ANALYSIS OF ELASTOHYDRODYNAMIC CIRCULAR AND NON-CIRCULAR JOURNAL BEARINGS WITH MICROPOLAR LUBRICANTS

A THESIS SUBMITTED TO THE UNIVERSITY OF CALICUT

IN FULFILMENT OF THE REQUIREMENT FOR THE

AWARD OF THE DEGREE OF

DOCTOR OF PHILOSOPHY

IN

MECHANICAL ENGINEERING

BY

SUKUMARAN NAIR V. P.

DEPARTMENT OF MECHANICAL ENGINEERING
NATIONAL INSTITUTE OF TECHNOLOGY
CALICUT, KERALA - 673 601

MAY 2004

Dedicated

To

My Parents

DECLARATION

I hereby certify that the work which is being presented in the thesis entitled "**ANALYSIS OF ELSASTOHYDRODYNAMIC CIRCULAR AND NON-CIRCULAR JOURNAL BEARINGS WITH MICROPOLAR LUBRICANTS**" in fulfillment of the requirement for the award of the Degree of Doctor of Philosophy, submitted to Calicut University, is an authentic record of my work carried out during a period from June 1997 to May 2004 under the supervision of Dr. K Prabhakaran Nair, Professor in Mechanical Engineering Department of National Institute of Technology, Calicut.

The matter embodied in the thesis has not been submitted by me for the award of any other degree.

Sukumaran Nair V. P.

This is to certify that the statement made by the candidate is correct to the best of my knowledge.

25/5/04

Dr. K Prabhakaran Nair,
Professor,
Department of Mechanical Engineering,
National Institute of Technology,
Calicut.

Date: 25/05/2004

ACKNOWLEDGEMENT

I would like to express my sincere gratitude and indebtedness to my guide Dr. K Prabhakaran Nair, Professor, Department of Mechanical Engineering, National Institute of Technology, Calicut for his invaluable guidance and constant encouragement during my work and preparation of the report. He has been the strong motive behind this amount of work. I sincerely feel that working with him has been a great research experience.

I am thankful to Dr. V George, Dr. R Ravindran Nair and Dr. N M Nagaraj, former Heads of the Department of Mechanical Engineering, NIT, Calicut for providing me the necessary facilities during my course of the work.

I am thankful to Prof. A.R. Gopinathan Kartha, former Professor, Mechanical Engineering Department, NSS Engineering College, Palakkad for all the encouragements given to me during the course of the work.

I am thankful to my colleagues especially Mr. D. Prakash of Mechanical Engineering Department, N.S.S. College of Engineering, Palakkad for his helps and suggestions.

Finally, I wish to thank my wife Maya and daughters Shyama and Silpa for their patience, constant cooperation and forbearance.

Date: 25/05/2004 **Sukumaran Nair V. P.**

ANALYSIS OF ELASTOHYDRODYNAMIC CIRCULAR AND NON-CIRCULAR JOURNAL BEARINGS WITH MICROPOLAR LUBRICANTS

ABSTRACT

The subject of elastohydrodynamic lubrication, during the initial stages of its development, conventionally included the lubricated point and line contacts. However, recently the area of elastohydrodynamic lubrication has been widened to encompass the lubricated surface contact problems such as slider and journal bearings. Though bearings are generally designed using the data developed with the assumption that their surfaces are rigid, bearings carrying heavy loads need analysis and design, which take into account their elastic deformation. The bearing deformations may quite often have magnitudes of the order of the film thickness, thus affecting the clearance space geometry of the bearing to an extent such that the actual performance characteristics may become significantly different from those computed with rigid bearing assumption.

Modern large capacity turbogenerators running usually at 3000 to 4000 rpm and producing power in the range of 500 MW to 1400 MW require large hydrodynamic bearings to support heavy rotor loads. In future, these bearings may even operate at higher speeds. In high speed applications where bearing stiffness and stability are major considerations, non circular bearing configurations give better dynamic performance of journal bearing systems and also reduce the power loss and increase the oil flow as compared to those of plain journal bearings.

To enhance certain characteristics of the lubricants various additives i.e. solids or liquids in the form of small particles are added to the lubricant. These additives along with contaminants form a dilute suspension of solid particles in the oil. These suspended solid particles produce thickening of lubricating oil, which in turn affect various performance characteristics of journal bearings. So it

is felt that there is a need to compute the static and dynamic characteristics of elastohydrodynamic journal bearings operating with micropolar lubricants.

This thesis is concerned with the analysis of circular and noncircular (two lobe and three lobe) journal bearings taking deformability of the bearings liner and variation of viscosity due to the presence of various additives in the lubricant. A survey of literature shows that a few investigations have been carried out on circular bearings operating with micropolar lubricants. Literatures are available on static analysis of such bearings, but literature on dynamic analysis is scarce. Literature survey also shows that no work has been carried out on EHD analysis of circular and non circular bearings operating with micropolar lubricants. So it is felt that there is a need to compute static and dynamic characteristics of elastohydodynamic journal bearings operating with micropolar lubricants.

In the present analysis a two dimensional modified Reynold's equation was derived from Navierstoke's equation and Fick's mass transfer equation and this modified Reynold's equation and three dimensional elasticity equations were used to compute the pressure distribution of the flow field and deformation of the bearing liner respectively. The solutions of the lubricant flow and elasticity equations were obtained using finite element method and a direct iteration scheme.

Based on the normalization of the governing equations, a non dimensional deformation coefficient ($\overline{\psi}$), as a function of runner speed, geometry of the lubricated contact, viscosity of the lubricant, modulus of elasticity and the thickness of the bearing linear, giving the measure of the bearing flexibility is defined. The effects of these variables (in terms of various values of deformation coefficient) on the pressure distribution, bearing deformation and on the performance characteristics of the journal bearing are studied.

In the work carried out, the static and dynamic characteristics of rigid or deformable and circular or non-circular (two lobe or three lobe) bearings have been studied. The static characteristics in terms of load capacity, attitude angle, end leakage and frictional force and dynamic characteristics in terms of stiffness

coefficients, damping coefficients, threshold speed and damped frequency of whirl have been determined for different values of eccentricity ratios and volume concentrations of additives for circular bearings, two lobe bearings and three lobe bearings. In the case of rigid circular and non-circular bearings, static and dynamic characteristics are obtained for different values of eccentricity ratios and wide range of volume concentration of additives. These characteristics are also evaluated for different values of mass transfer rate of additives in the fluid. For flexible bearings operating with Newtonian and micropolar fluids these performance characteristics are obtained for various eccentricity ratios and deformation coefficients.

The results of the study show that the effect of bearing deformation on the performance characteristics of the hydrodynamic bearings is quite appreciable when either the deformation coefficient or eccentricity ratio becomes large. The variation of viscosity with volume concentration and mass transfer rate of additives also introduces significant changes in the performance characteristics.

CONTENTS

NOMENCLATURE

$B_{XX}, B_{XY}, B_{YX}, B_{YY}$	- Fluid film damping coefficients
C	- Radical clearance
c	- Volume concentration of additives
c_o	- Percentage volume concentration of additives
c_r	- Volume concentration of the additives at the journal surface
D	- Journal diameter
E	- Modulus of elasticity of bearing linear material
$\overline{f}$	- Body force density
h	- Film thickness
K_d	- Diffusion coefficient
K_s	- Mass transfer rate
L	- Length of the bearing
M_C	- Critical mass of journal
$\overline{F}$	- Frictional power loss in L^{th} lobe
p	- Pressure acting on the journal
$\overline{p}$	- Nondimensional pressure acting on the journal
Q_Z	- End leakage of the bearing
$\overline{q}$	- Velocity vector
R	- Radius of the journal
r	- Radial co-ordinate
$S_{XX}, S_{XY}, S_{YX}, S_{YY}$	- Fluid film stiffness coefficients
T_{tr}	- Surface traction force
t_h	- Thickness of bearing liner
U	- Velocity of journal at the surface
u	- Velocity of the fluid in the circumferential direction

V_r, V_O, V_Z	- Components of bearing deformation in r, θ, z directions
V	- Velocity of the fluid in the radial direction at the journal surface
v	- Velocity of the fluid in the radial direction
W_X	- Horizontal component of load capacity
W_y	- Vertical component of load capacity
W	- Load carrying capacity of the bearing
w	- Velocity of the fluid in the axial direction
ε	- Eccentricity ratio
ε_p	- Ellipticity
μ	- Viscosity of the lubricant containing additives
μ_o	- Viscosity of the lubricant at reference temperature and pressure
ν	- Possion's ratio
ω	- Angular velocity of the journal
ω_d	- Damped frequency of whirl
ω_{th}	- Threshold speed
ξ, η	- Co-ordinates perpendicular to and along the line of centers
ρ	- Mass density of fluid
θ	- Co-ordinate in the circumferential direction
ϕ, ϕ_1	- Attitude angles
ψ	- Deformation coefficient

Matrices

$[\bar{B}]$ - Matrix for damping coefficients

$[D]$ - Elasticity matrix

$[\bar{d}]$ - Matrix for nodal displacement components

$[F]$ - Column vector for nodal force components

$[J]$ - Operator matrix

$[K]$ - Stiffness matrix for displacement field of bearing bush

$[K_f]$ - Fluidity matrix for the entire assemblage

$[\bar{M}]$ - Matrix for journal mass

$[N]$ - Shape function matrix

$[p]$ - Column matrix for nodal pressures for the entire assemblage

$[\bar{q}]$ - Velocity vector

$[\bar{s}]$ - State vector for journal centre perturbation co-ordination

$[T_{tr}]$ - Column matrix for surface traction force

Normalizing Factors

Non–Dimensional Quantities	*Multiplication Factor*
$\bar{B}_{ij}\,;i,j=1,2$	$\mu_0 \;\; R_j \;\; (R_j/C)^3$
$\bar{h}$, $\bar{h}_{\min}$	C
$\bar{M}_j$	$(\mu_0 \;\; R_j/\omega_{j)} \;\; (R_j/C)^3$
$\bar{p}$	$\mu_0\omega_j \;\; (R_j/C)^2$
$\bar{Q}_z$	$\frac{1}{2}\omega_j \; R_j \; Lc$
$\bar{r}$	C, for lubricant film t_h, for bearing body
$\bar{S}_{ij}\,;i,j=1,2$	$\mu_0\omega_j \;\; R_j \;\; (R_j/C)^3$
$\bar{u},\bar{v},\bar{w}$	$\omega_j R_j$

$\overline{W}_x \ \overline{W}y$	$\mu_0 \omega_j \ R_j^2 \ (R_j / C)^2$
$\bar{z}$	R_j
$\overline{\omega}_d, \overline{\omega}_{th}$	ω_j

Subscripts and Superscripts

e	- Superscript for the element
i, j	- Subscript for the element
L	- Subscript for the lobe
T	- Superscript for transpose of a matrix
$-(bar)$	- Superscript for non-dimensional quantities
$.(dot)$	- Superscript for the derivative with respect to time
$..(doubledot)$	- Superscript for acceleration
ξ, η	- Subscript for the axis along the perpendicular to the line of centers.

LIST OF FIGURES

LIST OF TABLES

INTRODUCTION

Sukumaran Nair V.P. "Analysis of elastohydrodynamic circular and non-circular journal bearings with micropolar lubricants" Thesis. Department of Mechanical Engineering , NIT Calicut, University of Calicut, 2004

Chapter 1

INTRODUCTION

1.1 GENERAL

A bearing is a system of machine elements whose function is to support an applied load by reducing friction between relatively moving surfaces. Hydrodynamic journal bearing is a fluid film bearing in which the load applied on the shaft is supported by the pressure developed in the lubricating film due to hydrodynamic action, (Fig.1.1).

Modern large capacity machines such as turbogenerators usually run at high speed and support heavy load. In high speed applications where bearing stiffness and stability are major considerations, non circular bearings give better dynamic performance.

When bearing is subjected to heavy loads the bearing shell deforms. The deformation of the bearing shell modifies the film thickness and this in turn affects the performance characteristics of the bearing. Therefore elastohydrodynamic analysis is considered to recompute the performance characteristics of circular and non circular bearings.

Various additives are added to the lubricant oil to enhance certain characteristics of the lubricant. These materials commonly known as additives are used as rust inhibitors (amine phosphates), corrosion inhibitors (sulphurised olefins), fire resistors (halogenated hydrocarbons), viscosity index improvers (polymethacrylate), powders of graphite and molybdenum disulphide) etc. The additives along with the contaminants form a dilute suspension of solid particles in the oil and it is treated as micropolar fluid. These suspended solid particles in the lubricating oil produce thickening of the oil affecting various performance characteristics of the journal bearing. Also there is an increase of viscosity in the part of the lubricating film, which is in the vicinity of the journal and bearing surfaces due to adhesion and other surface phenomena. The lubricant becomes

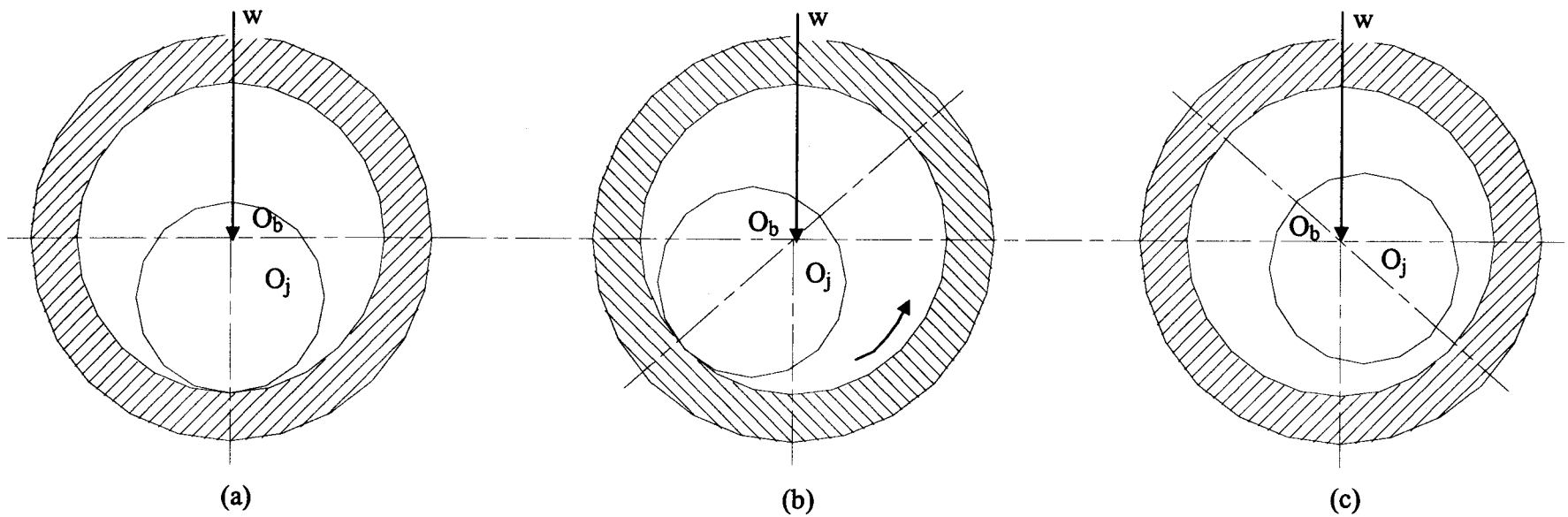

Fig. 1.1 Hydrodynamic Action of a Journal Bearing

non isoviscous. The non uniform distribution of the solid particles builds up concentration gradient which results in mass transfer of these particles across the film thickness and this affects bearing performance characteristics.

In the present work the static and dynamic performance characteristics of circular and non circular journal bearings are determined by considering the effect of deformation of the bearing liner and micropolar properties of the lubricant.

1.2 LITERATURE SURVEY

To identify the problem a survey of available literature on rigid hydrodynamic and elastohydrodynamic bearings is carried out. A literature survey is also carried out in the analysis of hydrodynamic journal bearings using micropolar lubricants.

1.2.1 Literature on Hydrodynamic Analysis

Conventionally, journal bearings are designed using the performance data computed on the assumptions that the bearing shell is rigid and viscosity of oil is constant. Based on these assumptions several investigations [1-8] are available on hydrodynamic analysis of circular and non circular bearings.

Hydrodynamic analysis of bearings are done by various methods. Singh et. al [9] determined various performance characteristics of a finite circular hydrodynamic bearing by solving Navier Stoke's equation for the flow field in the clearance space by using finite element method. Heller [10] solved fluid film equations for externally pressurized bearings for steady state performance and spring and damping coefficients using finite differences and a variable grid model. Ettler and Anderson [11] analyzed thrust bearings by using higher order finite elements for better accuracy in results. Chandrawat and Sinhasan [12] analyzed plain and two groove bearings by Gauss-Siedel iterative scheme and linear complementary problem approach. The results for these bearings wre compared when they operated in the laminar regime.

Goenka [13] presented a finite element formulation for the transient analysis of a journal bearing, which can be used for a partial or full arc bearing.

The results obtained for different cases of connecting rod bearings were presented. Chang [14] presented a new pressure starting boundary condition for calculating the oil film stiffness and damping coefficients of journal bearings using a perturbation method. Akers et. al [15] proved that in the case of journal bearings when out of balance load is added, the bearing becomes more stable if friction is included. Nikolajsen [16] investigated the stability of plain journal bearings and floating ring journal bearing against fractional frequency of whirl under laminar fluid film flow conditions. Shelly and Ettlest [17] applied finite element method for the whirl analysis of plain bearings. He presented several locus paths to show the separate and combined effects of rotor unbalance and unidirectional loading over a range of rotational speeds.

Rohde and Ezzat [18] analyzed hybrid journal bearing considering the compressibility of the lubricant in the bearing. Etsion and Pinkus [19] analyzed short journal bearings and showed that the bearing performance characteristics are functions of Sommerfeld number, length over diameter ratio and starting conditions at the film inlet. Taylor [20] obtained a numerical solution for the pressure distribution in a porous thrust bearing. He showed that the dynamic spring force and dynamic damping force vary with displacement for a given frequency.

Bearings may operate in the turbulent regime at high speeds. Analysis has been done by considering the variation in viscosity of the lubricating oil due to turbulence. Hydrodynamic bearings were analyzed by considering turbulence in oil flow by Wilcock [21]. He proved that in turbulent lubrication greater film thickness and larger power loss occur than from laminar theory. Venkateswarlu et.al [22] analyzed journal bearings considering the three dimensional motion in the lubricant layer operating from laminar to turbulent condition. Velocity and pressure fields were calculated from the governing differential equations using an iterative numerical method. Gardner and Ulshmid [23] determined the operating characteristics of two different types of journal bearings to indicate the effects of turbulence on these characteristics.

Literatures are available considering the non Newtonian nature of fluids in lubrication [24-26]. Dien and Elrod [27] analyzed a modified form of Reynold's Equation for fluids showing inelastic and non-Newtonian characteristics. The static and dynamic characteristics of a plane journal bearing were determined by Malik et. al [28] for non-Newtonian lubricants. He solved Reynold's Equation and the steady state pressure distribution was established by an iteration scheme.

Finite element method has been used for the hydrodynamic analysis of non circular bearings also. Goenka and Booker [29] extended the finite element formulation of cylindrical bearing to include non cylindrical bearings. In his analysis he determined the optimum bearing shape to maximize the minimum film thickness. Ashok Kumar et.al [30] determined the static and dynamic characteristics of an elliptical bearing by using a variational solution. Kumar Vaidyanathan et.al [31] analyzed non circular bearings considering the effects of turbulence and cavitation. Different static characteristics were determined for circular and two lobe bearings. Malik et.al[32] studied three lobe bearings assuming the viscosity to be constant. Malik et. al [33] analyzed the performance characteristics of tilted three lobe bearings. The effect of tilt angle on the dynamic performance characteristics was studied. Li et. al [34] analyzed the stability of elliptical, offset elliptical, three lobe and four lobe bearings using a numerical fast Fourier transform analysis.

1.2.2 Literature on EHD Analysis

Elastohydrodynamic analysis is considered as important because the effect of elastic deformations of the bearings shell on the performance characteristics of the journal bearing system is quite significant particularly for heavily loaded bearings. Flexibility of the bearing shell affects the performance of the bearing especially at higher values of deformation coefficient. During the last two decades elastohydrodynamic studies have received considerable attention with the recognition that large changes in the performance characteristics occur with flexibility of bearing liner under heavy load.

One of the first attempts on the study of EHD lubrication was made by Osterle and saibel [35 – 36]. For slider bearings, assuming the bearing pad to be a semi infinite elastic body, they determined the deformation and pressure field by neglecting the side leakage. They concluded that due to bearing deformation, pressure distribution and load capacity are different from those calculated for rigid bearings. For an infinitely long bearing, Higginson [37] studied the effects of elastic deformation of bearing shell on the journal bearing performance; these results were only qualitatively good because of his simplified approach to the calculation of elastic deformation. The theoretical investigation for elastic deformation of bearings was prompted by the experimental work of Carl [38] presented in 1964. He experimentally demonstrated the effect of bearing deformation on the pressure distribution in the clearance space of the journal bearing and showed that the distortion of bearing was important at pressures of the order of 13.8 Mpa. O' Donoghue et. al [39] studied the effect of elastic deformation of bearing on the performance of infinitely long journal bearing. Their studies also indicated that the elastic deformation of bearing introduces marked changes in bearing performance characteristics and their results confirmed the findings of Carl's experiments of maximum pressure and the extent of positive pressure film. An iterative procedure was used to find the pressure distribution satisfying both the hydrodynamic and elastic equations. A similar analysis for short bearings with flexible liners was also described by O'Donaghue et al [40]. Other studies [41-43] also demonstrated significant changes in pressure distribution in the clearance space of bearings when the deformation of the bearing shell was considered.

Benjamin and Castelli [44] solved Reynold's equation and three dimensional elasticity equations for analyzing journal bearings and they proved that the load capacity and attitude angle are reduced when deformations of bearing liner are considered. They showed that the elastohydrodynamic pressure distribution is significantly different from that obtained by neglecting the elastic deformation. Oh and Hubner [45] used finite element technique to solve elastohydrodynamic finite journal bearing problem. Reynold's equation for fluid

film and three dimensional elasticity equations for the bearing housing were solved simultaneously using an iteration scheme. The analysis yielded pressure distribution and displacement distribution. From these distribution s stresses in the bearing and minimum film thickness in the lubricant were determined. Jain et. al [46] determined the various static performance characteristics of the bearing. Reynold's equation was solved to obtain the pressure distribution by using FEM. Three dimensional elasticity equations were used to determine the bearing shell deformations. The final pressure was obtained by using an iteration scheme.

Stafford et. al [47] used simplified equations for studying elastohydrodynamic lubrication. Elastohydrodynamic analysis of a connecting rod big end bearing was done by them assuming a two dimensional structural model. They also assumed half Sommerfeld conditions to simplify calculations. Frene et. al [48-49] analyzed bearings by using flow field equations and two dimensional elasticity equations. Labouff and Booker [50] studied the effect of mesh density and housing flexibility on bearing performances. They also proved that there is change in the maximum film thickness and maximum film pressure obtained in the bearing when flexibility is considered.

Conway et. al [51-53] studied the effect of pressure on viscosity of the lubricating oil in EHD analysis. The oil was first assumed to be isoviscous and the analysis was then extended to the case of pressure dependent viscosity and they showed that the performance characteristic depend on both flexibility of the bearing liner and the dependence of viscosity on pressure. Taylor and Callaghan [54] determined pressure distribution in elastic isoviscous and elastic viscous cases. The effect of increasing the effective elastic modulus of the cylinder material on minimum film thickness also is discussed. Jain et. al [55-56] analyzed flexible bearings considering the variation of viscosity in pressure and they proved that piezo viscous lubricants support more loads

Elastohydrodynamic analysis of two axial groove journal bearings operating in laminar and super laminar regimes was done by Sinhasan and Chadrawat [57]. Literature is available on the analysis of porous flexible bearings

[58-60]. . Performance characteristics of capillary and orifice compensated flexible thrust bearings were analyzed by Sinhasan et. al [61]. Fantino et. al [62] analyzed connecting rod bearing operating with piezo viscous lubricants. In the analysis, plane elasticity relations were used by them to calculate the bearing displacement. Partial bearing in different flow regimes were analyzed by Jain et. al [63]. Kohnos et al [64] analyzed the elastohydrodynamic lubrication characteristics of journal bearings with combined use of the boundary-element method and finite-element method. The boundary-element method was used to calculate the elastic deformation of the bearing housing and the finite-element method was applied to the solution of the Reynolds equation.

Literatures are available on EHD Analysis of non circular bearings also. Hamrock and Dowson [65] analyzed elliptical contacts for materials with low elastic modulus. Tae Jo Park and Kyung – Woom Kim [66] analyzed elastohydrodynamic lubrications of elliptical contacts and determined pressure distribution for various film thicknesses. Prabhakaran Nair et. al. [67] determined various static and dynamic characteristics of elliptical bearings by using finite element method. Three dimensional Navier Stoke's equation and continuity equation governing lubricant flow in the clearance space of the journal bearing and the three dimensional elasticity equations governing the displacement field in the bearing shell were solved to get the pressure distribution in the bearing. Various characteristics of the bearing were presented for a range of deformation coefficients, which take in to account the flexibility of the bearing liner. Goyal and Sinhasan [68] presented static and dynamic performance characteristics of two-lobe journal bearings with non-Newtonian lubricants. The Navier-Stokes and continuity equations were solved for Newtonian fluids using the finite element method in the cylindrical coordinates representing the flow field in the clearance space of a two-lobe journal bearing. The non-Newtonian effect was introduced by modifying the viscosity term for the model in each iteration. Deformation of the bearing shell was obtained by solving the three-dimensional elasticity equations. Chandrawat and Sinhasan [69] studied two-lobe journal bearing and determined the static performance characteristics of a flexible shell two-lobe bearing

operating in laminar and turbulent (including transitional flow) regimes in the case of isoviscous and piezoviscous lubricants. Prabhakaran Nair et. al [70] extended the analysis used for elliptical bearings to include three lobe bearings. Chandrawat and Sinhasan [71] determined various static performance characteristics of a flexible shell three lobe bearing operating in the laminar and turbulent regime using isoviscous and piezoviscous lubricants.

Prabhakaran Nair et. al [72-81] analyzed circular and non circular bearings with flexible shell placed in a rigid housing considering also the change in temperature of Newtonian lubricants.

1.2.3 Literature on Micropolar Lubricants

The behaviour of micropolar fluids is explained by the theory of 'fluid microcontinua'. In this theory the intrinsic motion of molecular or granular constiluents of the medium is taken into account. The earliest formulation of a theory considering micromotions and deformations was done by Eringen [82]. He considered the continuum media as a set of structured micro volume elements whose kinematics can be independent of the motion of macrovolume. This theory has been further simplified to the theory of micropolar fluids [83] by ignoring the deformation of micro elements. Assuming the solid contaminants and additives in the lubricant oil to be rigid spherical particles, dilute suspensions of the same in the oil can be treated as micropolar fluids.

Allen and Kline [84] analyzed two dimensional problem of lubrication with micropolar fluids to get an approximate solution to the problem of a slider bearing. Shukla [85] studied the effects of additives on load carrying capacity of a hydrostatic bearing. He showed that the load carrying capacity increases with increase in the concentration of additives. Khader and Vachon [86] analysed laminar flow of micropolar fluids between two circular disks. The analysis indicated that significantly larger resultant pressures and shear stress occur in the lubricant due to the presence of the microstructures. They showed that load carrying capacity increases when compared with the result of a similar analysis employing nonmicropolar fluids. A one dimensional slider bearing with

micropolar fluid was analyzed by Shukla and Isa [87] by considering a generalized form of Reynold's equation including micropolarity. The derivation of a generalized Reynold's equation and an analysis for steady state characteristics of one dimensional journal bearing under the condition of micropolar lubrication was presented by Zaheeruddin and Isa [88]. Prakash and Sinha [89] studied the behaviour of micropolar fluids when it passes through narrow passages. The studies on the squeeze film characteristics of micropolar fluid lubricated journal bearing for both full and half bearings were also done by Prakash and Sinha. [90]. A practical example of using micropolar model is in the design of journal bearings in the area of nuclear power where heat transfer agent sodium is used as lubricant [91]. Albert et. al [92] studied hydrodynamic lubrication of a slider bearing with oil containing additives. It was shown that the load capacity and the frictional force of the slider bearing increase with increase in concentration of additives. The static characteristics of a journal bearing with micropolar lubricants were determined by Prakash and Prawal Sinha [93] considering the problem as that of a steady laminar flow of an incompressible micropolar fluid. The steady state performance of infinitely long journal bearing based on the theory of micropolar fluids revealed that the prominent feature of a micropolar fluid is an increased effect of viscosity which in conformity with experimental results. Alber et. al [94] developed an analytical hydrodynamic model to predict the behaviour of a two phase lubricant. Analysis showed that the presence of suspended solid particles in a Newtonian lubricant enhanced the load carrying capacity. The short bearing performance with micropolar fluids has been analyzed by Nicolae Tipei [95]. The performance of finite width journal bearings lubricated with micropolar fluids is analysed by Tsai-Wang HuangCheng-I Weng and Chao-Kuang Chen [96] using the finite difference method to solve the generalized three-dimensional Reynolds equation. The characteristics of finite journal bearings with micropolar and Newtonian fluids are obtained and presented graphically. The analysis reveals that the prominent feature of increasing load capacity and decreasing friction coefficient for micropolar fluids is more pronounced at higher eccentricity ratio. Khonsari and Brewe [97] studied the performance parameters for a journal

bearing of finite length lubricated with micropolar fluids. They proved that a significantly higher load-carrying capacity than with Newtonian fluids result, depending on the size of the material characteristic length and the coupling number. It is also shown that, although the frictional force associated with a micropolar fluid is in general higher than that of a Newtonian fluid, the friction coefficient of micropolar fluids tends to be lower than that of Newtonian fluids. A modified momentum equation and continuity equation were used to analyze the bearing. Prabhakaran Nair et. al [98] analyzed hydrodynamic circular journal bearing with micropolar fluids. Prabhakaran Nair et. al [99] also determined the static and dynamic characteristics of circular rigid bearings operating with micropolar fluids. Albert E. Yousif and Thamir M. Ibrahim [100] determined the characteristics of conventional infinitely long thrust bearings by solving numerically the modified Reynolds equation for the steady laminar flow of an incompressible micropolar fluid that has an increased effective viscosity, especially in thin films. They proved that the bearing performance, in general, is improved by micropolar lubricants. The static and dynamic characteristics of a hydrostatic circular thrust bearing were studied by Jaw-Ren Lin [101]. Modified Reynold's equation and flow continuity equation were used to solve the problem and results were obtained by using a perturbation technique. The convergence to the stationary solution for large viscosity flows was analyzed by Lukaszewicz [102]. He determined long time behaviour of micropolar fluids in two dimensional flows. Raghunandana et.al [103] studied the effect of non Newtonian behaviour of lubricants, resulting from addition of polymers, on the performance of hydrodynamic journal bearings. Das et. al [104] solved a modified Reynold's equation based on the theory of micropolar lubricant by using finite difference method to obtain the film pressure for a hydrodynamic bearing with misalignment. With the help of this pressure, steady state characteristics of the bearing were determined. Literature survey shows that the performance characteristics of hydrodynamic circular bearings considering the effect of deformation of bearing liner and mass transfer of micropolar lubricant on the performance have not been investigated. It is also seen that no literature is

available for static and dynamic analysis of elastohydrodynamic noncircular bearings operating under micropolar lubricant. So it is felt that there is a need to compute the performance characteristics of circular and noncircular bearings considering the effect of deformation of bearing liner and mass transfer of micropolar lubricants.

1.3 OBJECTIVES OF THE PRESENT WORK

In the present work the static and dynamic characteristics of the rigid or deformable, circular or non-circular (two lobe or three lobe) bearings operating under micropolar lubricants have been studied A two dimensional Reynold's equation was derived from Navier Stoke's equation and Fick's mass transfer equation and this modified Reynold's equation and three dimensional elasticity equations were solved to compute the pressure distribution of the flow field and deformation of the bearing respectively. The finite element method, which offers several advantages, when applied to lubrication problems is used to analyze bearings.

In the case of micropolar fluids the variation of viscosity is governed by the following relation [85].

$$\mu = \mu_0 (1+\lambda c_r) \tag{1.1}$$

where λ is a parameter which specify the shape, size, deformation, distribution and material properties of the additive particles.

Assuming spherical non deformable additive particles according to Einstein's relation [94].

$$\mu = \mu_0 (1+2.5c_r). \tag{1.2}$$

The static characteristics in terms of load capacity, attitude angle, end leakage and frictional force and dynamic characteristics in terms of stiffness coefficients, damping coefficients, threshold speed and damped frequency of whirl have been determined for rigid and deformable, circular and non circular bearings operating with Newtonian and micropolar lubricants. Results are obtained for a wide range of deformation coefficients and volume concentration of

additives.The effect of mass transfer of additives on the performance characteristics of bearings are also analysed

The computed results show that the presence of additives in the lubricating oil affects the performance characteristics. The change in volume concentration of additives and mass transfer rate produce significant effects in the performance characteristics of the bearing especially when the bearing operates at higher eccentricity ratios. The deformation of the bearing liner also affects the performance characteristics of the bearing.

1.4 THESIS ORGANIZATION

The work carried out is organized into five chapters. The first chapter Introduction high lights the literature survey and states the objectives and scope of investigation. The second chapter deals with the theoretical analysis of bearings. Governing differential equations and finite element formulations for fluid flow field and displacement field with boundary conditions are discussed in this chapter.

The static and dynamic performance characteristics of the bearing are described in Chapter 3.

The fourth chapter contains details of solution schemes. Flow charts for various segments of solution procedure are also given in this chapter.

The results and discussions are given in Chapter 5. Scope for future studies of the work also is given in this chapter.

The non circular bearing geometries and details of FEM formulations are given in Appendices A_1 and A_2.

THEORETICAL ANALYSIS

Sukumaran Nair V.P. "Analysis of elastohydrodynamic circular and non-circular journal bearings with micropolar lubricants" Thesis. Department of Mechanical Engineering , NIT Calicut, University of Calicut, 2004

Chapter 2

THEORETICAL ANALYSIS

2.1 GENERAL

This chapter deals with the generalized formulation of problems concerning circular (Fig. 2.1) and non circular (Fig. 2.2 - 2.3) bearings with micropolar lubricants. Elastohydrodynamic (EHD) studies require simultaneous solutions of the following:

1. Two dimensional modified Reynold's equation derived from Navier Stoke's, continuity and Fick's second law equations.
2. The three dimensional elasticity equations to determine the deformation of the bearing liner.

The representative models for the fluid flow field and the displacement field with boundary conditions to be adopted are described in this chapter. To achieve the analysis the two dimensional modified Reynold's equation and the three dimensional elasticity equations are to be solved to obtain the pressure distributions in the fluid flow field and the deformation of the bearing liner. In the present work, it is proposed to use the powerful technique, finite element method, to obtain the numerical solution of the elastohydrodynamic problem.

2.2 HYDRODYNAMIC ANALYSIS

To obtain the hydrodynamic pressure distribution in the fluid flow field in the clearance space of journal bearing, Reynold's equation is used. To consider micropolar effect in the pressure field, Reynold's equation is modified by incorporating Fick's second law of diffusion in the equation.

2.2.1 Governing Equations

Navier-Stoke's equation for incompressible fluid is written as

$$\rho\left(\frac{\partial \vec{q}}{\partial t} + \vec{q}.\nabla\vec{q}\right) = \rho\vec{f} - \nabla p + \nabla.\mu\nabla\vec{q} \qquad (2.1)$$

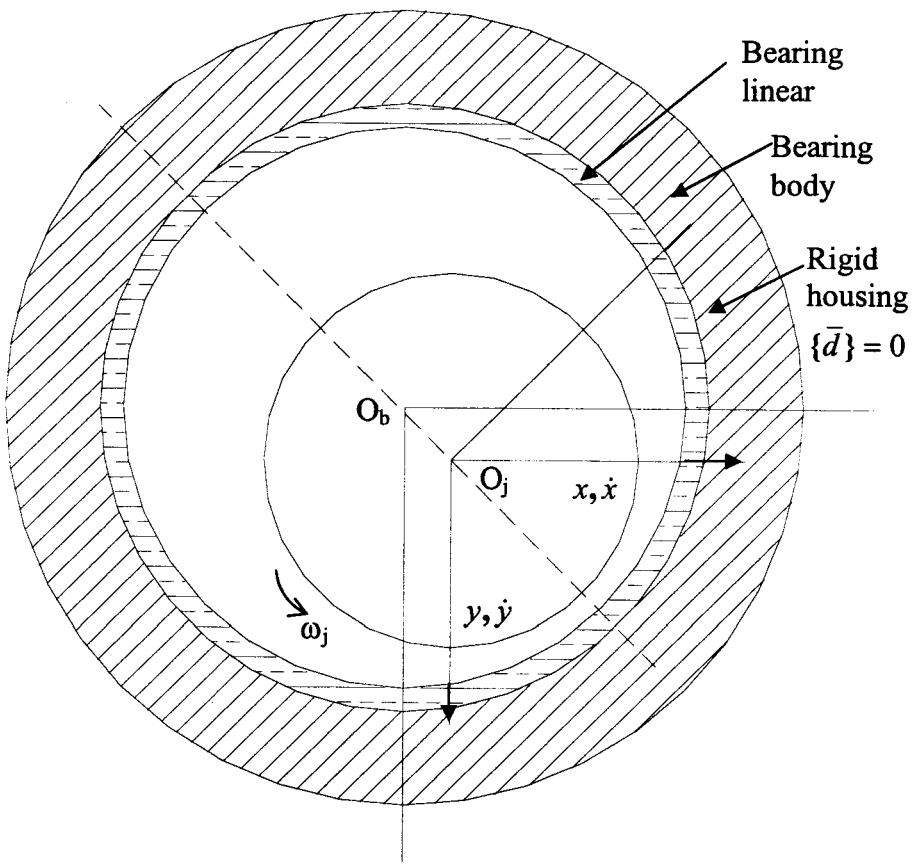

Fig. 2.1 Circular Bearing Geometry

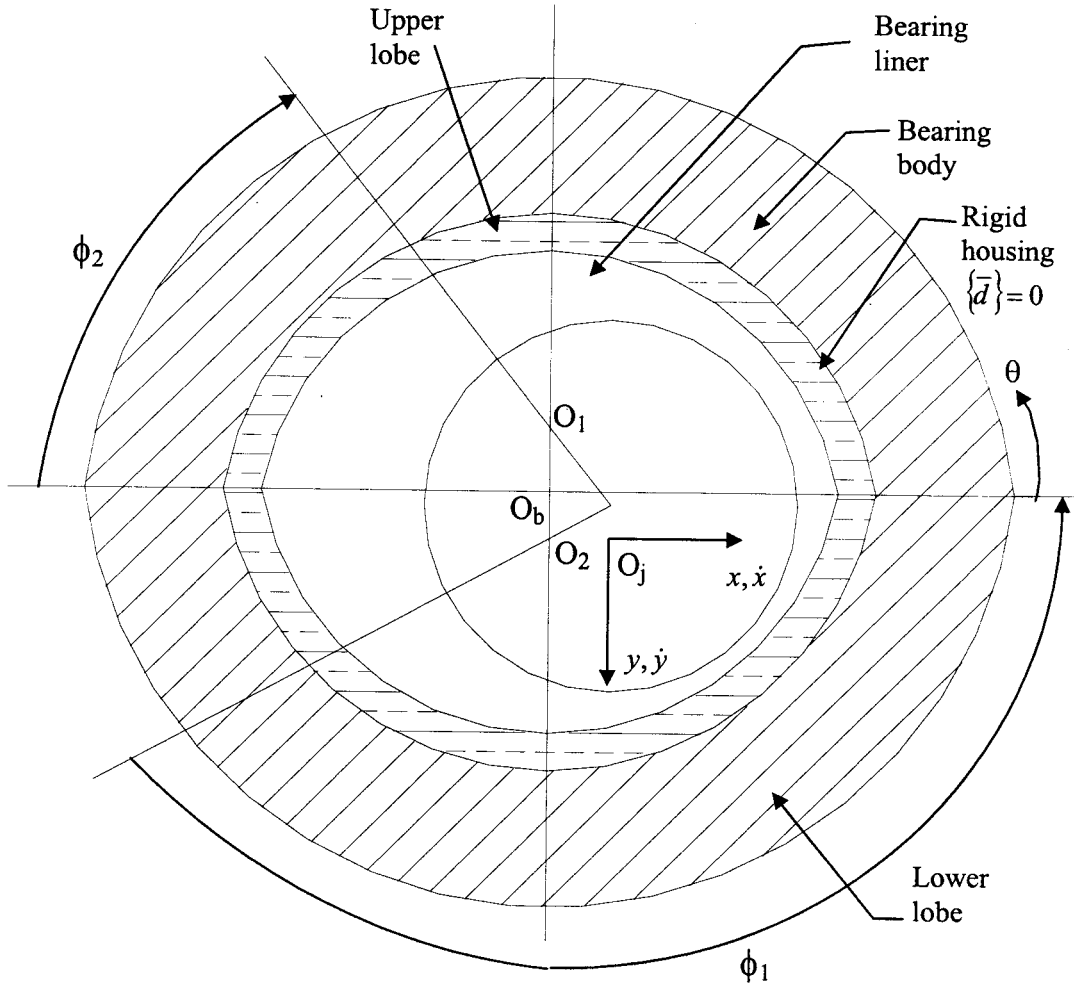

Fig. 2.2 Two Lobe Bearing Geometry

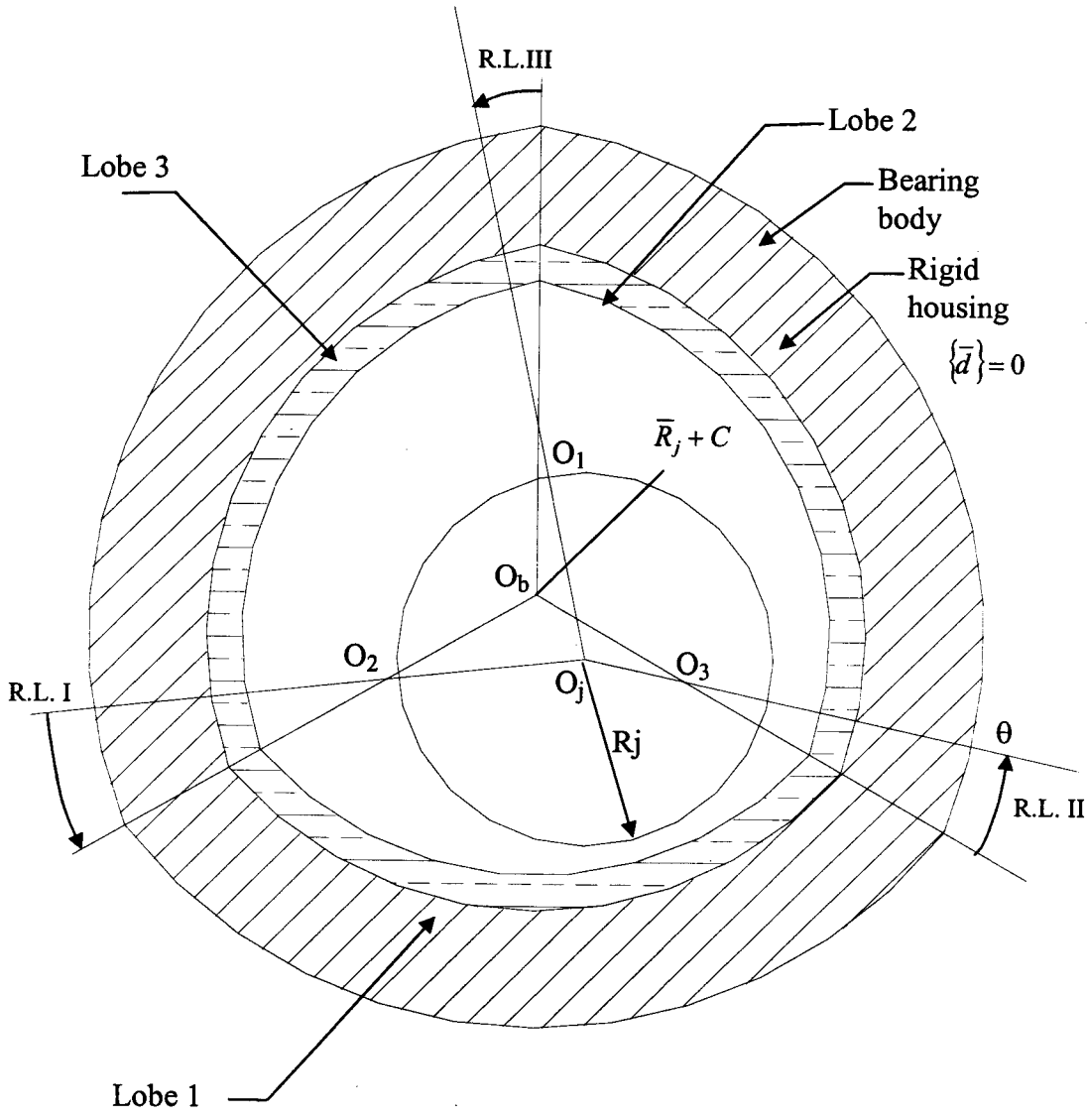

Fig. 2.3 Three Lobe Bearing Geometry

Continuity equation for steady flow of an incompressible fluid is given by

$$\nabla.\vec{q} = 0 \tag{2.2}$$

Fick's Second law of mass diffusion is written as

$$\frac{\partial c}{\partial t} + \bar{q}.\nabla c = K_d \nabla^2 c \tag{2.3}$$

For the case of a steady, uniform flow [92] Eq.(2.3) reduces to

$$K_d \left\{ \frac{\partial^2 c}{\partial y^2} + \frac{\partial^2 c}{\partial z^2} \right\} = w \frac{\partial c}{\partial z} \tag{2.4}$$

Since $\frac{\partial c}{\partial z} << 1$ and $\frac{\partial^2 c}{\partial z^2} << \frac{\partial^2 c}{\partial y^2}$ Eq. (2.4) becomes

$$\frac{\partial^2 c}{\partial y^2} = 0 \tag{2.5}$$

Eq. (2.5) can be solved for 'c' subject to the boundary conditions

$c = c_r$ at $y = 0$ and

$$K_d \frac{\partial c}{\partial y} = -K_s c_r \text{ at } y = h \tag{2.6}$$

Thus we get

$$c = c_r \left(1 + \frac{K_s y}{K_d} \right) \tag{2.7}$$

Eq. (2.7) with Eq. (1.1) gives the relation for viscosity in the following form.

$$\mu = \mu_0 \left[1 + \lambda c_r \left\{ 1 + \frac{K_s y}{K_d} \right\} \right] \tag{2.8}$$

For getting modified Reynold's equation from Eqs. (2.1), (2.2) and (2.8), the following assumptions are made.

1. Inertia and body forces are negligible when compared with the pressure and viscous forces.

2. There is no variation of pressure across the fluid film. i.e., $\frac{\partial p}{\partial y} = 0$

3. There is no slip in the fluid-solid boundaries.

4. Flow is laminar and incompressible.

5. Compared with the two velocity gradients $\frac{\partial u}{\partial y}$ and $\frac{\partial w}{\partial y}$, all other velocity gradients are considered to be negligible.

6. The height of the fluid film is very small. This permits us to ignore the curvature of the fluid film.

Using the relevant assumptions given, Eq. (2.1) can be written as

$$\frac{\partial p}{\partial x} = \frac{\partial}{\partial y}\left[\mu \frac{\partial u}{\partial y}\right] \tag{2.9}$$

and

$$\frac{\partial p}{\partial z} = \frac{\partial}{\partial y}\left[\mu \frac{\partial w}{\partial y}\right] \tag{2.10}$$

Integrating Eq. (2.9) with respect to y twice we get

$$u = \frac{\partial p}{\partial x}\int\frac{y}{\mu}dy + \int\frac{C_1}{\mu}dy + C_2 \tag{2.11}$$

From Eq. (2.8) and Eq. (2.11) we get the following relation.

$$u = \frac{K_d}{\mu_0 K_s \lambda c_r}\frac{\partial p}{\partial x}\left\{y - \frac{(1+\lambda c_r)K_d}{K_s \lambda c_r}\ln \mu(y)\right\} + \frac{C_1 K_d}{\mu_0 K_s \lambda C_r}\ln \mu(y) + C_2 \tag{2.12}$$

Similarly integrating Eq.(2.10) and using Eq.(2.8) we obtain

$$w = \frac{K_d}{\mu_0 K_s \lambda c_r}\frac{\partial p}{\partial z}\left\{y - \frac{(1+\lambda c_r)K_d}{K_s \lambda c_r}\ln \mu(y)\right\} + \frac{C_3 K_d}{\mu_0 K_s \lambda C_r}\ln \mu(y) + C_4 \tag{2.13}$$

The boundary conditions are given below.

$$u = U,\ w = 0 \quad \text{at } y = 0$$
$$u = 0,\ w = 0 \quad \text{at } y = h \tag{2.14}$$

Using Eqs. (2.14) in Eq. (2.12) we get

$$u = \left[-U \ln \frac{\mu(y)}{\mu(h)} + \frac{K_d}{\mu_0 K_s \lambda C_r} \frac{\partial p}{\partial x} \left\{ \left[y \ln \frac{\mu(h)}{\mu(0)} \right] + h \ln \left[\frac{\mu(y)}{\mu(0)} \right] \right\} \right] \div \ln \frac{\mu(h)}{\mu(0)} \tag{2.15}$$

Using boundary conditions in Eq. (2.13) we have

$$w = \frac{\dfrac{K_d}{\mu_0 K_s \lambda C_r} \dfrac{\partial p}{\partial z} \left[y \ln \dfrac{\mu(h)}{\mu(0)} - h \ln \dfrac{\mu(y)}{\mu(0)} \right]}{\ln \dfrac{\mu(h)}{\mu(0)}} \tag{2.16}$$

Differentiating Eq. (2.15) with respect to x and Eq. (2.16) with respect to y we get

$$\frac{\partial u}{\partial x} = -\frac{\partial}{\partial x} \left[\frac{U \ln \dfrac{\mu(y)}{\mu(h)}}{\ln \dfrac{\mu(h)}{\mu(0)}} \right] + \frac{\partial}{\partial x} \left[\frac{\dfrac{\partial p}{\partial x} \dfrac{K_D}{\mu_0 K_s \lambda C_r}}{\ln \dfrac{\mu(h)}{\mu(0)}} \right] \left\{ y \ln \frac{\mu(h)}{\mu(0)} + h \ln \frac{\mu(y)}{\mu(0)} \right\} \tag{2.17}$$

$$\frac{\partial w}{\partial z} = \frac{K_d}{\mu_0 K_s \lambda C_r} \frac{\partial}{\partial z} \left[\frac{\dfrac{\partial p}{\partial z} \left[y . \ln \dfrac{\mu(h)}{\mu(0)} - h \ln \dfrac{\mu(y)}{\mu(0)} \right]}{\ln \dfrac{\mu(h)}{\mu(0)}} \right] \tag{2.18}$$

Integrating continuity equation, Eq (2.2) we get

$$v = -\int \frac{\partial u}{\partial x} dy - \int \frac{\partial w}{\partial z} dy + C_5 \tag{2.19}$$

The boundary conditions are

$$y = 0 \qquad \text{at } v = V$$
$$y = h \qquad \text{at } v = 0 \tag{2.20}$$

Using Eqs. (2.17), (2.18) and boundary conditions given by Eq. (2.20) in Eq. (2.19) and neglecting higher order terms we get the following relation.

$$V = -\int_0^h \frac{\partial}{\partial x}\left\{\frac{U \ln \dfrac{\mu(y)}{\mu(h)}\, dy}{\ln \dfrac{\mu(h)}{\mu(0)}}\right\} + \int_0^h \frac{\partial}{\partial x}\left\{\frac{\dfrac{K_d}{\mu_0 K_s \lambda C_r}\dfrac{\partial p}{\partial x}}{\ln \dfrac{\mu(h)}{\mu(0)}}\, y \ln \frac{\mu(h)}{\mu(0)}\, dy\right\}$$

$$+ \int_0^h \frac{\partial}{\partial z}\left\{\frac{\dfrac{K_d}{\mu_0 K_s \lambda C_r}\dfrac{\partial p}{\partial z}}{\ln \dfrac{\mu(h)}{\mu(0)}}\, y \ln \frac{\mu(h)}{\mu(0)}\, dy\right\} \qquad (2.21)$$

Simplifying equation (2.21) we get

$$\frac{\partial}{\partial x}\left[\frac{h^3}{12\mu_0}\left\{1-\lambda c_r\left(1+\frac{K_s h}{2K_d}\right)\right\}\frac{\partial p}{\partial x}\right] + \frac{\partial}{\partial z}\left[\frac{h^3}{12\mu_0}\left\{1-\lambda c_r\left(1+\frac{K_s h}{2K_d}\right)\right\}\frac{\partial p}{\partial z}\right]$$

$$= \frac{U\partial}{\partial x}\left[\frac{h}{2}\left\{1-\frac{\lambda c_r K_s h}{6K_d}\right\}\right] + V \qquad (2.22)$$

Changing in to polar co ordinates and non dimensionalising

$$\frac{\partial}{\partial \theta}\left[\frac{\bar{h}^3}{12\bar{\mu}}\left\{1-\lambda c_r\left(1+\frac{\bar{K}_s \bar{h}}{2}\right)\right\}\frac{\partial \bar{p}}{\partial \theta}\right] + \frac{\partial}{\partial \bar{z}}\left[\frac{\bar{h}^3}{12\bar{\mu}}\left\{1-\lambda c_r\left(1+\frac{\bar{K}_s \bar{h}}{2}\right)\right\}\frac{\partial \bar{p}}{\partial \bar{z}}\right]$$

$$= \frac{\bar{U}\partial}{\partial \theta}\left[\frac{\bar{h}}{2}\left\{1-\frac{\lambda c_r \bar{K}_s \bar{h}}{6}\right\}\right] + \bar{R}\bar{V} \qquad (2.23)$$

The following relations are used for the velocity components in the tangential and radial directions.

$$\bar{U} = 1 + \frac{\dot{\eta}}{\bar{R}}\sin\theta - \frac{\varepsilon\dot{\xi}}{\bar{R}}\cos\theta \qquad (2.24)$$

$$\bar{V} = \frac{\dot{\eta}}{\bar{R}}\cos\theta - \frac{\varepsilon\dot{\xi}}{\bar{R}}\sin\theta \qquad (2.25)$$

$$\frac{\partial \bar{U}}{\partial \theta} = \frac{\dot{\eta}}{\bar{R}}\cos\theta + \frac{\varepsilon\dot{\xi}}{\bar{R}}\sin\theta \qquad (2.26)$$

Using Eqs. (2.24), (2.25) and (2.26) in Eq. (2.23) we get

$$\frac{\partial}{\partial \theta}\left[\frac{\bar{h}^3}{12\bar{\mu}}\left[1-\lambda c_r\left[1+\frac{\bar{K}_s \bar{h}}{2}\right]\right]\frac{\partial \bar{p}}{\partial \theta}\right] + \frac{\partial}{\partial \bar{z}}\left[\frac{\bar{h}^3}{12\bar{\mu}}\left[1-\lambda c_r\left[1+\frac{\bar{K}_s \bar{h}}{2}\right]\right]\frac{\partial \bar{p}}{\partial \bar{z}}\right]$$

$$= \frac{1}{2}\frac{\partial \bar{h}}{\partial \theta}\left[1-\frac{\lambda c_r \bar{K}_s \bar{h}}{6}\right]+\dot{\eta}\cos\theta-\varepsilon\dot{\xi}\sin\theta \qquad (2.27)$$

2.2.2 Finite Element Formulation

The flow field in the clearance space of circular bearing and in each lobe of non circular bearing has been descretized into four noded isoparametric elements. The total region has been divided into 14 elements in circumferential direction and 4 elements in axial direction. It has been descretized by decreasing the size of the elements in circumferential direction, so that the steep variation of pressure gradient at the trailing edge of the fluid film is accurately calculated. The element numbering is done in such a way that the bandwidth is a minimum. The descretization of the flow field is given in Fig 2.4.

The Langrangian interpolation function for the four nodded isoperimetric elements are given below.

$N_1 = 0.25\,(1 - \xi)\,(1 - \eta)$

$N_2 = 0.25\,(1 - \xi)\,(1 + \eta)$

$N_3 = 0.25\,(1 + \xi)\,(1 + \eta)$

$N_4 = 0.25\,(1 + \xi)\,(1 - \eta)$

Where ξ and η are the local co-ordinates as shown in Fig. 2.5.

Applying the orthogonality condition of Galerkin's method for Eq(2.27) we have

$$\iint_{\Omega^e}\left\{\frac{\partial}{\partial\theta}\left[\frac{\bar{h}^3}{12\bar{\mu}}\left\{1-\lambda c_r\left(1+\frac{\bar{K}_s\bar{h}}{2}\right)\frac{\partial\bar{p}}{\partial\theta}\right\}+\frac{\partial}{\partial\bar{z}}\frac{\bar{h}^3}{12\bar{\mu}}\left\{1-\lambda c_r\left(1+\frac{\bar{K}_s\bar{h}}{2}\right)\frac{\partial\bar{p}}{\partial\bar{z}}\right\}\right]\right.$$

$$\left.-\frac{\partial}{\partial\theta}\left[\frac{\bar{h}}{2}\left[1-\frac{\lambda c_r\bar{K}_s\bar{h}}{6}\right]\right]-\dot{\eta}\cos\theta+\varepsilon\dot{\xi}\sin\theta\right\}N_i\,d\theta\,d\bar{z}=0 \qquad (2.28)$$

where N_i (i = 1, 2, 3, 4) are the Langrangian interpolation functions. Since $\bar{p} = N_j\bar{p}_j$ and $\bar{h} = N_j\bar{h}_j$ (j = 1, 2, 3, 4).

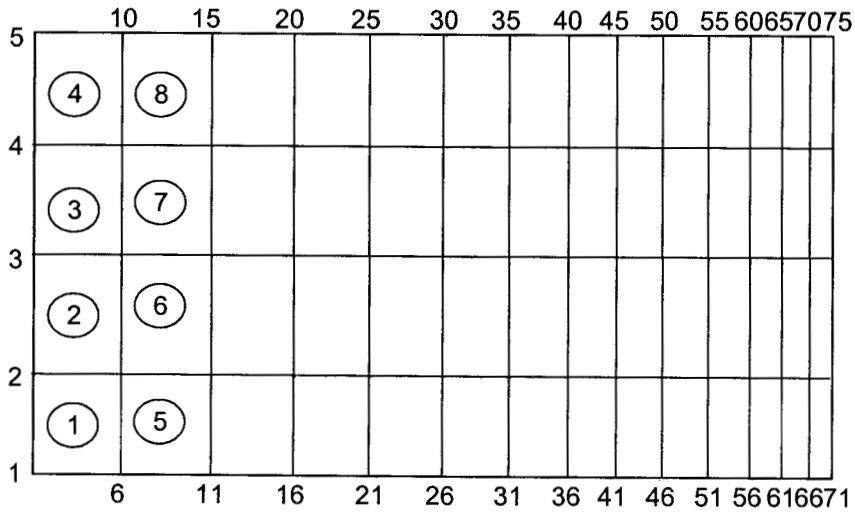

Fig. 2.4 Descretization of Flow Field

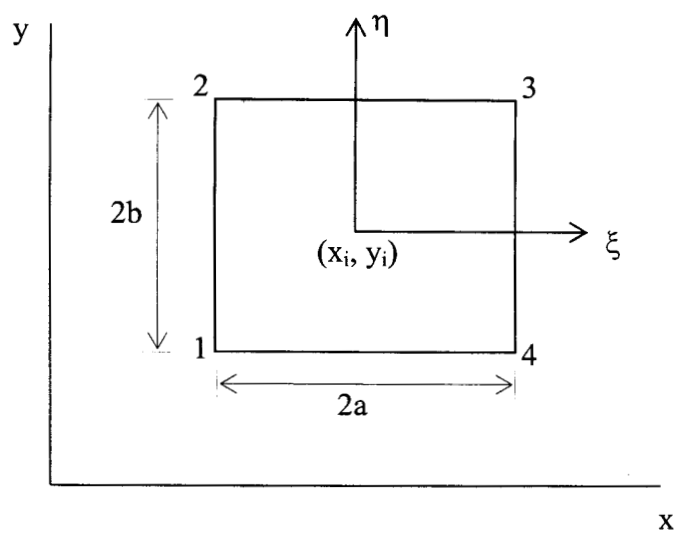

Fig. 2.5 Local Coordinate System

We have on integrating by parts

$$\int_{\Gamma^e} N_i \frac{\bar{h}^3}{12\bar{\mu}}\left\{1-\lambda c_r\left(1+\frac{\bar{K}_s\bar{h}}{2}\right)\frac{\partial \bar{p}}{\partial \theta}\right\}d\bar{z} - \int_{\Gamma^e}\iint\left[\frac{\bar{h}^3}{12\bar{\mu}}\left\{1-\lambda c_r\left(1+\frac{\bar{K}_s\bar{h}}{2}\right)\frac{\partial N_i}{\partial \theta}\frac{\partial \bar{p}}{\partial \theta}d\theta\right\}\right]d\bar{z}$$

$$+\int_{\Gamma^e} N_i \frac{\bar{h}^3}{12\bar{\mu}}\left\{1-\lambda\, c_r\left(1+\frac{\bar{K}_s\bar{h}}{2}\right)\frac{\partial \bar{p}}{\partial \bar{z}}\right\}d\theta - \int_{\Gamma^e}\iint\left[\frac{\bar{h}^3}{12\bar{\mu}}\left\{1-\lambda\, c_r\left(1+\frac{\bar{K}_s\bar{h}}{2}\right)\frac{\partial N_i}{\partial \bar{z}}\frac{\partial \bar{p}}{\partial \bar{z}}d\bar{z}\right\}\right]d\theta$$

$$= \int_{\Gamma^e} N_i \frac{\bar{h}}{2}\frac{1-\lambda c_r\bar{K}_s\bar{h}}{6}d\bar{z} - \iint_{\Omega^e}\left[\frac{\bar{h}}{2}\left(\frac{1-\lambda\, c_r\bar{K}_s\bar{h}}{6}\right)\right]\frac{\partial N_i}{\partial \theta}\; d\theta\, d\bar{z}$$

$$+\dot{\eta}\left[\int_{\Gamma^e} N_i \sin\theta d\bar{z} - \iint_{\Omega^e}\left[\sin\theta.\frac{\partial N_i}{\partial \theta}d\theta\right]d\bar{z}\right]$$

$$+\varepsilon\dot{\xi}\left[\int_{\Gamma^e} N_i \cos\theta d\bar{z} - \iint_{\Omega^e}\left[\cos\theta.\frac{\partial N_i}{\partial \theta}d\theta\right]d\bar{z}\right] \qquad (2.29)$$

Single integral terms can be removed since integration is being carried out over a closed loop.

Simplifying Eq. (2.29) we have

$$\iint_{\Omega^e}\frac{\bar{h}^3}{12\bar{\mu}}\left[1-\lambda c_r\left(1+\frac{\bar{K}_s\bar{h}}{2}\right)\right]\left[\frac{\partial N_i}{\partial \theta}\frac{\partial N_j}{\partial \theta}+\frac{\partial N_i}{\partial \bar{z}}\frac{\partial N_j}{\partial \bar{z}}\right]\bar{p}_j d\theta d\bar{z}$$

$$= \iint_{\Omega^e}\frac{\bar{h}}{2}\frac{\partial N_i}{\partial \theta}\left(1-\frac{\lambda c_r\bar{K}_s\bar{h}}{6}\right)d\theta d\bar{z} - \dot{\eta}\iint_{\Omega^e}\frac{\partial N_i}{\partial \theta}\sin\theta d\theta d\bar{z} - \varepsilon\dot{\xi}\iint\frac{\partial Ni}{\partial \theta}\cos\theta\, d\theta\, d\bar{z} \qquad (2.30)$$

This can be written in matrix form as:

$$[\mathrm{K_f}]^e\ \{\bar{p}\}^e = \{R_1\}^e + \{R_2\ \}^e + \varepsilon\{R_3\ \}^e \qquad (2.31)$$

where $R^e_{1i} = \iint_{\Omega^e}\frac{\partial N_i}{\partial \theta}.\frac{\bar{h}}{2}\left(1-\frac{\lambda c_r\bar{K}_s\bar{h}}{6}\right)d\theta d\bar{z}$

$$R^e_{2i} = -\dot{\eta}\iint_{\Omega^e}\frac{\partial N_i}{\partial \theta}.\sin\theta d\theta d\bar{z} \qquad R^e_{3i} = -\dot{\xi}\iint_{\Omega^e}\frac{\partial N_i}{\partial \theta}.\cos\theta d\theta d\bar{z}$$

and

$$[K_{ij}]^e = \iint_{\Omega^e}\left[\frac{\bar{h}^3}{12\bar{\mu}}1-\lambda c_r\left(1+\frac{\bar{K}_s\bar{h}}{2}\right)\right]\left[\frac{\partial N_i}{\partial \theta}\frac{\partial N_j}{\partial \theta}+\frac{\partial N_i}{\partial \bar{z}}\frac{\partial N_j}{\partial \bar{z}}\right]\bar{p}_j d\theta\, d\bar{z}$$

$[K_{ij}]^e$ is the element stiffness matrix. Ω^e refers to domain of the eth element and Γ^e refers to the boundary of the e^{th} element.

Numerical integration is carried out by using Gauss quadrature formula.

In the case of multilobe bearing, each of the lobes can be treated as a partial bearing with an active film from the leading edge tot the trailing edge.

where $\frac{\partial p}{\partial \theta} = 0$

Then Eq. (2.28) becomes

$$\iint_{\Omega^e}\left\{\frac{\partial}{\partial\theta}\left[\frac{h^{-3}}{12\bar{\mu}}\left\{1-\lambda c_r\left(1+\frac{\bar{K}_s\bar{h}}{2}\right)\frac{\partial\bar{p}}{\partial\theta}\right\}+\frac{\partial}{\partial\bar{z}}\frac{h^{-3}}{12\bar{\mu}}\left\{1-\lambda c_r\left(1+\frac{\bar{K}_s\bar{h}}{2}\right)\frac{\partial\bar{p}}{\partial\bar{z}}\right\}\right]\right.$$

$$\left.-\frac{\partial}{\partial\theta}\left[\frac{\bar{h}}{2}\left[1-\frac{\lambda c_r\bar{K}_s\bar{h}}{6}\right]\right]-\dot{\eta}\cos(\theta+\beta)+\varepsilon\dot{\xi}\sin(\theta+\beta)\right\}N_i\,d\theta d\bar{z}=0 \qquad (2.32)$$

where β locates the leading edge of each lobe.

The film variation up to trailing edge of each lobe in non-circular bearing is given by.

$\bar{h} = 1 + \varepsilon_1 \cos(\theta + \beta_1)$ for first lobe

$\bar{h} = 1 + \varepsilon_2 \cos(\theta + \beta_2)$ for second lobe

$\bar{h} = 1 + \varepsilon_3 \cos(\theta + \beta_3)$ for third lobe

2.2.3 Global System Equations

The element fluidity matrices are assembled to get global matrices. The final global equation for the entire flow field can be written as

$$[K_f]\,[\bar{p}] = \{R_1\} + \{R_2\} + \{R_3\} \qquad (2.33)$$

2.2.4 Boundary Conditions

The boundary conditions for each lobe may be given by

$$\bar{p}(\theta,\bar{z}) = 0 \quad \text{at } \theta = 0, \theta_2^i$$

$$\bar{p}(\theta,\bar{z}) = 0 \quad \text{at } \bar{z} = \pm 1 \qquad (2.34)$$

$$\frac{\partial p}{\partial\theta}(\theta,\bar{z}) = 0 \text{ at } \theta = \theta_2^i$$

where θ_2^i is the unknown extent of positive pressure fluid for the i^{th} lobe.

Solution of Eq. (2.33) after applying boundary conditions (2.34) gives nodal pressures and nodal flows

2.3 ELASTO HYDRODYNAMIC ANALYSIS

2.3.1 General

The bearing liner is a finite length cylinder subjected to hydrodynamic loading due to the fluid film pressure on its internal surfaces. The distribution of the fluid film pressure is such that it causes the bush to deform in all directions, i.e., radial, axial and circumferential. It is however seen that the bush in a journal bearing is usually enclosed in a housing which is comparatively rigid.

2.3.2 Finite Element Formulation

The bearing liner is discretized by 8 nodded hexagonal isoparametric elements. In the case of circular bearing, the bearing liner is discretized into 64 elements (16 elements in the circumferential direction and 4 elements in the axial direction) (Fig. 2.6), in the case of two lobe journal bearing into112 elements (28 elements in the circumferential direction and four elements in the axial direction) (Fig 2.7) and in the case of three lobe journal bearing into144 elements (36 in the circumferential direction and four elements in the axial direction) (Fig 2.8). The displacement components are considered to vary linearly in the elements. Using the elasticity theory the expression for the potential energy of an element when bearing is subjected only to traction forces, T_{tr} is given by

$$\pi^e = 1/2 \iiint [\delta]^{eT} [J]^{eT} [D]^e [J]^e [\delta]^e \ \mathrm{r d\theta\ dr\ dz}$$

$$- \iint [T_{tr}]^e [\delta]^e \ \mathrm{r d\theta\ dz} \qquad (2.35)$$

The displacement δ for the bearing liner is

$$(\delta) = \begin{bmatrix} V_\theta(r,\theta,z) \\ V_r(r,\theta,z) \\ V_z(r,\theta,z) \end{bmatrix}$$

The element equation can be obtained by minimizing the potential energy over each element.

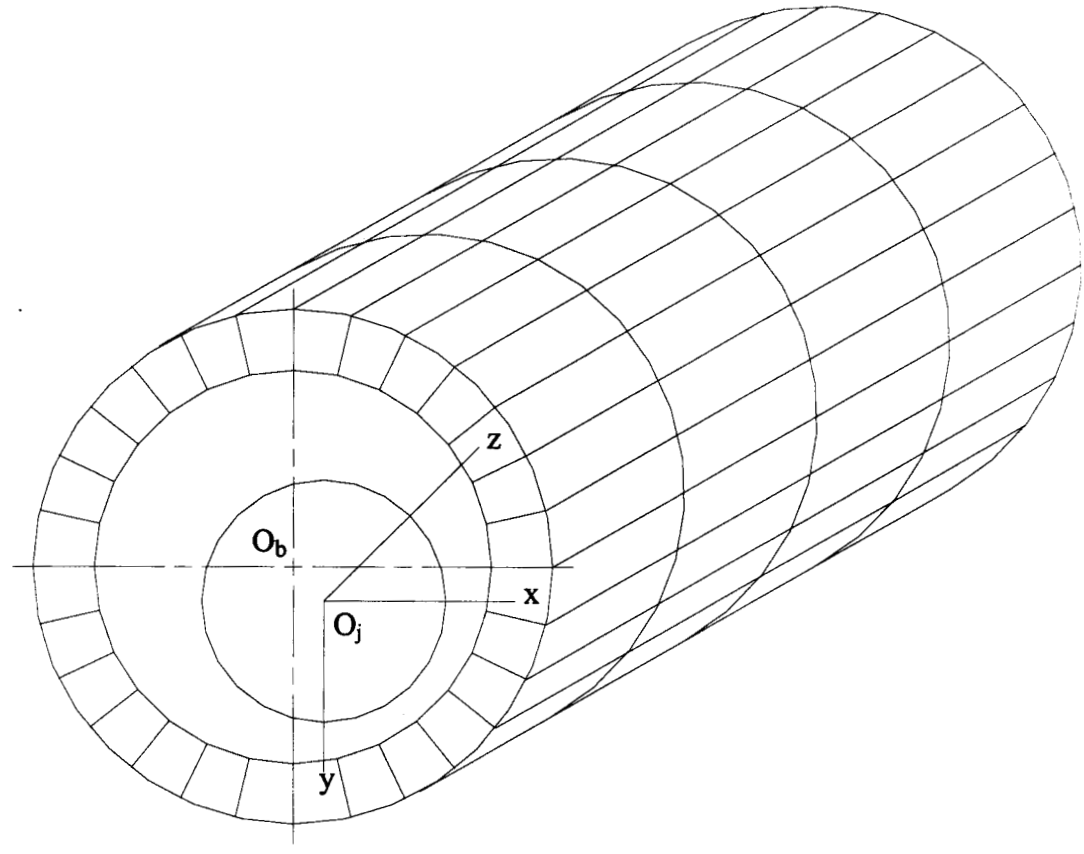

Fig. 2.6 Discretization of Circular Bearing

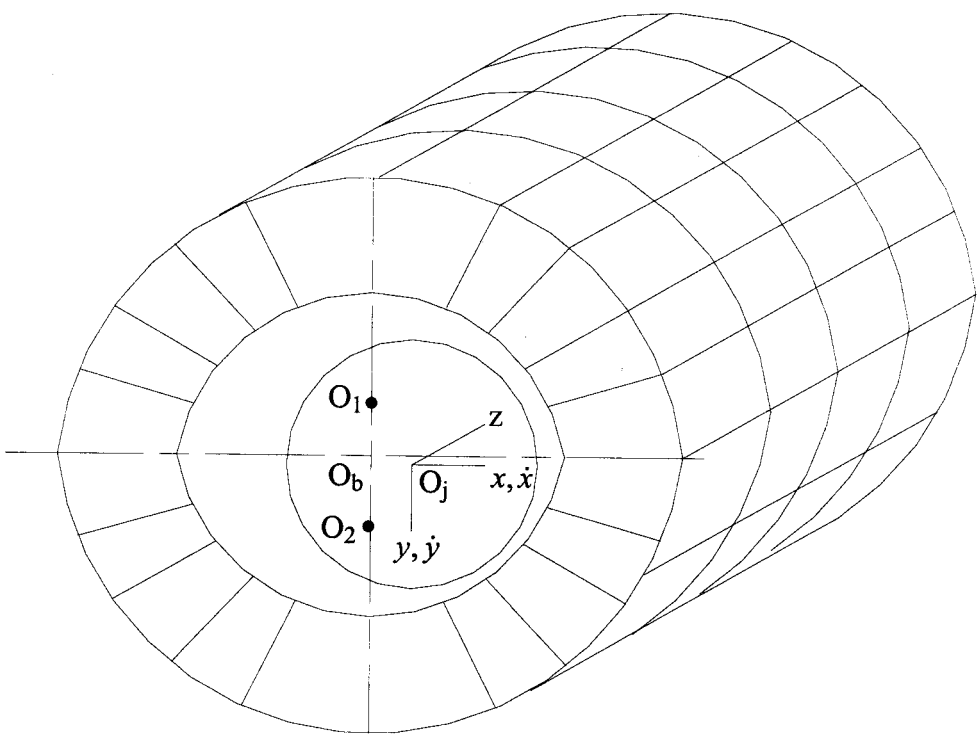

Fig. 2.7 Discretization of Two Lobe Bearing

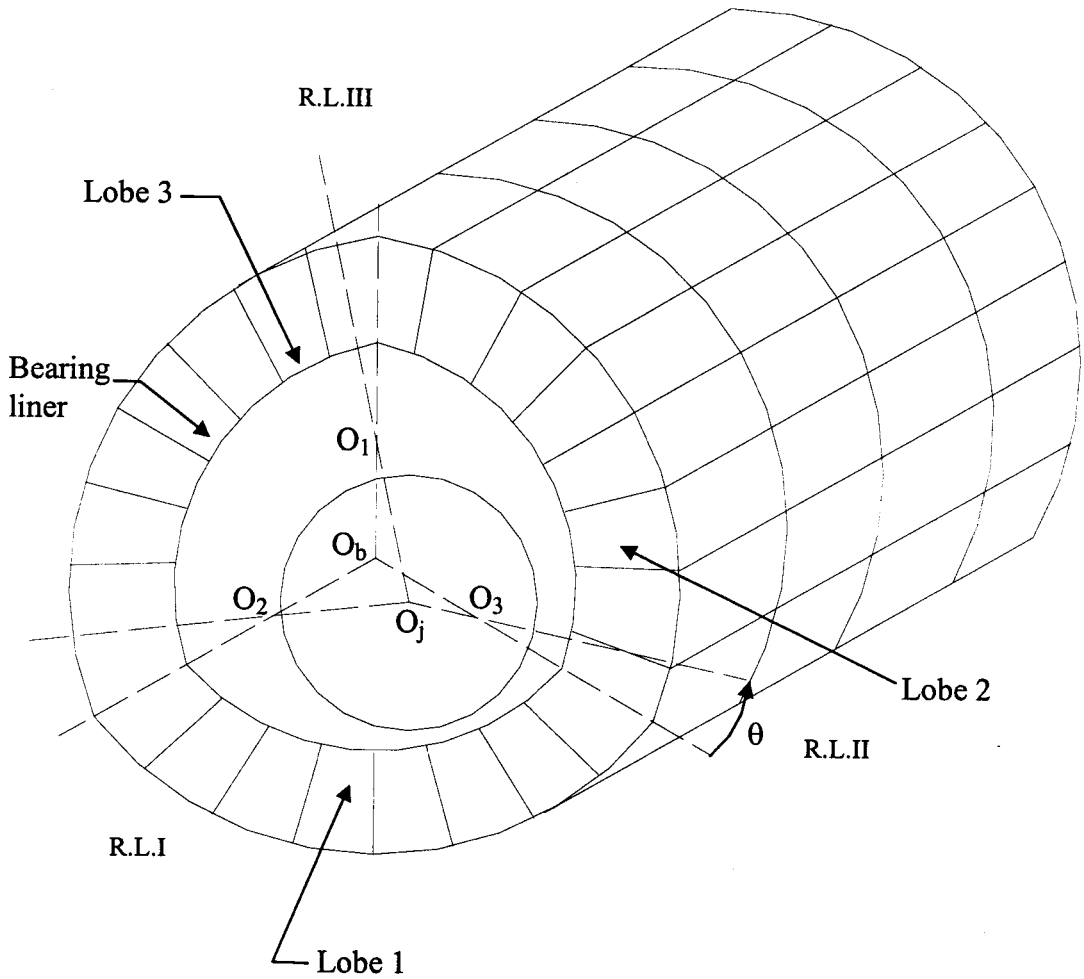

Fig. 2.8 Discretization of Three Lobe Bearing

The displacement field $[\delta]^e$ in e^{th} element can be written as

$$[\delta]^e = \begin{bmatrix} V_\theta \\ V_r \\ V_z \end{bmatrix} = [N]^e [\bar{d}]^e \tag{2.36}$$

where $[N]^e$ represent the element shape function matrix.

$$V_\theta = \sum_{i=1}^{m} V_{\theta i} \bar{N}_i, \quad V_r = \sum_{i=1}^{m} V_{ri} \bar{N}_i, \quad V_z = \sum_{i=1}^{m} V_{zi} N_i$$

and

$$[d]^e = [V_{\theta 1}, V_{r1}, V_{z1}, \ldots\ldots\ldots\ldots V_{\theta m}, V_{rm}, V_{zm}]^T \tag{2.37}$$

where m is the number of nodes per element.

Since in the equilibrium position, potential energy of the system is minimum, we have

i.e.,
$$\sum_{e=1}^{n_e} \begin{Bmatrix} \frac{\partial \pi^e}{\partial V_{\theta i}} \\ \frac{\partial \pi^e}{\partial V_{ri}} \\ \frac{\partial \pi^e}{\partial V_{zi}} \end{Bmatrix} = 0 \tag{2.38}$$

where e = 1, 2, ... n_e and i =1, ..., m

n_e = number of elements

Using the above condition, system equations are reduced to

$$\sum_{e=1}^{n_e} \left[\iiint [J]^{eT} [D]^e [J]^e \, r d\theta \, dr \, dz - \iint [N][T_{tr}]^e \, r d\theta \, dz \right] = 0 \tag{2.39}$$

where

$$[J]^e = \begin{bmatrix} \frac{1}{r}\left[\frac{\partial}{\partial\theta}\right] & \frac{1}{r} & 0 \\ 0 & \frac{\partial}{\partial r} & 0 \\ 0 & 0 & \frac{\partial}{\partial z} \\ \frac{\partial}{\partial r} & \frac{1}{r}\left[\frac{\partial}{\partial\theta}\right] & 0 \\ \frac{\partial}{\partial r} & 0 & \frac{1}{r}\left[\frac{\partial}{\partial\theta}\right] \\ 0 & \frac{\partial}{\partial z} & \frac{\partial}{\partial r} \end{bmatrix}$$

$$[D] = \begin{bmatrix} D_2 & D_2 & D_1 & 0 & 0 & 0 \\ D_1 & D_2 & D_2 & 0 & 0 & 0 \\ D_2 & D_1 & D_2 & 0 & 0 & 0 \\ 0 & 0 & 0 & D_2 & 0 & 0 \\ 0 & 0 & 0 & 0 & D_3 & 0 \\ 0 & 0 & 0 & 0 & 0 & D_3 \end{bmatrix}$$

and

$$D_1 = E(1-\gamma)(1+\gamma)(1-2\gamma)$$

$$D_2 = E\gamma/(1+\gamma)(1-2\gamma)$$

$$D_3 = E/2\ (1+\gamma)$$

the above element equation may be written in the matrix form as

$$[K]^e\ [d]^e = [F]^e \tag{2.40}$$

where $[K]^e$ is the element stiffness matrix and is given by

$$[K]^e = \iiint [J]^{eT}[D]^e[J]^e\ r\,d\theta\,dr\,dz \tag{2.41}$$

$$[F]^e = \iiint [N]^{eT}[T_{tr}]^e\ r\,d\theta\,dz \tag{2.42}$$

$$[T_{tr}]^e = [0\ [T_{tr}]^e\ 0] \tag{2.43}$$

By non dimensionalising, using

$r = \bar{r}t_h, z = t_h\bar{z}, [D] = E[\bar{D}], d = C[\bar{d}]$ and $p = \mu\varpi_j(R_j/C)^2\bar{p}$ and by using the general assembly procedure, the following global system equations are obtained

$$[K][\bar{d}] = \bar{\psi}[\bar{F}] \tag{2.44}$$

where

$$\bar{\psi} = \frac{\mu_0\varpi_j(R_j/C)^3}{E}\frac{t_h}{R_j}$$

[K] Stiffness Matrix

[d] Displacement Matrix

[F] Force matrix

2.3.3 Boundary Conditions for The Deformations

Here it is assumed that the bearing liner is contained in a comparatively rigid housing. So the outer surface of the housing does not deform, implying that the nodes in contact with the rigid surface are restrained from moving.

Hence

$$\begin{Bmatrix} \bar{V}_{\theta i} \\ \bar{V}_{ri} \\ \bar{V}_{zi} \end{Bmatrix} = \{0\} \tag{2.45}$$

where 'i' is the number of nodes on the bearing liner of rigid housing interface.

2.3.4 Modification of Film Thickness

For the flexible journal bearing system, the non-dimensional fluid film thickness is expressed as

$$\bar{h} = 1 + \varepsilon\cos\theta + \bar{V}_r \tag{2.46}$$

where $\bar{V}_r$ is the non-dimensional deformation of the bearing bush in the radial direction.

PERFORMANCE CHARACTERISTICS

Sukumaran Nair V.P. "Analysis of elastohydrodynamic circular and non-circular journal bearings with micropolar lubricants" Thesis. Department of Mechanical Engineering , NIT Calicut, University of Calicut, 2004

Chapter 3

PERFORMANCE CHARACTERISTICS

3.1 GENERAL

The static and dynamic performance characteristics of both rigid and flexible bearings are calculated from the computed nodal pressures. The expressions for static and dynamic performance characteristics are derived as the functions of the nodal pressures, and the shape functions. The static characteristics include the load capacity, attitude angle, power loss and end leakage. The dynamic performance characteristics are studied in terms of fluid film stiffness and damping coefficients, threshold speed and damped frequency of whirl. The expressions for the static and dynamic performance characteristics of journal bearings are given in the following sections. Using the linearized equations of disturbed motion of the journal centre and Routh's criteria, the expressions for the critical mass and the threshold speed are derived.

3.2 FLUID FILM REACTIONS

For a general dynamic situation, the hydrodynamic pressure 'p' depends on the journal bearing spin velocity and the velocity components $(\dot{\xi},\dot{\eta})$. The components of fluid film reactions (forces and moments) along ξ and η directions are given by the following relations.

$$W_{\xi} = \int_{0}^{\theta r} \int_{-1}^{1} p\cos\theta \; r d\theta \, dz \tag{3.1}$$

$$W_{\eta} = \int_{0}^{\theta r} \int_{-1}^{1} p\sin\theta \; r d\theta \, dz \tag{3.2}$$

3.3 LOAD CAPACITY AND ATTITUDE ANGLE

The fluid film reaction components along and perpendicular to the line of centers for an element in the bearing lobe are determined by integrating the components of pressure force.

$$\overline{W}_{\xi}^{e} = \iint \overline{p}^{e} \cos\theta \, \bar{r} d\theta \, d\bar{z} \tag{3.3}$$

$$\overline{W}_{\xi}^{e} = \iint \overline{p}^{e} \sin\theta \, \bar{r} d\theta \, d\bar{z} \tag{3.4}$$

These reactive forces are recalculated along x and y axes for each element in each lobe. The total fluid film reaction components along x and y axes for each lobe of the non-circular bearing are obtained by summing the contributions of all the elements of the flow field on the bearing lobe.

$$\overline{W}_{XL} = \sum_{e=1}^{n_e} \overline{W}_{X}^{e} \qquad \overline{W}_{YL} = \sum_{e=1}^{n_e} \overline{W}_{Y}^{e} \tag{3.5}$$

where n_e is the number of the elements and L represents the L^{th} lobe. From the above fluid film reaction components, load components of the multi-lobe journal bearing can be obtained as:

$$\overline{W}_{X} = \sum_{L=1}^{n_L} \overline{W}_{XL} \quad \text{and} \quad \overline{W}_{Y} = \sum_{L=1}^{n_L} \overline{W}_{YL}$$

where n_L represents the number of the lobes of the journal bearing.

$$\overline{W} = \left[\overline{W}_{x}^{2} + \overline{W}_{Y}^{2}\right]^{1/2} \tag{3.6}$$

The angle between the line of the centers and the load line is known as attitude angle and is given by

$$\phi = \tan^{-1} \frac{W_Y}{W_X} \tag{3.7}$$

Attitude angle is an important parameter. Although it is considered as a static characteristic, it has implications on the stability of the bearing system.

3.4 BEARING OIL FLOW

Using the nodal velocity components obtained from the solution vector of the flow-field equations, the end leakage for each bearing is computed from the following relation.

$$Q_Z^L = \int_{\bar{R}}^{\bar{R}+\bar{h}} \int_{0}^{\theta_r} W_{Z=-1} r \, d\theta \, dr + \int_{\bar{R}}^{\bar{R}+\bar{h}} \int_{0}^{\theta_r} W_{Z=+1} r \, d\theta \, dr \tag{3.8}$$

In the case of bearings, end leakage is kept small so that only small amount of lubricant need be supplied. But when thermal effects are significant, a

large end leakage is desirable to take away heat generated due to viscous dissipation.

3.5 FRICTIONAL FORCE

Frictional power loss for each lobe of the nearing is obtained by the following expression

$$\overline{F} = \iint \overline{\mu}\left[\frac{1}{\overline{h}} + \frac{\overline{h}}{2}\frac{\partial \overline{p}}{\partial \theta}\right]\overline{r}\,d\theta\,d\overline{z} \tag{3.9}$$

It is important to keep power loss a minimum.

Friction parameter is defined by the following relation.

$$\bar{f} = \frac{\overline{F}}{\overline{W}}$$

3.6 FLUID FILM STIFFNESS COEFFICIENTS

The non-dimensional fluid film stiffness coefficients are defined as

$$\begin{bmatrix} \overline{S}_{XX} & \overline{S}_{XY} \\ \overline{S}_{YX} & \overline{S}_{YY} \end{bmatrix} = -\begin{bmatrix} \dfrac{\partial \overline{W}_X}{\partial \overline{x}} & \dfrac{\partial \overline{W}_X}{\partial \overline{y}} \\ \dfrac{\partial \overline{W}_Y}{\partial \overline{x}} & \dfrac{\partial \overline{W}_Y}{\partial \overline{y}} \end{bmatrix} \tag{3.10}$$

where $\overline{W}_X$ and $\overline{W}_Y$ the film force components in the x and y directions respectively.

The first subscript of the stiffness coefficient denotes the direction of force and the second, the direction of displacement. The resultant stiffness coefficients for non-circular bearings will be obtained by adding the contribution of all lobes.

3.7 FLUID FILM DAMPING COEFFICIENTS

The damping coefficients are defined as

$$\begin{bmatrix} \overline{B}_{XX} & \overline{B}_{XY} \\ \overline{B}_{YX} & \overline{B}_{YY} \end{bmatrix} = -\begin{bmatrix} \dfrac{\partial \overline{W}_x}{\partial \dot{\overline{x}}} & \dfrac{\partial \overline{W}_x}{\partial \dot{\overline{y}}} \\ \dfrac{\partial \overline{W}_y}{\partial \dot{\overline{x}}} & \dfrac{\partial \overline{W}_y}{\partial \dot{\overline{y}}} \end{bmatrix} \tag{3.11}$$

where $\dot{\bar{x}}$ and $\dot{\bar{y}}$ are the journal centre velocities in x and y directions respectively. The first subscript of the damping coefficients denotes the direction of force and the second, the direction of velocity.

The resultant damping coefficients will be obtained by adding the contributions of each lobe.

3.8 EQUATION MOTION

The equations of disturbed motion of the journal can be expressed as

$$[\bar{M}]\,[\ddot{\bar{s}}] = \{\nabla \bar{F}(\bar{s},\dot{\bar{s}})\} \tag{3.12}$$

where $[\bar{M}]$ is a diagonal mass matrix and $\{\nabla \bar{F}(\bar{s},\dot{\bar{s}})\}$ represents the out of balance hydrodynamic film force components which depend on the instantaneous position and velocity of the journal centre. These force components are usually non-linear functions of $\{\bar{s}\}$ and $\{\dot{\bar{s}}\}$. However, within a small neighbourhood of the equilibrium position of the journal, the fluid film force components may be assumed to be linear functions of the components of vectors $\{\bar{s}\}$ and $\{\dot{\bar{s}}\}$. Equation (3.14) can be written as

$$[\bar{M}]\,[\ddot{\bar{s}}] + [B][\dot{\bar{s}}] + [S][\bar{s}] = 0 \tag{3.13}$$

$$\begin{bmatrix} \bar{M}_j & 0 \\ 0 & \bar{M}_j \end{bmatrix} \begin{bmatrix} \ddot{\bar{x}} \\ \ddot{\bar{y}} \end{bmatrix} + \begin{bmatrix} \bar{B}_{XX} & \bar{B}_{XY} \\ \bar{B}_{YX} & \bar{B}_{YY} \end{bmatrix} \begin{bmatrix} \dot{\bar{x}} \\ \dot{\bar{y}} \end{bmatrix} + \begin{bmatrix} \bar{S}_{XX} & \bar{S}_{XY} \\ \bar{S}_{YX} & \bar{S}_{YY} \end{bmatrix} \begin{bmatrix} \bar{x} \\ \bar{y} \end{bmatrix} = 0$$

The characteristic equation of the linearized equation of lateral motion is written in the following form.

$$\bar{\sigma}^4 + \bar{A}_1\bar{\sigma}^3 + \bar{A}_2\bar{\sigma}^2 + \bar{A}_3\bar{\sigma} + \bar{A}_4 = 0 \tag{3.14}$$

where $\bar{\sigma}$ of a complex variable and A_i (i = 1,.....4) are functions of the journal mass $\bar{M}_j$ and the dynamic coefficients. The real part of the roots of the characteristic equation indicates damping in the system and the imaginary part the frequency of oscillations of the journal.

$$\bar{A}_1 = \frac{1}{\bar{M}_j}(\bar{B}_{xy} + \bar{B}_{yy}) \tag{3.15}$$

$$\bar{A}_2 = \frac{1}{\bar{M}_j}\left\{\bar{B}_{xy}\bar{B}_{yy} + \bar{M}_j(\bar{S}_{xx} + \bar{S}_{yy}) - \bar{B}_{xy}\bar{B}_{yx}\right\} \tag{3.16}$$

$$\bar{A}_3 = \frac{1}{\bar{M}_j^2}\left\{\bar{S}_{yy}\bar{B}_{xx} + \bar{B}_{yy}\bar{S}_{xx} - (\bar{B}_{yx}\bar{S}_{xy} + \bar{S}_{yx}\bar{B}_{xy})\right\} \tag{3.17}$$

$$\bar{A}_4 = \frac{1}{\bar{M}_j^2}(\bar{S}_{xx}\bar{S}_{yy} - \bar{S}_{yx}\bar{S}_{xy}) \tag{3.18}$$

From Routh's criteria, the necessary and the sufficient conditions for the linearized system to be stable are

$$\bar{A}_i \geq 0 \qquad (\text{i} = 1,.....4) \tag{3.19}$$

$$\bar{A}_1\bar{A}_2 - \bar{A}_2 \geq 0 \tag{3.20}$$

$$\bar{A}_1\bar{A}_2\bar{A}_3 - \bar{A}_3^2 - \bar{A}_1^2\bar{A}_4 => 0 \tag{3.21}$$

By satisfying these conditions, equations (3.19-3.21) the stability margin in terms of critical mass is obtained

3.9 THRESHOLD SPEED

The journal speed at which the journal bearing system become unstable is given by

$$\bar{\omega}_{th} = \frac{\bar{M}_c}{\bar{W}} \tag{3.22}$$

3.10 THE DAMPED FREQUENCY OF WHIRL

The damped frequency of whirl id defined by the following expression

$$\bar{\omega}_d = \frac{(\bar{S}_{xx} - \bar{K}_l)(\bar{S}_{yy} - \bar{K}_l) - \bar{S}_{xy}\bar{S}_{yx}}{\bar{B}_{xx}\bar{B}_{yy} - \bar{B}_{xy}\bar{B}_{yx}} \tag{3.23}$$

where

$$\bar{K}_l = \frac{\bar{S}_{xx}\bar{B}_{yy} + \bar{S}_{yy}\bar{B}_{xx} - \bar{S}_{xy}\bar{B}_{yx} - \bar{S}_{yx}\bar{B}_{xy}}{\bar{S}_{xx} + \bar{B}_{yy}}$$

A negative of ω_d implies an absence of whirl.

SOLUTION PROCEDURE

Sukumaran Nair V.P. "Analysis of elastohydrodynamic circular and non-circular journal bearings with micropolar lubricants" Thesis. Department of Mechanical Engineering , NIT Calicut, University of Calicut, 2004

Chapter 4

SOLUTION PROCEDURE

4.1 GENERAL

The solution procedure to be adopted for determining the static and dynamic performance characteristics of elastohydrodynamic circular and noncircular bearing problems with Newtonian and micropolar lubricants is presented in the chapter. The procedure comprises the coupled solution of

1) The two dimensional modified Reynold's equation
2) The three dimensional elasticity equation to obtain the displacement field.

The simultaneous solutions of all these equations have to be obtained by using finite element method and a direct iterative procedure. Additional iterations are required to establish the Reynold's boundary conditions at the trailing edge of fluid film in circular bearing and each lobe of the non-circular bearing and to establish the equilibrium journal centre for the vertical load support in the case of non circular bearings.

4.2 SOLUTION SCHEME

The solution scheme used for solving elastohydrodynamic lubrication involves the determination of various quantities. The flow charts for determining these quantities with various iterative segments and convergence criteria are presented here.

4.2.1 Solution of Nodal Pressures

The Reynold's equation representing the flow field in the clearance space of the journal bearing is solved to obtain the pressure and velocity components in the flow field.

After discretizing the flow field as explained in Chapter 2 the element fluidity matrix is formed for each element. The boundary conditions are applied at the element equation stage and the element fluidity matrices are assembled to form the global fluidity matrix. The global system of equations (2.33) thus

formed are solved to get nodal pressure components. The flow chart of the scheme for obtaining nodal pressures is given in Fig 4.1.

4.2.2 Computation of Reynold's Boundary

Reynold's boundary condition is established based on that the pressure gradient $\frac{\partial p}{\partial \theta} = 0$ at the boundary ($\theta = \theta_r$) of positive pressure fluid film.

Initially a value of θ_r is assumed for the film extent. The pressure gradient $\left(\frac{\partial p}{\partial \theta}\right)$ at its trailing edge is computed and depending on whether the pressure gradient is negative or positive, a respectively positive or negative correction on the first trial value of θ_r is made. The pressure gradient at the trailing edge is calculated again for the modified value of the film extent. In subsequent iterations, the new trial value θ_r is selected by linear interpolation or extrapolation using the two closest values from the previous iterations. The iteration is terminated when the magnitude of the pressure gradient becomes smaller than an arbitrarily assigned small value, 0.01.

In noncircular bearings, for a given journal centre position (ε, ϕ), each lobe has its own positive pressure fluid film, the extent of which has to be determined. For circular and noncircular flexible bearings, the film extent of deformable bearing at any eccentricity ratio, is obtained using the same iterative procedure starting with the value of θ_r for the corresponding rigid bearing, as the first trial value. The flow diagram for determining Reynold's boundary is shown in Fig. 4.2.

4.2.3 Determination of Attitude Angle for Non-Circular Bearings

In the case of non circular bearings, the direction of load when specified with reference to the lobe geometry, requires a unique unknown attitude angle. The attitude angle for a given operating eccentricity is determined by using the iteration scheme described below.

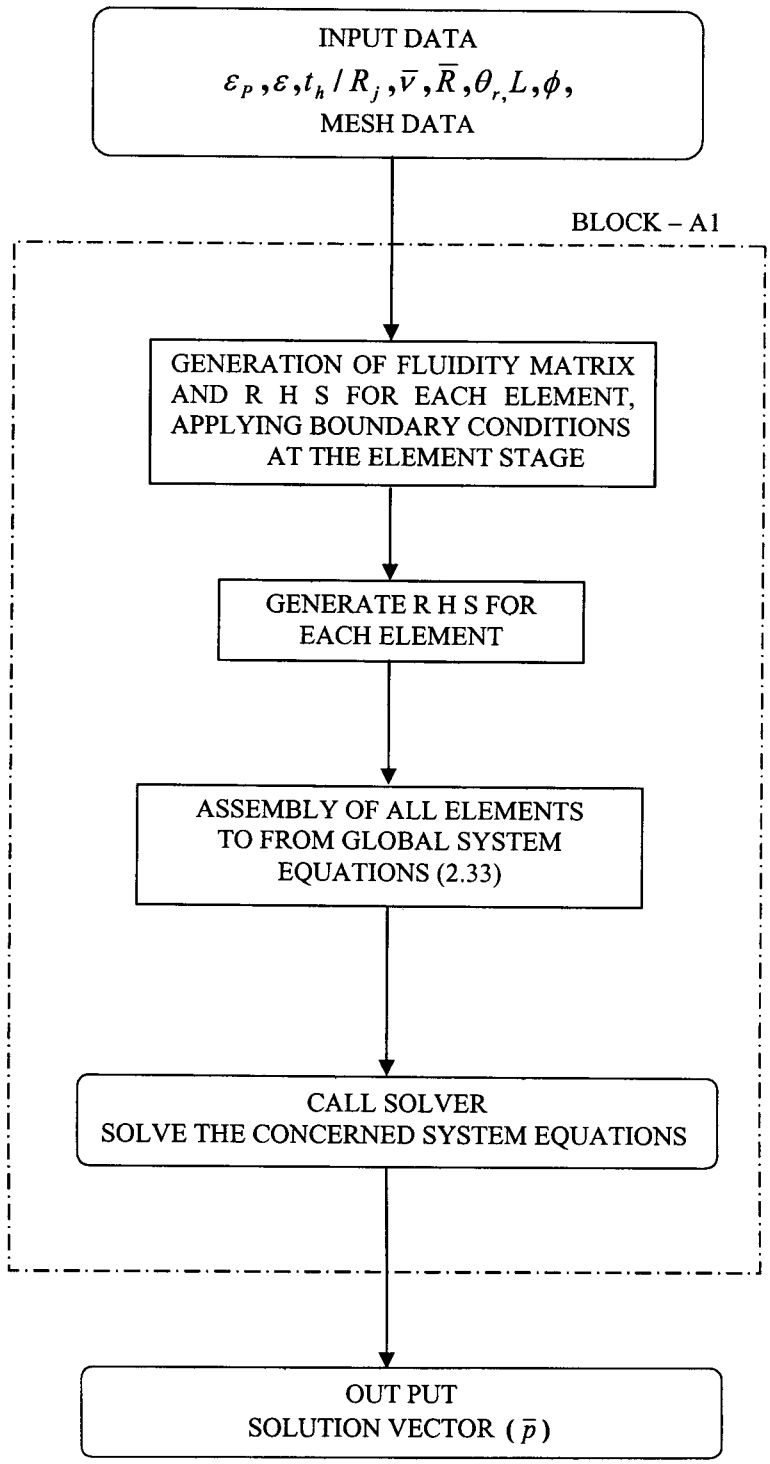

Fig. 4.1 Flow Diagram for Determining Nodal Pressure

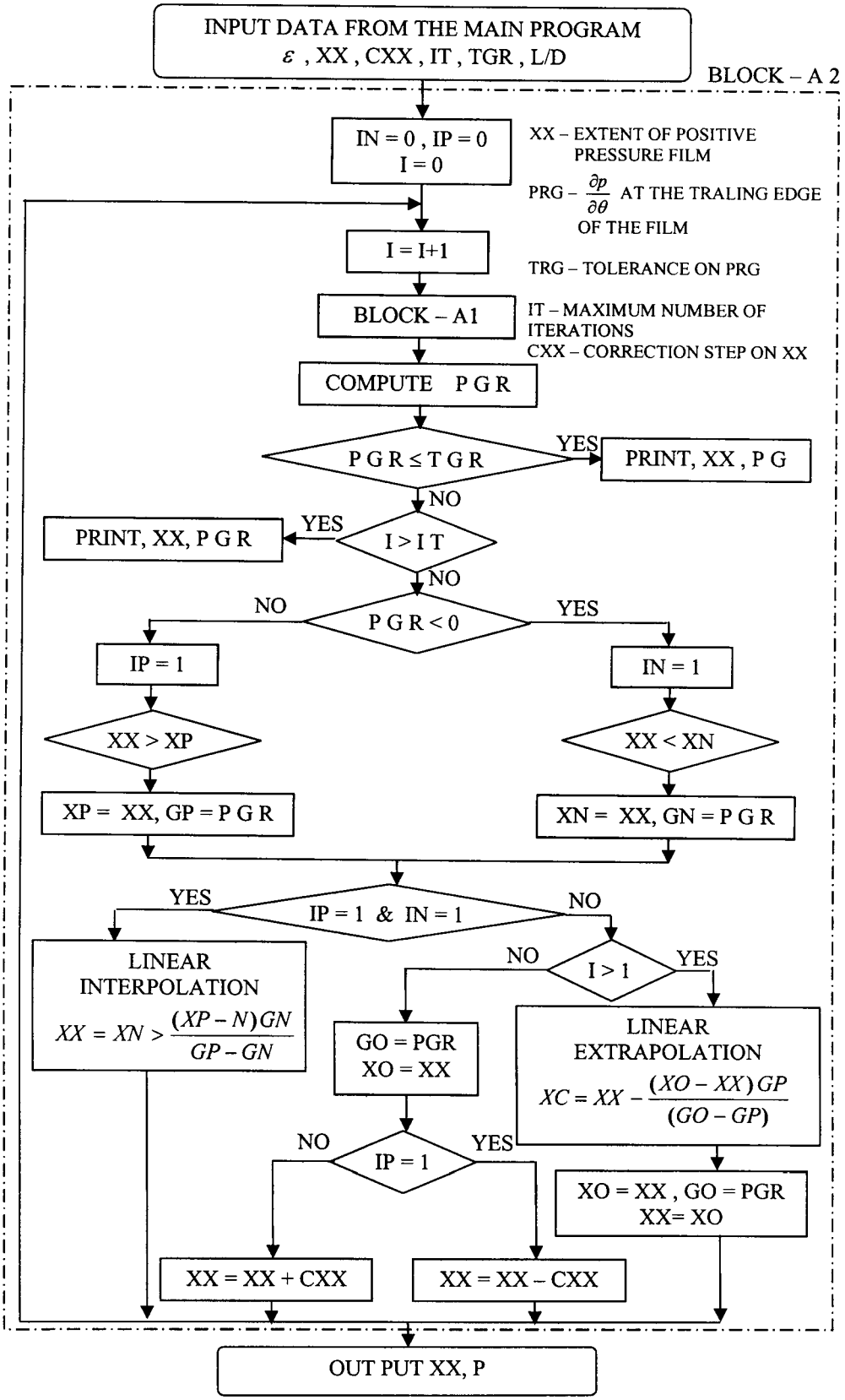

Fig. 4.2 Flow Diagram for Reynolds Boundary

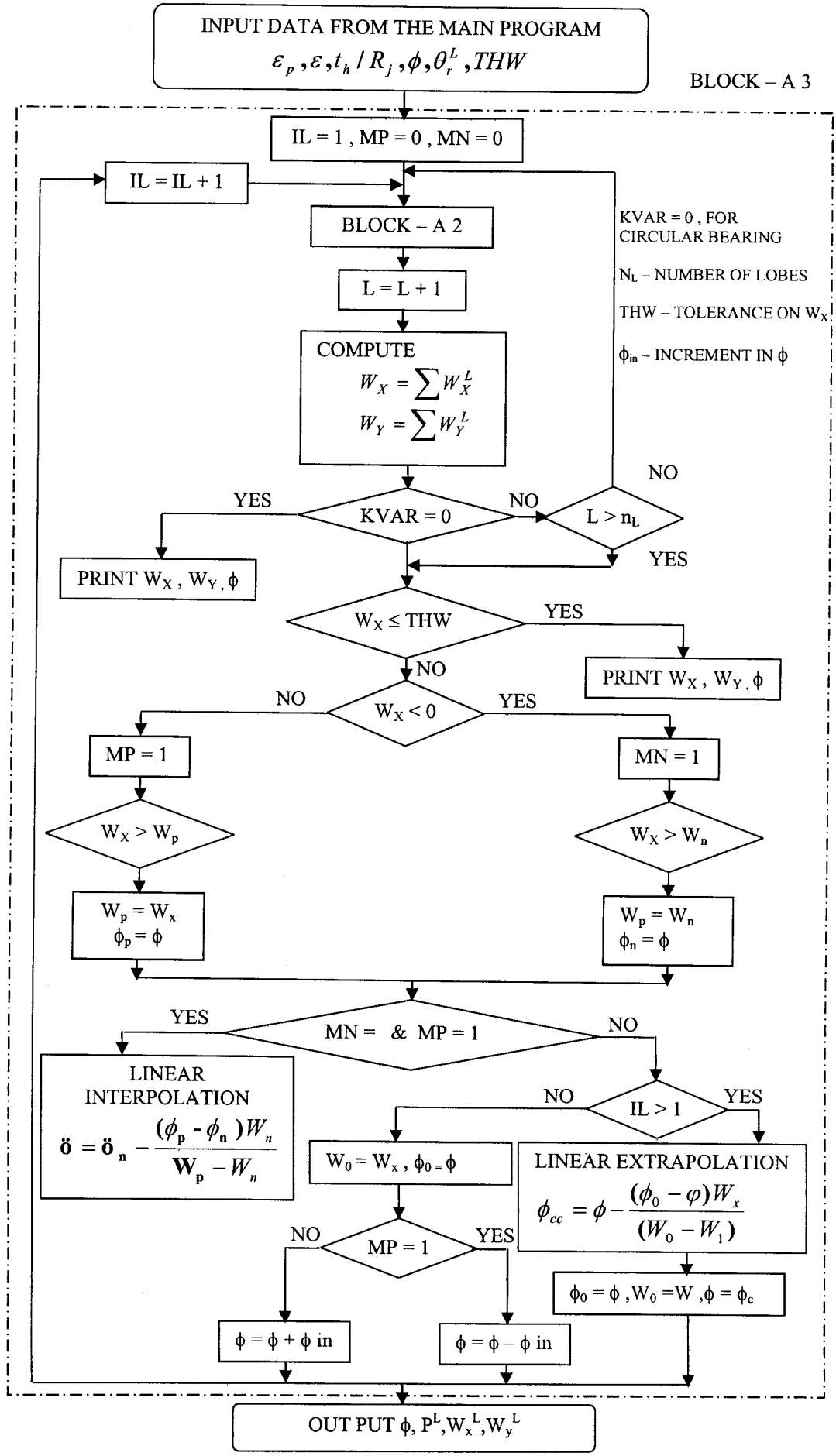

Fig.4.3 Flow Diagram for Attitude Angle for Non-Circular Bearings

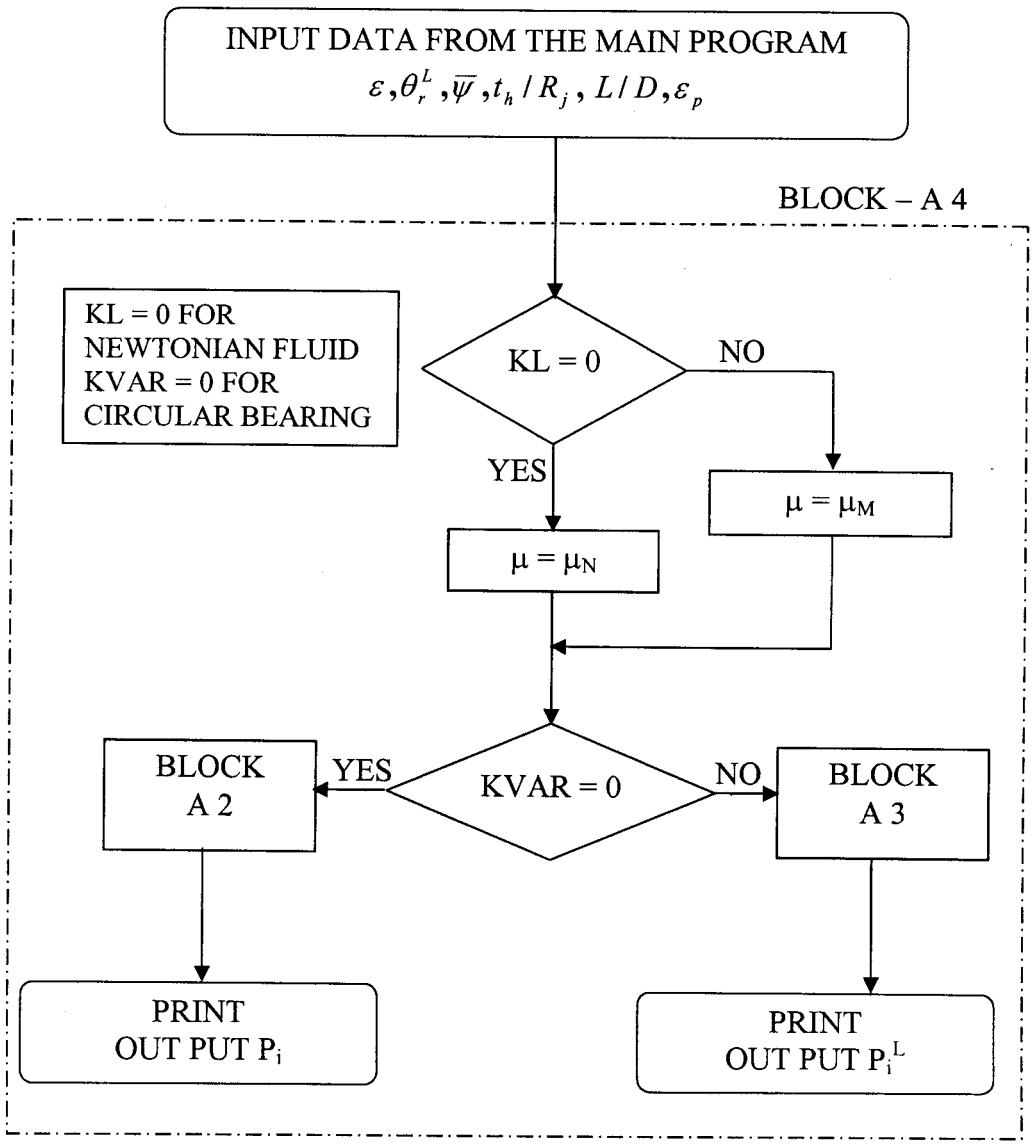

Fig. 4.4 Flow Diagram for Determining Nodal Pressure for Circular and Noncircular Bearing with Newtonian and Micropolar Lubricants

First a trial value of ϕ is chosen for which the horizontal component of load capacity is obtained from Eq. (3.5) for each lobe of a bearing with given eccentricity ratio ε. Depending on whether the horizontal component of the load capacity is positive or negative, a respective positive or negative correction is made in the first trial value of ϕ. For the corrected value of ϕ, the component of load is again calculated. The next value of ϕ is obtained using linear interpolation or extrapolation considering the two closest values of ϕ obtained from the previous iterations. These iteration are terminated when the horizontal component of the load carrying capacity achieves a value less than a pre assigned arbitrarily small value (0.01).

For flexible noncircular bearings, the attitude angle is computed using the procedure explained above after modifying the film thickness by taking into account the elastic deformation of the bearing liner in the radial direction. The flow diagram for determining attitude angle is given in Fig 4.3.

4.2.4 Computation of Nodal Pressures for Circular and non Circular Bearings with Newtonian and Micropolar Lubricants

The flow diagram for calculating the nodal pressures for circular and noncircular bearing with Newtonian and micropolar lubricants is given in Fig 4.4. The viscosity for micropolar fluid is determined from Eq. (1.1) in the case of computing nodal pressures for bearing with micropolar fluids.

4.2.5 Computation of Nodal Displacements

For computing nodal displacements, the stiffness matrix for each element is generated by the Subroutine STIFF, using Eq. (2.41). The right hand side of Eq. (2.40) is formed in the subroutine LOAD for each element using the nodal pressures obtained from the solution of lubricant flow-field. The global system equations are then obtained by assembling the stiffness matrices and RHS (Subroutine FRONT). The global stiffness matrix and column vector of the nodal forces are also modified by the subroutine FRONT, for the specified boundary conditions and the global system equations are solved to obtain nodal

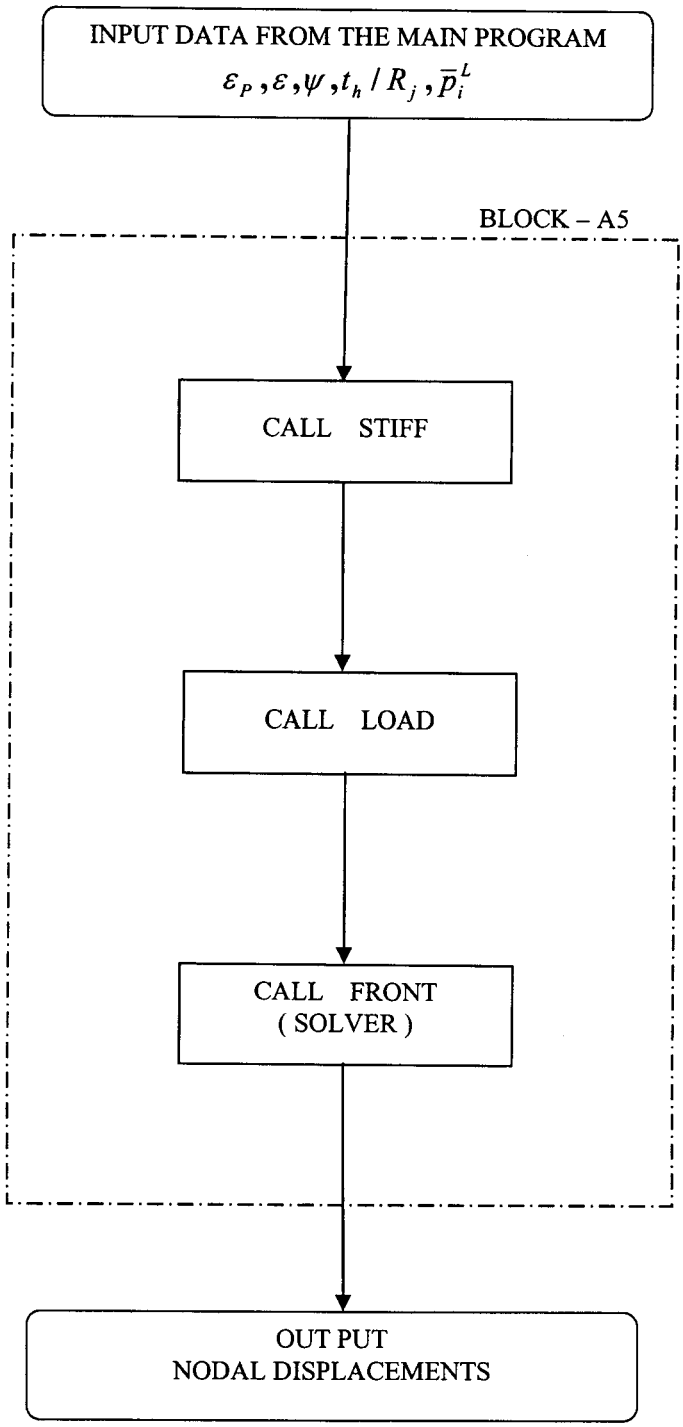

Fig. 4.5 Flow Diagram for Determination of Nodal Displacements

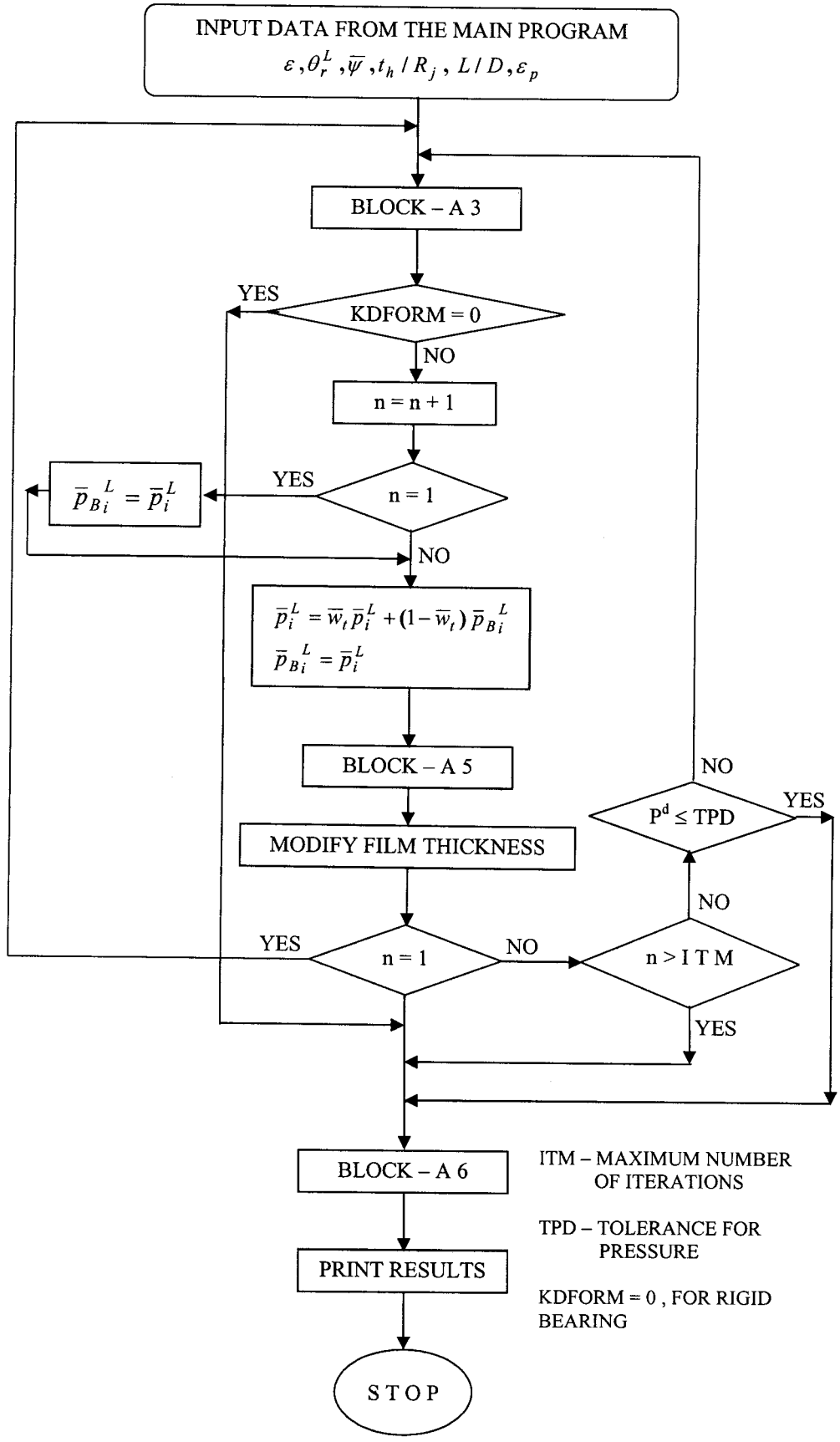

Fig. 4.6 Solution Scheme for Journal Bearings with Newtonian and Micropolar Lubricants

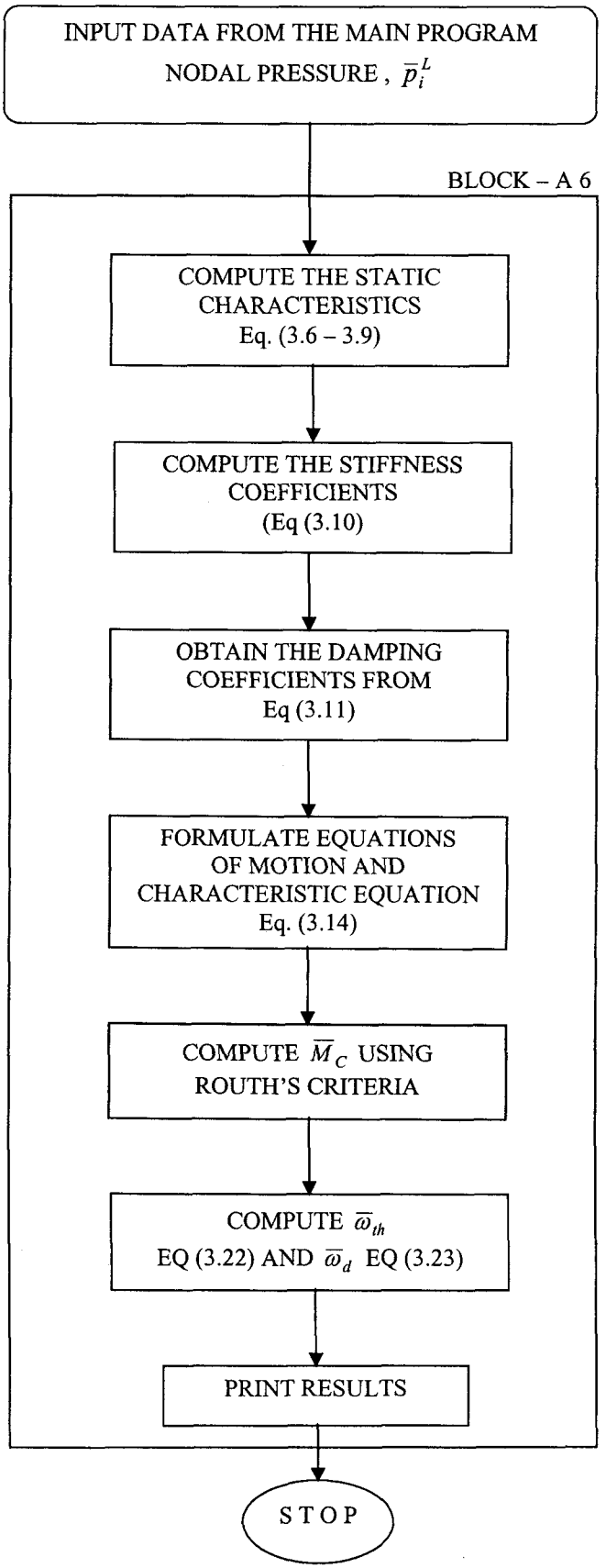

Fig. 4.7 Flow Diagram for Computing the Journal Performance Characteristics

displacements ($\bar{v}_\theta, \bar{v}_r$ and $\bar{v}_z$) by the same subroutine. The flow diagram for determination of nodal displacements is given in Fig. 4.5.

4.2.6 Results for Journal Bearings with Newtonian and Micropolar Lubricants

Fig 4.6 shows the solution scheme for obtaining the results of circular and noncircular journal bearings taking the bearing liner deformation in to account. The iterative scheme for EHD analysis of flexible circular and noncircular bearings involve the following steps, (i) assuming the bearing to be rigid, the film extent in the circular bearing or in each lobe of the non circular bearing and the nodal pressures are computed as the first trail value for EHD iteration, and (ii) considering the bearing liner to be flexible with a deformation coefficient, $\overline{\psi}$, and using the nodal pressures calculated in step (i), the nodal displacements are determined. Using these nodal displacements, the film thickness is modified. The pressure distribution is then recomputed for the modified film geometry. Iterations are repeated by solving the governing equations of flow and elastic fields till convergence is satisfied.

4.2.7 Performance Characteristics

The performance characteristics of the bearing are calculated from the computed pressures. The static characteristics in terms of load capacity, attitude angle, end leakage and frictional force are obtained from equations given in Chapter 3.

The stiffness coefficients are determined using Eq. (3.10). A linear perturbation method considering the perturbations of the journal centre in the radial and circumferential directions are considered to evaluate the stiffness coefficients.

For determining the damping coefficients using Eq. (3.11), the fluid force components in ξ and η directions are calculated separately for the cases $\dot{\xi} = 0, \dot{\eta} = 0$ by giving values of $\dot{\xi}$ and $\dot{\eta}$.

Threshold speed and damped frequency of whirl are obtained, using the stiffness and the damping coefficients and Routh's criteria from expressions given in Chapter 3. The flow chart for computing the bearing performance characteristics is given in Fig 4.7.

4.3 REMARKS

A large number of iterations were required to obtain the pressure and elastic fields at higher eccentricity ratios and large values of deformation coefficients. The iterations required for the solution were considerably reduced when the weighted averages of nodal pressures were used to calculate the effective nodal pressures.

RESULT DISCUSSIONS AND CONCLUSIONS

Sukumaran Nair V.P. "Analysis of elastohydrodynamic circular and non-circular journal bearings with micropolar lubricants" Thesis. Department of Mechanical Engineering , NIT Calicut, University of Calicut, 2004

Chapter 5

RESULT DISCUSSIONS AND CONCLUSIONS

This chapter contains the results obtained from the analysis used to compute the performance characteristics of bearings and discussions there on. The static characteristics in terms of load carrying capacity, end leakage, attitude angle and frictional force and dynamic characteristics in terms of stiffness coefficients, damping coefficients, threshold speed and damped frequency of whirl are computed for rigid and flexible circular and non circular (two lobe and three lobe) journal bearings for the following cases.

(i) Newtonian lubricant

(ii) Micropolar lubricant.

The modification in fluid film thickness due to bearing deformation and consequently in the pressure distribution depends on the bearing geometric and operating parameters and the elastic properties of the material of the bearing liner. In the present study, a non dimensional deformation coefficient ($\overline{\psi}$), which is a measure of the flexibility of bearing liner, is defined in terms of parameters μ_0, ω_j, R_j, C, E and t_h. The effects of these parameters on the performance characteristics of circular and non circular journal bearings are studied for Newtonian and micropolar lubricants.

In the first part of this chapter the static and dynamic performance characteristics are presented for rigid ($\overline{\psi} = 0$) and deformable circular bearings lubricated with (i) Newtonian fluid and (ii) Micropolar fluid. The various performance characteristics for rigid and deformable two lobe bearings operating with Newtonian and micropolar lubricants are presented in the second part. The results obtained from the analysis of rigid and flexible three lobe bearings lubricated with Newtonian and micropolar fluids are discussed in the final part of this chapter.

Table 5.1 shows the summary of the cases studied. In all the cases of bearings studied, the aspect ratio (L/D) is taken as unity, ratio of bearing liner thickness to journal bearing radius $\left(\frac{t_h}{R_j}\right)$ is taken as 0.1 and the ratio of journal radius to the radial clearance $\left(\frac{R_j}{C}\right)$ is taken as 625. In the case of non circular bearings ellipticity is taken as 0.5.

To provide a physical feel of the results obtained, a set of dimensional values of bearing performance characteristics are calculated using the following geometry and operating conditions. These values are presented for rigid ($\overline{\psi} = 0$) and flexible bearings.

Bearing geometry and operating conditions.

Journal radius, R_j = 25 mm

Speed, N = 2500 rpm

Viscosity of the lubricant, μ_0 = 0.04 Pa.s

Table 5.2 shows different materials and their deformation coefficients.

The following sections contain the results of (and discussion on) the static and dynamic characteristics obtained for circular and noncircular rigid and flexible bearings operating with Newtonian and micropolar lubricants.

5.1 CIRCULAR BEARINGS

The static and dynamic characteristics are obtained for rigid and deformable circular bearings considering lubricant as (1) Newtonian and (2) micropolar and in both cases the results are obtained for different values of eccentricity ratios and deformation coefficients.

5.1.1 Circular Rigid Bearings

The effect of volume concentration of additives (λ_{Cr}) and mass transfer rate (K_s) on the performance characteristics of rigid circular journal bearings are presented in Figs. 5.1-5.14. To authenticate the solution algorithm and computer program developed the results obtained in the case of circular bearing are

compared with published results [99] in Fig.5.1. It is seen that the results are in full agreement with the published results.

Fig. 5.1 shows the variation of load carrying capacity with respect to the volume concentration of additives for circular bearings. It is observed that load carrying capacity increases with increase in volume concentration of additives, mass transfer rate and eccentricity ratio. The increase in volume concentration of additives (λ_{Cr}) increases the viscosity of the lubricant and in turn increases the load carrying capacity. When the mass transfer rate of additives (K_s) increases, the load carrying capacity increases for any value of volume concentration of additives and eccentricity ratio.

The change of end leakage with increase in volume concentration of additives is shown in Fig. 5.2. From this Figure it is observed that end leakage increases with increase in volume concentration of additives and mass transfer rate. It is also observed that end leakage does not depend on the volume concentration of additives when mass transfer rate is zero. This can be explained as follows. When the volume concentration of additives increases, viscosity of lubricant and pressure increase. Increase in lubricant viscosity reduces end leakage, but increase in pressure will increase the end leakage. The combined effect may produce the end leakage to be almost constant at any value of volume concentration of additives when there is no mass transfer. When there is mass transfer (K_s), the end leakage increases at any value of volume concentration of additives and eccentricity ratio.

The variation of attitude angle with volume concentration of additives is shown in Fig. 5.3. From this Figure it is seen that the attitude angle decreases with increase in eccentricity ratio for any value of volume concentration of additives; but at any value of eccentricity ratio, attitude angle increases with increase in λ_{Cr}. It may also be noted that at low values of eccentricity ratio ($\varepsilon = 0.2$) and volume concentration of additives, increase in mass transfer rate may not produce significant change in attitude angle.

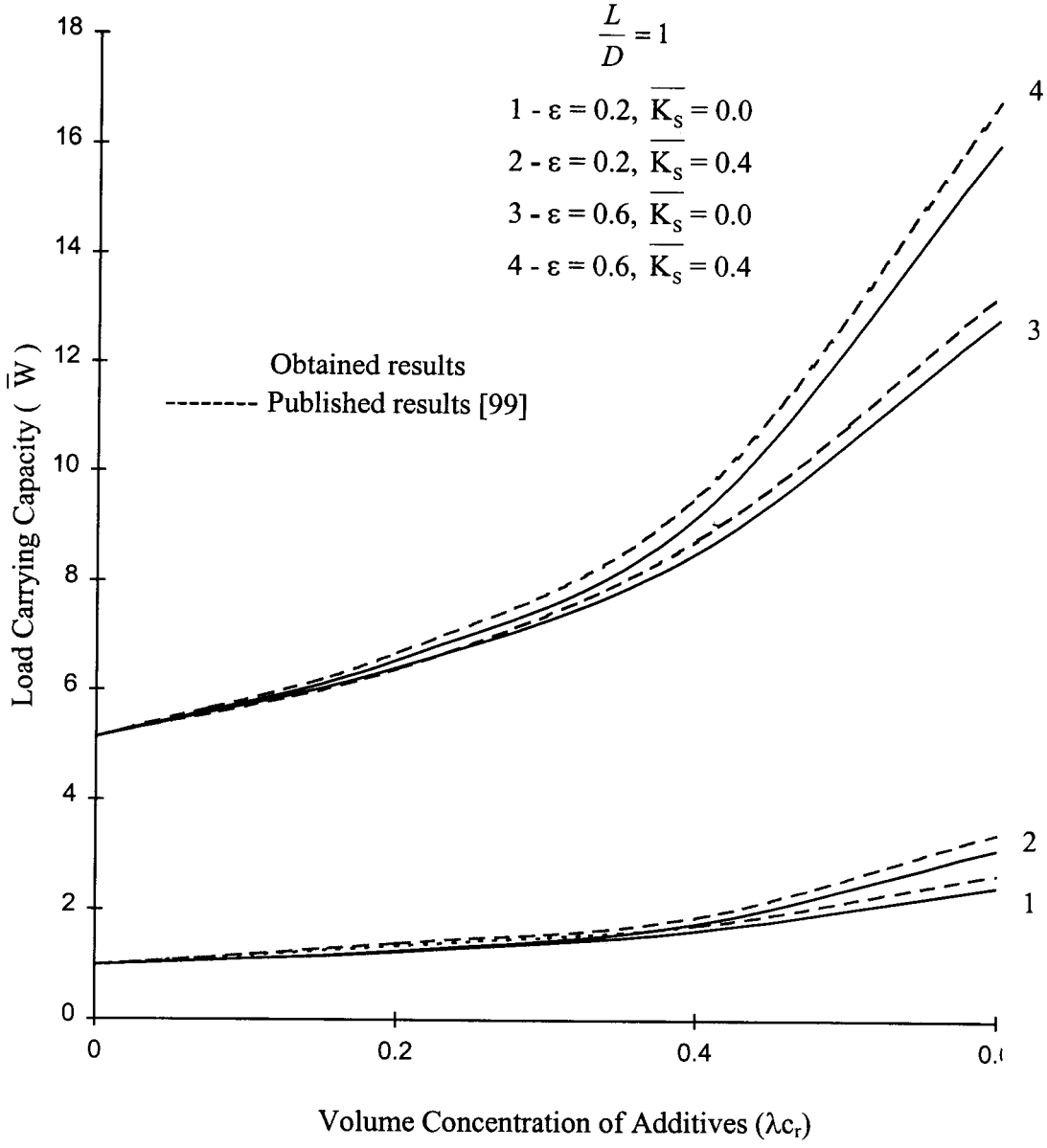

Fig. 5.1 - Load carrying Capacity ($\bar{W}$) vs Volume Concentration of Additives (λc_r) in Circular Bearing

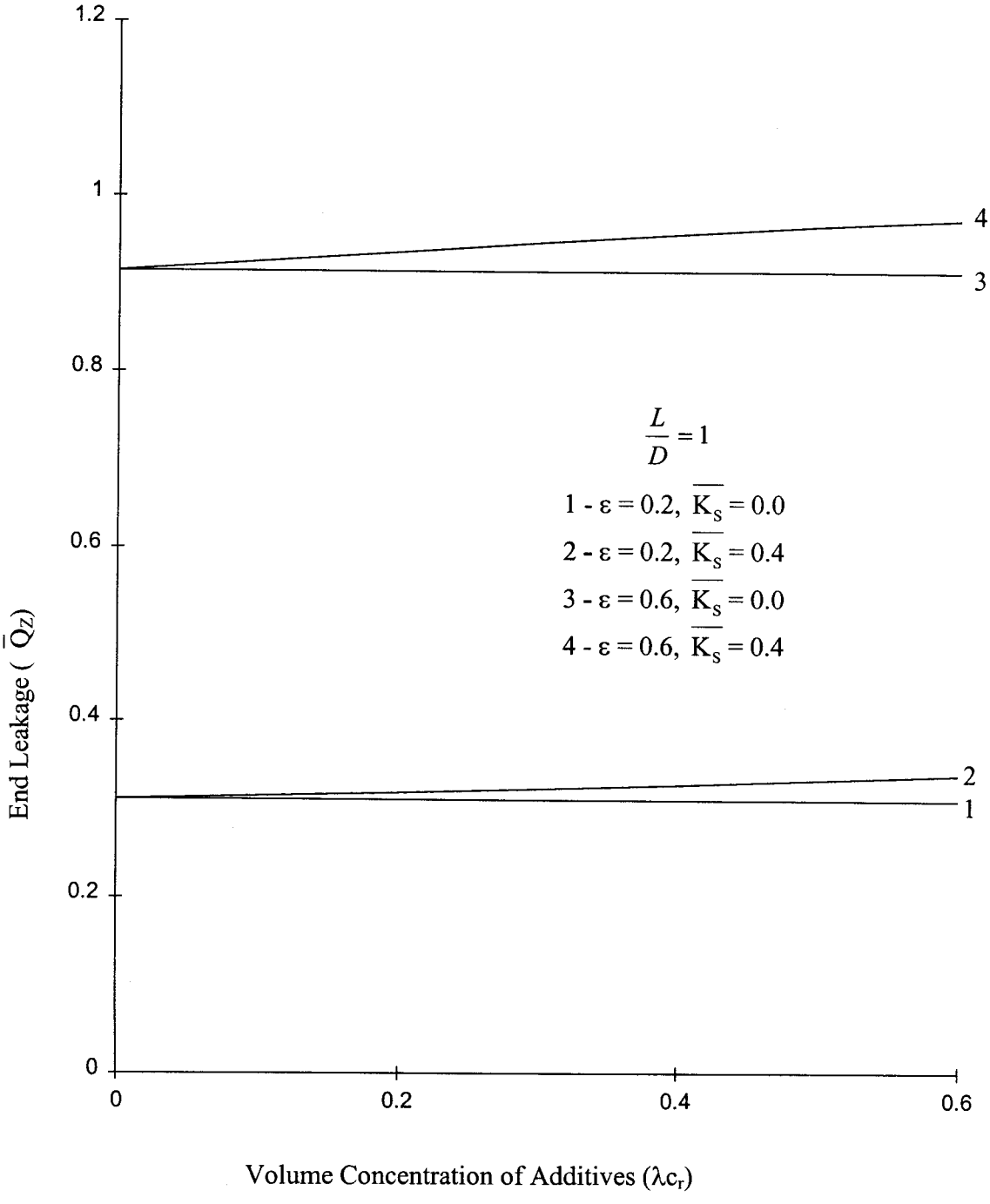

Fig. 5.2 – End Leakage ($\bar{Q}_z$) vs Volume Concentration of Additives (λc_r) in Circular Bearing

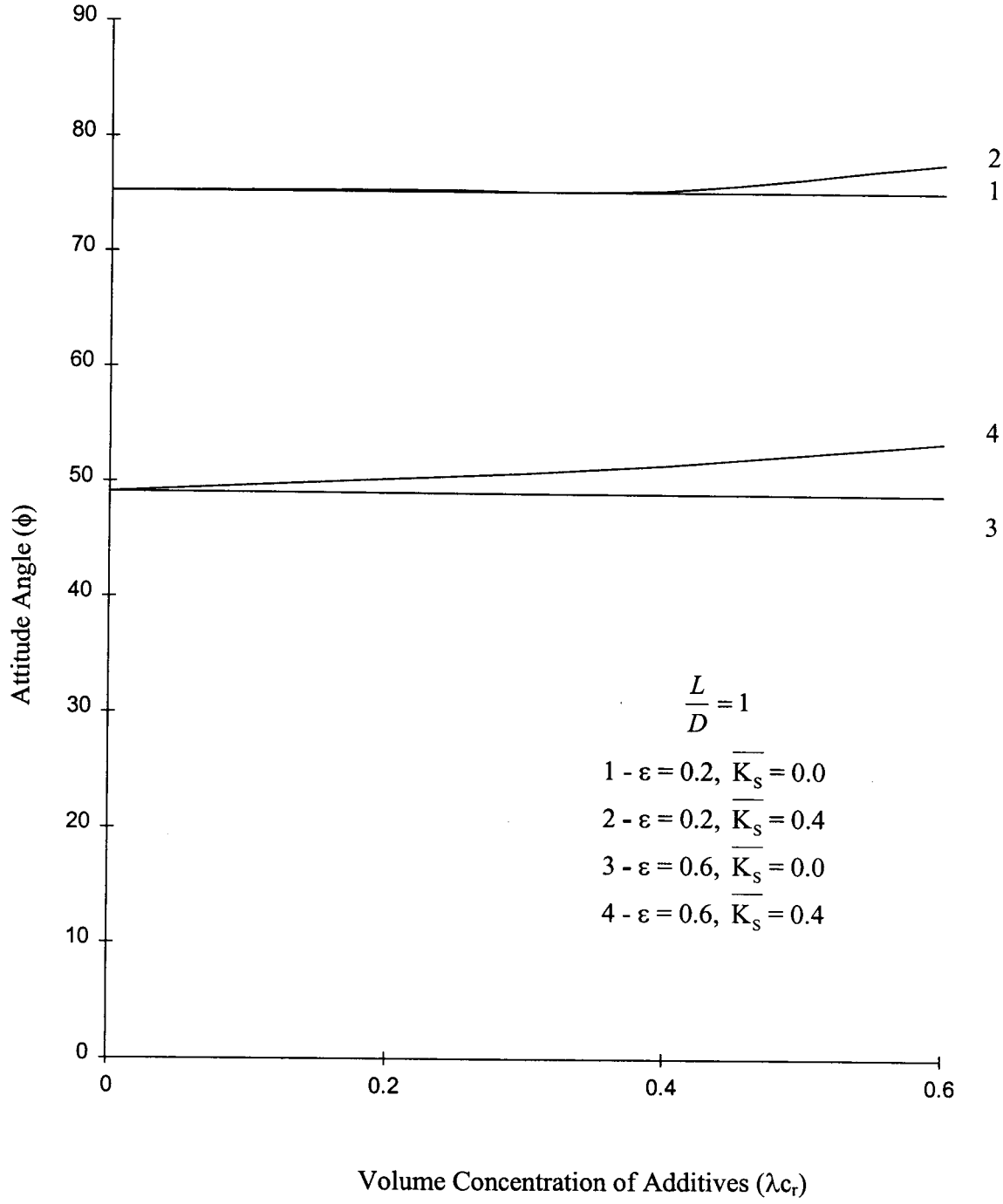

Fig. 5.3 – Attitude Angle (ϕ) vs Volume Concentration of Additives (λc_r) in Circular Bearing

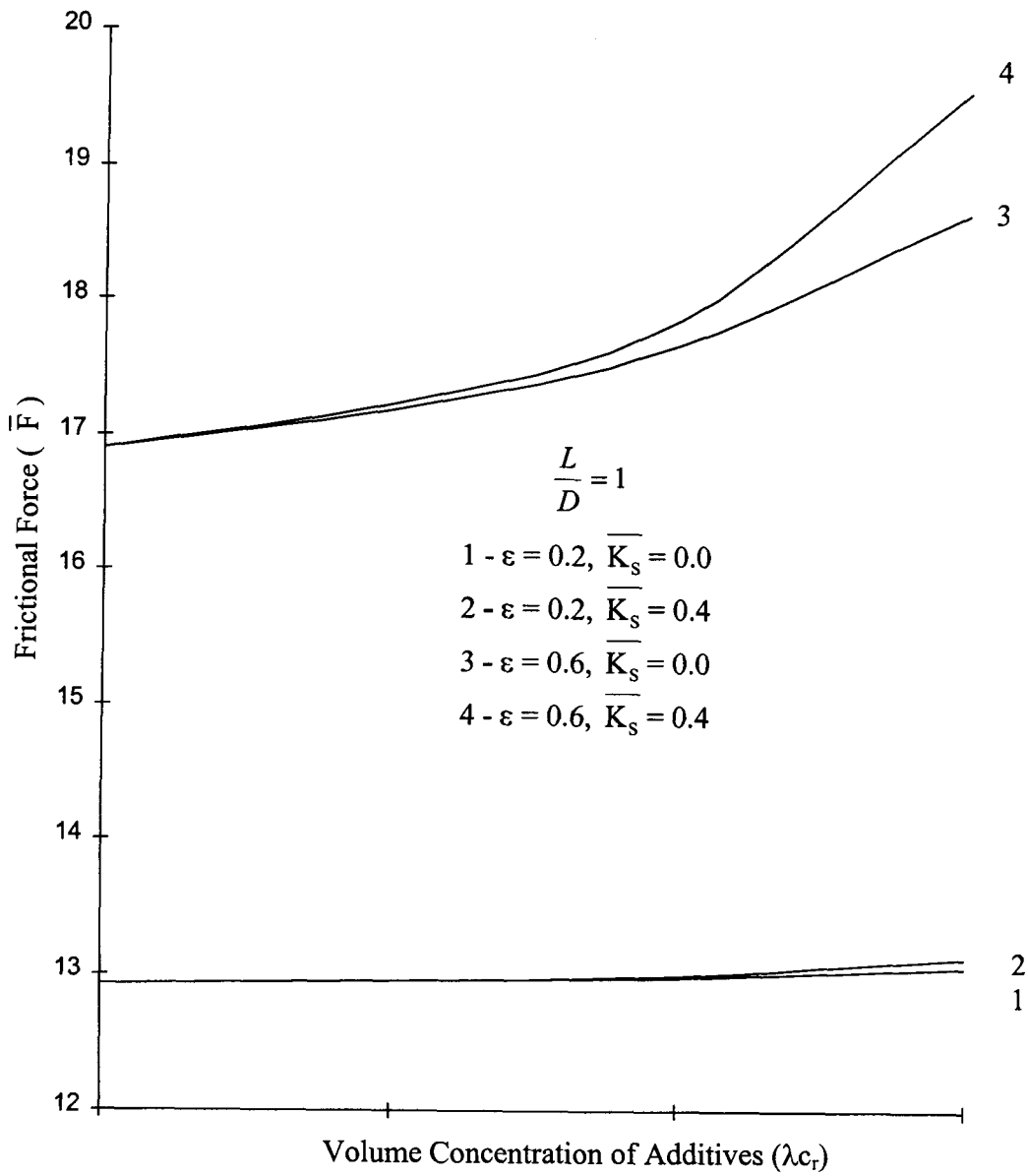

Fig. 5.4 - Frictional Force ($\bar{F}$) vs Volume Concentration of Additives (λc_r) in Circular Bearing

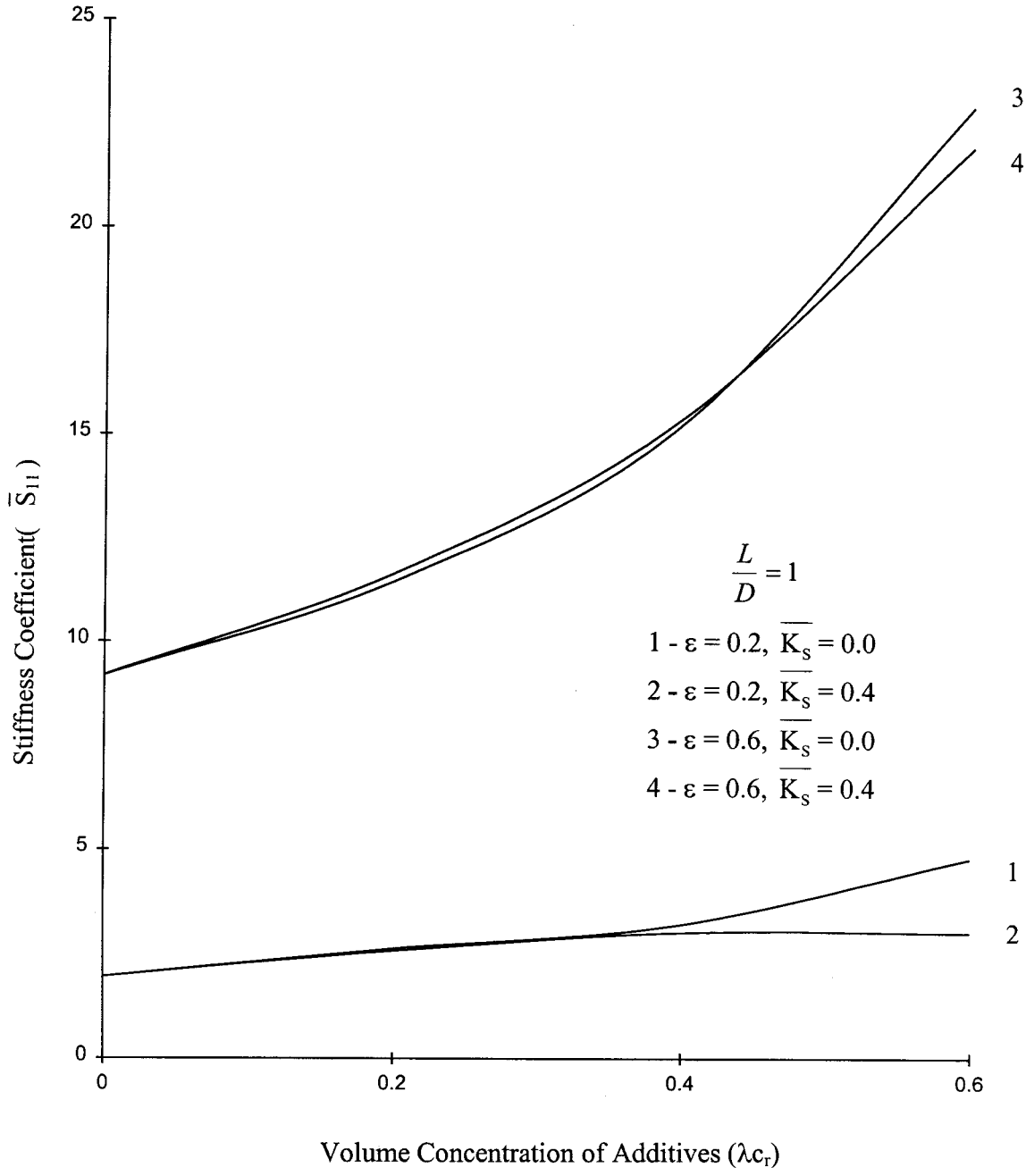

Fig. 5.5 – Stiffness Coefficient($\bar{S}_{11}$) vs Volume Concentration of Additives (λc_r) in Circular Bearing

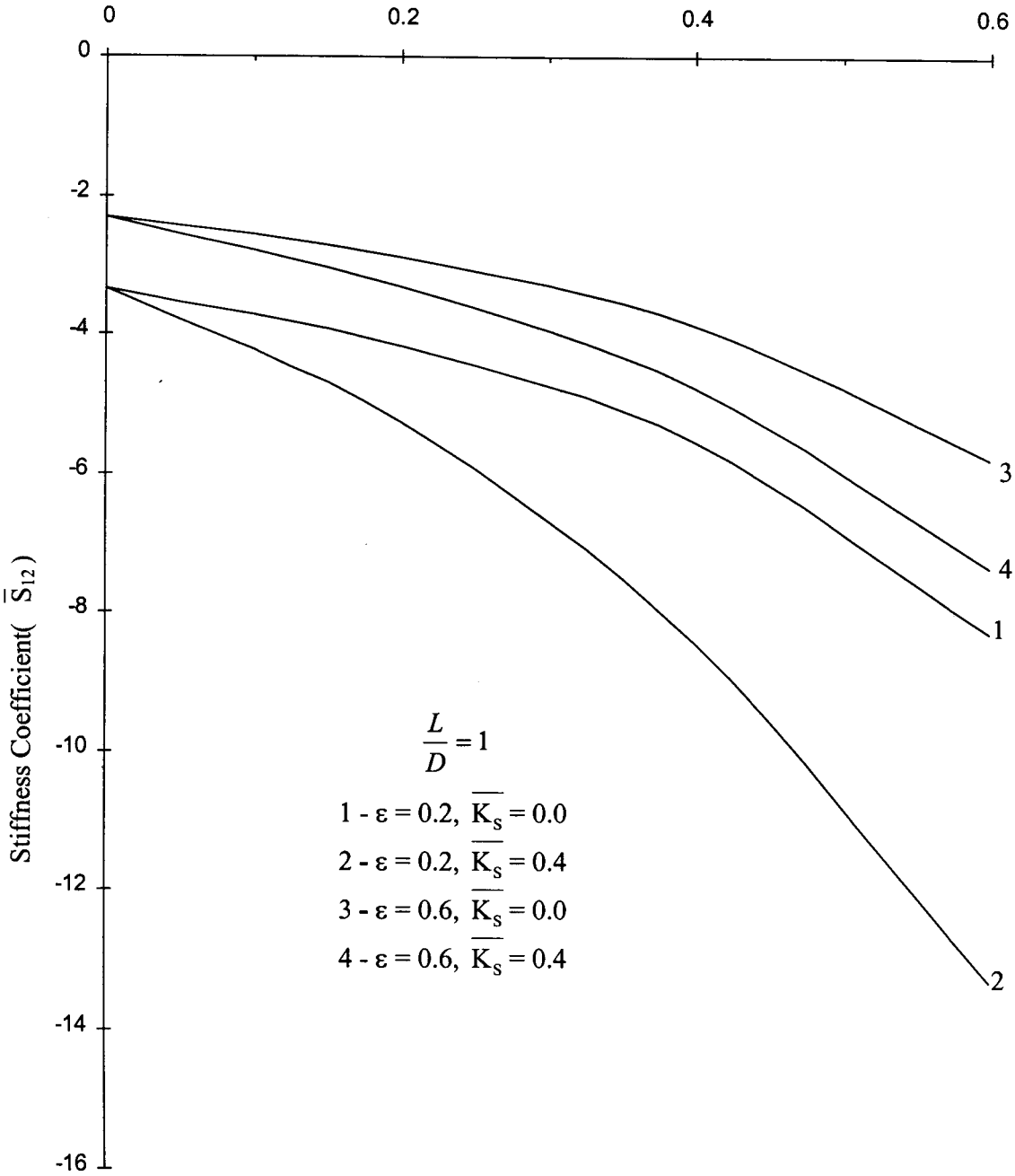

Fig. 5.6 – Stiffness Coefficient ($\bar{S}_{12}$) vs Volume Concentration of Additives (λc_r) in Circular Bearing

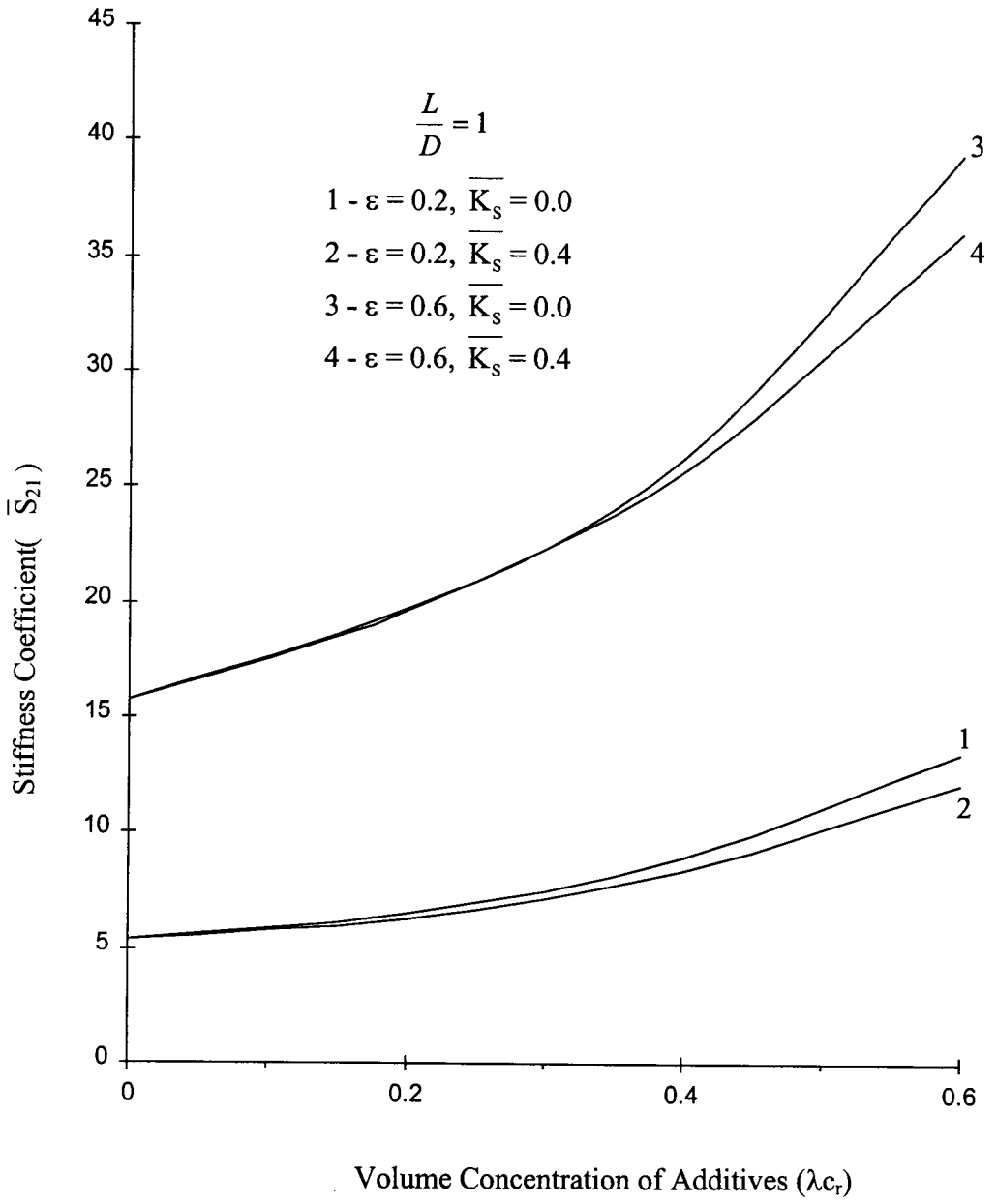

Fig. 5.7 – Stiffness Coefficient ($\bar{S}_{21}$) vs Volume Concentration of Additives (λc_r) in Circular Bearing

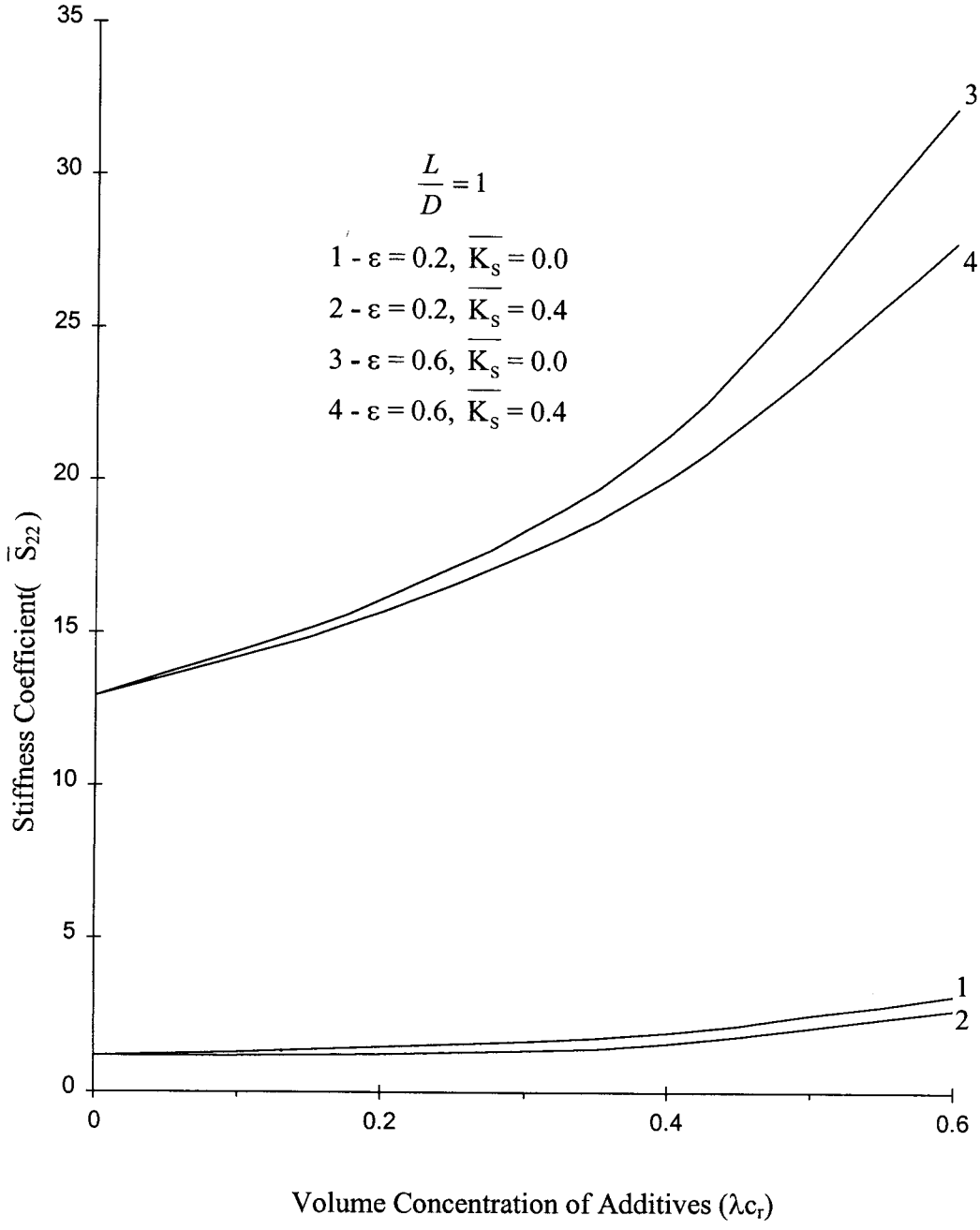

Fig. 5.8 – Stiffness Coefficient ($\bar{S}_{22}$) vs Volume Concentration of Additives (λc_r) in Circular Bearing

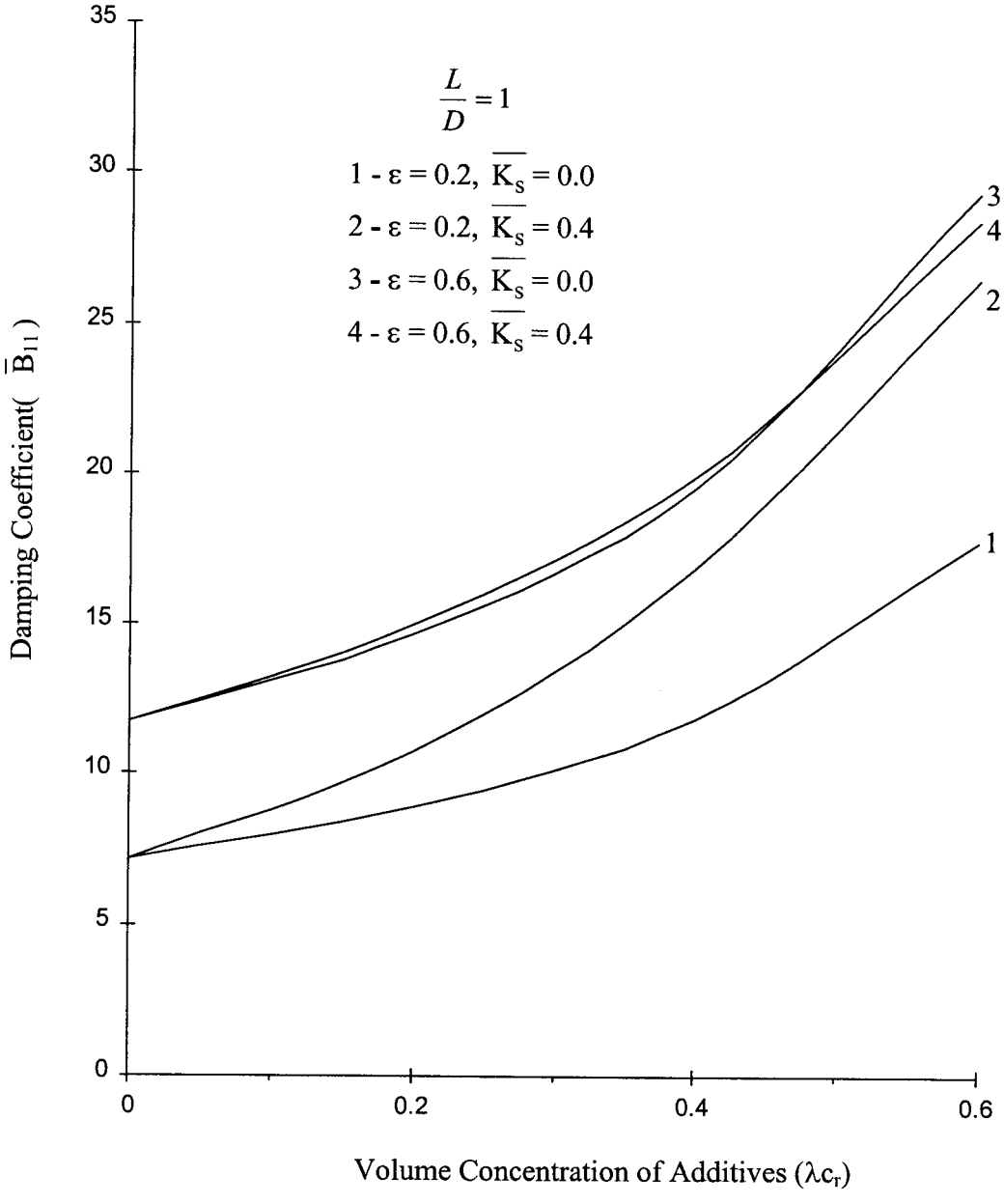

Fig. 5.9 – Damping Coefficient($\overline{B}_{11}$) vs Volume Concentration of Additives (λc_r) in Circular Bearing

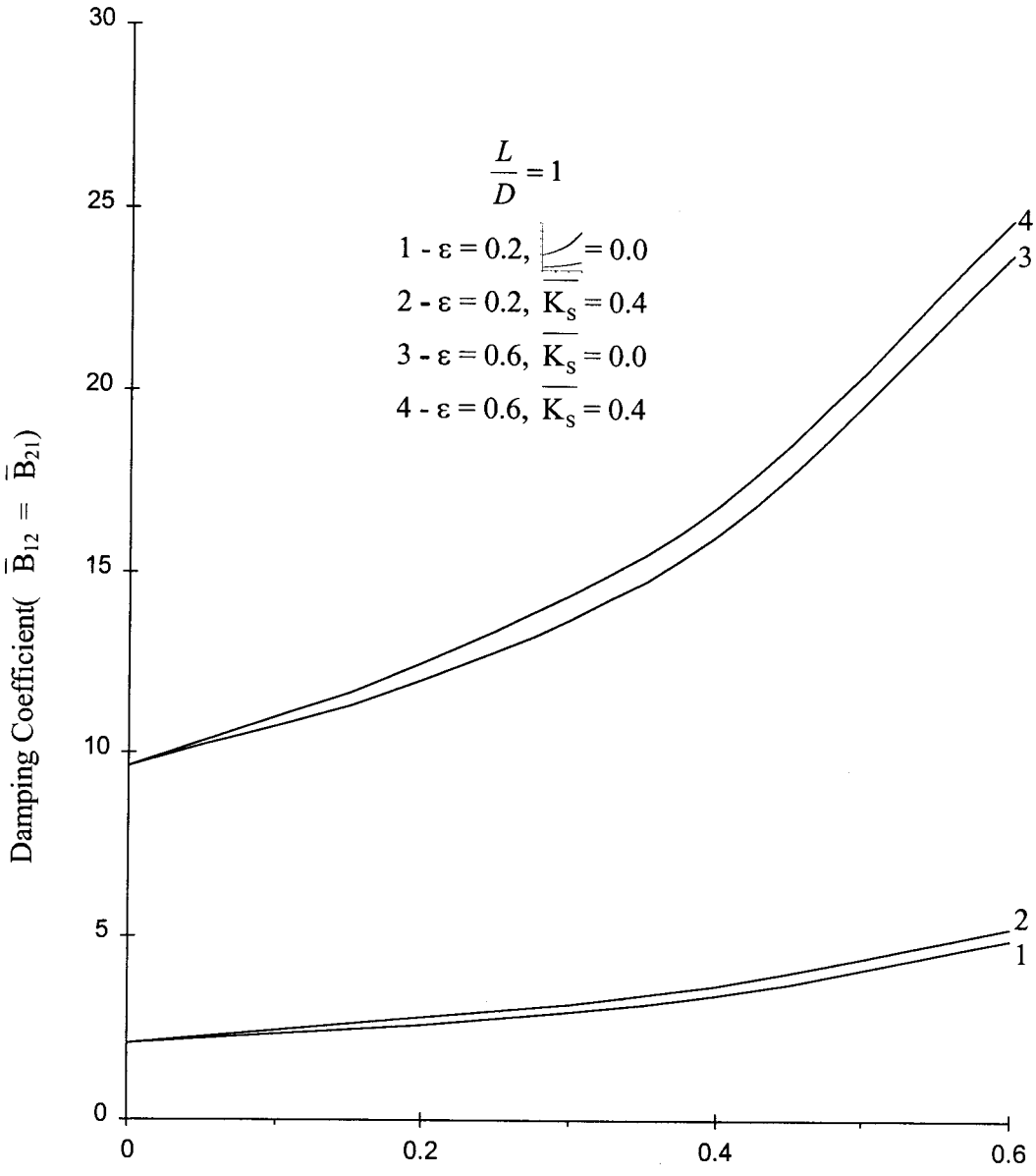

Fig. 5.10 – Damping Coefficient($\bar{B}_{12} = \bar{B}_{21}$) vs Volume Concentration of Additives (λc_r) in Circular Bearing

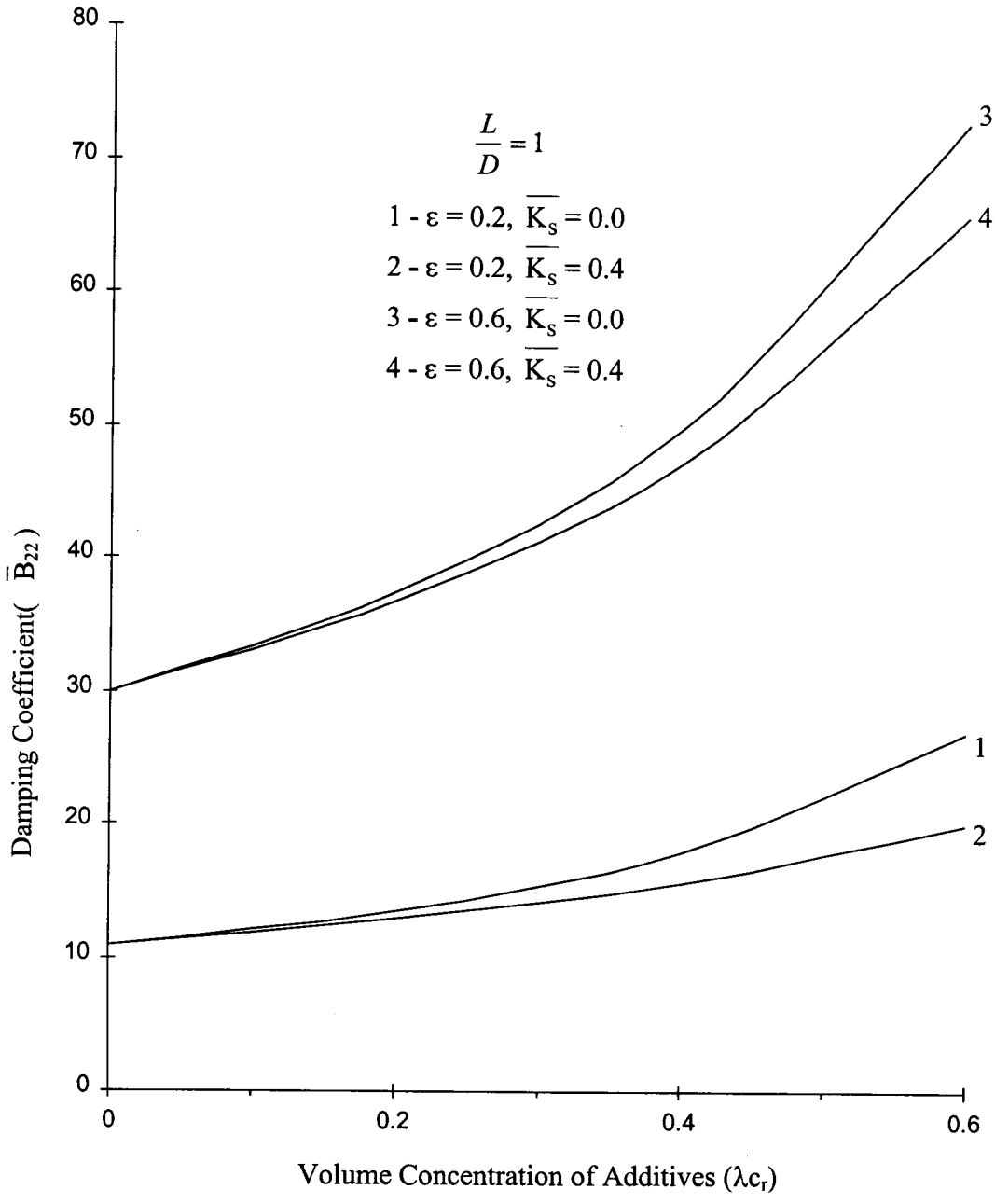

Fig. 5.11 – Damping Coefficient($\bar{B}_{22}$) vs Volume Concentration of Additives (λc_r) in Circular Bearing

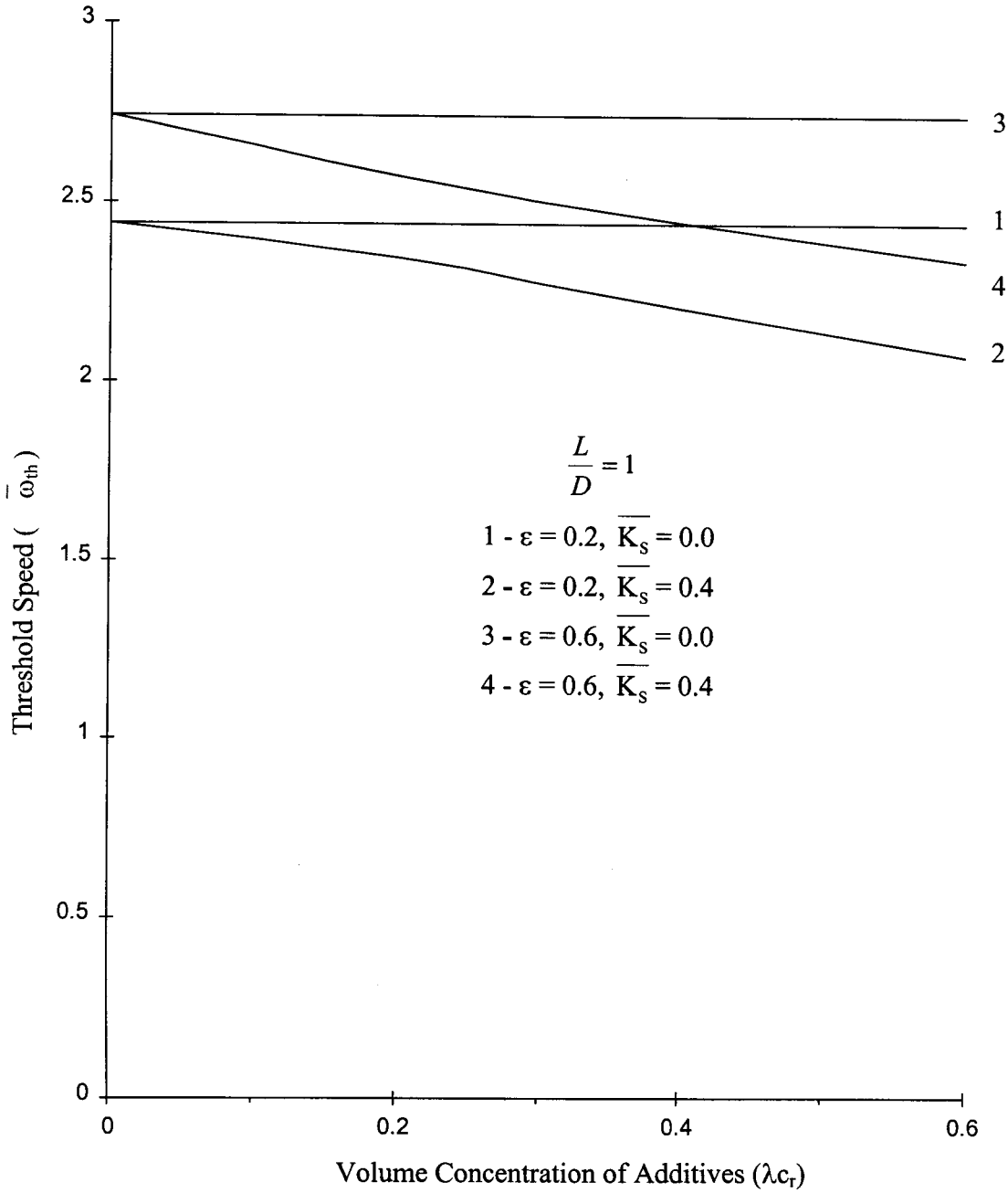

Fig. 5.12 – Threshold Speed ($\bar{\omega}_{th}$) vs Volume Concentration of Additives (λc_r) in Circular Bearing

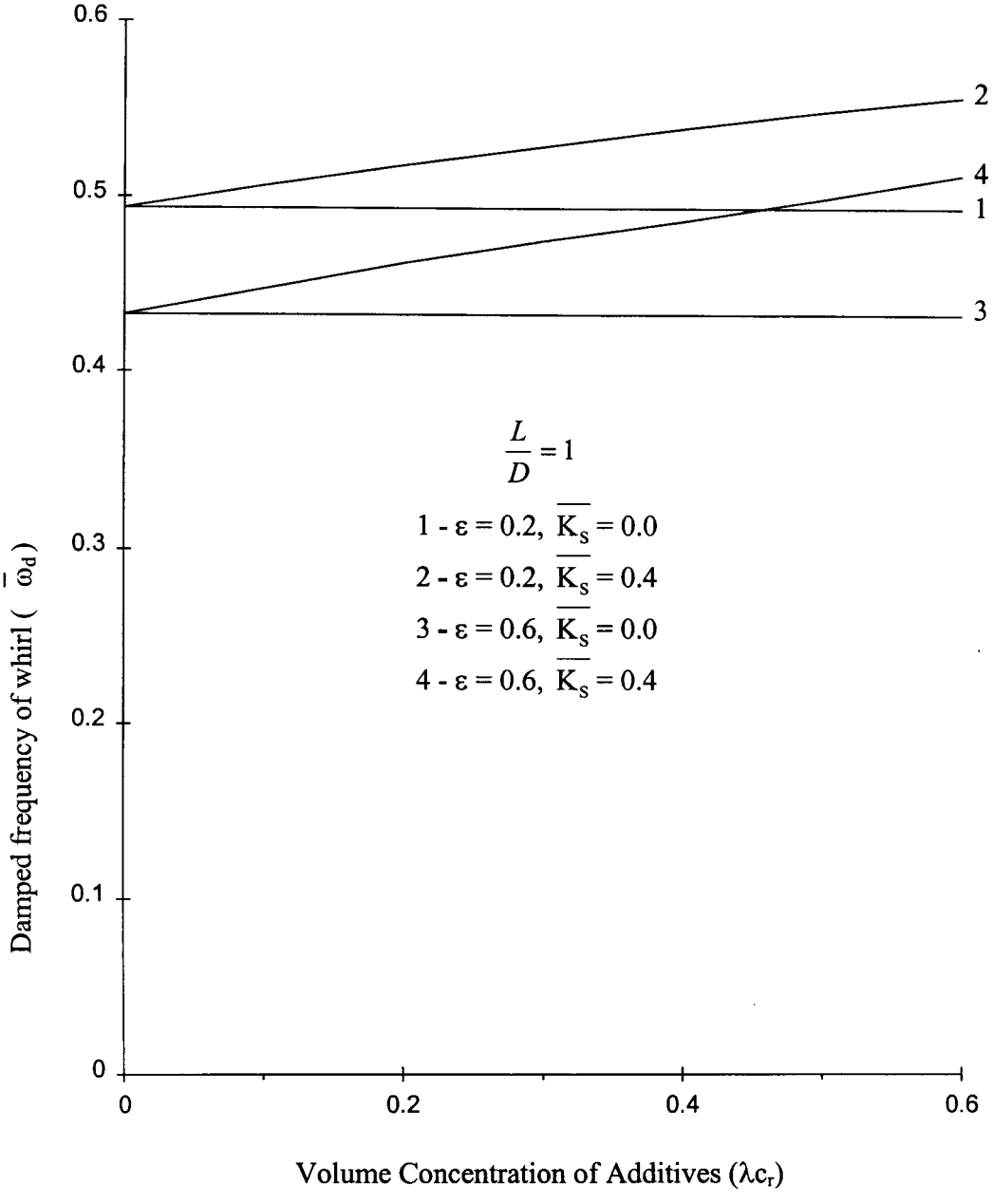

Fig. 5.13 – Damped frequency of whirl ($\bar{\omega}_d$) vs Volume Concentration of Additives (λc_r) in Circular Bearing

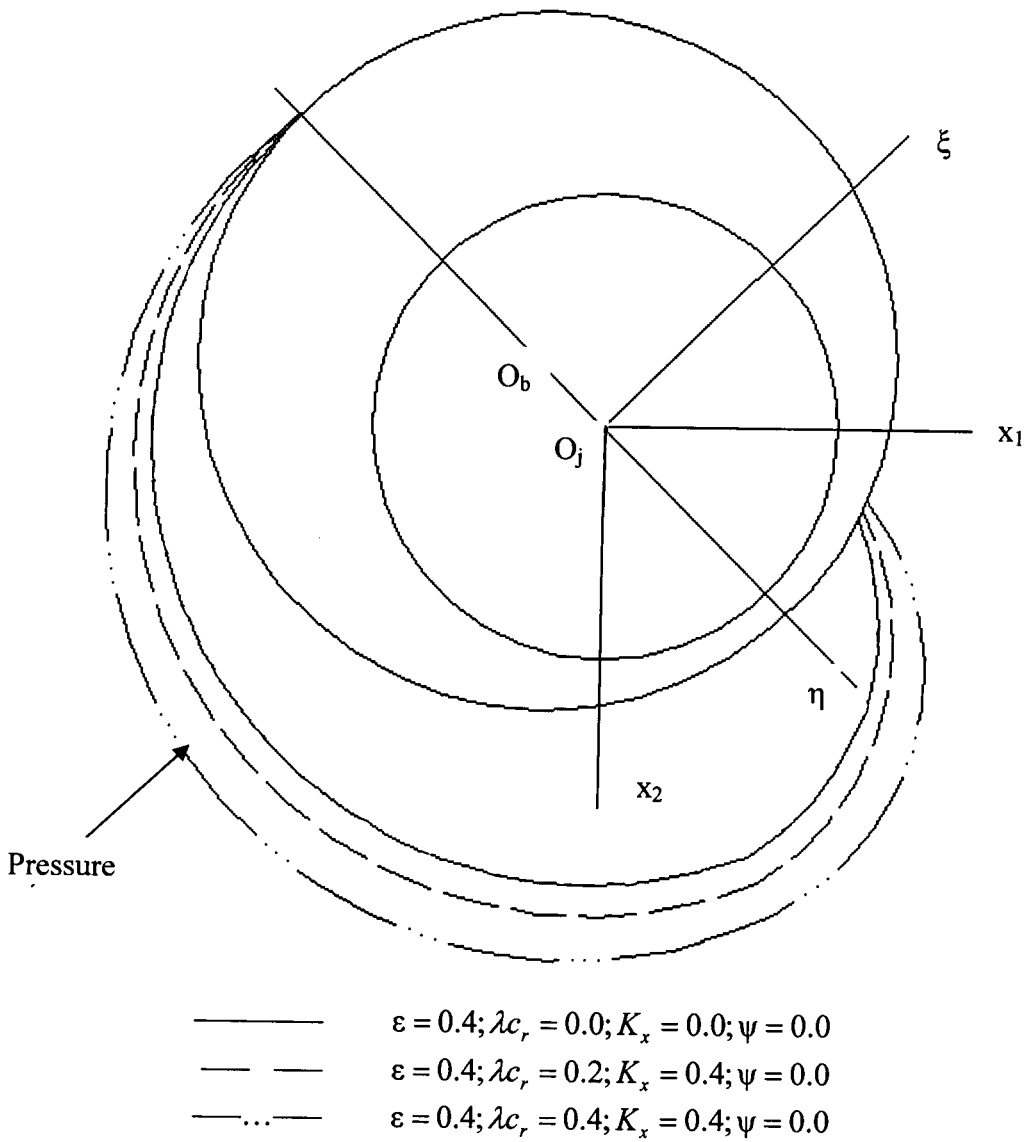

Fig. 5.14 Computed Pressure Field for Circular Rigid Bearing

The change in frictional force with increase in volume concentration of additives in the case of circular bearings is shown in Fig. 5.4. From this Figure it is observed that the frictional force increases with increase in eccentricity ratio, volume concentration of additives and mass transfer rate. It is also noted from this graph that the effect of volume concentration and mass transfer rate on frictional force is significant when the eccentricity ratio is high.

Figs. 5.5-5.11 show the variation of stiffness and damping coefficients $\bar{S}_{11}, \bar{S}_{12}, \bar{S}_{21}, \bar{S}_{22}$ and $\bar{B}_{11}, B_{12} \approx \bar{B}_{21}, \bar{B}_{22}$ respectively with increase in volume concentration of additives and mass transfer rate for circular bearings. All stiffness coefficients (Figs. 5.5-5.8) except $\bar{S}_{12}$ increase with increase in volume concentration of additives for any value of eccentricity ratio. When the mass transfer rate increases, these values of stiffness coefficients decrease at any value of λ_{Cr} and ε. In the case of $\bar{S}_{12}$, its value decrease with increase in volume concentration of additives for any value of eccentricity ratio. It is also seen from Figs. 5.9-5.11, that all the damping coefficients $\bar{B}_{11}, B_{12} \approx \bar{B}_{21}, \bar{B}_{22}$ increase with increase in volume concentration of additives. At any value of λ_{Cr} and low values of ε, when mass transfer rate increases the damping coefficients $\bar{B}_{11}, B_{12} \approx \bar{B}_{21}, \bar{B}_{22}$ increases with increase in λ_{Cr}. At high values of eccentricity ratio, when mass transfer rate increases, all the damping coefficients increase with increase in λ_{Cr} up to a certain value and after that only $\bar{B}_{11}$ decreases.

The variations of threshold speed with increase in volume concentration of additives (λ_{Cr}) are shown in Fig. 5.12 for Newtonian and micropolar lubricants when the bearing operates at different eccentricity ratios ($\varepsilon = 0.2$ and $\varepsilon = 0.6$) and aspect ratio (L/D) equal to 1. It may be noted that when there is no mass transfer of additives ($K_s = 0$), threshold speed does not change with increase in λ_{Cr} for any value of eccentricity ratio. At this juncture, it may also be noted that the same observation was made in the case of attitude angle (Fig. 5.3), which is a measure of stability. But when the mass transfer rate of additives increases, threshold speed decreases at any value of λ_{Cr}. This indicates that the presence of additives

lowers the stability of bearing. At the value of $\lambda_{Cr} = 0.6$, $\varepsilon = 0.6$ and $K_s = 0.4$ there is 14.83 percent decrease in the value of threshold speed compared with that value obtained for Newtonian lubricant ($\lambda_{Cr} = 0$, $K_s = 0$).

Fig.5.13 shows the variation of damped frequency of whirl with increase in λ_{Cr} for eccentricity ratios $\varepsilon = 0.2$ and $\varepsilon = 0.6$. It is seen that damped frequency of whirl is independent of volume concentration of additive when there is no mass transfer of additives. When there is mass transfer of additives damped frequency of whirl increases at any value of ε and volume concentration of additives. It is also observed that the damped frequency of whirl decreases with increase in eccentricity ratio. A decrease in damped frequency of whirl indicates that there is increase in the stability of bearing system. In a nutshell, the effect of micropolar fluid is to reduce the stability of bearing system.

The computed pressure fields for circular rigid bearing $\varepsilon = 0.4$ is shown in Fig. 5.14 for different values of volume concentration of additives and mass transfer rate.

To have a physical feel, the dimensional values of the static and dynamic performance characteristics are computed for the bearing geometry and operating conditions mentioned at the beginning of the section. These dimensional values are given in Table 5.3. From this table it is seen that at $\varepsilon = 0.8$, load carrying capacity increases form 34.3 to 55.58 when the volume concentration of additives increases from zero to 0.4 and mass transfer rate increases from zero to 0.4. It may also be noted that at high values of eccentricity ratio, bearing system is always stable for both Newtonian and micropolar lubricant.

5.1.2 Elastic Circular Bearings

EHD analysis of bearings takes into consideration the deformation of the bearing liner while analyzing various types of elastic bearings.

Results obtained from EHD analysis of circular bearings using Newtonian and micropolar fluids are shown in Figs. 5.15-5.28. Various performance characteristics for elastic circular bearings are presented for different values of

eccentricity ratios, mass transfer rates and deformation coefficients in these figures.

Fig.5.15shows the variations of load capacity with increase in deformation coefficient for Newtonian (λc_r= 0, K_s= 0) and micropolar lubricants (λc_r=0.2/0.4, K_s= 0.4) for circular bearings. For micropolar lubricants the load carrying capacity obtained at any deformation coefficient (ψ) is greater than that obtained with Newtonian lubricant when bearing operates at any eccentricity ratio. It is noted that the load carrying capacity decreases with the increase in deformation coefficient for any value ε. It is also observed that in the case of micropolar lubricants, for a fixed value of mass transfer rate (K_s), when the volume concentration of additives increases, the load capacity increases for any deformation coefficient and eccentricity ratio. At low values of deformation coefficient and higher eccentricity ratio, the variation of load capacity with increase in deformation coefficient is more significant than the values obtained at lower eccentricity ratio, for any value of volume concentration of additives.

The change of end leakage with the variation of deformation coefficient is shown in Figs.5.16 for circular bearings. From this Figure it is observed that the end leakage decreases with increase in deformation coefficient. It is also seen that variation of end leakage with increase in deformation coefficient is appreciable when the bearing operates at higher eccentricity ratio compared to the values obtained at lower eccentricity ratios. When deformation coefficient is high the bearing is more flexible. This leads to the development of small pressures and small pressure gradients leading to a lower end leakage. In the case of small eccentricity ratios the load and hence the pressure are less leading to smaller pressure gradients and smaller end leakage. For any value of deformation coefficient and eccentricity ratio, when mass transfer rate of additives increases, the value of end leakage obtained increases. The increase in the value of volume concentration of additives also increases the value of end leakage at any value of mass transfer rate (K_s).

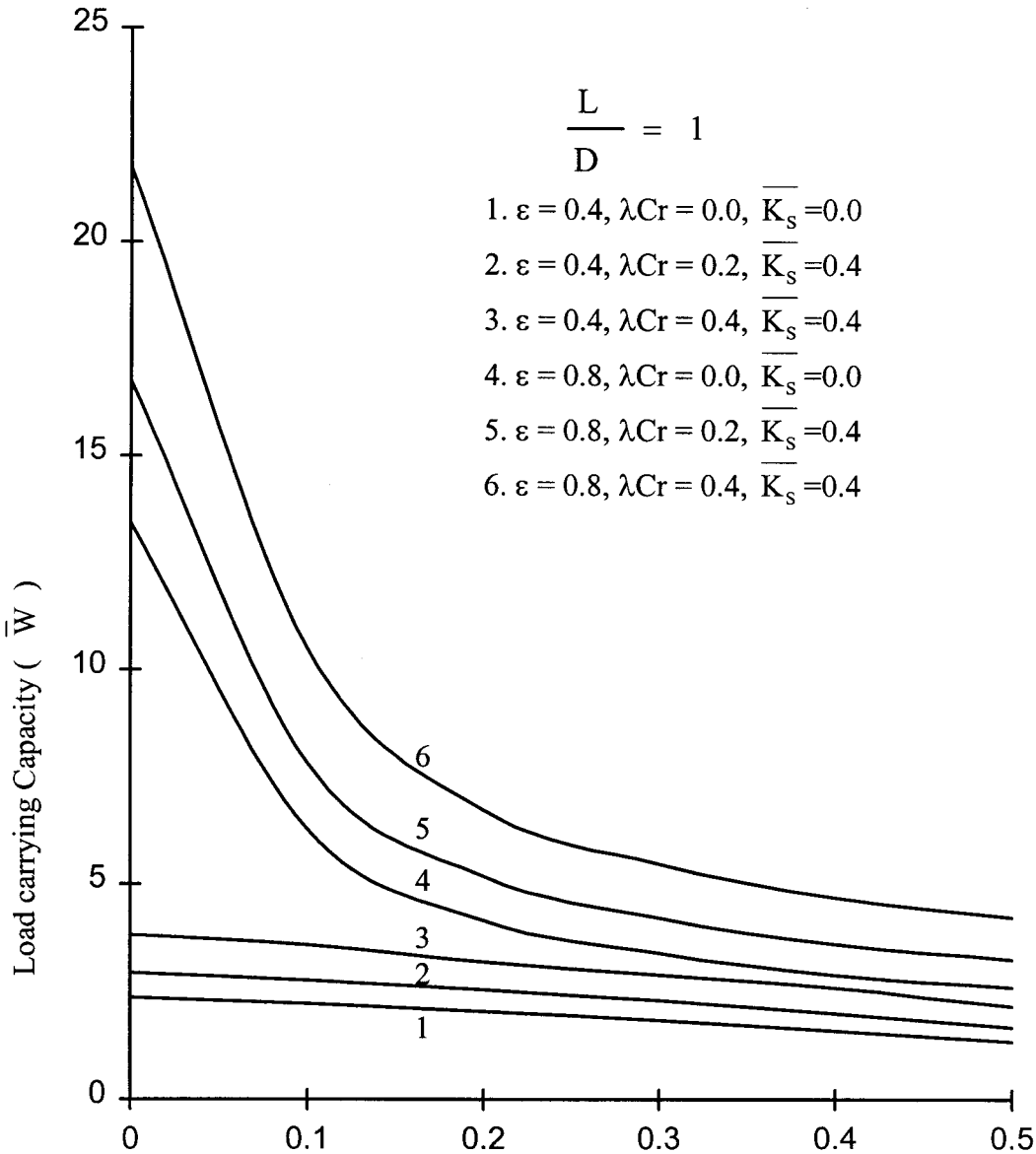

Fig. 5. 15- Load carrying Capacity ($\overline{W}$) vs Deformation Coefficient ($\overline{\psi}$) in Circular Bearing

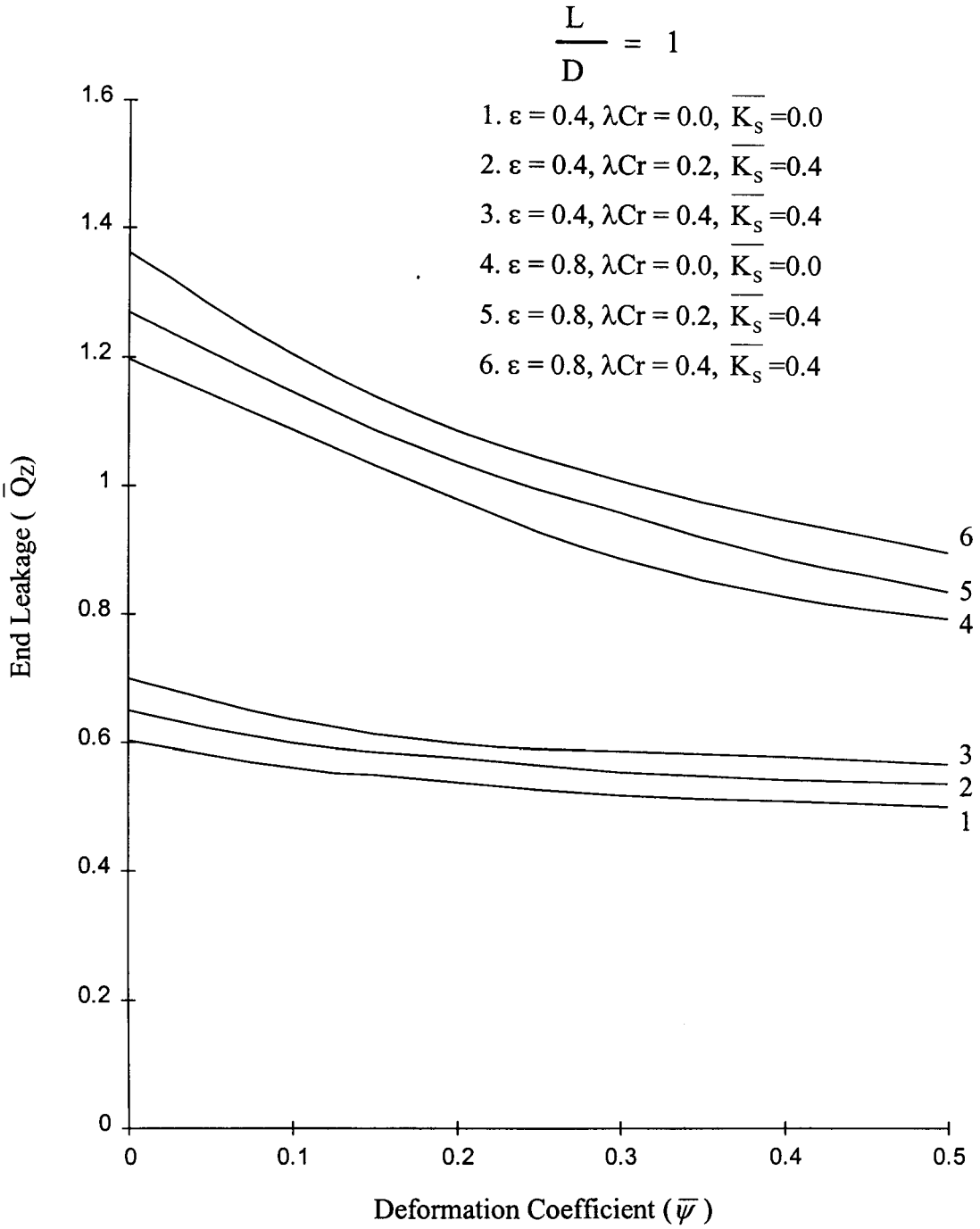

Fig. 5.16 – End Leakage ($\bar{Q}_Z$) vs Deformation Coefficient ($\overline{\psi}$) in Circular Bearing

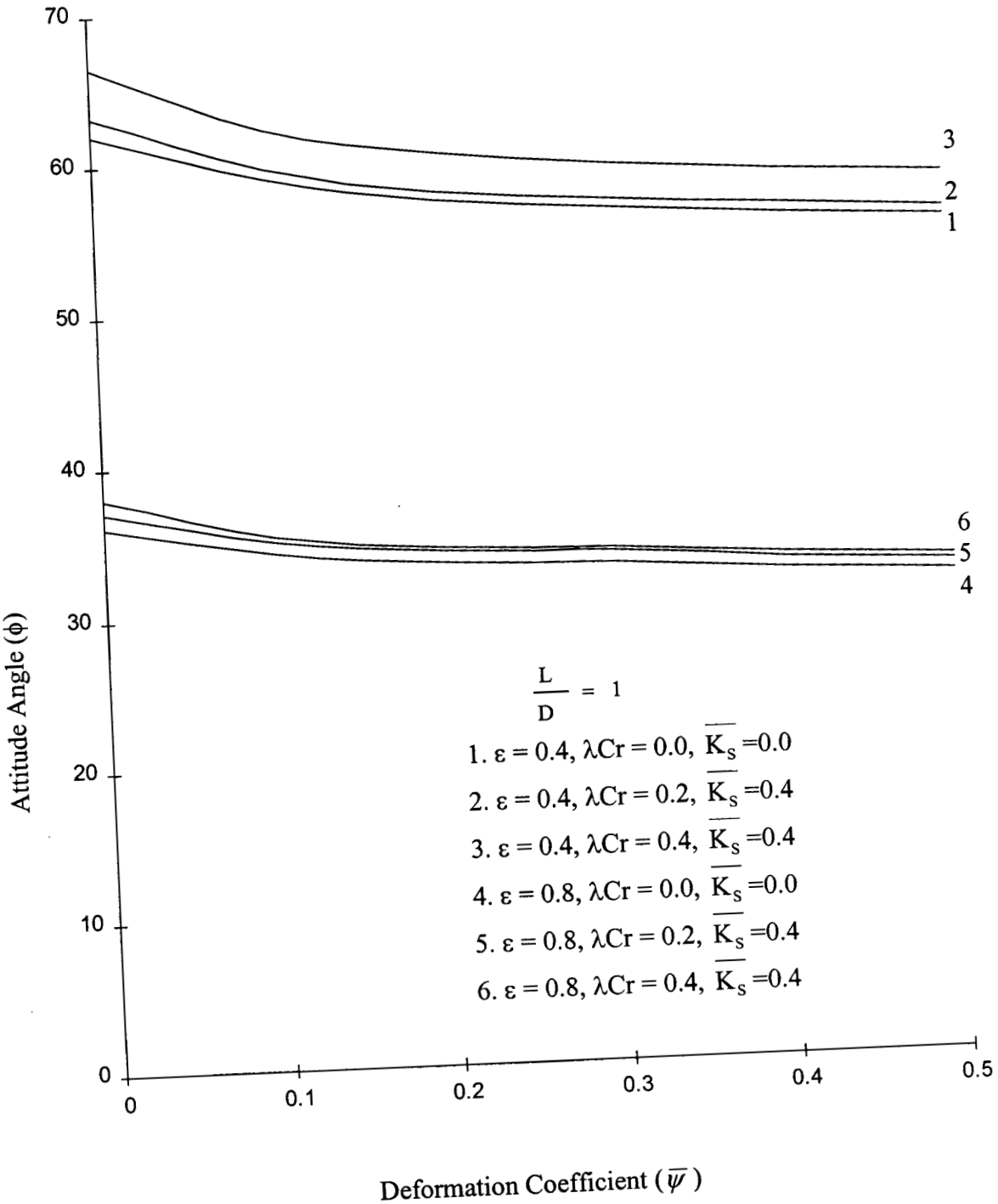

Fig. 5.17 – Attitude Angle (ϕ) vs Deformation Coefficient ($\overline{\psi}$) in Circular Bearing

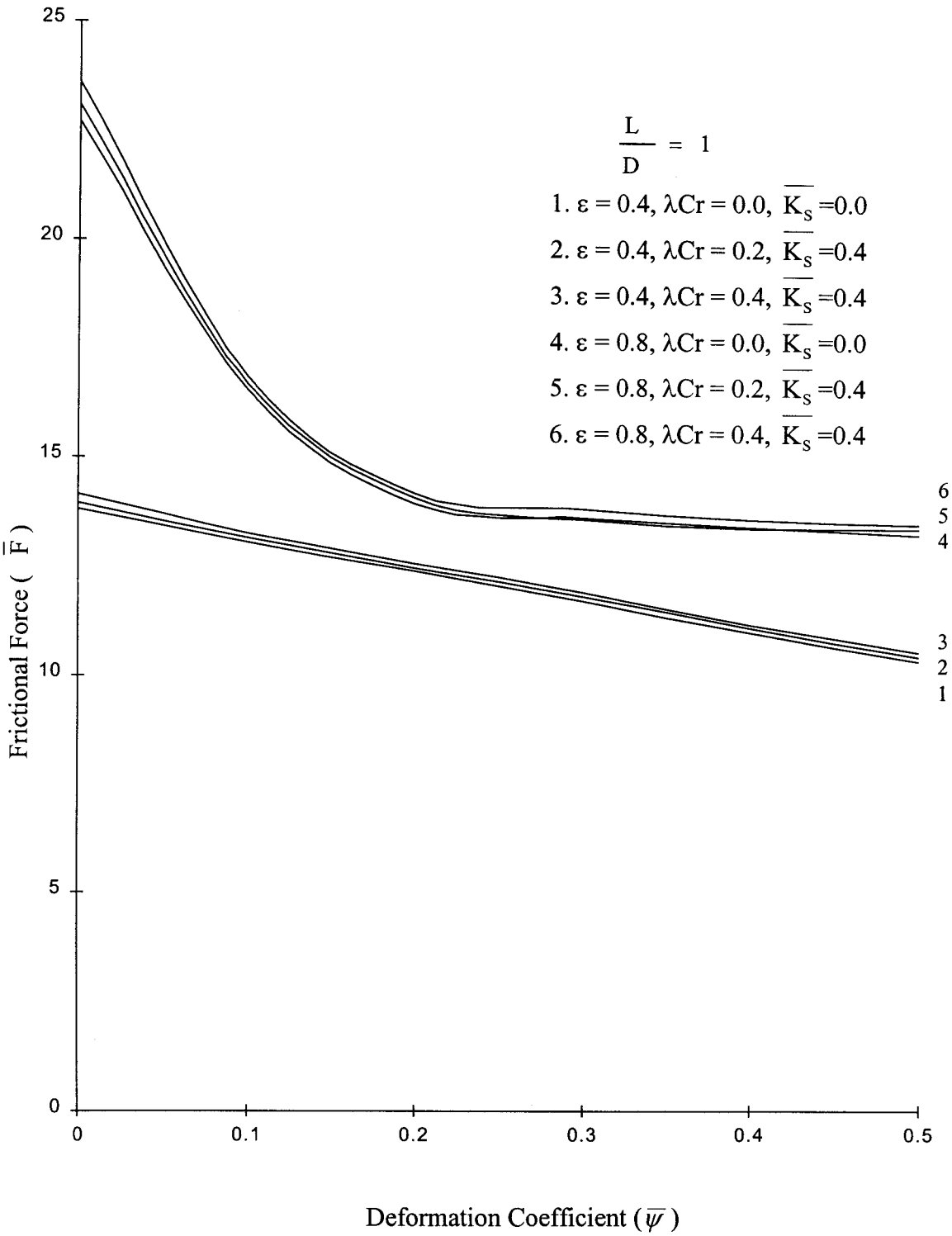

Fig. 5.18 - Frictional Force ($\bar{F}$) vs Deformation Coefficient ($\bar{\psi}$) in Circular Bearing

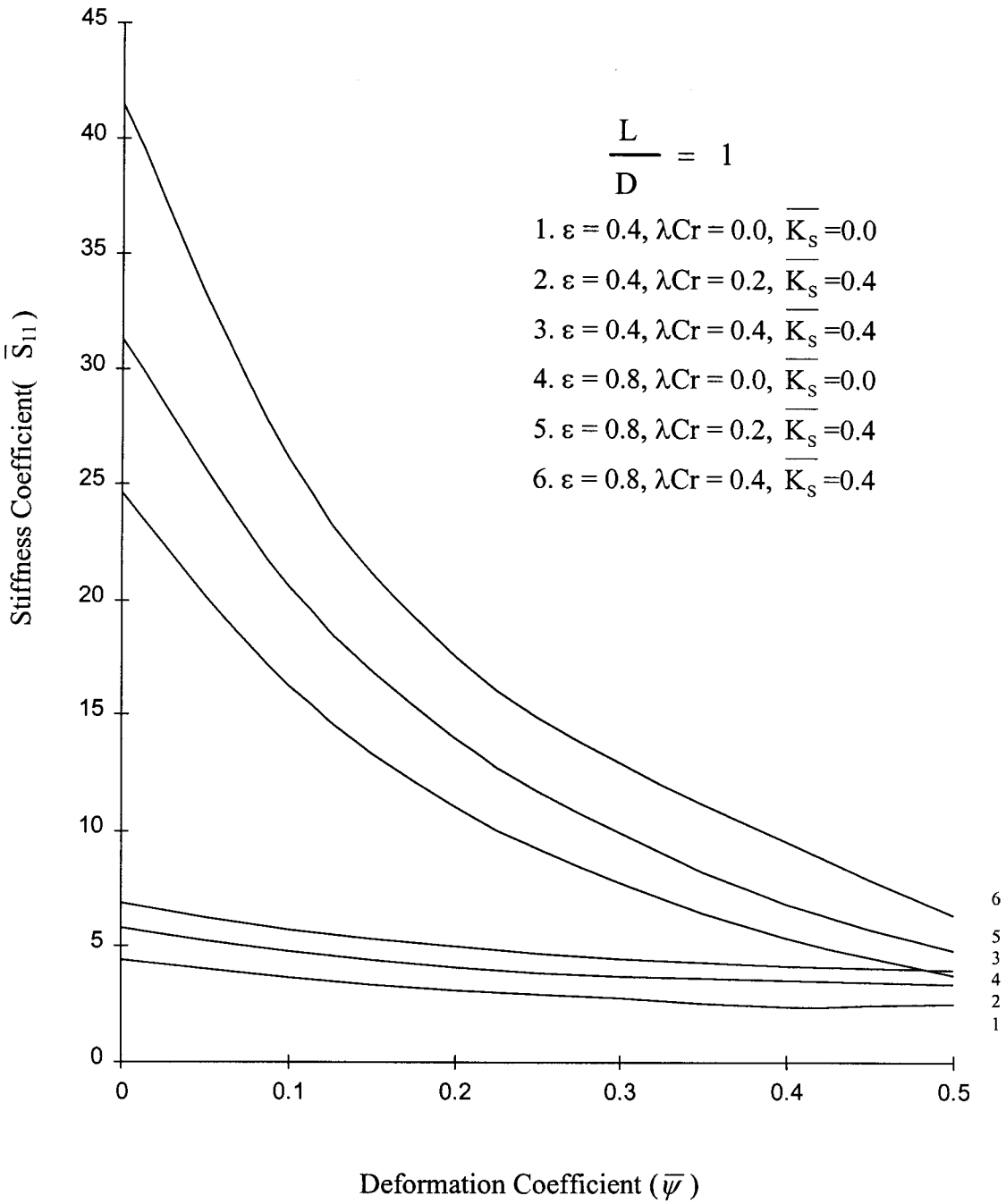

Fig. 5.19 – Stiffness Coefficient($\bar{S}_{11}$) vs Deformation Coefficient ($\bar{\psi}$) in Circular Bearing

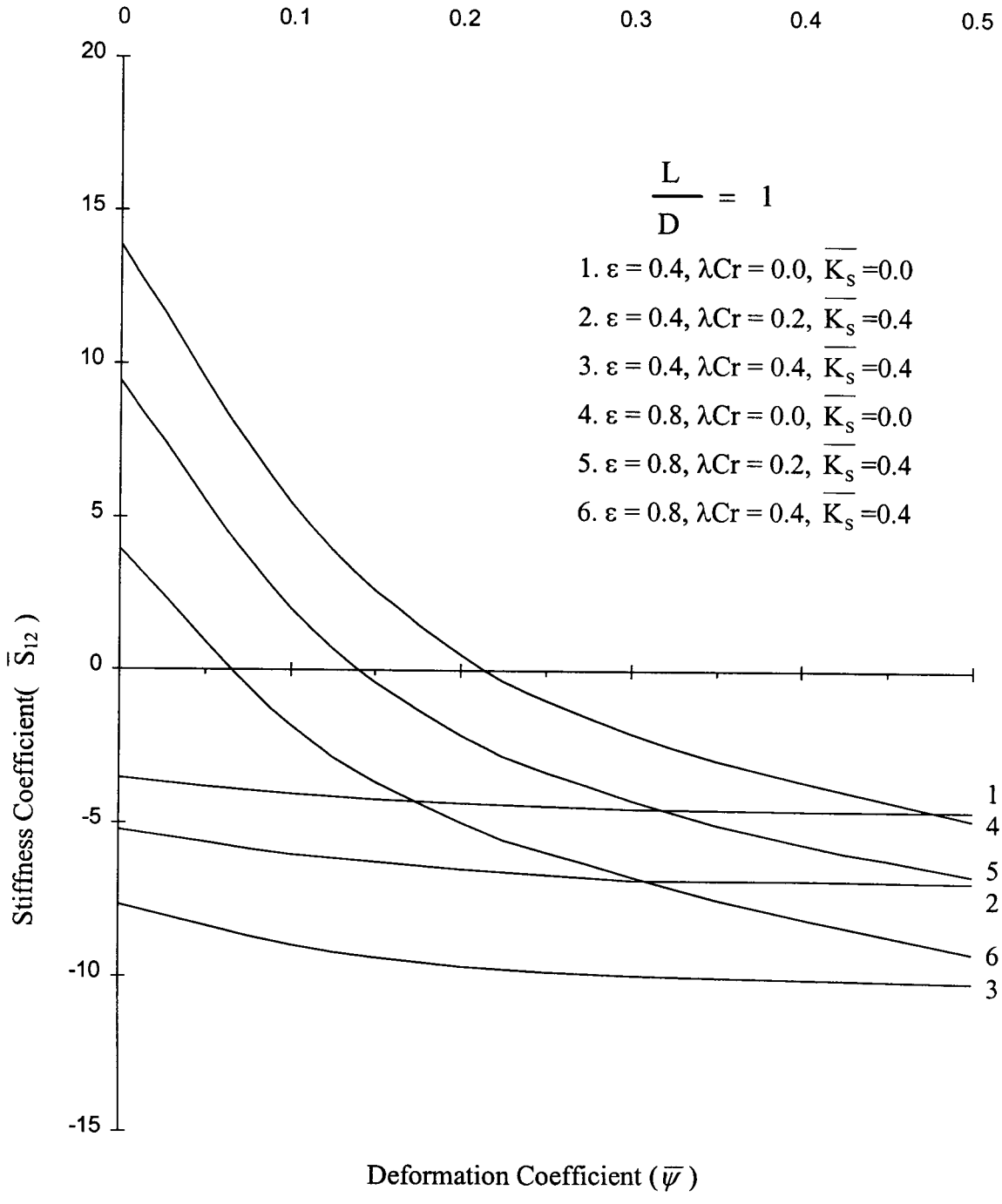

Fig. 5.20 – Stiffness Coefficient($\overline{S}_{12}$) vs Deformation Coefficient ($\overline{\psi}$) in Circular Bearing

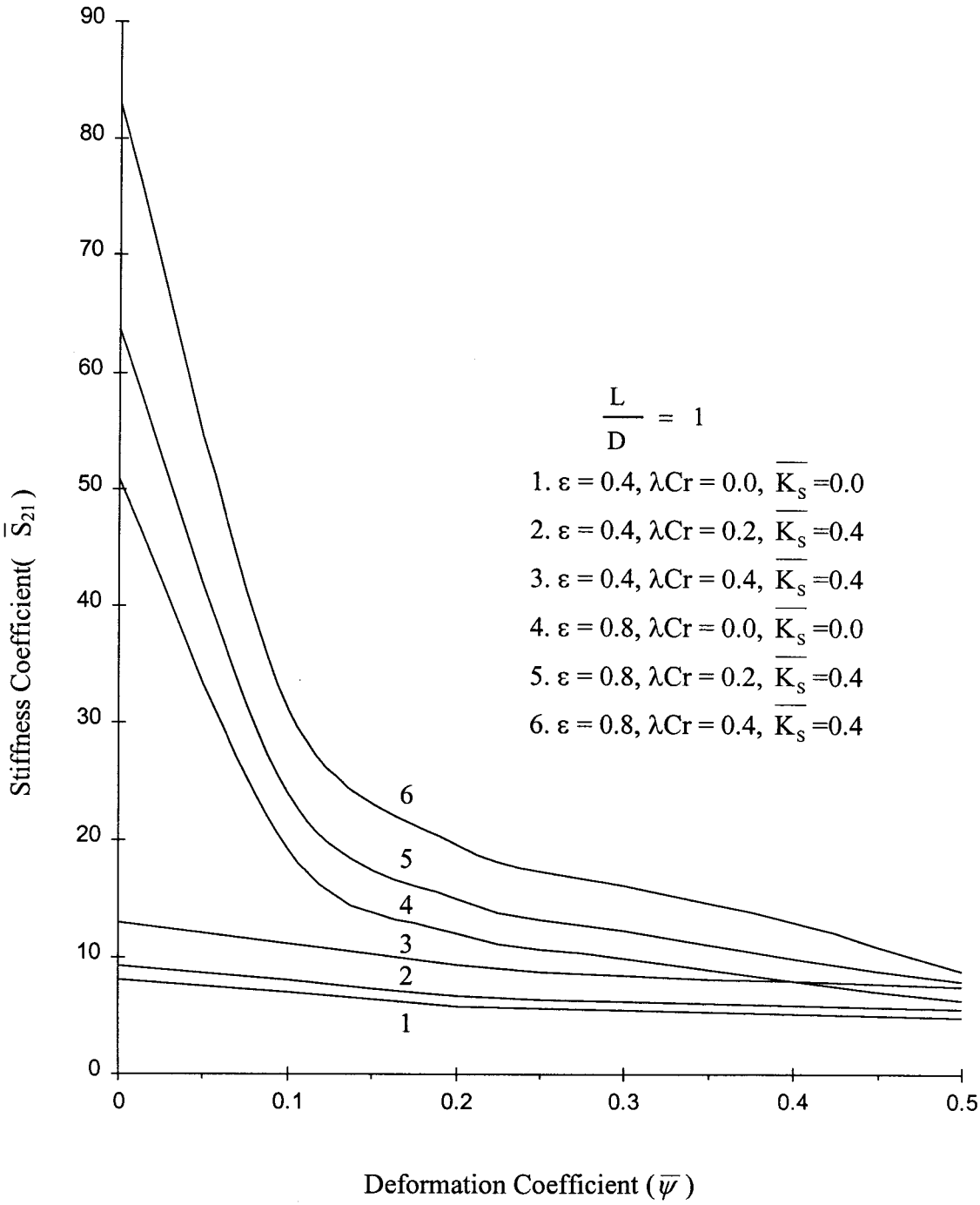

Fig. 5.21 – Stiffness Coefficient($\bar{S}_{21}$) vs Deformation Coefficient ($\bar{\psi}$) in Circular Bearing

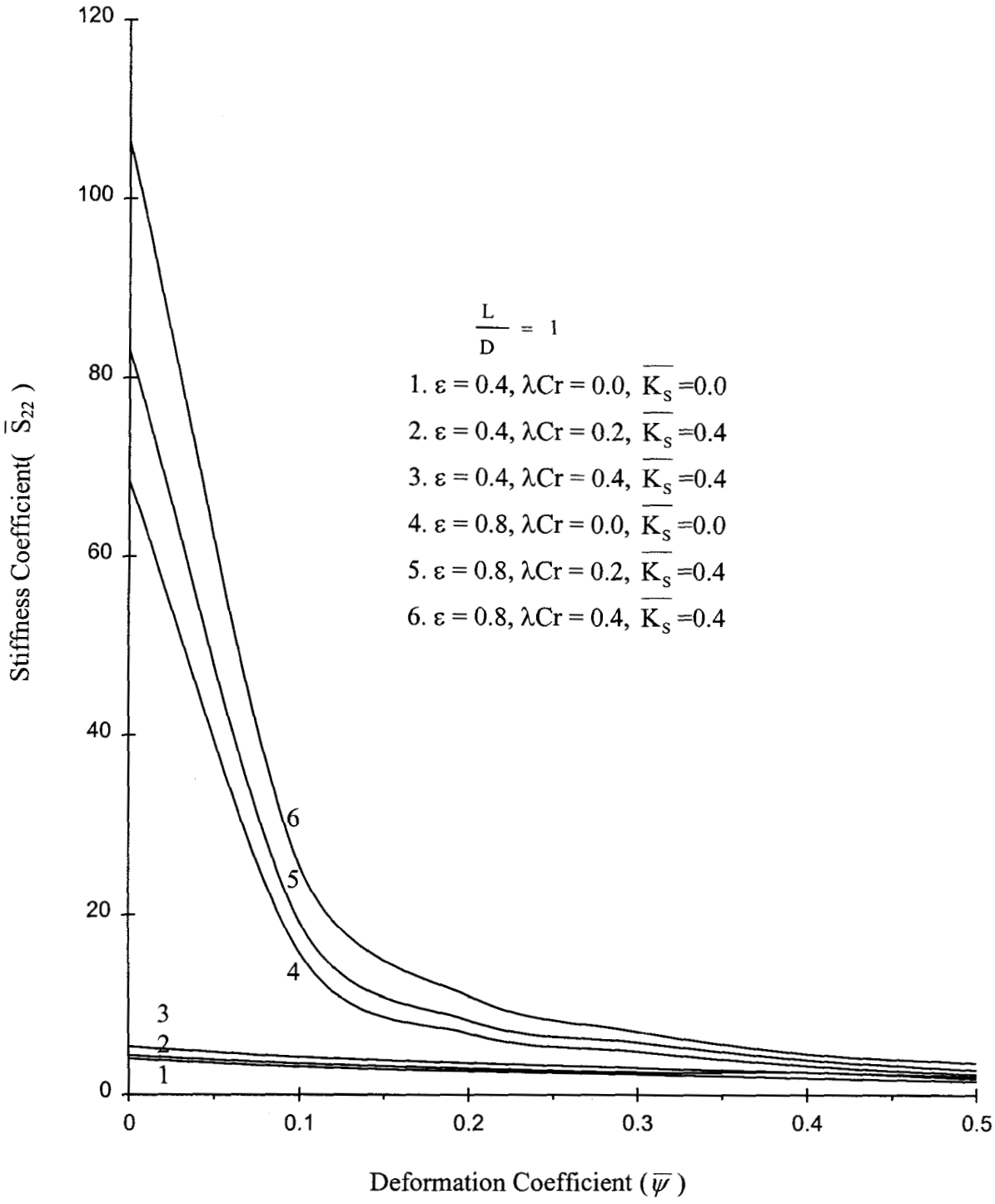

Fig. 5.22 – Stiffness Coefficient($\bar{S}_{22}$) vs Deformation Coefficient ($\bar{\psi}$) in Circular Bearing

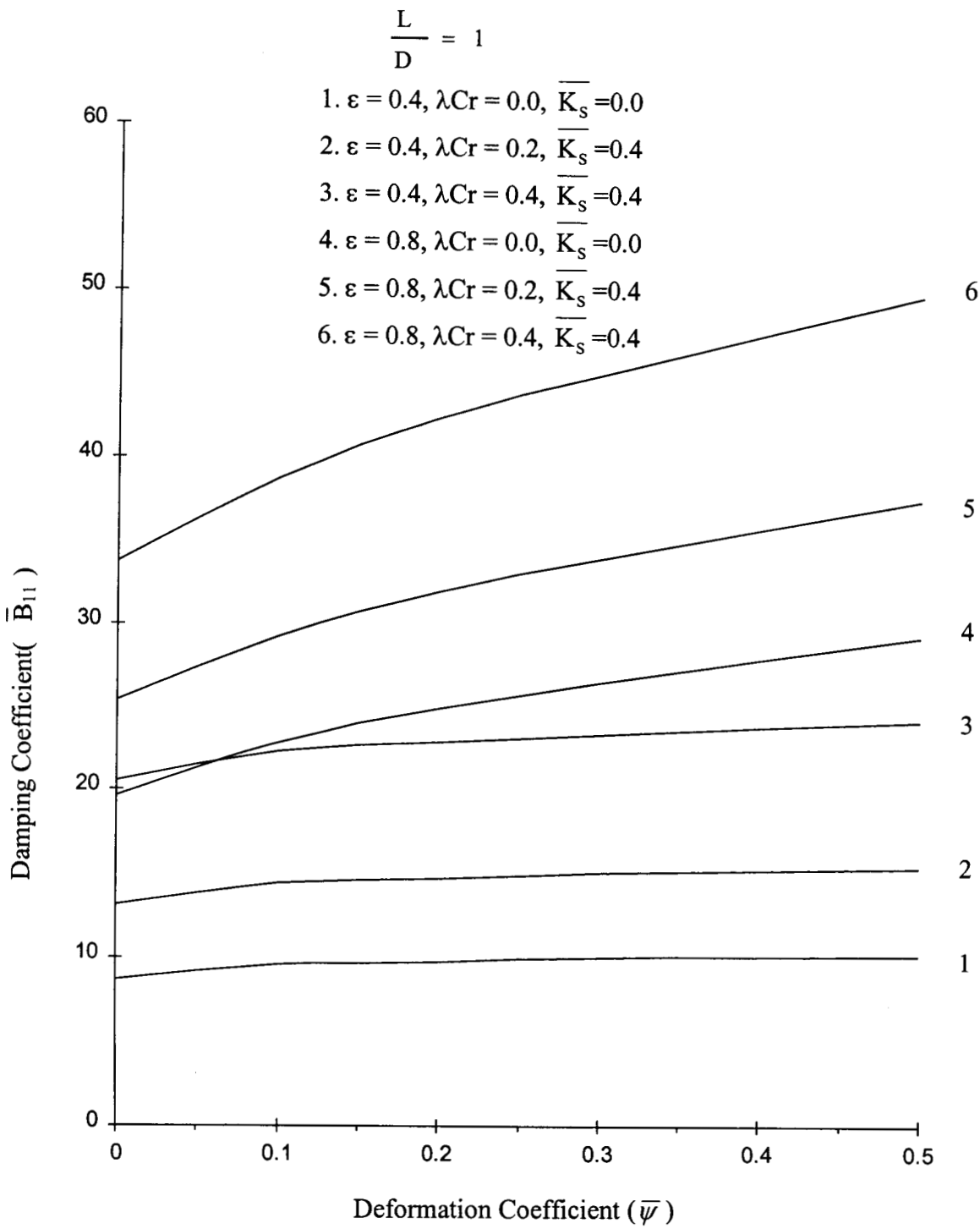

Fig. 5.23 – Damping Coefficient($\overline{B}_{11}$) vs Deformation Coefficient ($\overline{\psi}$) in Circular Bearing

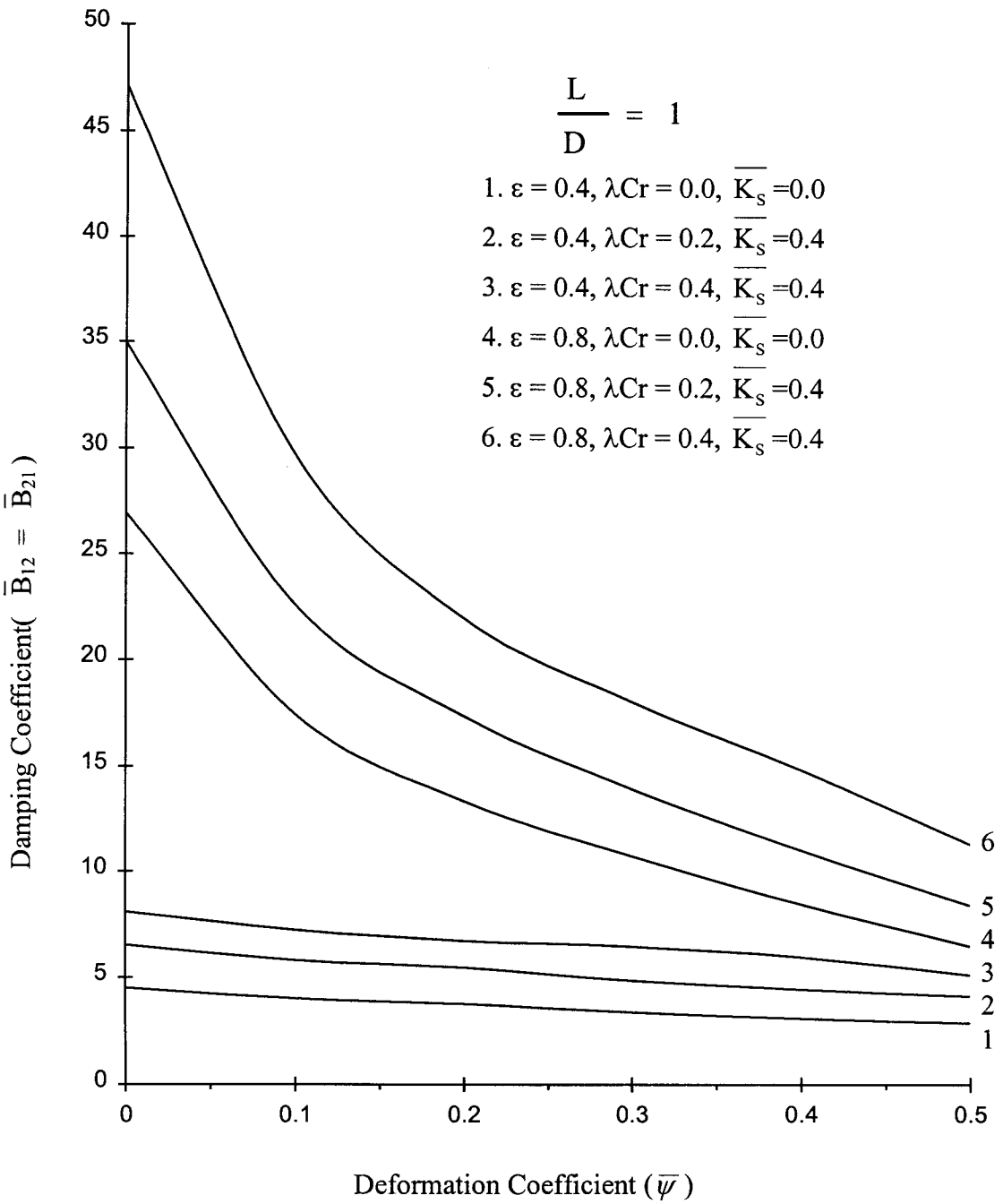

Fig. 5.24 – Damping Coefficient($\overline{B}_{12} = \overline{B}_{21}$) vs Deformation Coefficient ($\overline{\psi}$) in Circular Bearing

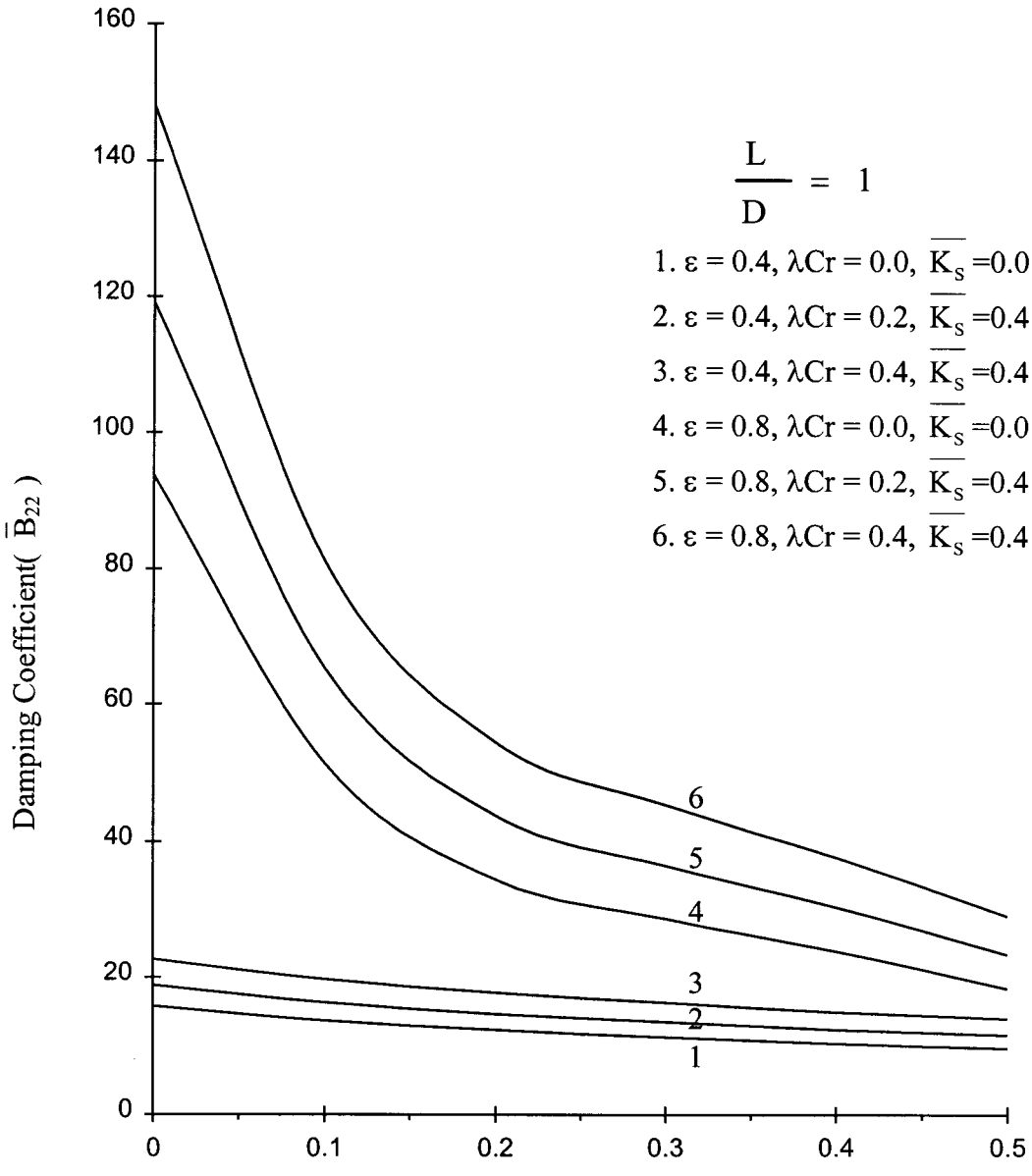

Fig. 5.25– Damping Coefficient ($\bar{B}_{22}$) vs Deformation Coefficient (ψ) in Circular Bearing

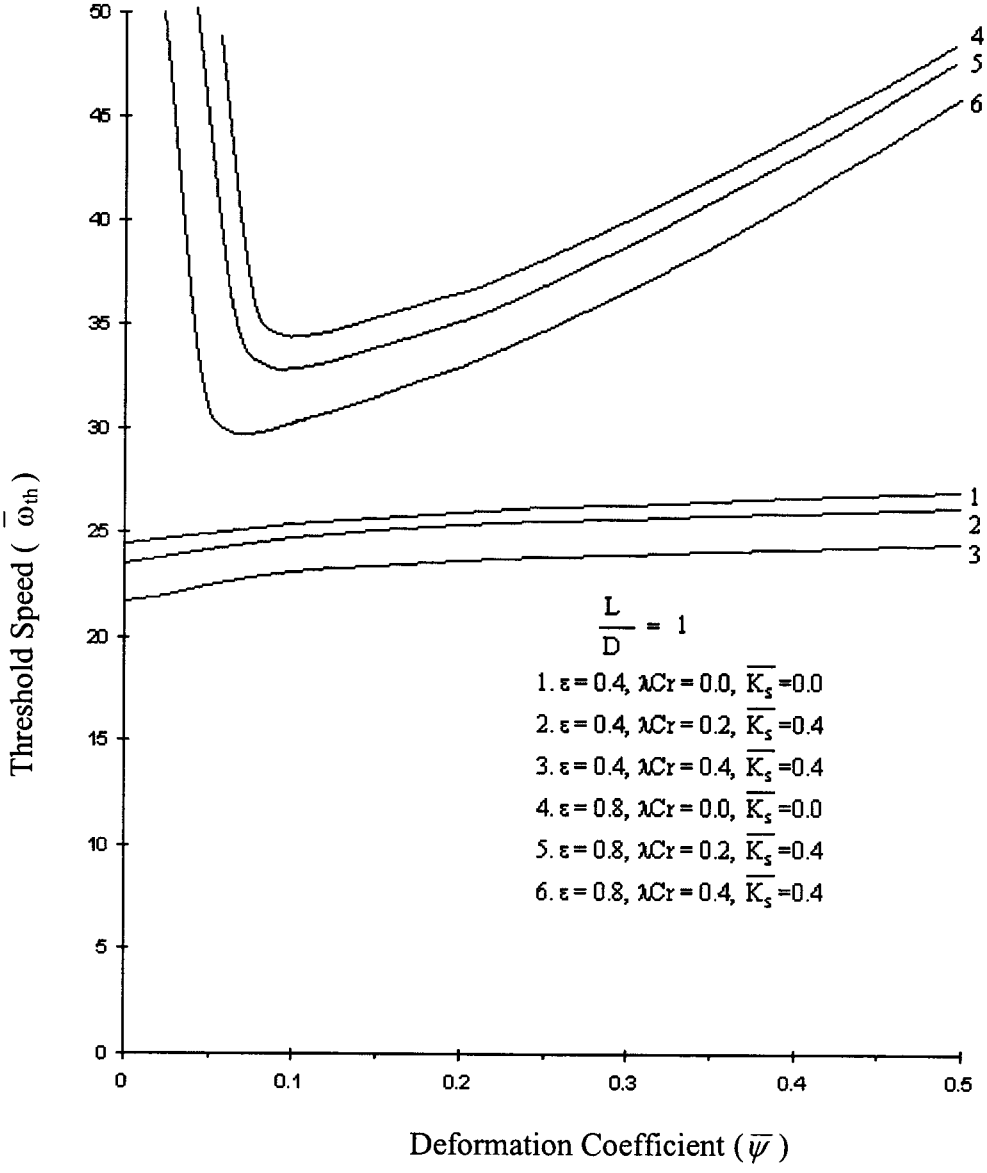

Fig. 5.26 – Threshold Speed ($\bar{\omega}_{th}$) vs Deformation Coefficient ($\bar{\psi}$) in Circular Bearing

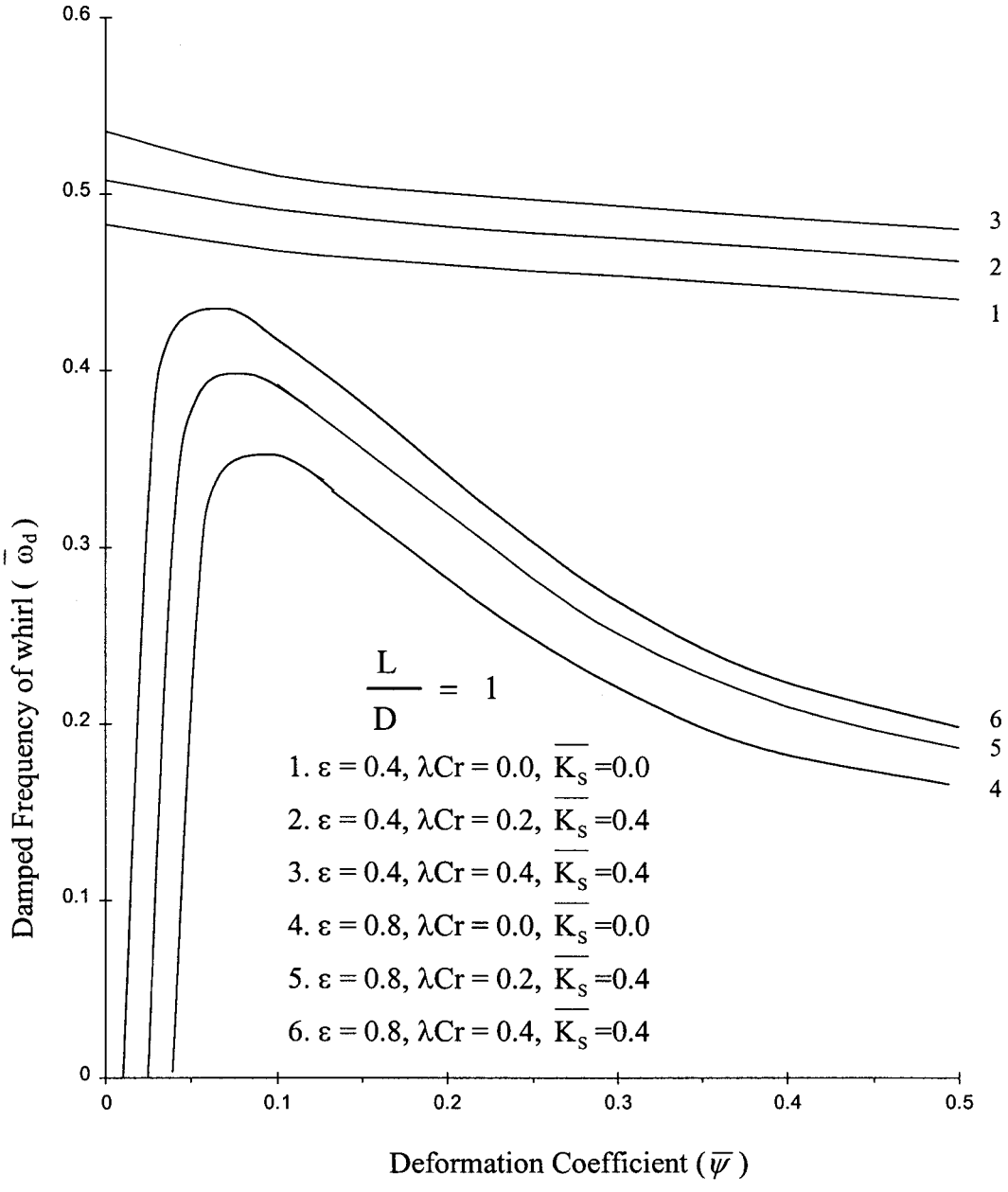

Fig. 5.27 – Damped Frequency of whirl ($\bar{\omega}_d$) vs Deformation Coefficient ($\bar{\psi}$) in Circular Bearing

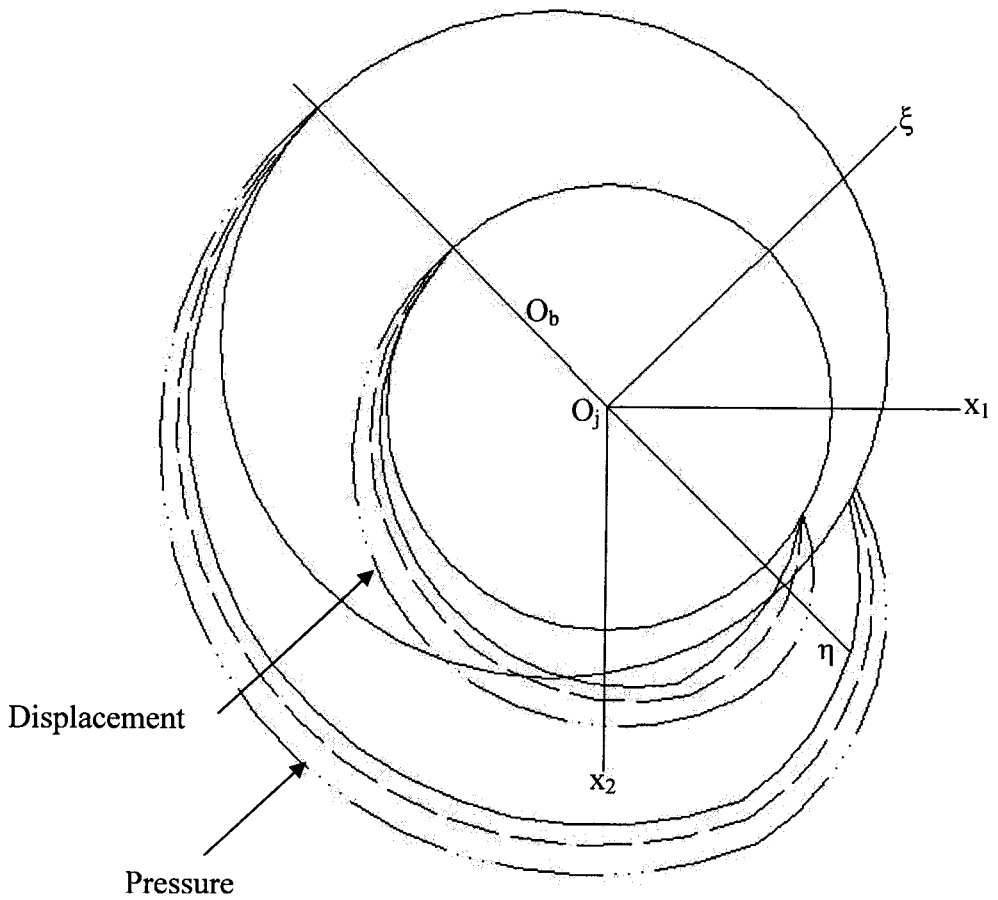

Fig. 5.28 Computed Pressure and Deformation Field for Circular Bearing

In Fig. 5.17 the variations in the values of attitude angle with the change in deformation coefficient for circular bearings are shown. It is observed that the change in volume concentration and mass transfer rate do not affect the values of attitude angles obtained for Newtonian lubricant significantly when the bearing operates at lower eccentricity ratio for any value of deformation coefficient ($\overline{\psi}$) .It is also observed that the attitude angle decreases with increase in deformation coefficient. For micropolar lubricant the value of attitude angle obtained is more than that obtained for Newtonian lubricant. These curves indicate that from the designers point of view micropolar fluids show less stability than Newtonian fluids.

Fig. 5.18 shows the variation of frictional force with the change in deformation coefficient for circular bearings. From Fig. 5.18 it is noted that at higher eccentricity ratio, a large reduction in frictional force is obtained with increase in deformation coefficient for circular bearings. For a fixed value of mass transfer rate the frictional force increase with increase in volume concentration of additives for any value of eccentricity ratio and deformation coefficient, but it decreases with increase in deformation coefficient.

The variations of stiffness coefficients $\overline{S}_{11}, \overline{S}_{12}, \overline{S}_{21}$ and $\overline{S}_{22}$ with increase in deformation coefficient are shown in Figs. 5.19-5.22. All these stiffness coefficients decrease with increase in $\overline{\psi}$, but all the values of stiffness coefficients except that of S_{12} increase with increase in λ_{Cr}.

The changes in damping coefficients with the increase in deformation coefficient are shown in Figs. 5.23-5.25. From these Figures it is observed that all the damping coefficients except B_{11} decrease with increase in deformation coefficient.

The variations of threshold speed with respect to deformation coefficient are shown in Fig. 5.26 for circular bearings. It is observed that threshold speed increases with increase in deformation coefficient at $\varepsilon = 0.4$. But at high values of eccentricity ratio ($\varepsilon = 0.8$) threshold speed decreases with increase in deformation

coefficient up to a certain value and after that it increases with increase in deformation coefficient. At any value of deformation coefficient and mass transfer rate the values of threshold speed obtained are less than those obtained for flexible bearings with Newtonian lubricant ($K_s = 0$, $\lambda_{Cr} = 0$). It is also observed from the graph that at low value of deformation coefficient and high eccentricity ratio the values of threshold speed tends to infinity which means that the system is always stable under the above conditions.

The changes of damped frequencies of whirl with respect to the deformation coefficient are shown in Fig. 5.27 for circular bearings. The damped frequency of whirl decreases with increase in deformation coefficient when eccentricity ratio is small ($\varepsilon = 0.4$). But at high eccentricity ratios ($\varepsilon = 0.8$), the damped frequency of whirl first increases, attains a maximum value and then decreases. It can be noted that at low values of deformation coefficient the damped frequency of whirl tends to become negative which indicates that the system will always be stable. It is also observed that at any value of deformation coefficients the increase in volume concentration of additives increases the value of damped frequency of whirl obtained for micropolar lubricants. The increase in mass transfer rate also affects the damped frequency of whirl. From all these curves it may noted that the flexibility of the bearing liner, volume concentration of additives and mass transfer rate affect both static and dynamic performance characteristics.

Fig.5.28 shows the pressure and deformation fields in the case of circular bearings.

The dimensional values of performance characteristics obtained from EHD analysis of circular bearings in some typical cases are given in Tables 5.4 and 5.5. From these Tables it is seen that the static characteristics $\overline{W}, \overline{Q}_z$ and ϕ and dynamic characteristics $\overline{S}_{11}, \overline{S}_{12}, \overline{S}_{21}, \overline{S}_{22}$ and $\overline{B}_{11}, B_{12} \approx \overline{B}_{21}, \overline{B}_{22}$, $\overline{\omega}_d$ and $\overline{\omega}_{th}$ are affected by the flexibility of bearing liner and volume concentration of additives of the lubricant. For eg., at $\varepsilon = 0.8$ and $\overline{\psi} = 0.1$ the load carrying capacity

decreases from 34.33 to 16.08 KN which indicates that there is 53.16 percent reduction in the load carrying capacity due to the presence of flexibility of bearing liner for Newtonian lubricants (Tables 5.3 and 5.4). The presence of volume concentration of additives ($\lambda c_r = 0.4$) increases load carrying capacity at flexibility $\overline{\psi} = 0.1$ from 16.08 to 26.02 there by reducing the load carrying capacity of bearing only by 24 percent. From this it is observed that the assumption of Newtonian lubricant will not be valid especially when the bearing operates at high eccentricity ratio because significant changes in the values of performance characteristics are obtained for micropolar lubricants.

The percentage deviations in all the performance characteristics of circular bearings are obtained and presented in Tables 5.6 and 5.7.

5.2 TWO LOBE BEARINGS

The various performance characteristics are obtained for two lobe bearings considering them as rigid and deformable when operating with Newtonian and micropolar lubricants. These characteristics are determined for different values of eccentricity ratios, volume concentration of additives, mass transfer rate and deformation coefficients.

5.2.1 Two Lobe Rigid Bearings

The results obtained from the analysis of rigid two lobe bearings operating with Newtonian and micropolar lubricants are presented in Figs. 5.29-5.42.

The changes in load carrying capacity with the change in volume concentration of additives for two lobe bearings operating at eccentricity ratios $\varepsilon = 0.25$ and $\varepsilon = 0.45$ are shown in Fig. 5.29. It is observed that the load carrying capacity increases significantly with increase in volume concentration of additives and mass transfer rate especially when the bearing operates at high eccentricity ratio($\varepsilon = 0.45$).Effect of mass transfer of additives on the load carrying capacity becomes significant at high values of volume concentration of additives.

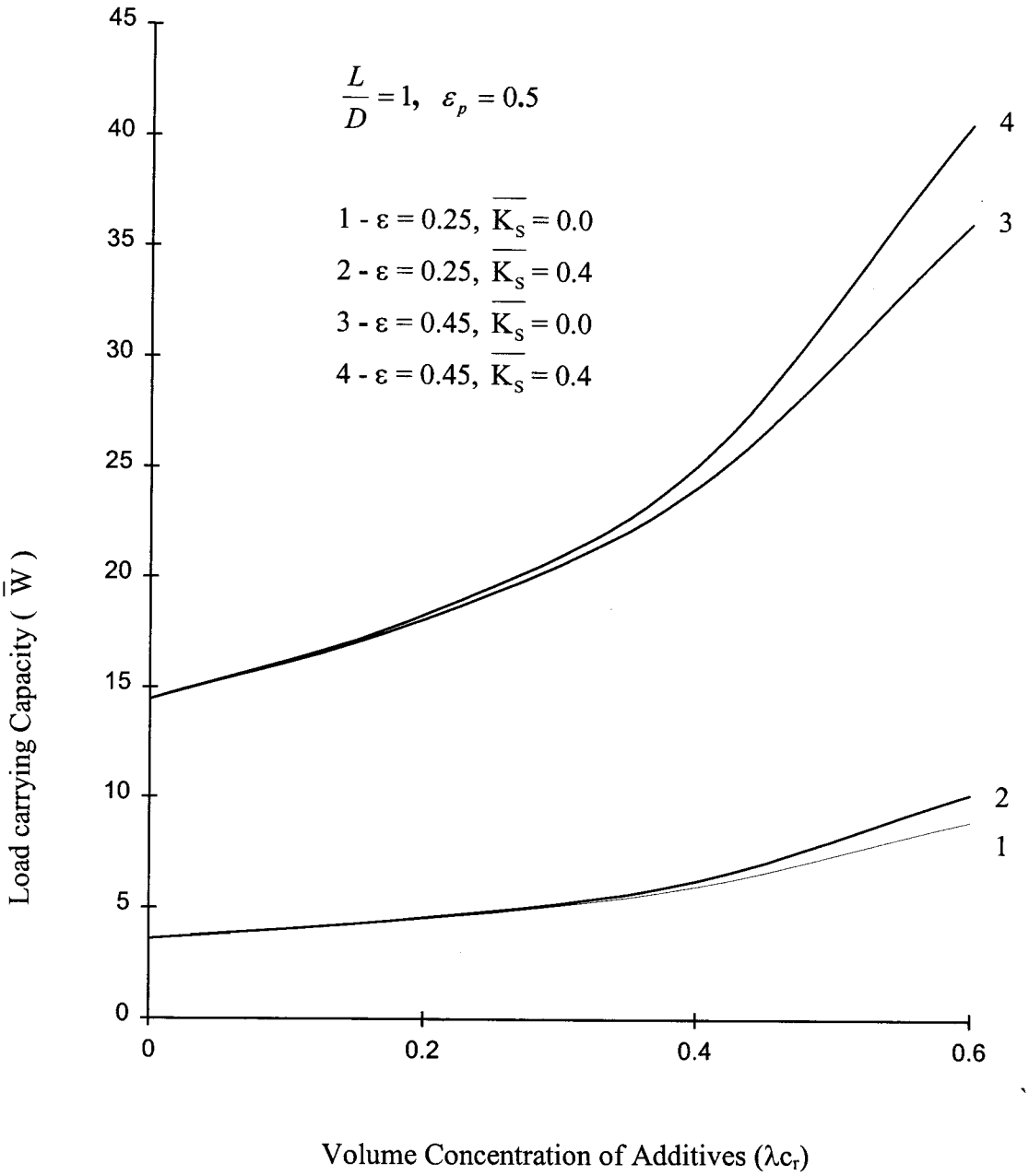

Fig. 5. 29 Load carrying Capacity ($\overline{W}$)vs Volume Concentration of Additives (λc_r) in Two Lobe Bearing

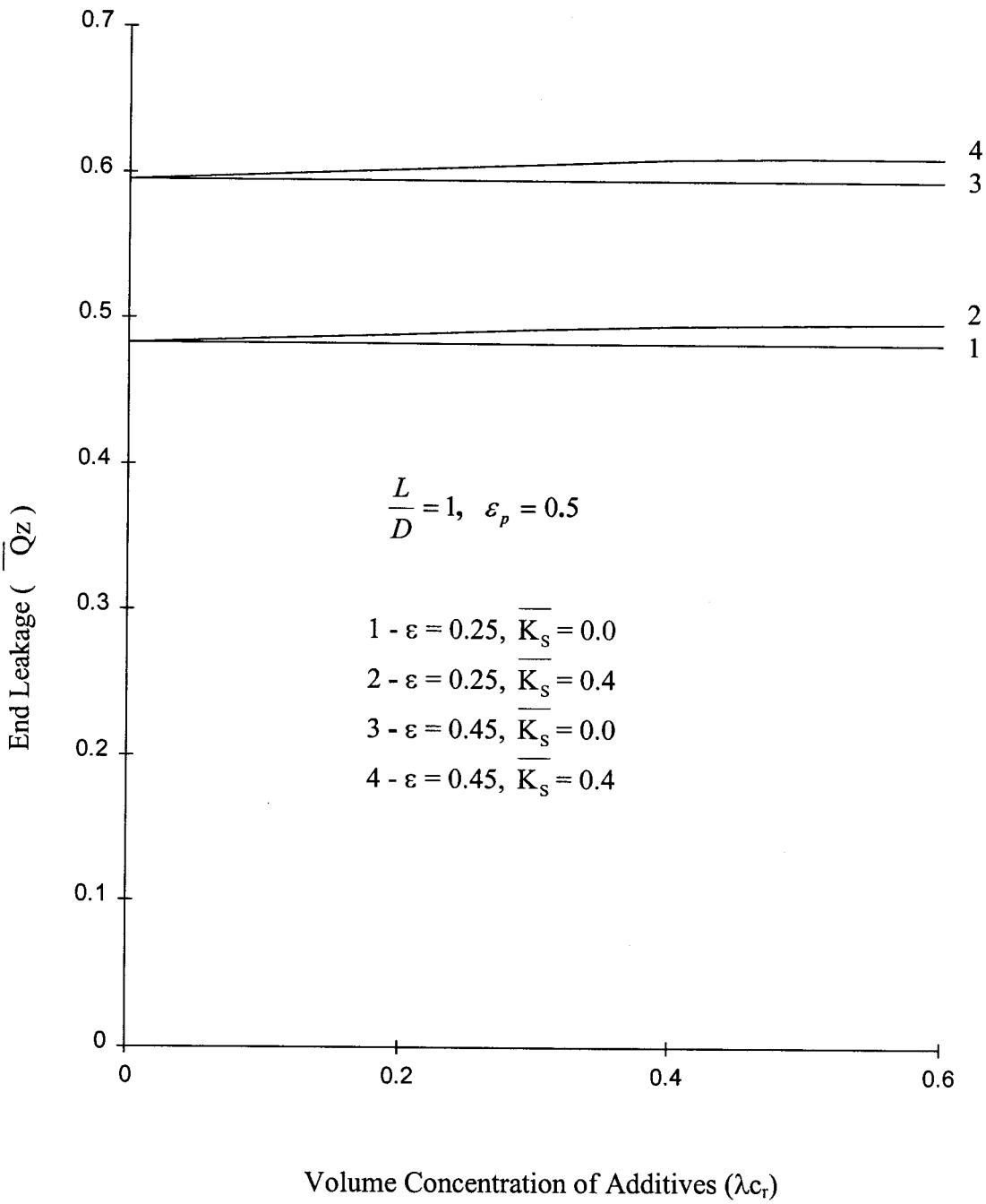

Fig. 5.30 End Leakage ($\overline{Q}_z$) vs Volume Concentration of Additives (λc_r) in Two Lobe Bearing

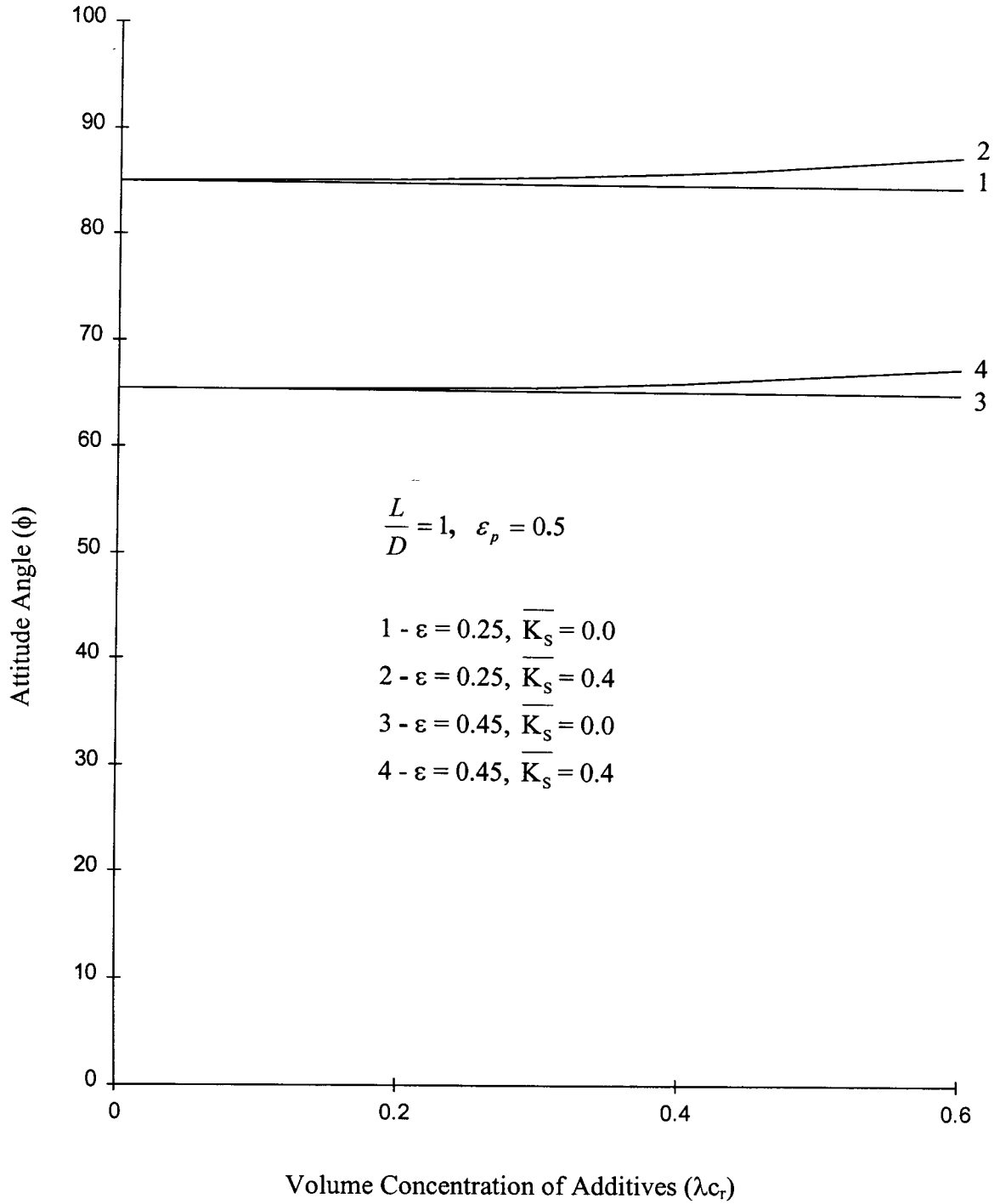

Fig. 5.31 Attitude Angle (ϕ) vs Volume Concentration of Additives (λc_r) in Two Lobe Bearing

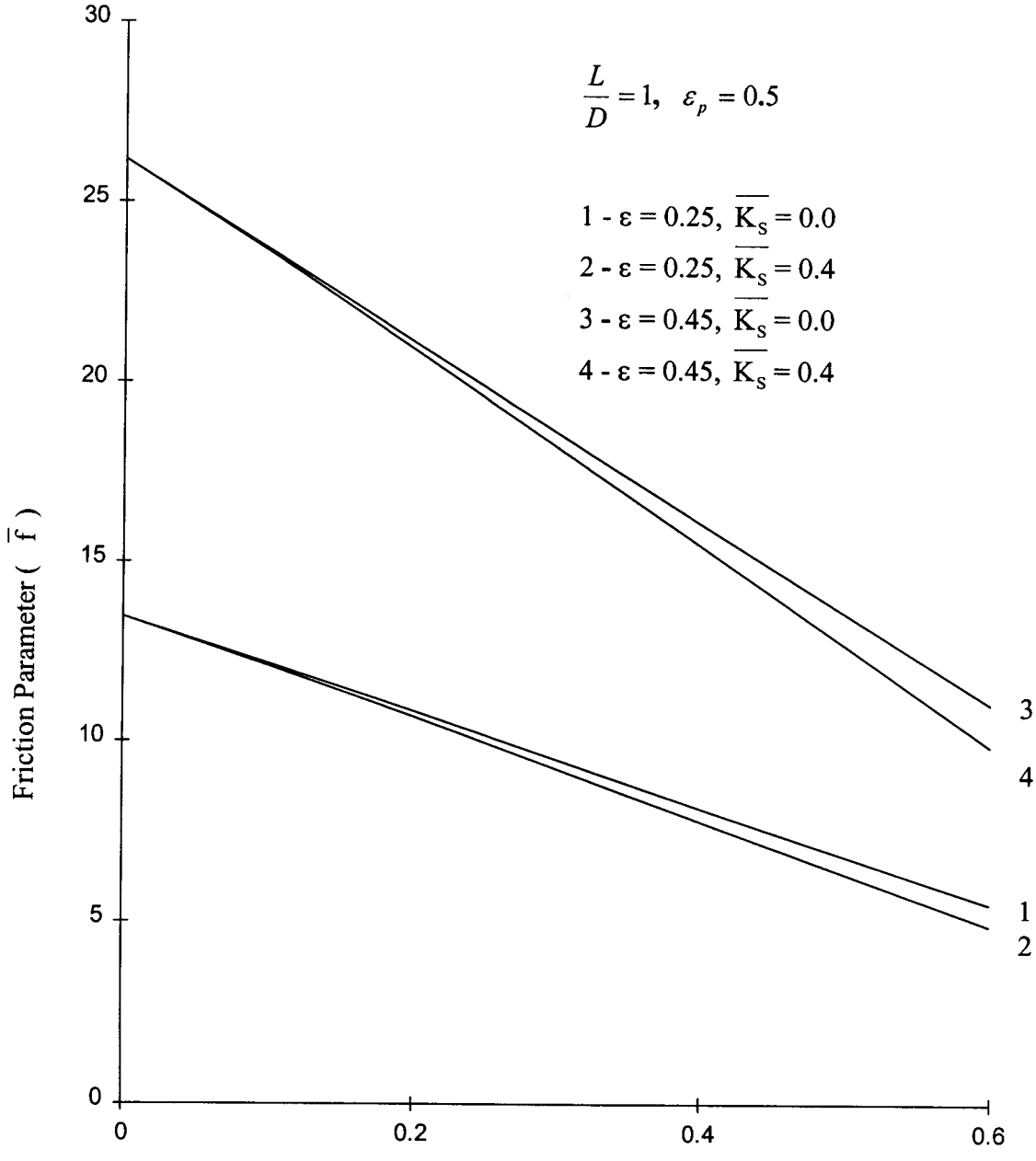

Fig. 5.32 Friction Parameter($\bar{f}$) vs Volume Concentration of Additives (λc_r) in Two Lobe Bearing

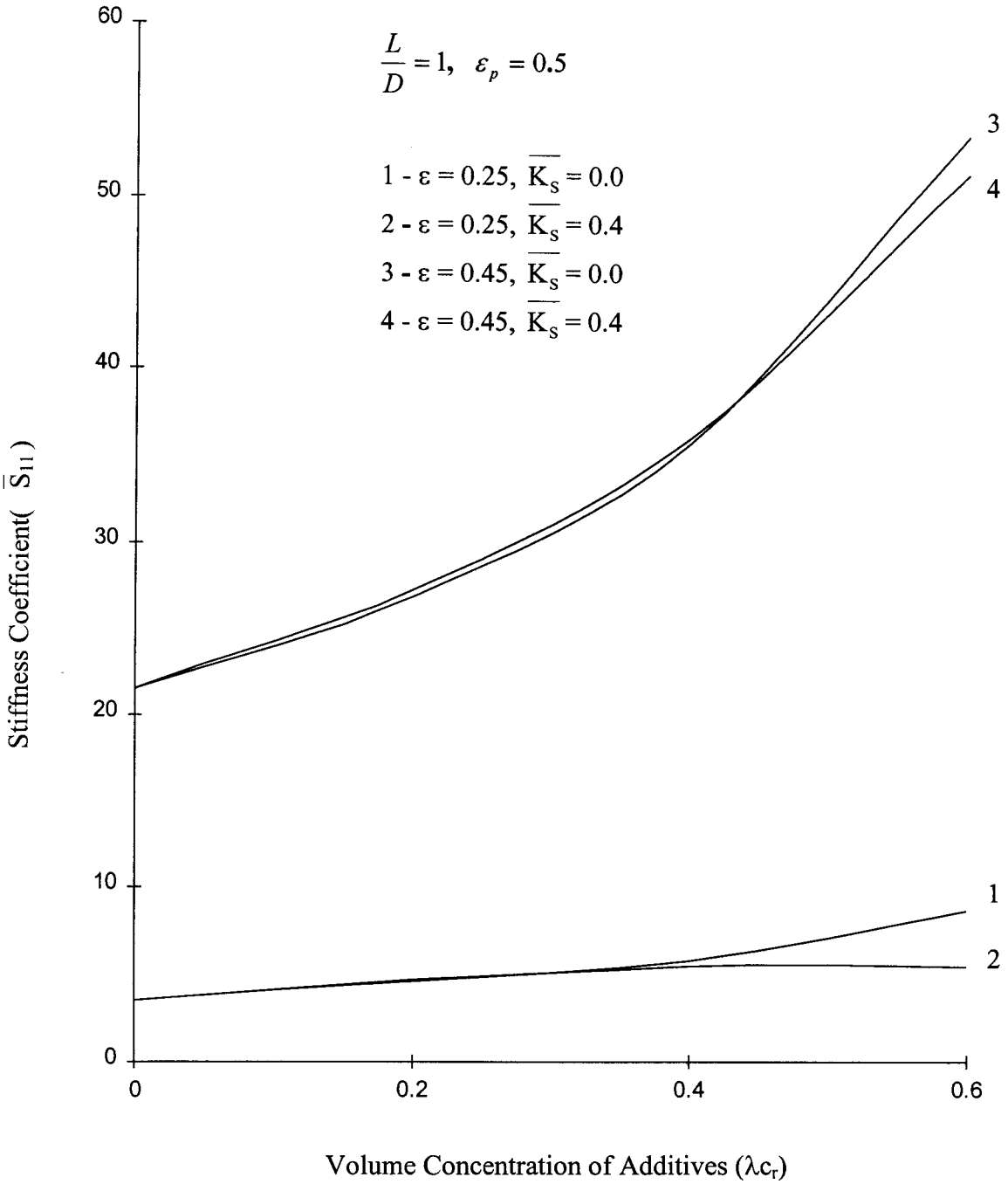

Fig. 5.33 Stiffness Coefficient($\overline{S}_{11}$) vs Volume Concentration of Additives (λc_r) in Two Lobe Bearing

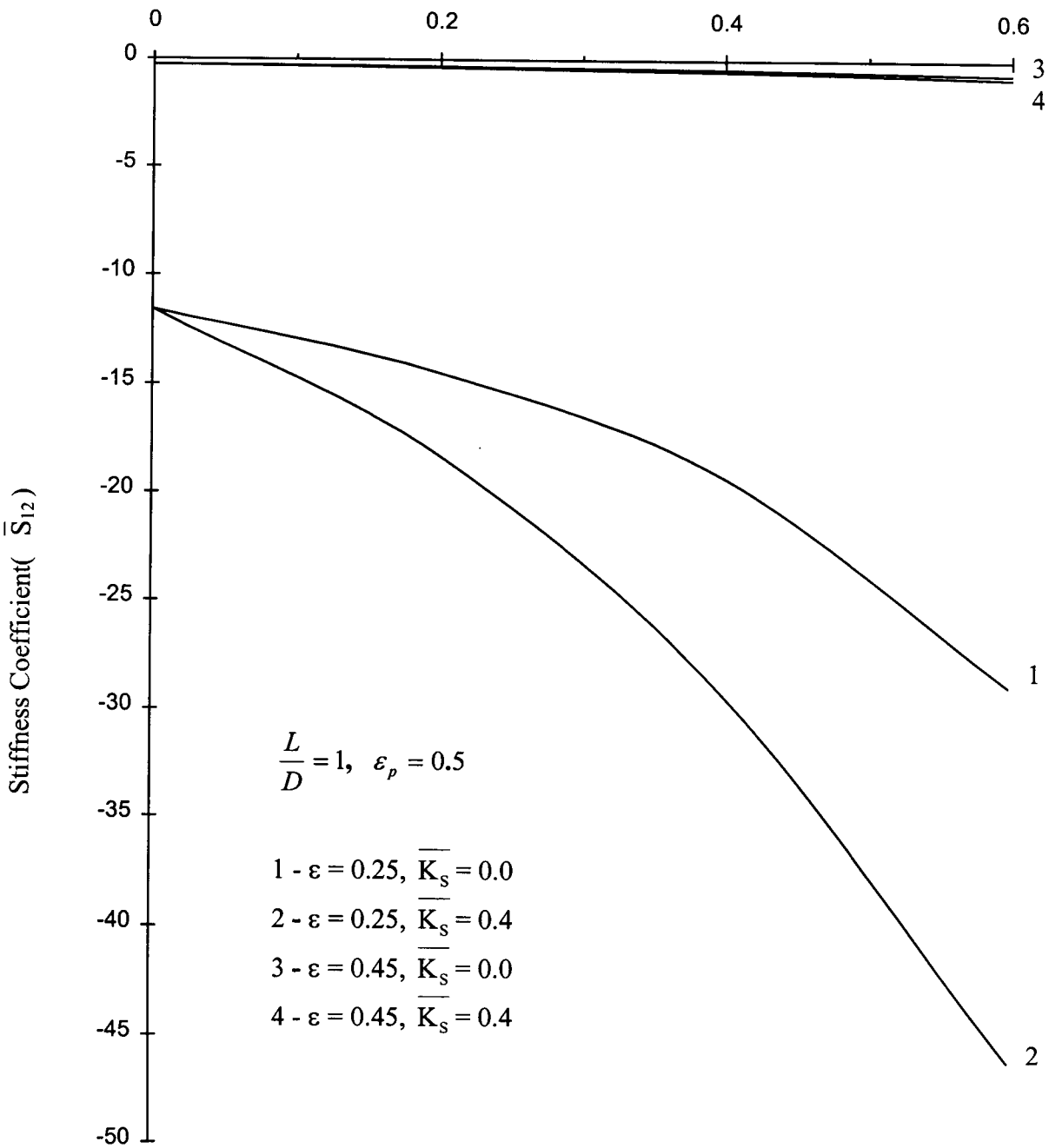

Fig. 5.34 Stiffness Coefficient($\bar{S}_{12}$) vs Volume Concentration of Additives (λc_r) in Two Lobe Bearing

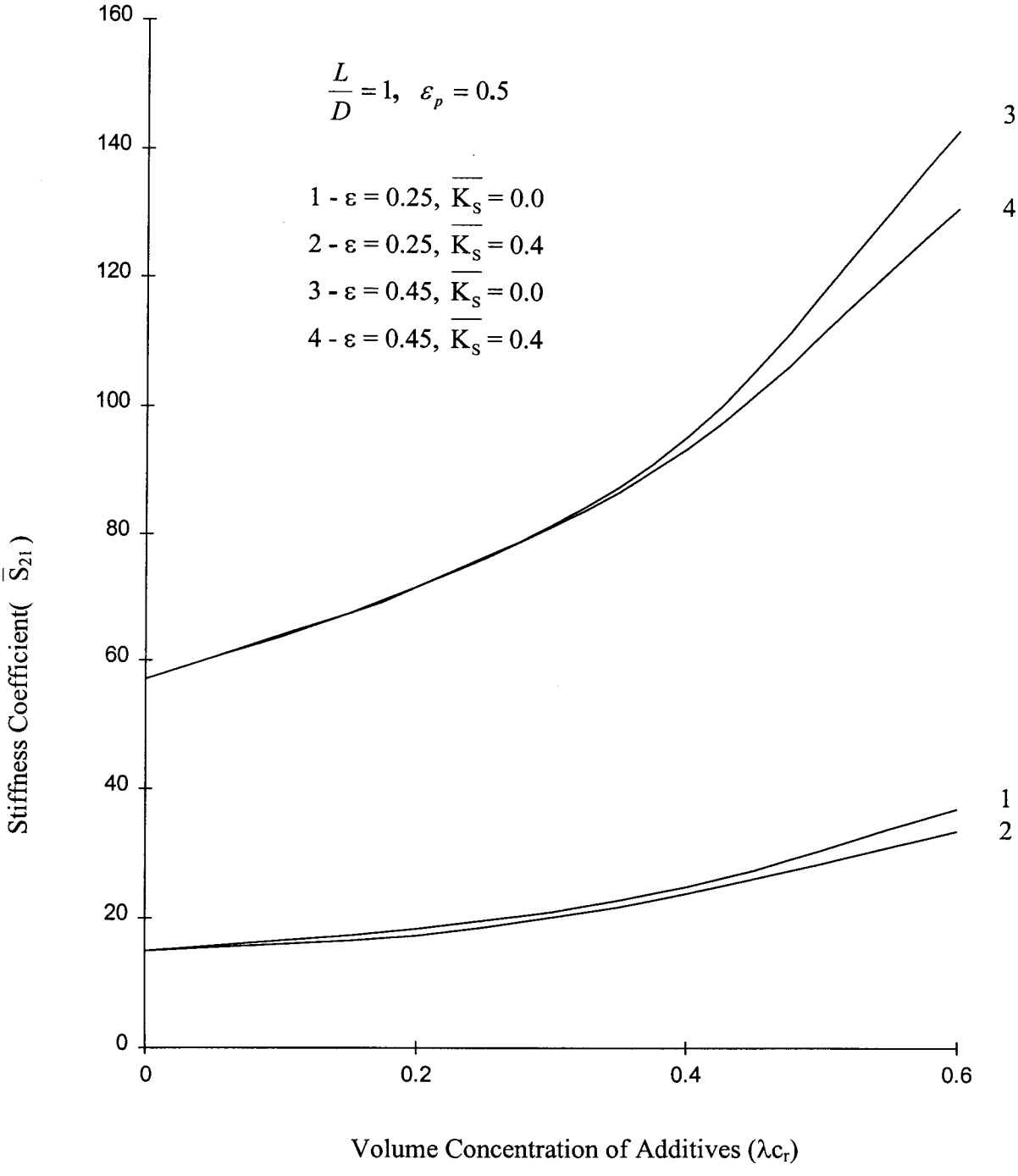

Fig. 5.35 Stiffness Coefficient($\overline{S}_{21}$) vs Volume Concentration of Additives (λc_r) in Two Lobe Bearing

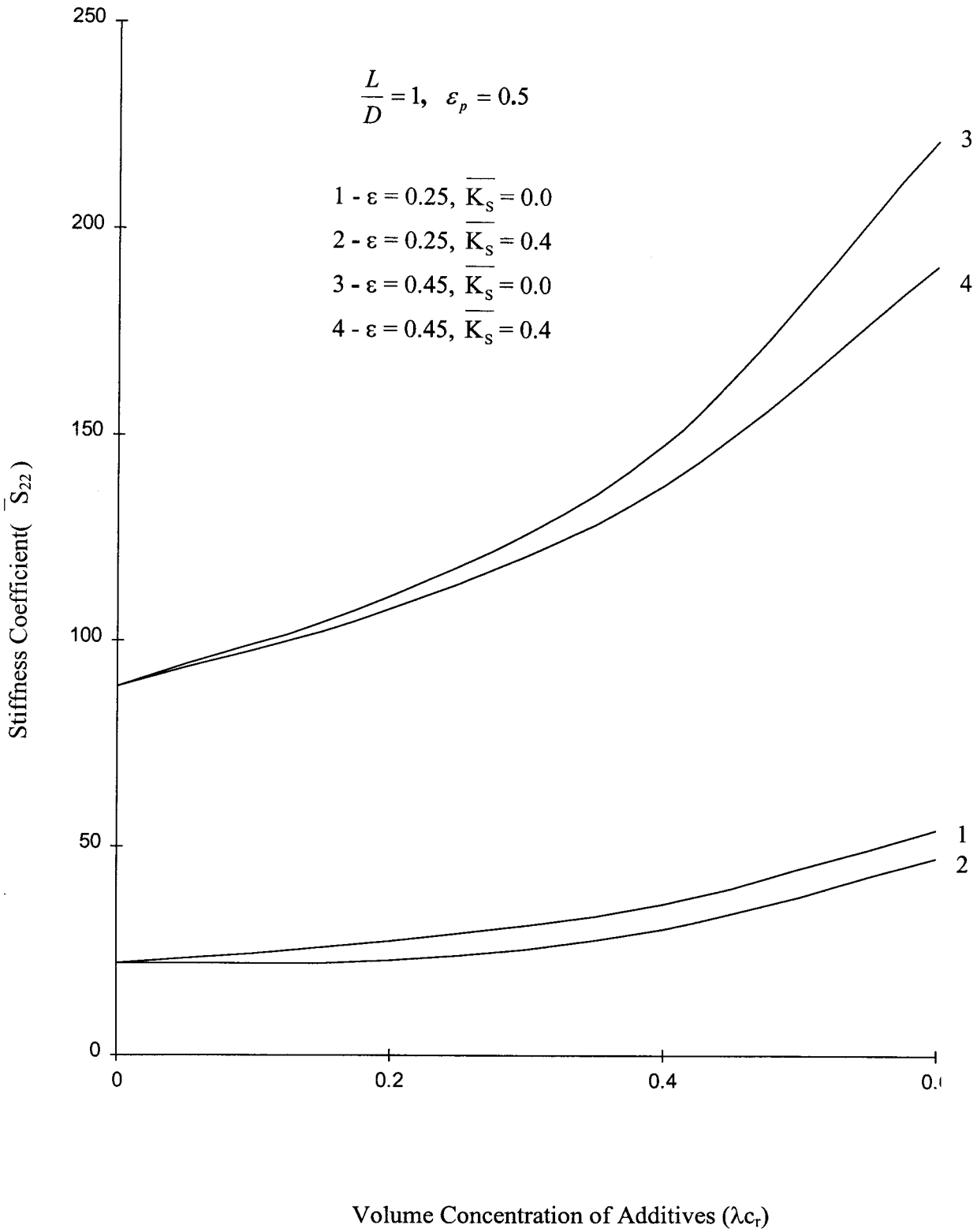

Fig. 5.36 Stiffness Coefficient($\overline{S}_{22}$) vs Volume Concentration of Additives (λc_r) in Two Lobe Bearing

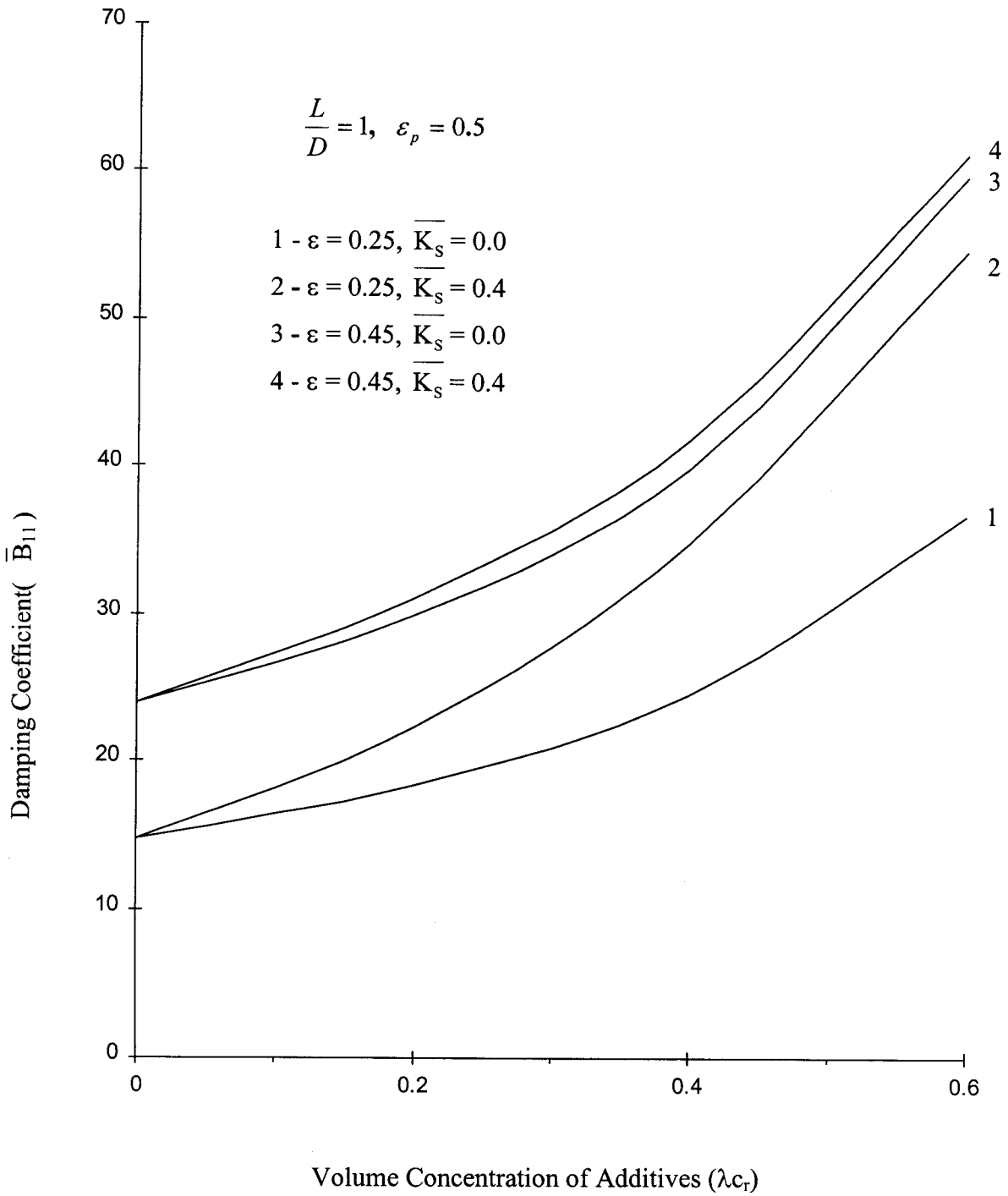

Fig. 5.37 Damping Coefficient($\bar{B}_{11}$) vs Volume Concentration of Additives (λc_r) in Two Lobe Bearing

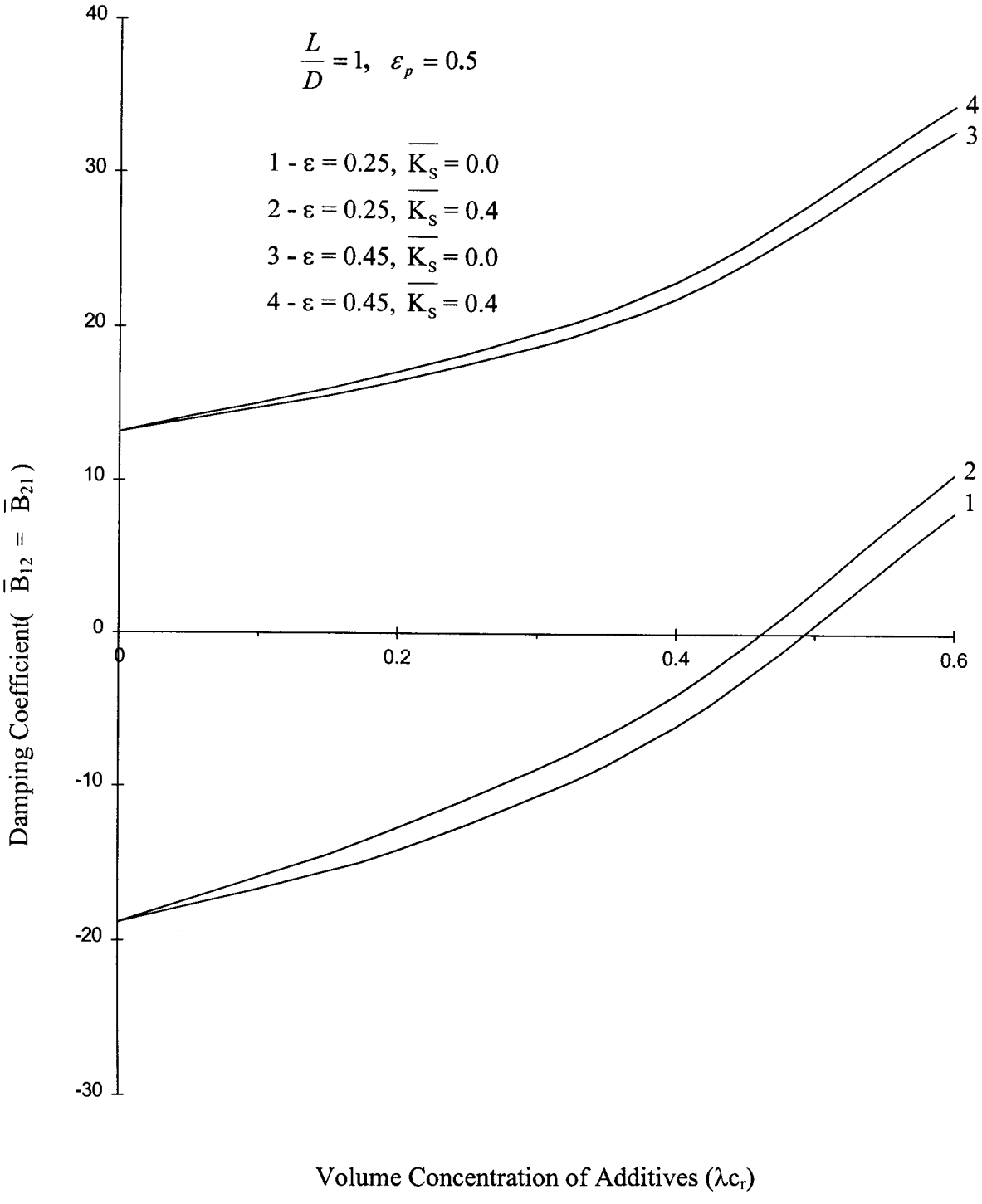

Fig. 5.38 Damping Coefficient($\bar{B}_{12} = B_{21}$) vs Volume Concentration of Additives (λc_r) in Two Lobe Bearing

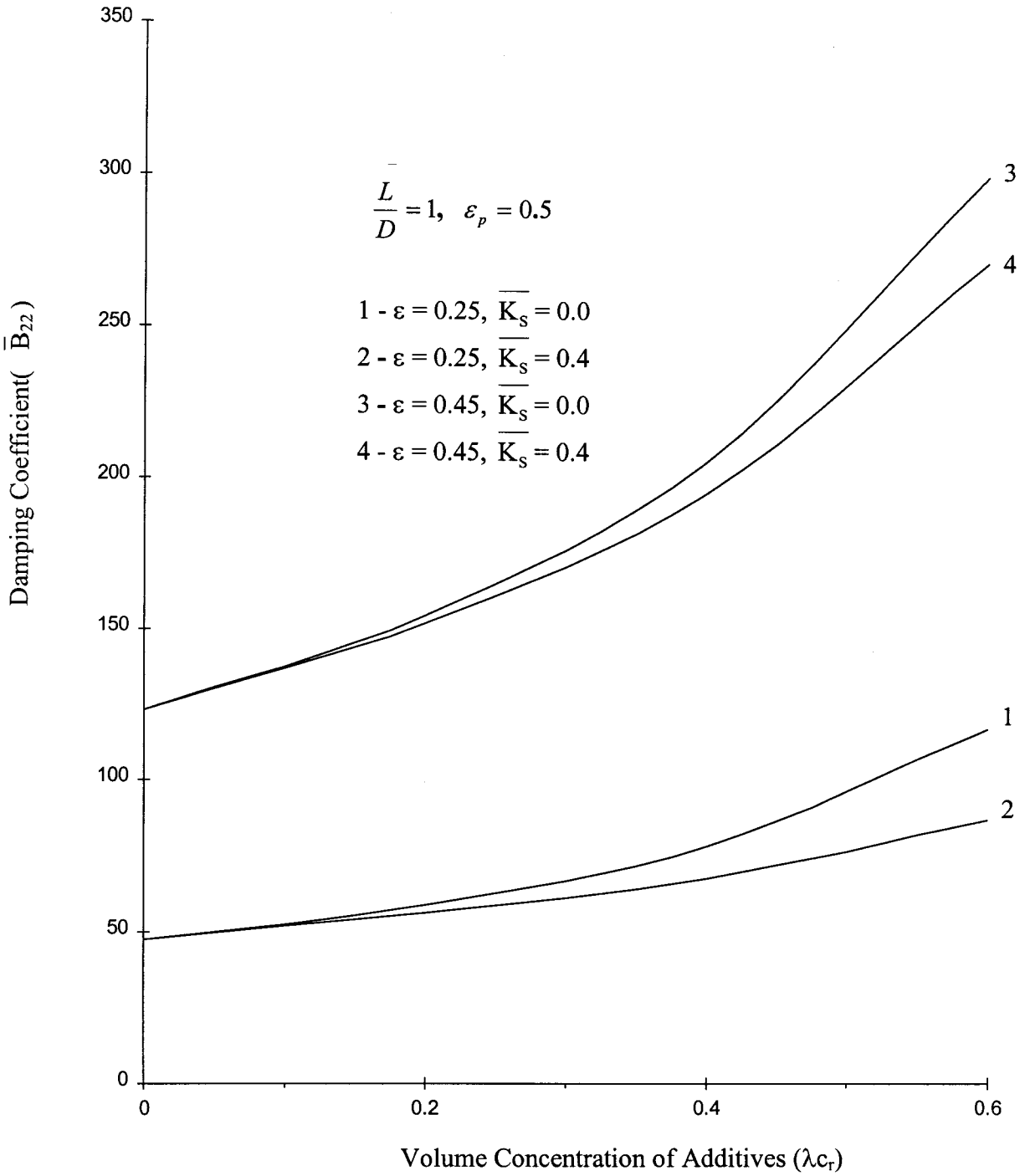

Fig. 5.39 Damping Coefficient($\bar{B}_{22}$) vs Volume Concentration of Additives (λc_r) in Two Lobe Bearing

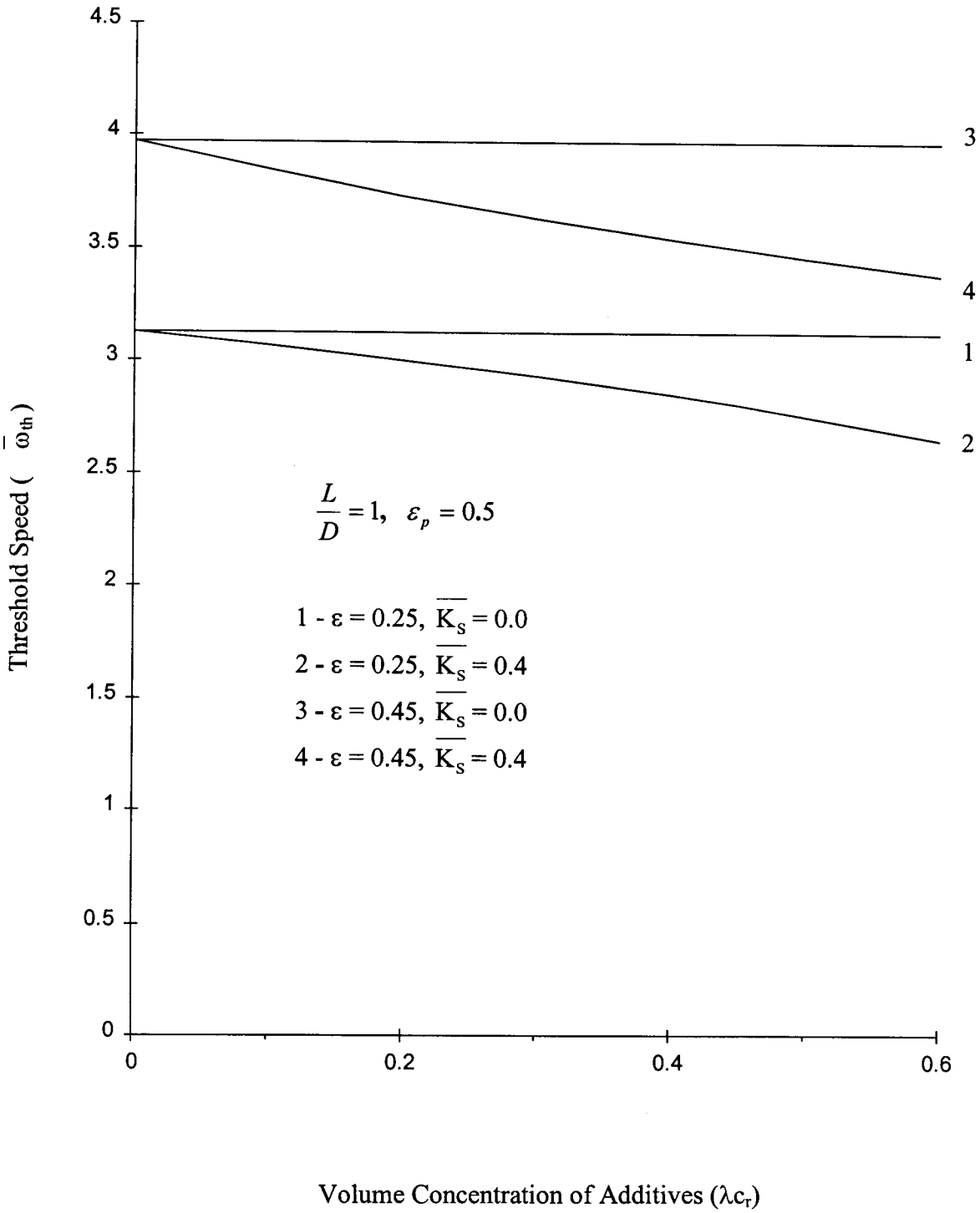

Fig. 5.40 Threshold Speed ($\bar{\omega}_{th}$) vs Volume Concentration of Additives (λc_r) in Two Lobe Bearing

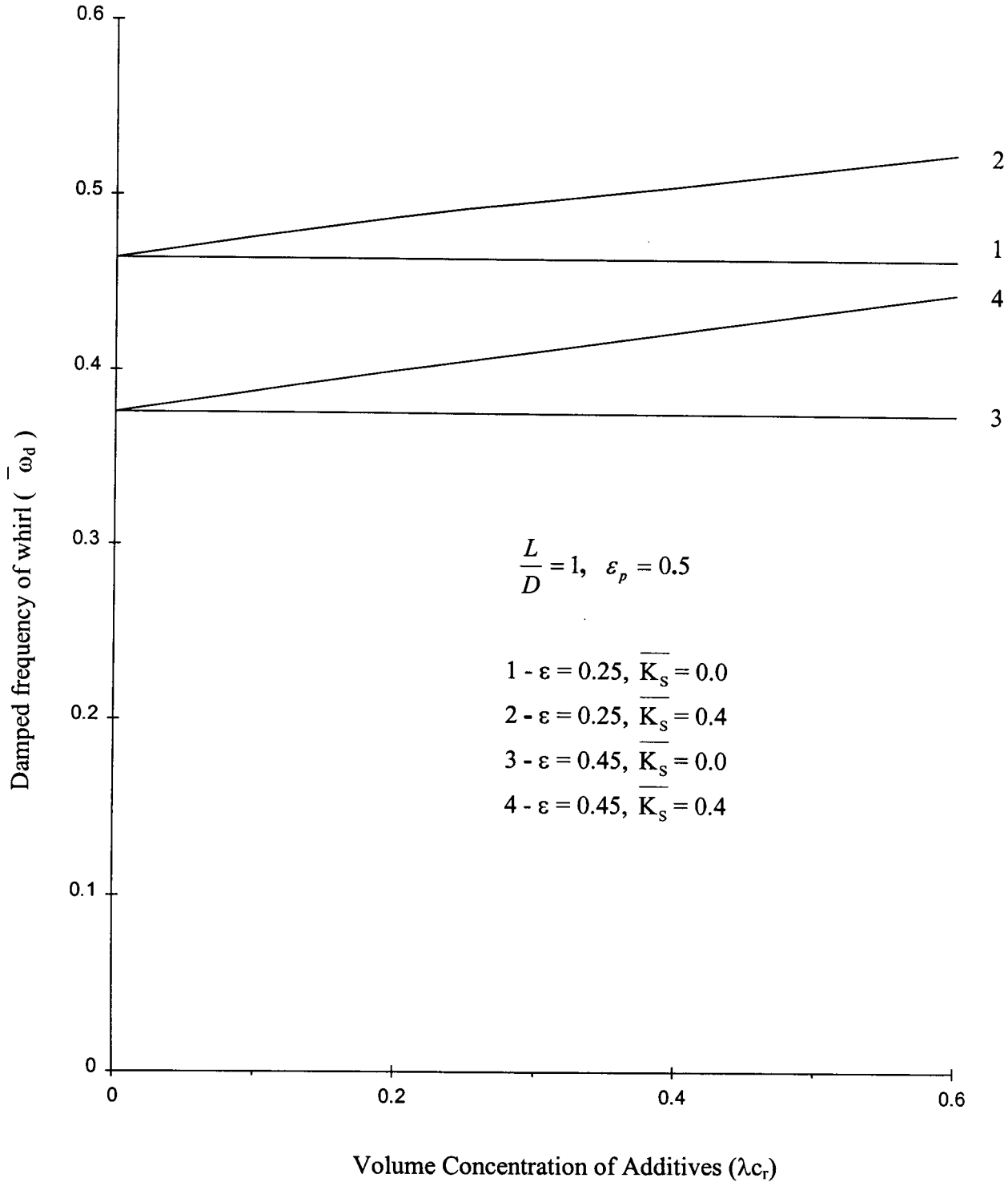

Fig. 5.41 Damped Frequency of Whirl ($\bar{\omega}_d$) vs Volume Concentration of Additives (λc_r) in Two Lobe Bearing

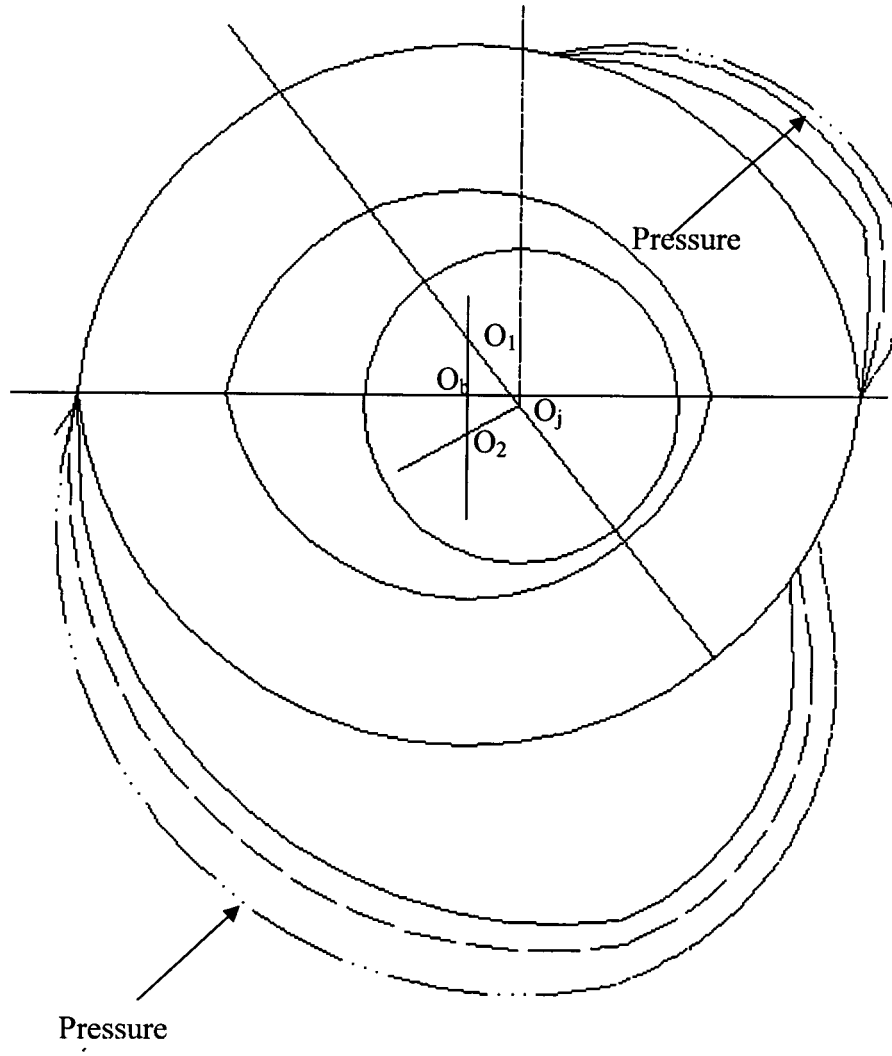

—————— $\varepsilon = 0.25; \lambda c_r = 0.0; K_x = 0.0; \psi = 0.0$

— — $\varepsilon = 0.25; \lambda c_r = 0.2; K_x = 0.4; \psi = 0.0$

—...— $\varepsilon = 0.25; \lambda c_r = 0.4; K_x = 0.4; \psi = 0.0$

Fig. 5.42 Computed Pressure Field for Two Lobe Rigid Bearing

The variations of end leakage and attitude angle with increase in volume concentration of additives are shown in Fig. 5.30 and 5.31 respectively. It is noted that these characteristics do not change with volume concentration when there is no mass transfer rate ($K_s = 0$). The same trend has been obtained in the circular bearings also. However when there is mass transfer rate, end leakage and attitude angle increase with increase in volume concentration of additives. They also increase with increase in mass transfer rate.

Fig. 5.32 shows the variation of friction parameter with the change in volume concentration of additives. From this Figure it is observed that the friction parameter decreases with increase in volume concentration of additives. This is because the increase in frictional force is less than the increase in load carrying capacity due to increase in volume concentration of additives. It is also noted that friction parameter decreases with increase in mass transfer rate.

The variations of stiffness and damping coefficients with the change in volume concentration of additives for two lobe bearings are shown in Figs. 5.33-5.39. All the coefficients except stiffness coefficients S_{12} increase with increase in volume concentration of additives.

The variations of threshold speed and damped frequency of whirl are shown in Fig. 5.40 and Fig. 5.41 respectively. It is observed that threshold speed and damped frequency of whirl are not affected by volume concentration of additives when there is no mass transfer rate as in the case of circular bearings. The threshold speed decreases with increase in volume concentration of additives, but damped frequency of whirl increases with increase in volume concentration. Threshold speed and damped frequency of whirl are affected by mass transfer of additives.

The pressure fields computed for two lobe rigid bearings with Newtonian and micropolar lubricants when the bearing operates at eccentricity ratio $\varepsilon = 0.25$ are shown in Fig. 5.42.

The dimensional values of the performance characteristics of two lobe rigid bearings operating at different eccentricity ratios are given in Table 5.8. The effect of volume concentration of additives and mass transfer rate on the various performance characteristics of rigid two lobe bearing is given in this Table. It shows that appreciable changes in the performance characteristics are obtained for micropolar lubricants when they are compared with the performance characteristics for Newtonian lubricants.

5.2.2 Elastic Two Lobe Bearings

Various performance characteristics for two lobe bearings considering the effect of deformation of bearing liner when the bearing operates with Newtonian and micropolar lubricants are obtained.

To authenticate solution algorithm and computer program developed the load carrying capacity obtained for flexible two lobe bearing with Newtonian lubricant is compared with published results [67] in Fig. 5.43. From this Figure it is seen that the results are in good agreement.

The effect of deformation coefficient on the load carrying capacity of two lobe bearings for both Newtonian and micropolar lubricants is shown in Fig. 5.44. Significant reductions in load carrying capacity are observed for both Newtonian and micropolar lubricants when bearing operates at high ε. It is also noted that at low values of eccentricity ratio ($\varepsilon = 0.25$) due to the presence of additives (micropolar fluids) the load carrying capacity obtained at any value of deformation coefficient is more than that obtained for lubricants without additives (Newtonian lubricants).

The variation of end leakage with increase in deformation coefficient for two lobe bearings is shown in Fig. 5.45. It is seen that an appreciable change in the end leakage is obtained at higher values of deformation coefficient for any eccentricity ratio when it is compared with rigid bearings. When mass transfer rate increases, values of end leakage obtained increases for any values of eccentricity ratio and volume concentration of additives.

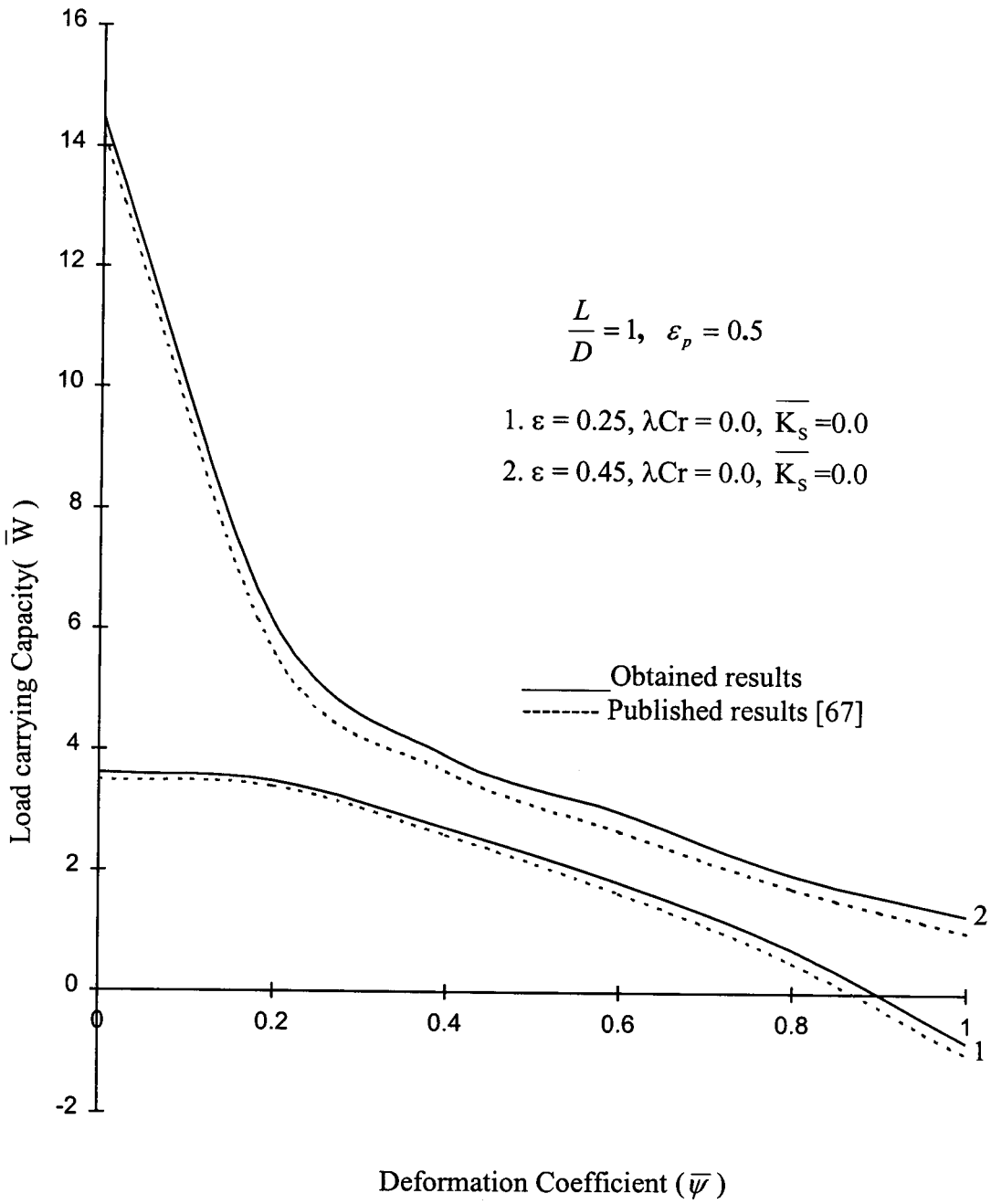

Fig. 5. 43 Load carrying Capacity ($\overline{W}$) vs Deformation Coefficient ($\overline{\psi}$) in Two Lobe Bearing with Newtonian Lubricants

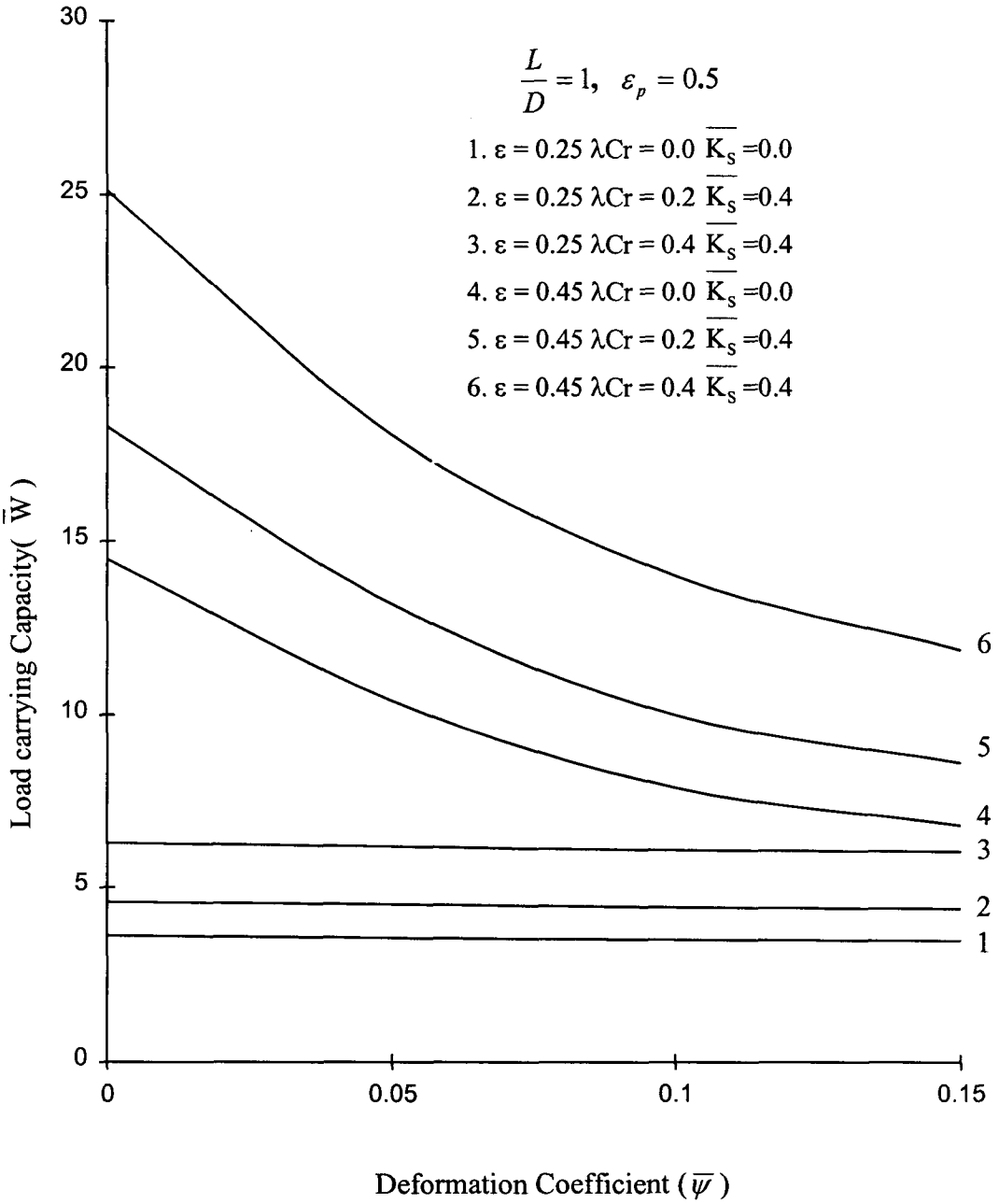

Fig. 5. 44- Load carrying Capacity ($\overline{W}$) vs Deformation Coefficient ($\overline{\psi}$) in Two Lobe Bearing

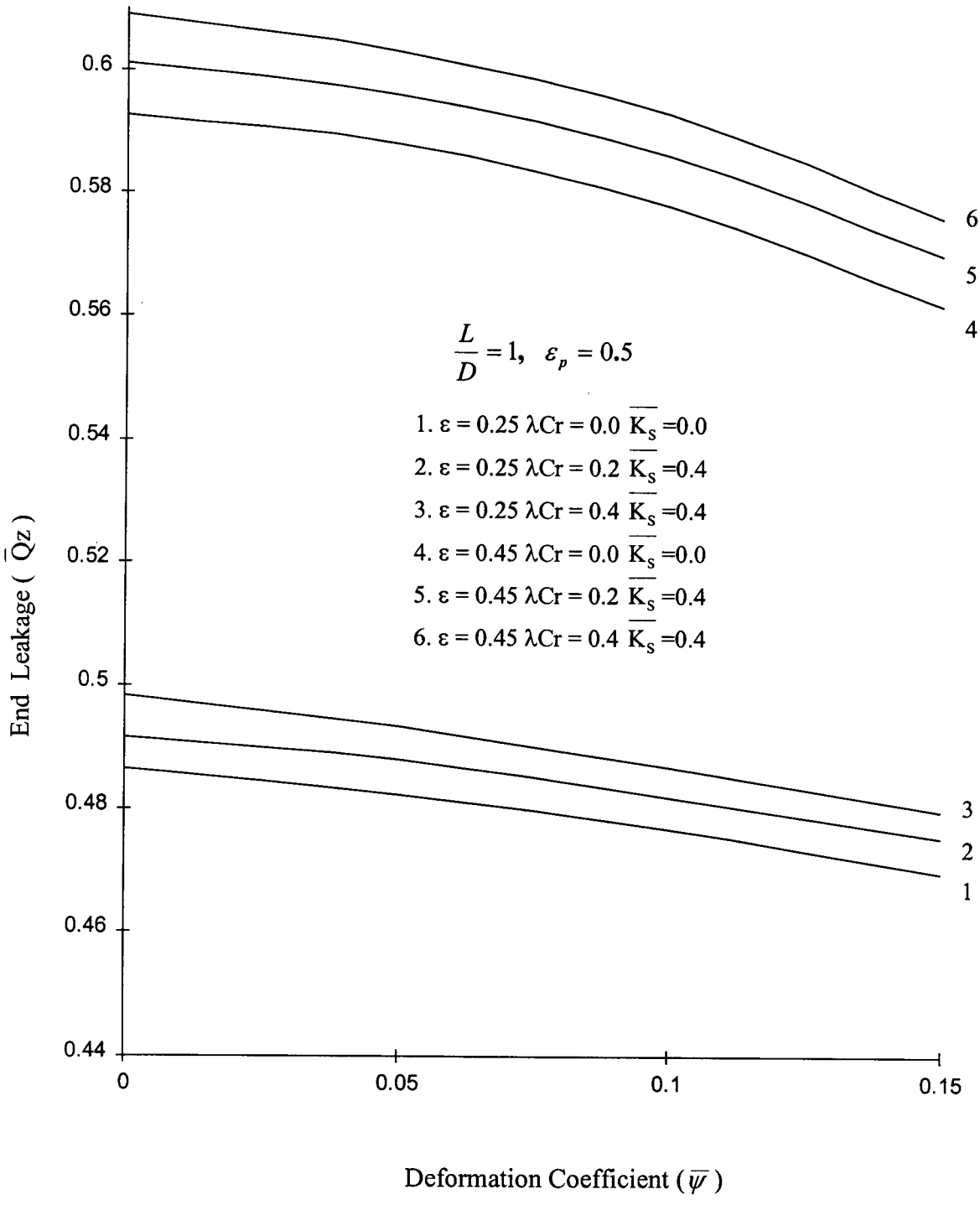

Fig. 5. 45 – End Leakage ($\bar{Q}_z$) vs Deformation Coefficient ($\bar{\psi}$) in Two Lobe Bearing

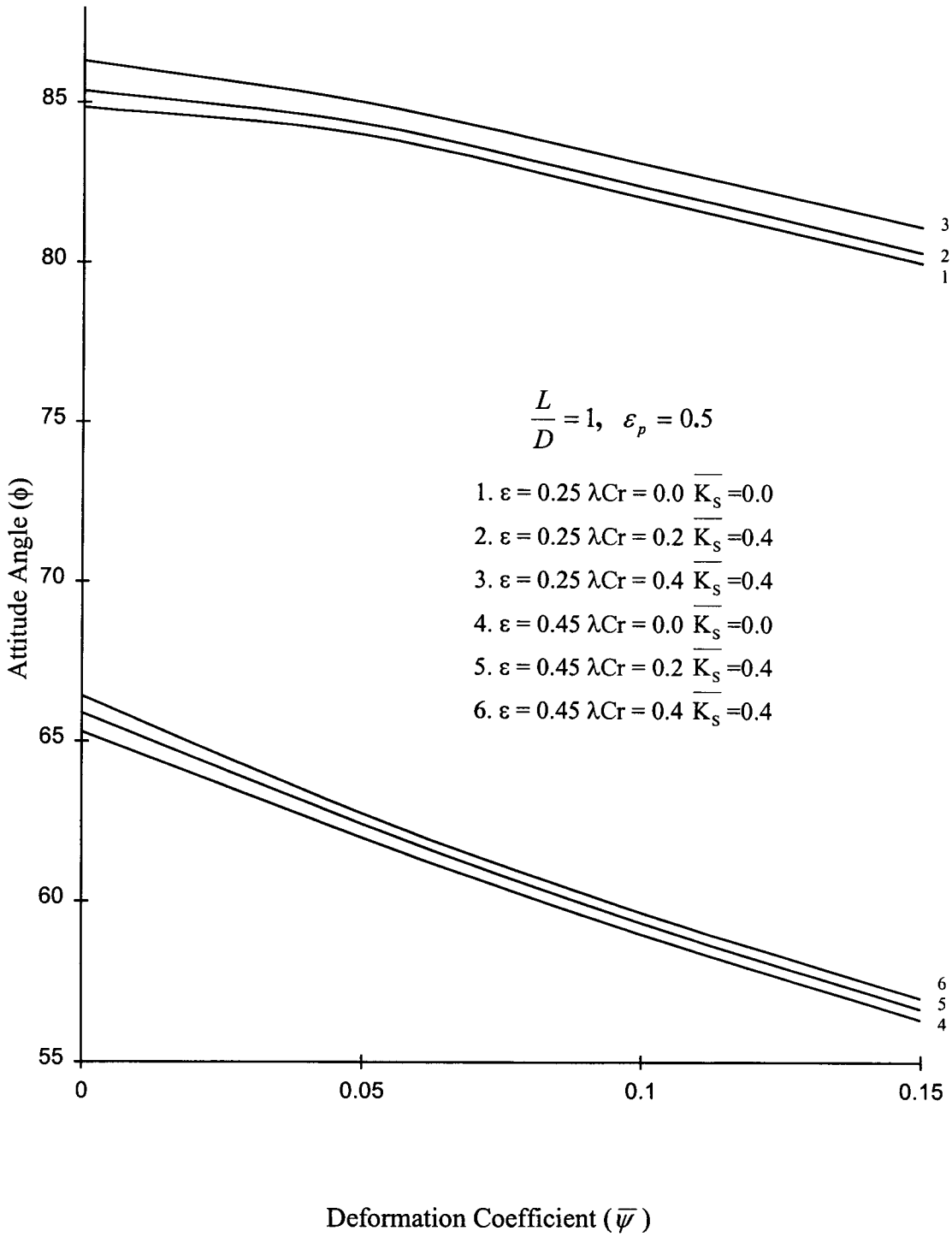

Fig. 5.46 – Attitude Angle (ϕ) vs Deformation Coefficient ($\overline{\psi}$)in Two Lobe Bearing

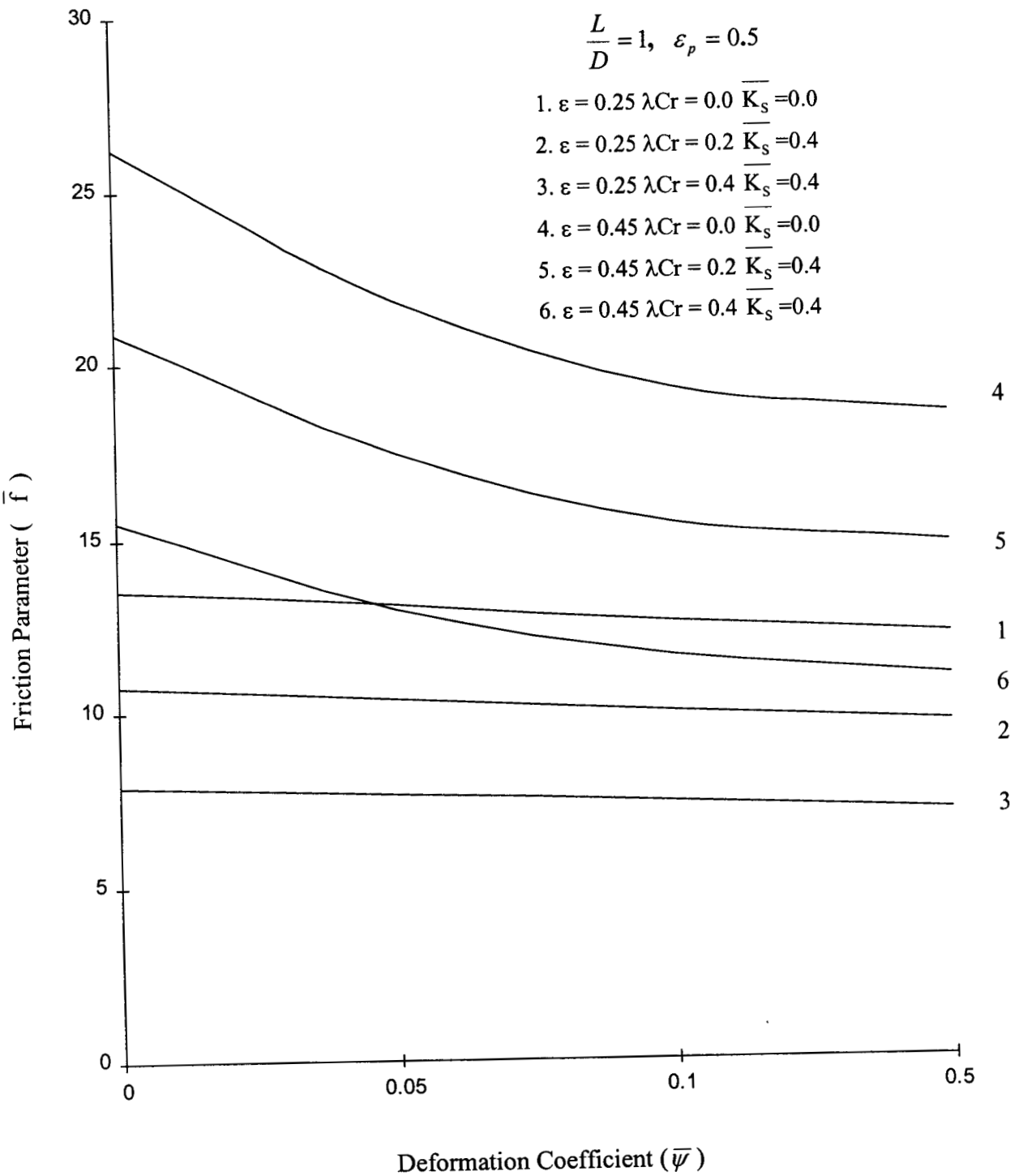

Fig. 5.47 – Friction Parameter ($\bar{f}$) vs Deformation Coefficient ($\overline{\psi}$) in Two Lobe Bearing

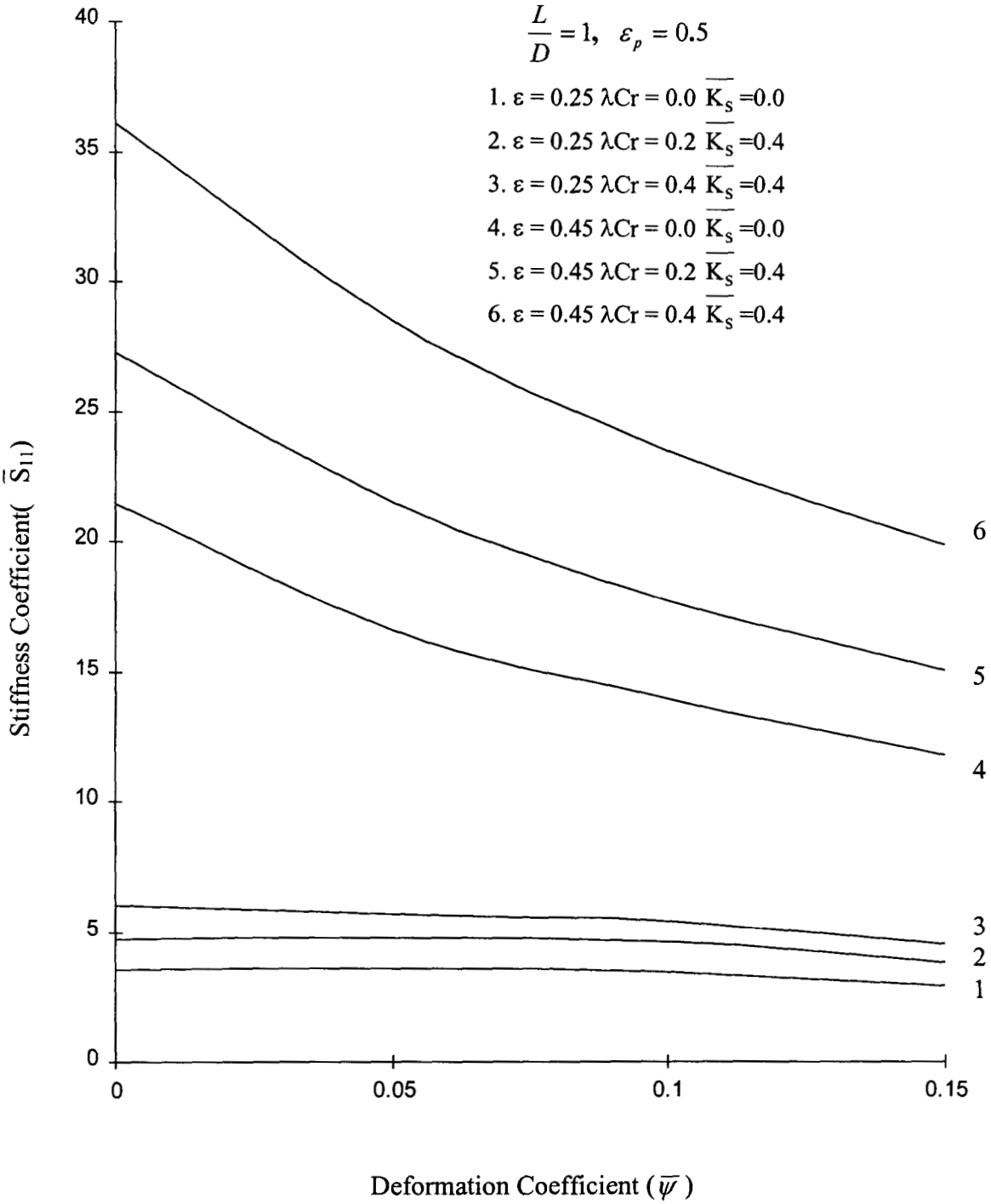

Fig. 5.48 – Stiffness Coefficient ($\overline{S_{11}}$) vs Deformation Coefficient ($\overline{\psi}$) in Two Lobe Bearing

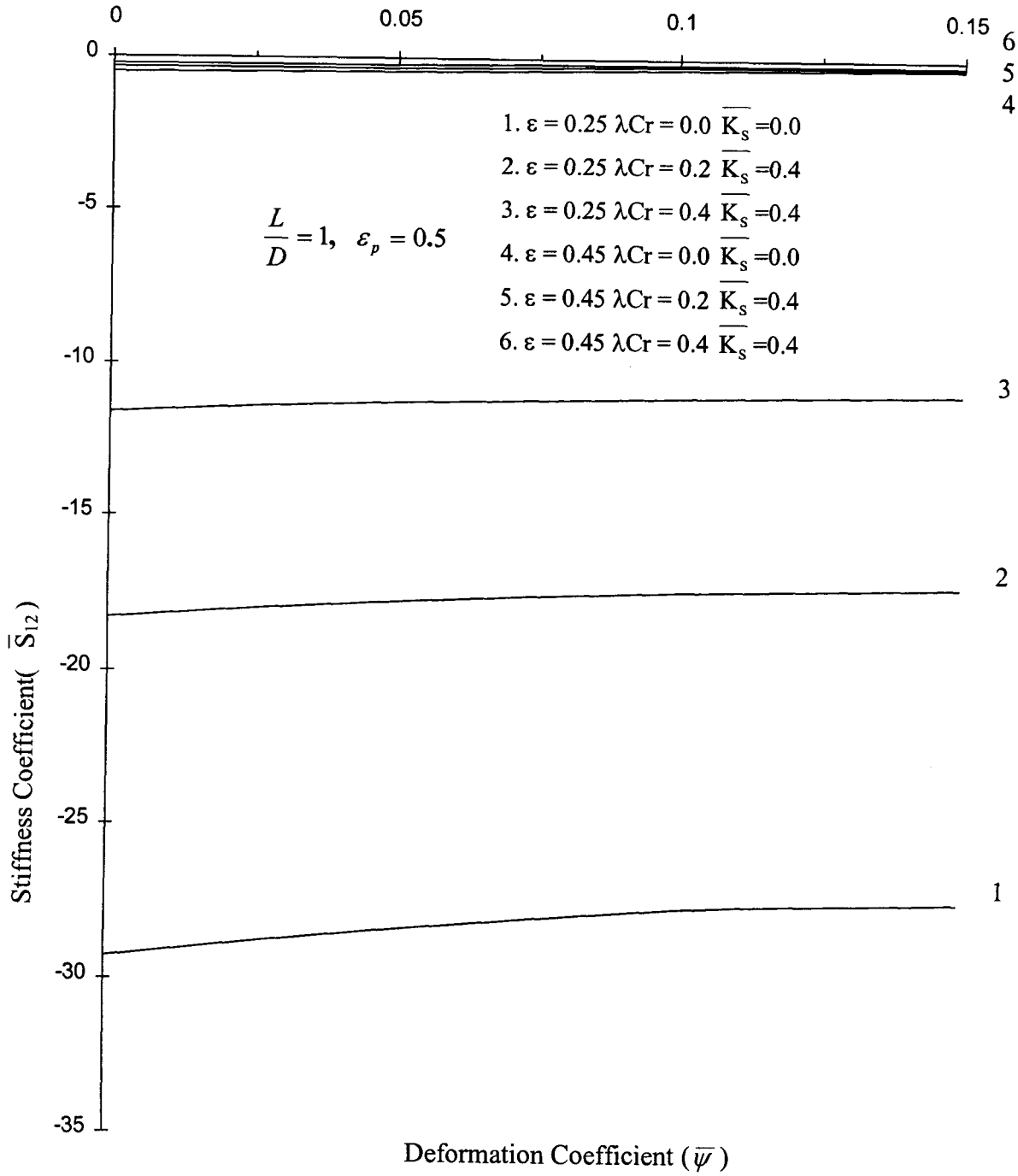

Fig. 5.49 – Stiffness Coefficient($\overline{S}_{12}$) vs Deformation Coefficient ($\overline{\psi}$) in Two Lobe Bearing

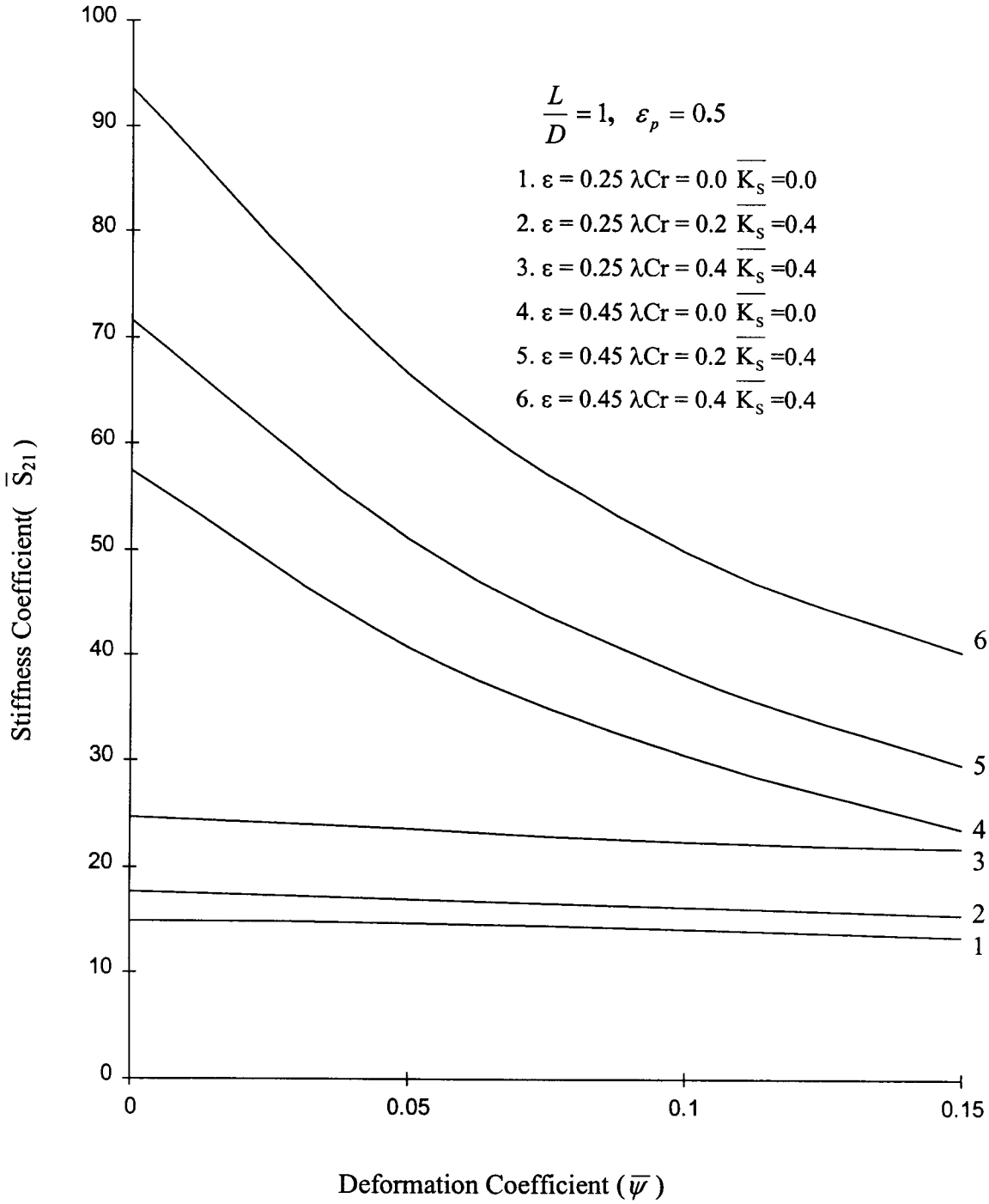

Fig. 5.50 – Stiffness Coefficient($\overline{S}_{21}$) vs Deformation Coefficient ($\overline{\psi}$) in Two Lobe Bearing

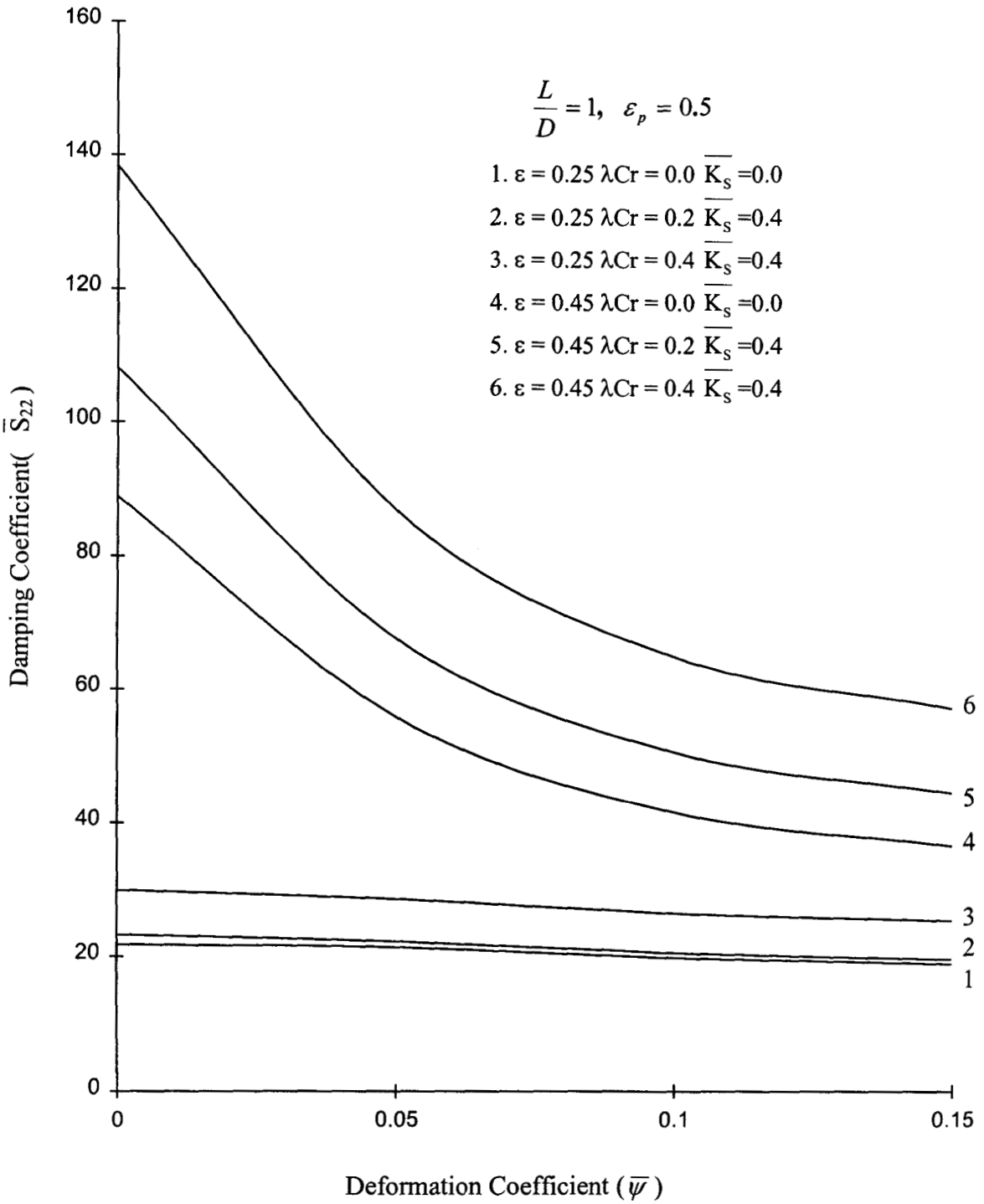

Fig. 5.51 – Stiffness Coefficient($\bar{S}_{22}$) vs Deformation Coefficient ($\bar{\psi}$) in Two Lobe Bearing

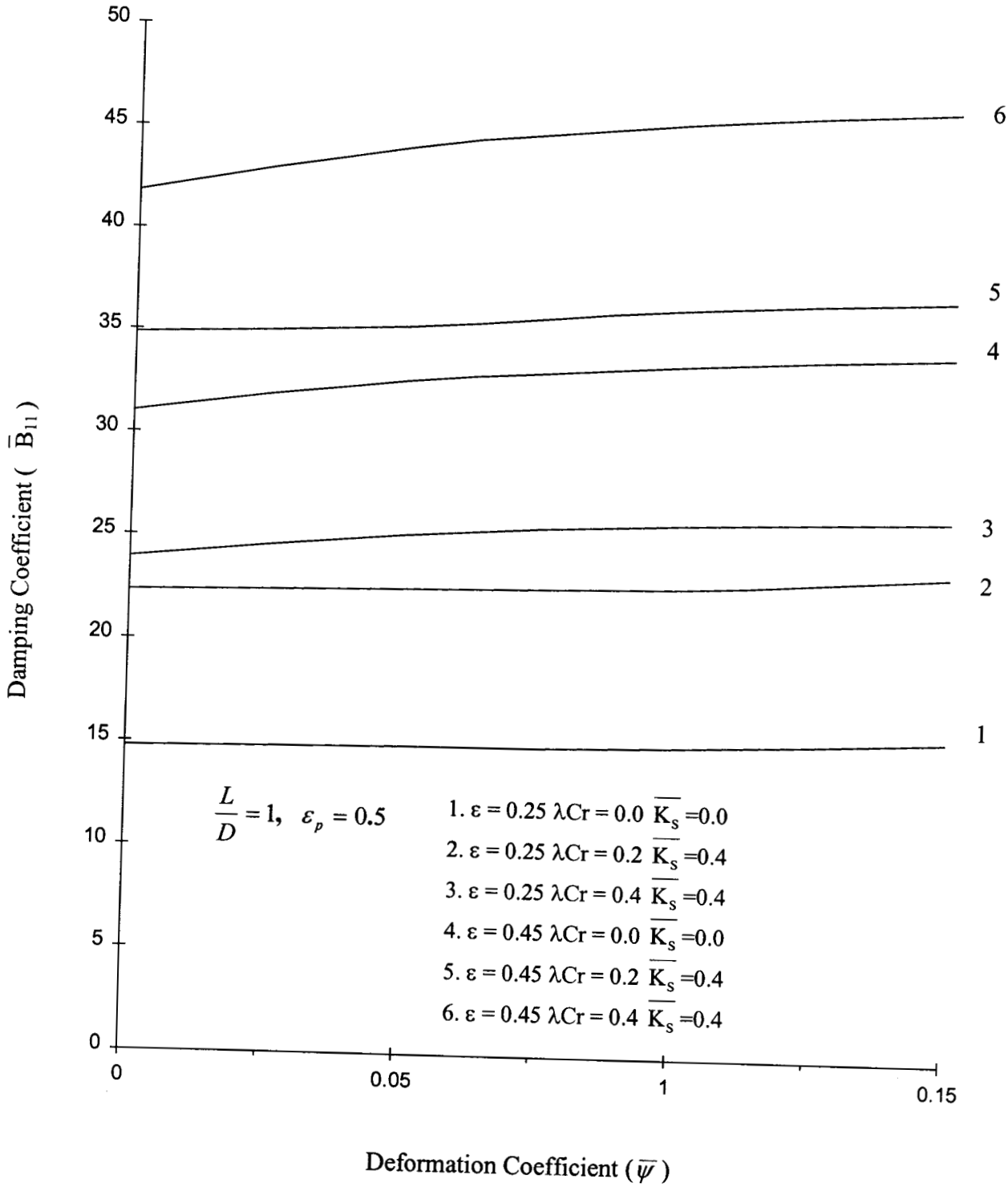

Fig. 5.52– Damping Coefficient($\bar{B}_{11}$) vs Deformation Coefficient ($\bar{\psi}$) in Two Lobe Bearing

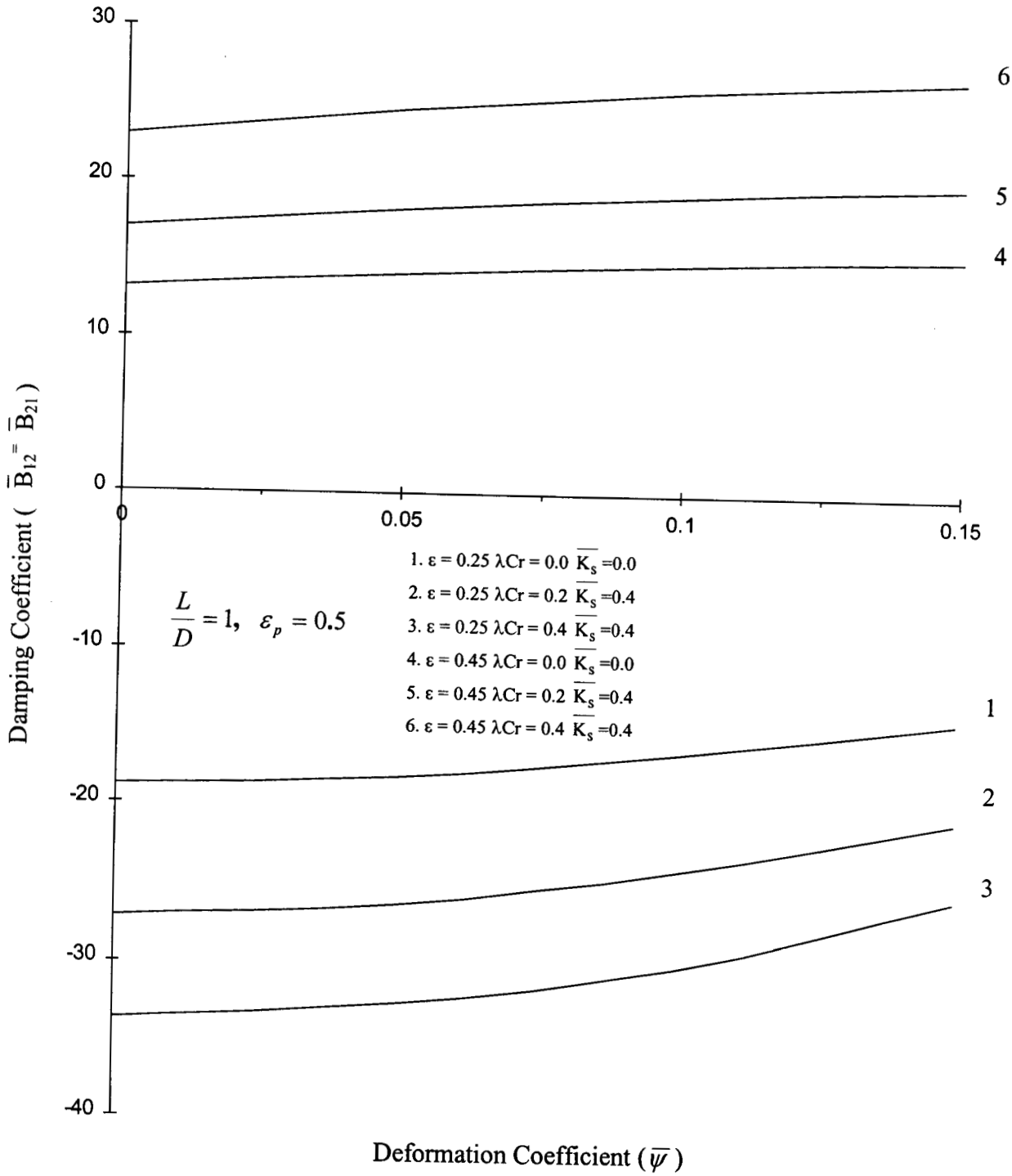

Fig. 5.53– Damping Coefficient($\bar{B}_{12} = B_{21}$) vs Deformation Coefficient ($\overline{\psi}$) in Two Lobe Bearing

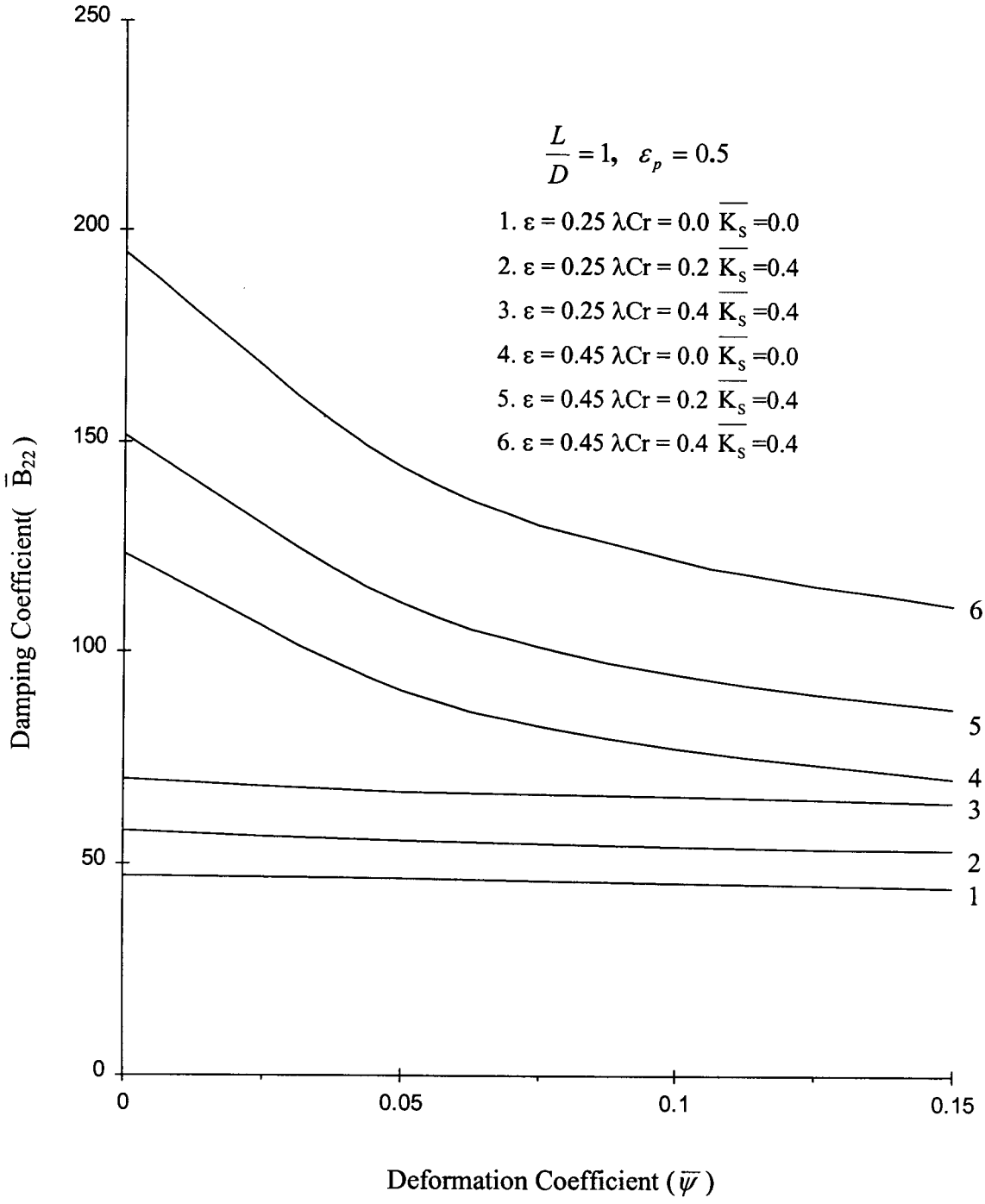

Fig. 5.54– Damping Coefficient($\overline{B}_{22}$) vs Deformation Coefficient ($\overline{\psi}$) in Two Lobe Bearing

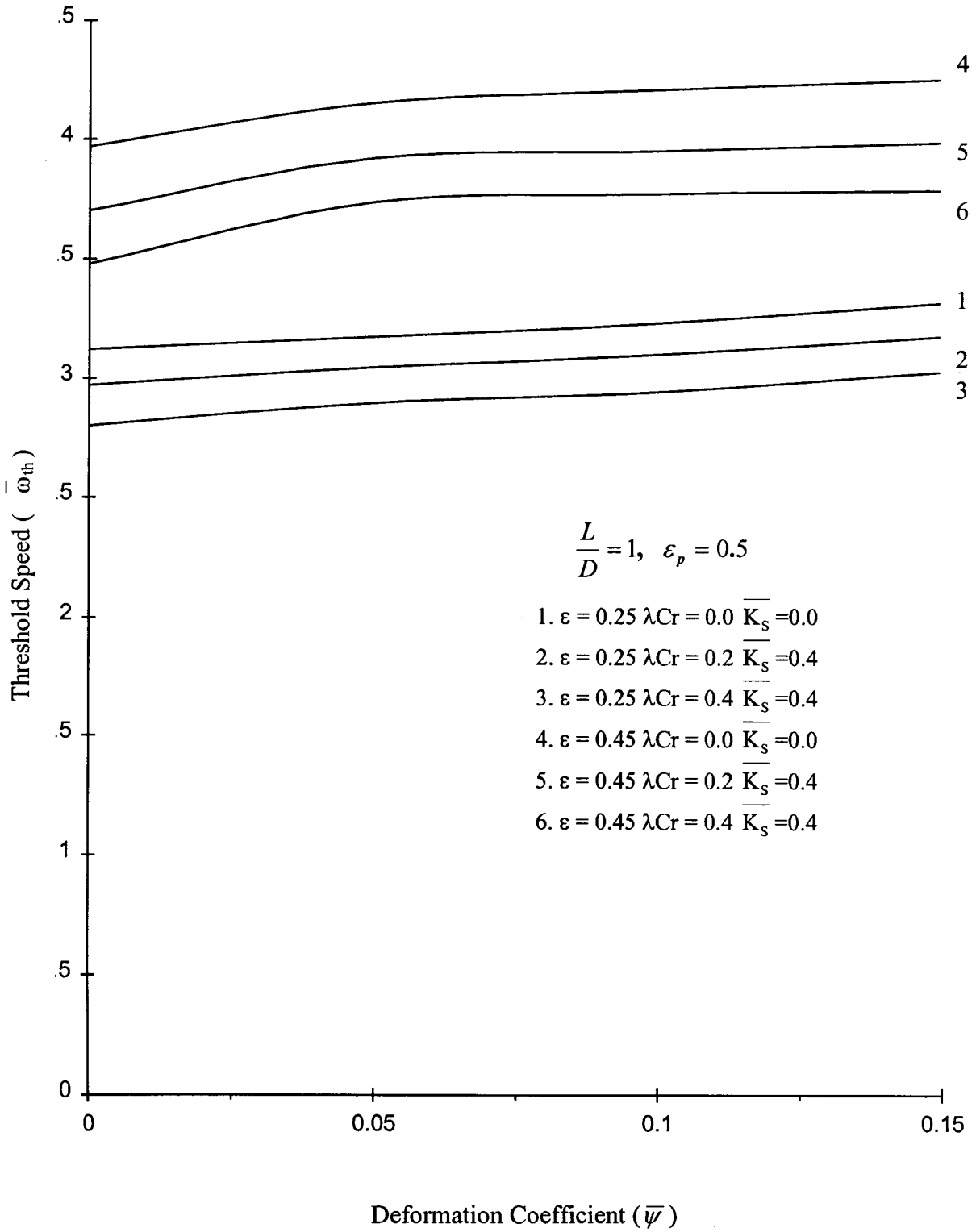

Fig. 5.55 – Threshold Speed ($\bar{\omega}_{th}$) vs Deformation Coefficient ($\bar{\psi}$) in Two Lobe Bearing

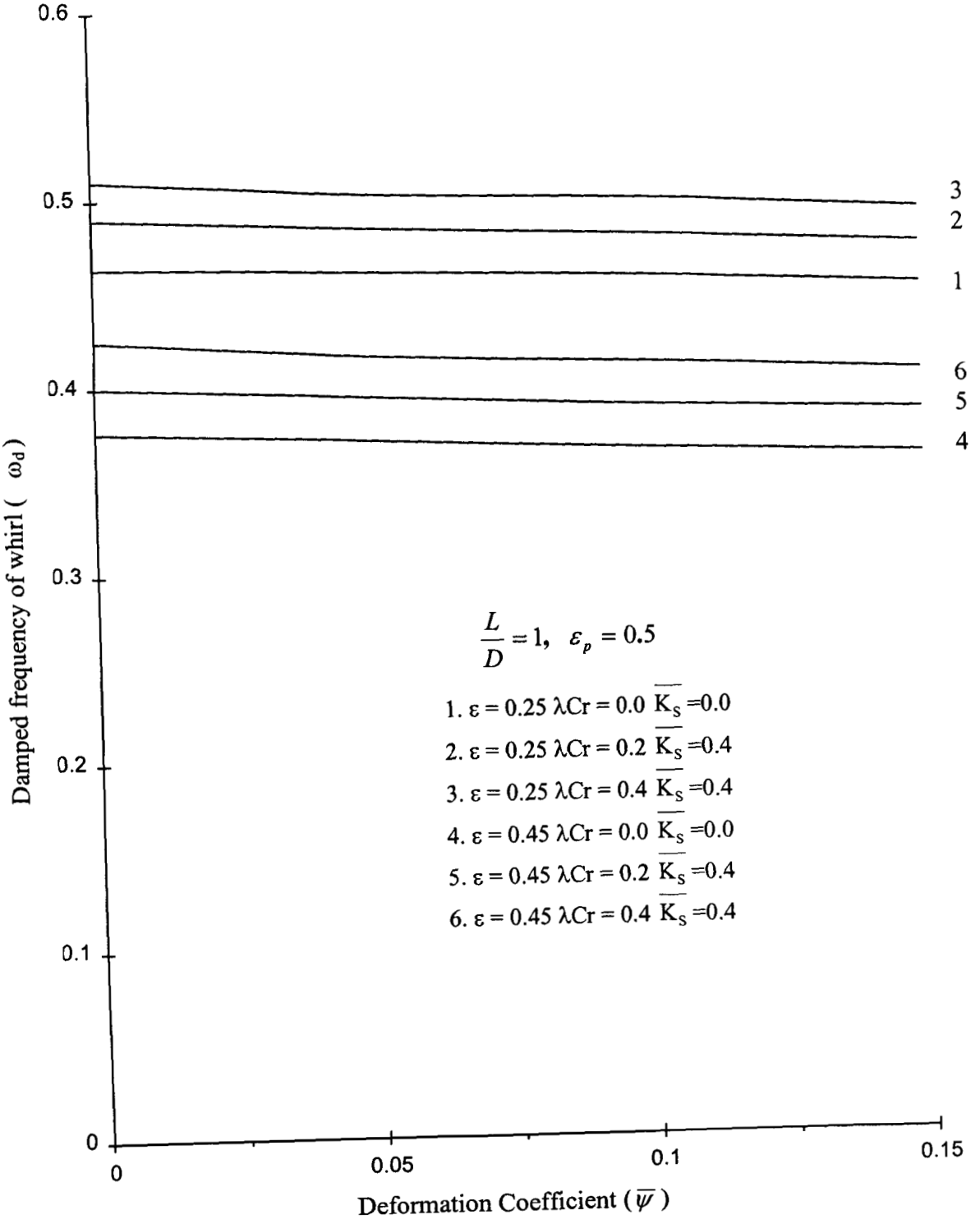

Fig. 5.56 – Damped frequency of whirl ($\bar{\omega}_d$) vs Deformation Coefficient ($\bar{\psi}$) in Two Lobe Bearing

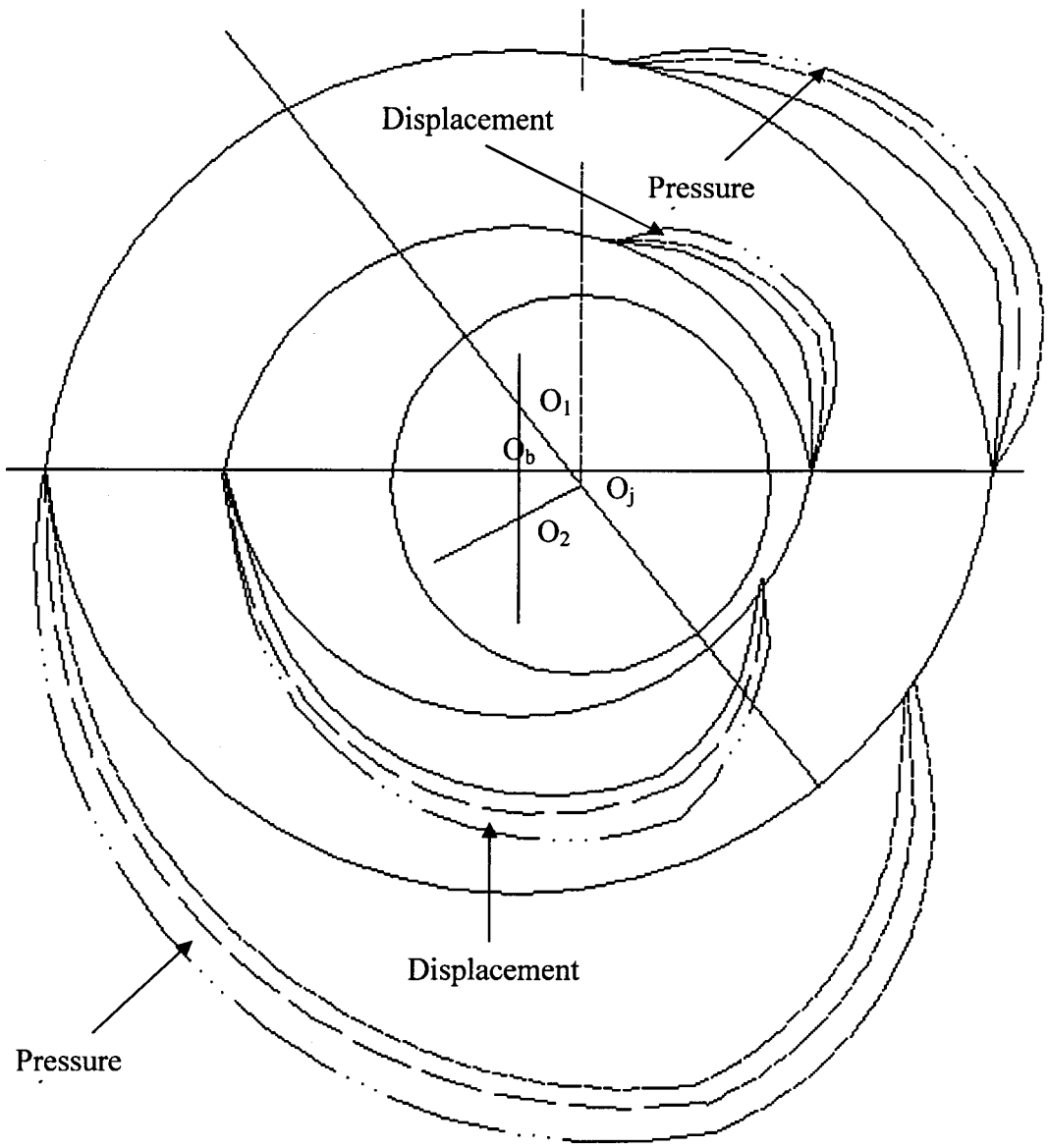

Fig. 5.57 Computed Pressure and Deformation Field for Two Lobe Bearing

The change of attitude angle with increase in deformation coefficient for a two lobe bearing is shown in Fig. 5.46. From this Figure it is observed that attitude angle decreases with increases in deformation coefficient and eccentricity ratio, but increases with volume concentration of additives when there is mass transfer. It is also noted that attitude angle is reduced considerably even at low values of deformation coefficient when the bearing operates at high eccentricity ratios for both Newtonian and micropolar fluids. The increase in attitude angle indicates that the stability of two lobe bearing system will be reduced for micropolar lubricants.

The variation of friction parameter with the increase in deformation coefficient is shown in Fig. 5.47. It is observed from this Figure that the friction parameter is reduced significantly with the increase in deformation coefficient when the bearing operates at high eccentricity ratio.

Changes in stiffness and damping coefficients due to the change in deformation coefficients are shown in Figs. 5.48-5.54. From these figures it can be noted that all the stiffness coefficient except $\bar{S}_{12}$ decrease with increase in deformation coefficient for any value of eccentricity ratio.

The variation of threshold speed with deformation coefficient is shown in Fig. 5.55. It is observed that threshold speed for bearings with micropolar lubricants is less than that for bearing with Newtonian lubricants for a given value of deformation coefficient and eccentricity ratio. In the case of two lobe bearings it is also noted that threshold speed increases with deformation coefficient for any value of eccentricity ratio.

The variation of damped frequency of whirl with increase in deformation coefficient is shown in Fig. 5.56. It is observed that the damped frequency of whirl decreases with increase in eccentricity ratio but increases with volume concentration of additives. It is also noted that damped frequency of whirl decreases with increase in deformation coefficient.

The pressure and deformation fields in the case of two lobe bearings are shown in Fig. 5.57.

The dimensional values of various performance characteristics of elastic two lobe bearings are given in Tables 5.9 and 5.10. The percentage variations in the performance characteristics of two lobe bearings compared to the corresponding values of rigid bearings operating with lubricants without additives are presented in Tables 5.11 and 5.12. At $\varepsilon = 0.45$ and $\overline{\psi} = 0.1$, for Newtonian lubricant there is 45.31 percent reduction in load carrying capacity when compared to that of rigid bearing. When micropolar effect is considered ($\lambda_{Cr} = 0.4$, $K_s = 0.4$) only 3.24 percent reduction in load carrying capacity was observed. At the same time when the bearing operates at $\varepsilon = 0.25$ and $\overline{\psi} = 0.1$ an increase of 68.71 percent increase in load carrying capacity was observed in the case of micropolar fluids ($\lambda c_r = 0.4$, $K_s = 0.4$) when compared to that of rigid bearing operating with Newtonian fluids. These indicate that micropolar characteristics of lubricant produce significant effect on the performance characteristics of the bearing. Therefore the effect of volume concentration of additives and mass transfer rate on the performance characteristics of the bearing must be considered in the analysis and design of bearings.

5.3 THREE LOBE BEARINGS

The result obtained in the case of three lobe bearings operating under Newtonian and micropolar lubricants are presented in Figs. 5.58-5.86.

5.3.1 Three Lobe Rigid Bearings

The static performance characteristics in terms of load carrying capacity, end leakage, attitude angle, friction parameter and dynamic characteristics in terms of stiffness and damping coefficients, threshold speed and damped frequency of whirl are computed for three lobe bearing when the bearing operates at eccentricity ratios $\varepsilon = 0.2$ and $\varepsilon = 0.4$. These results are obtained for both Newtonian and micropolar lubricants. The variations of $\overline{W}, \overline{Q}_z, \phi, \bar{f}$,

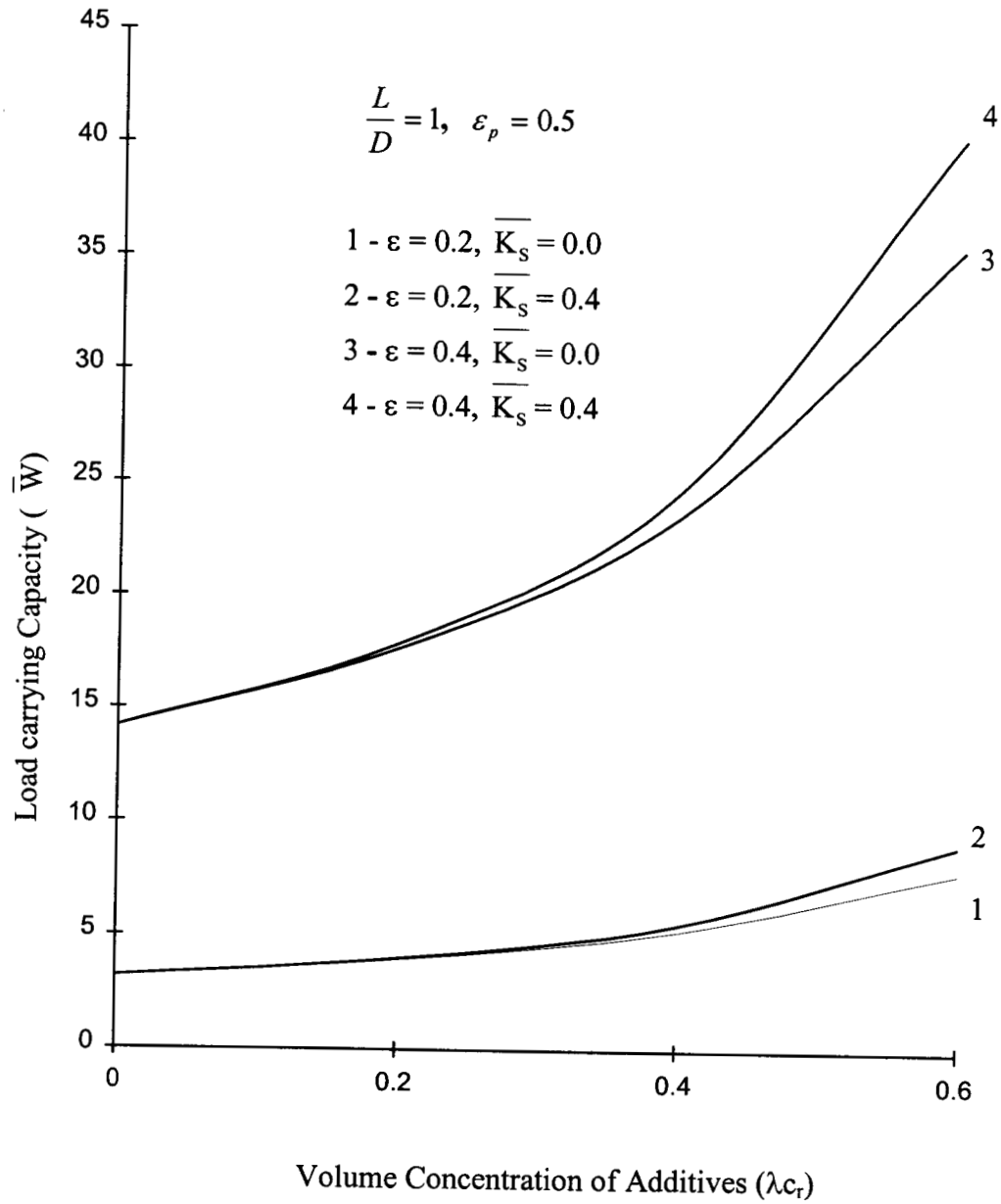

Fig. 5. 58 Load carrying Capacity ($\bar{W}$) vs Volume Concentration of Additives (λc_r) in Three Lobe Bearing

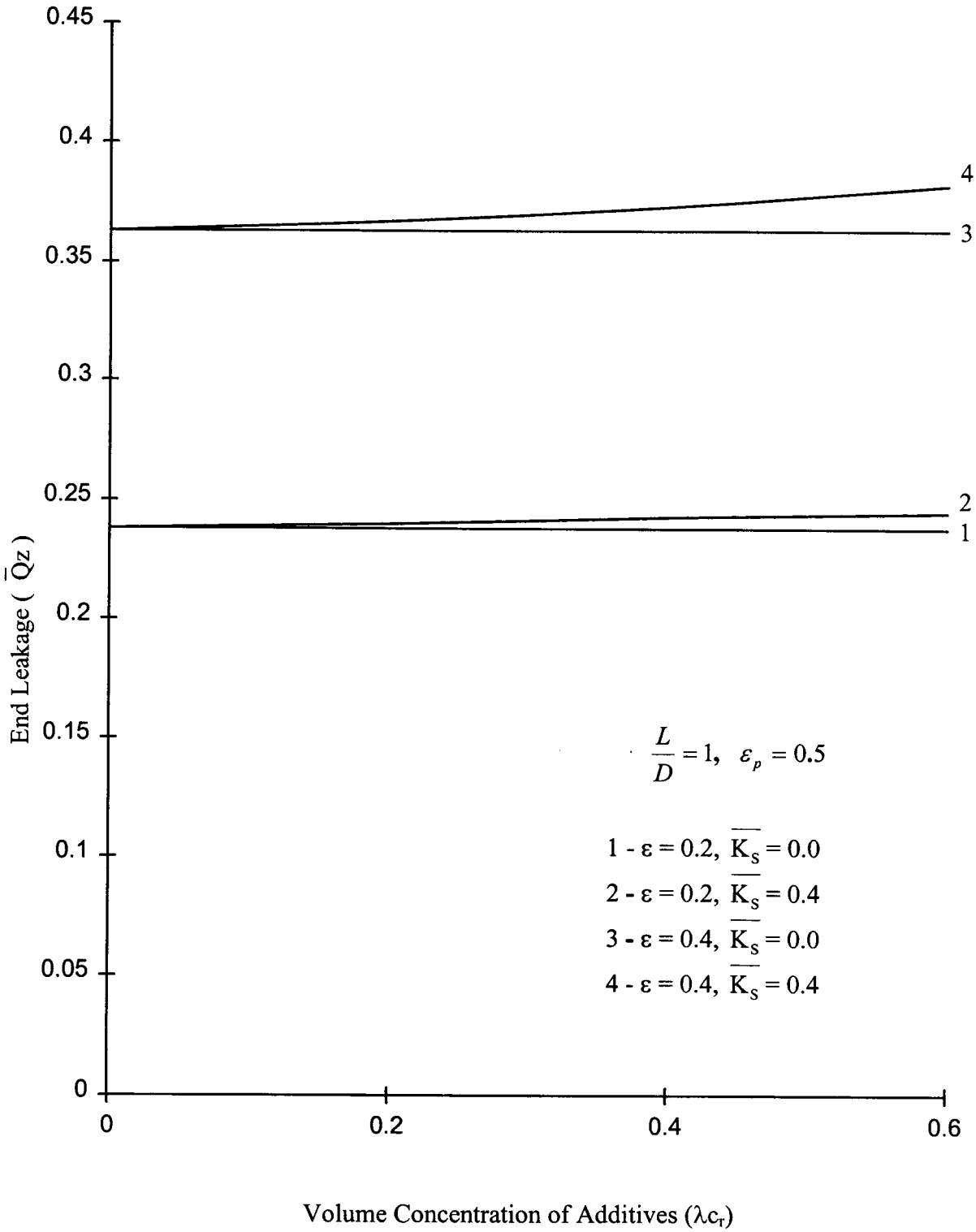

Fig. 5.59 End Leakage ($\bar{Q}z$) vs Volume Concentration of Additives (λc_r) in Three Lobe Bearing

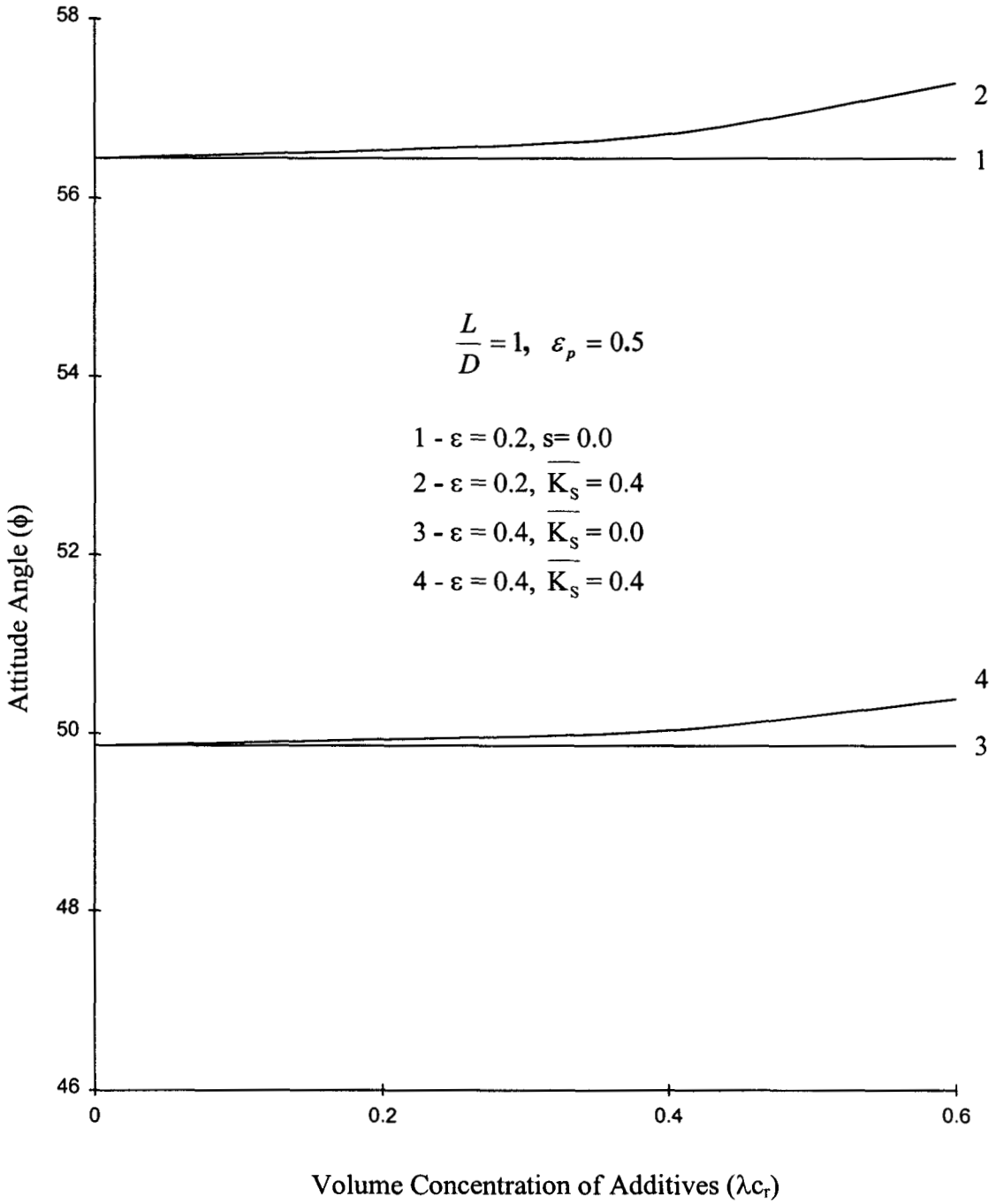

Fig. 5. 60 Attitude Angle (ϕ) vs Volume Concentration of Additives (λc_r) in Three Lobe Bearing

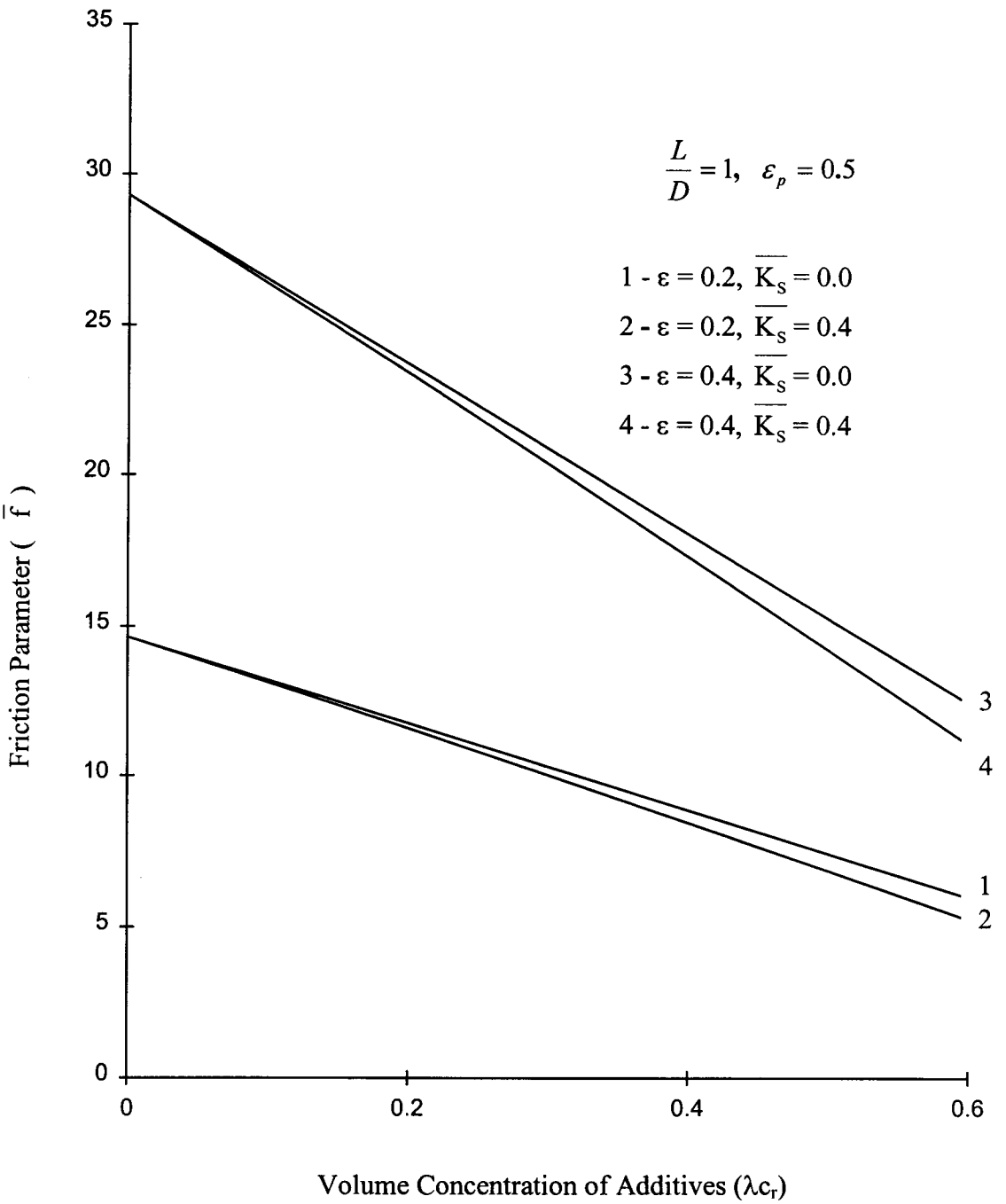

Fig. 5.61 Friction Parameter ($\bar{f}$) vs Volume Concentration of Additives (λc_r) in Three Lobe Bearing

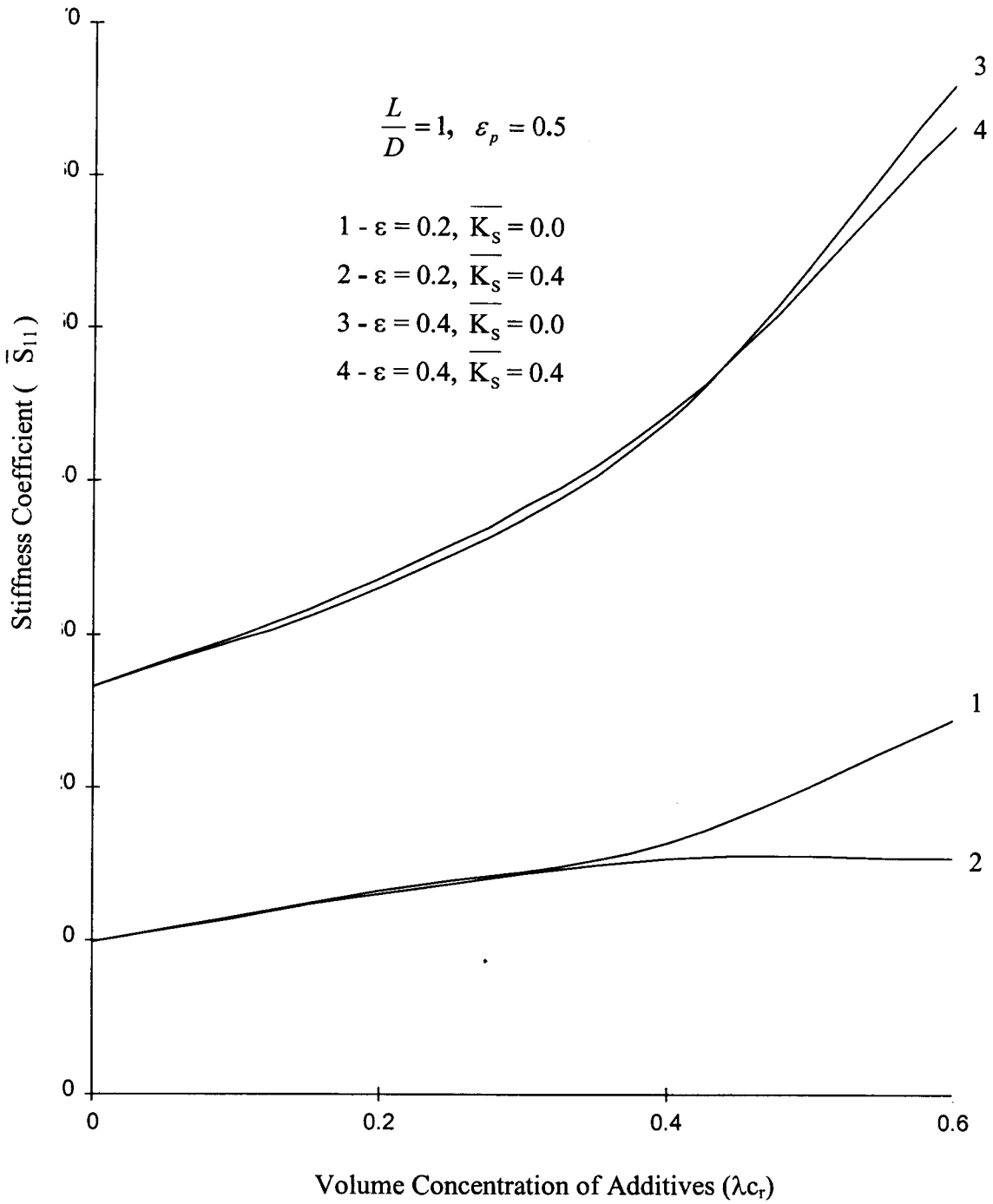

Fig. 5.62 Stiffness Coefficient($\bar{S}_{11}$) vs Volume Concentration of Additives (λc_r) in Three Lobe Bearing

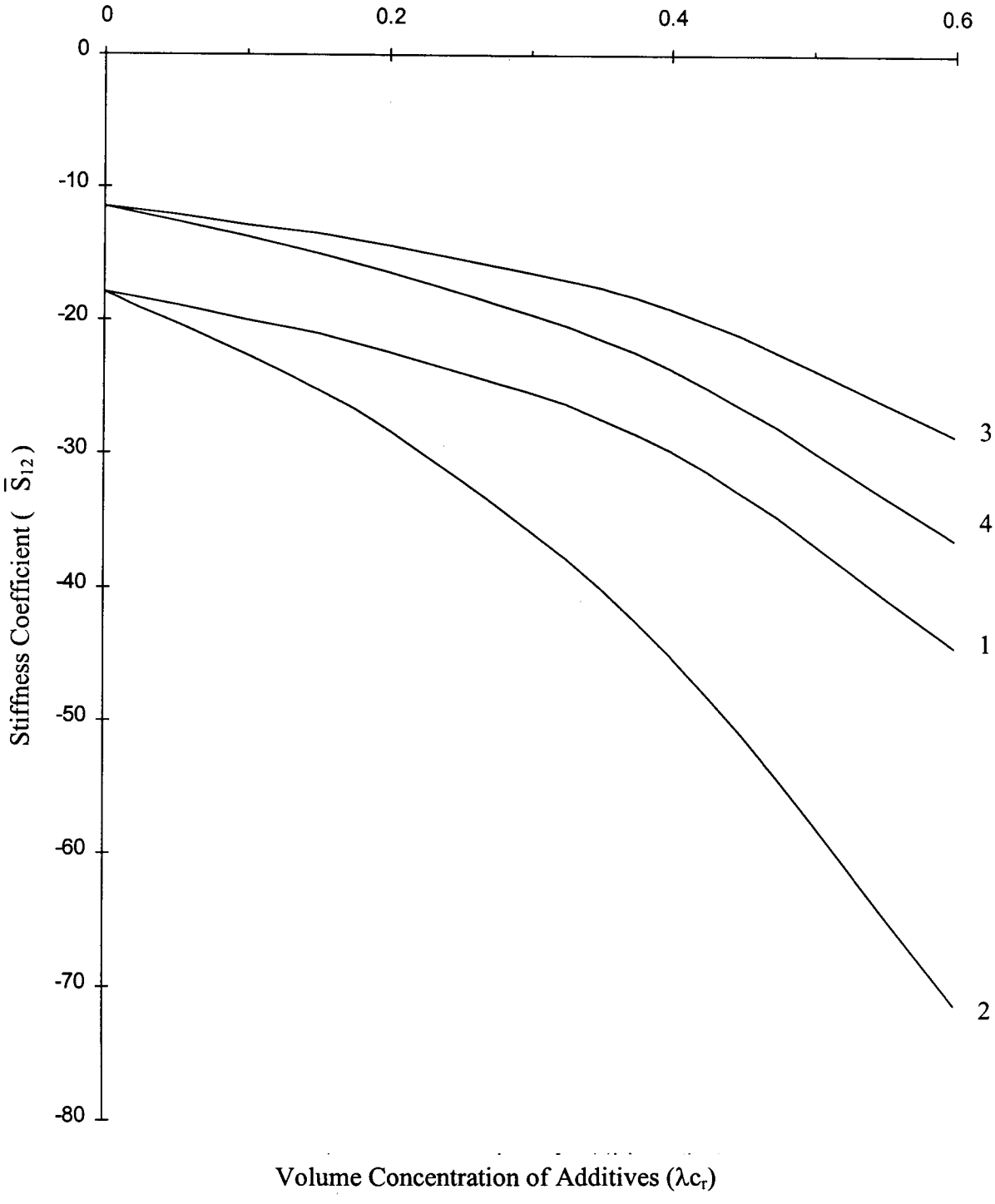

Fig. 5.63 Stiffness Coefficient($\bar{S}_{12}$) vs Volume Concentration of Additives (λc_r) in Three Lobe Bearing

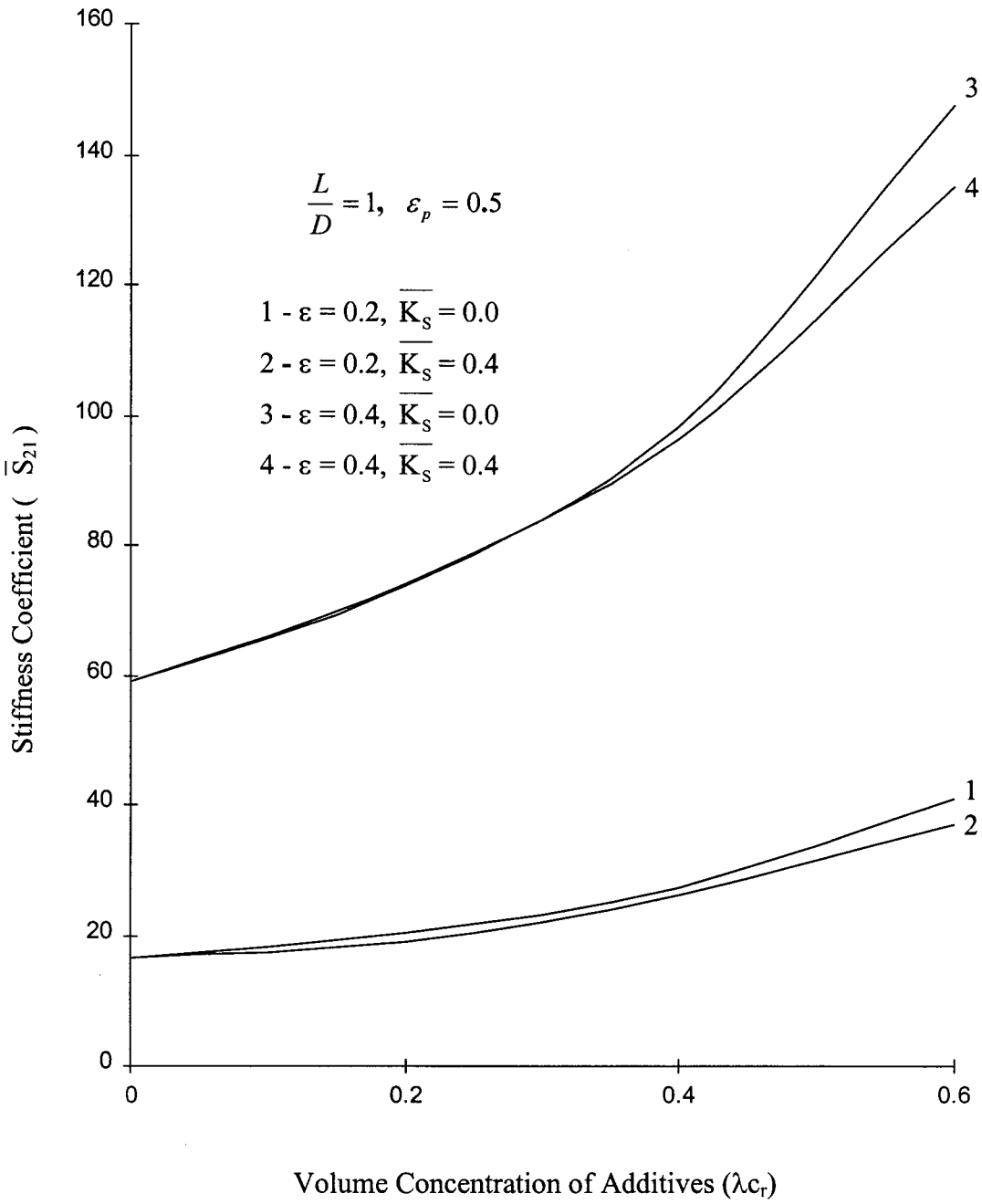

Fig. 5.64 Stiffness Coefficient($\bar{S}_{21}$) vs Volume Concentration of Additives (λc_r) in Three Lobe Bearing

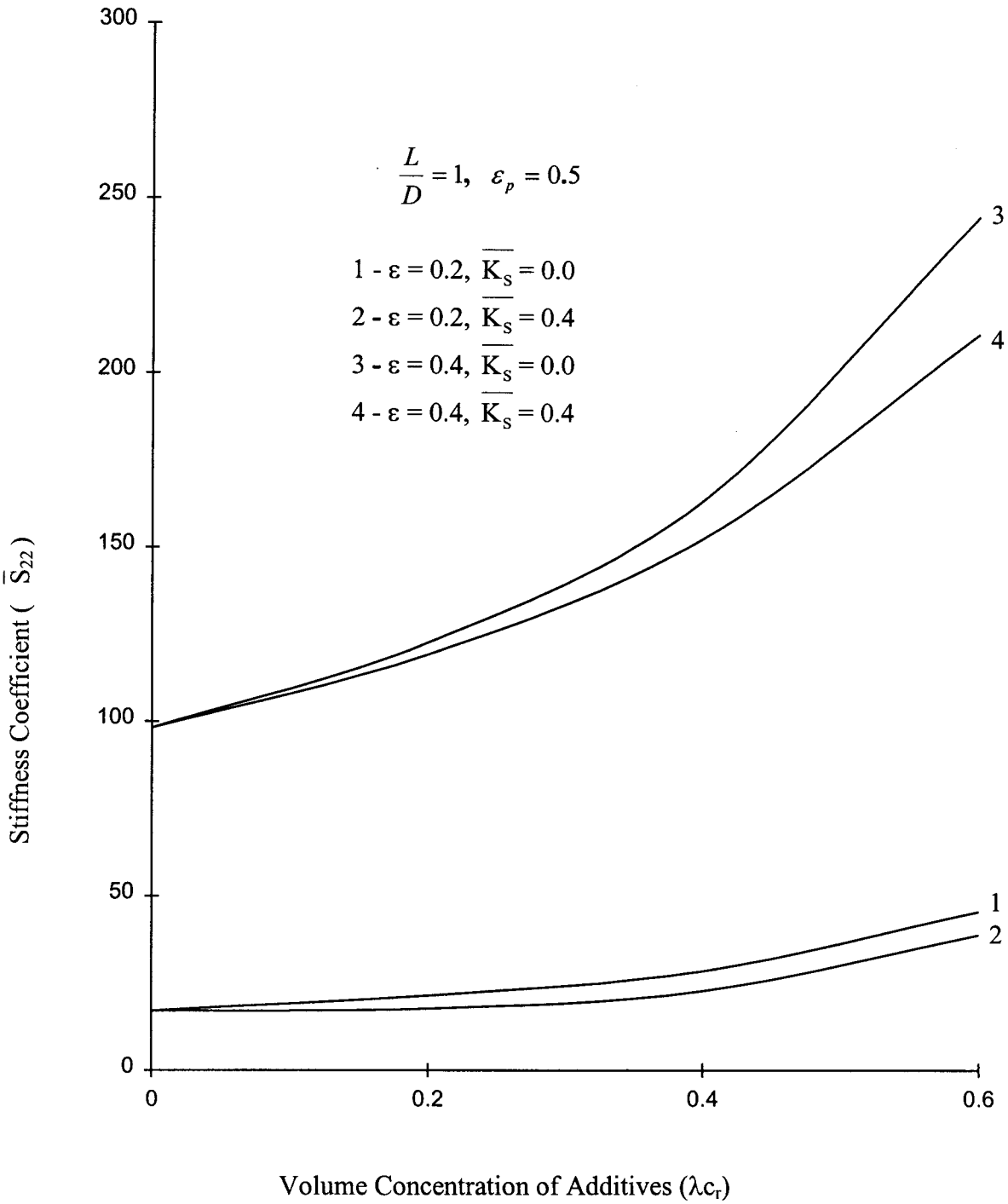

Fig. 5.65 Stiffness Coefficient($\bar{S}_{22}$) vs Volume Concentration of Additives (λc_r) in Three Lobe Bearing

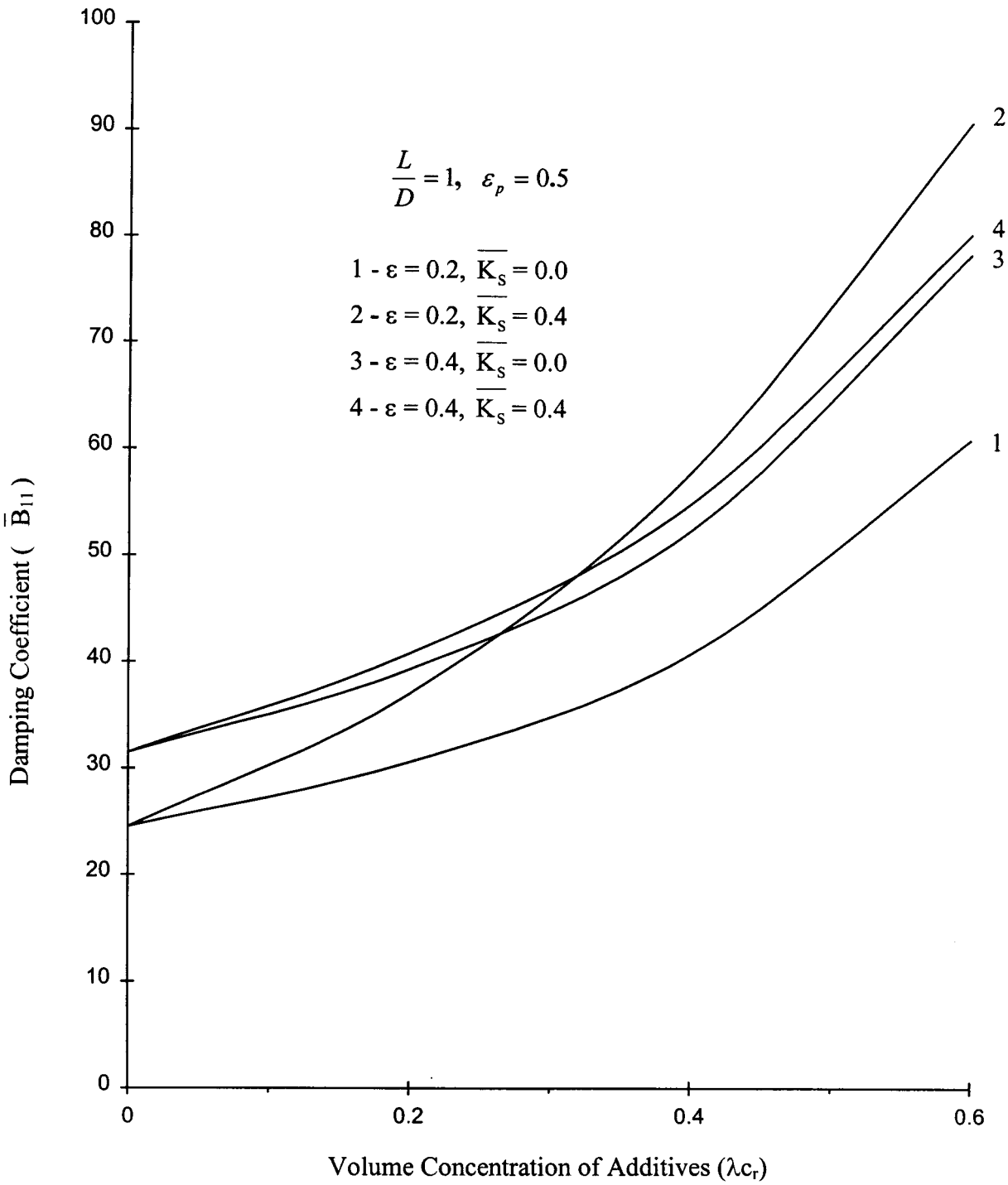

Fig. 5.66 Damping Coefficient($\overline{B}_{11}$) vs Volume Concentration of Additives (λc_r) in Three Lobe Bearing

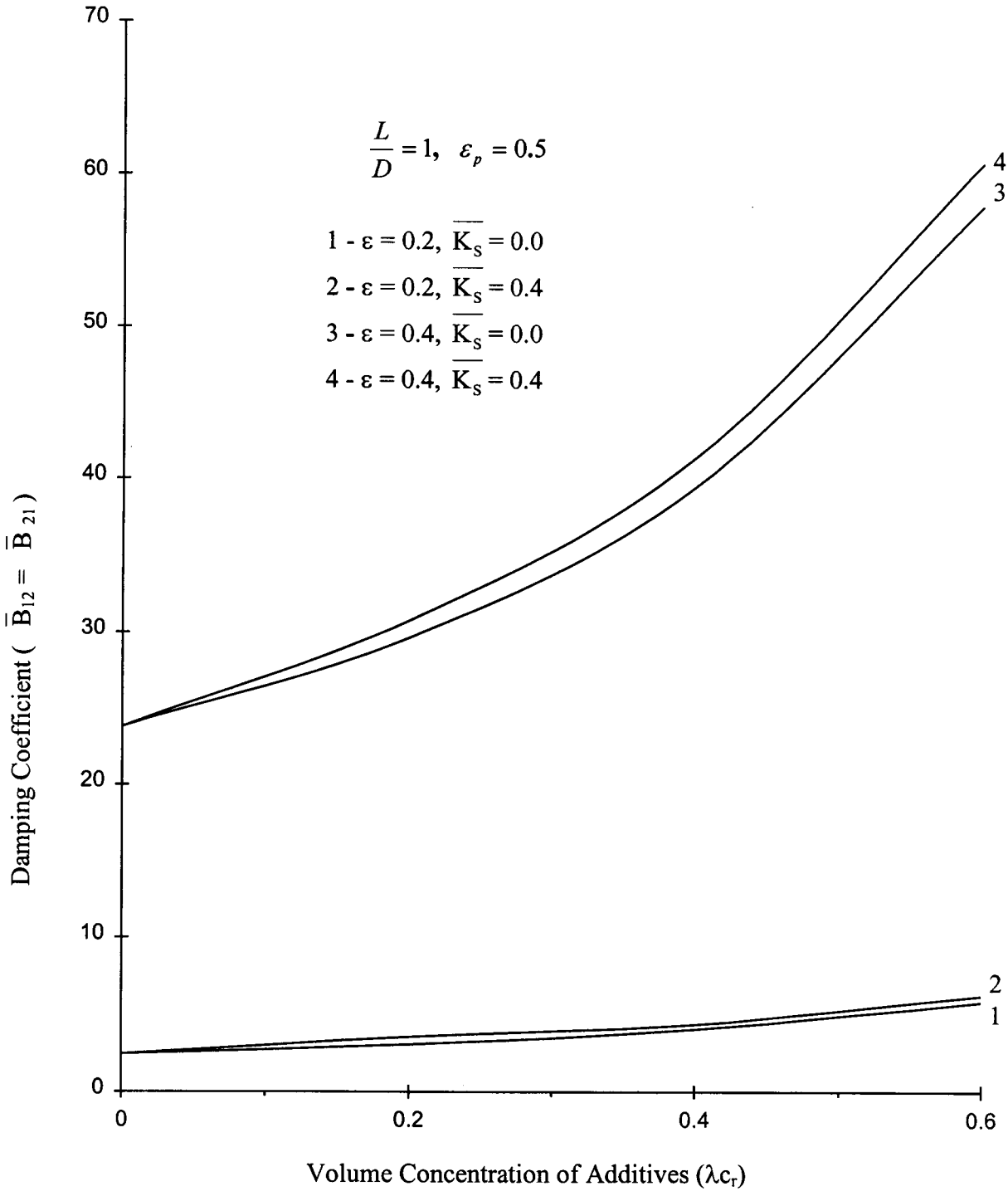

Fig. 5.67 Damping Coefficient($\overline{B}_{12} = \overline{B}_{21}$) vs Volume Concentration of Additives (λc_r) in Three Lobe Bearing

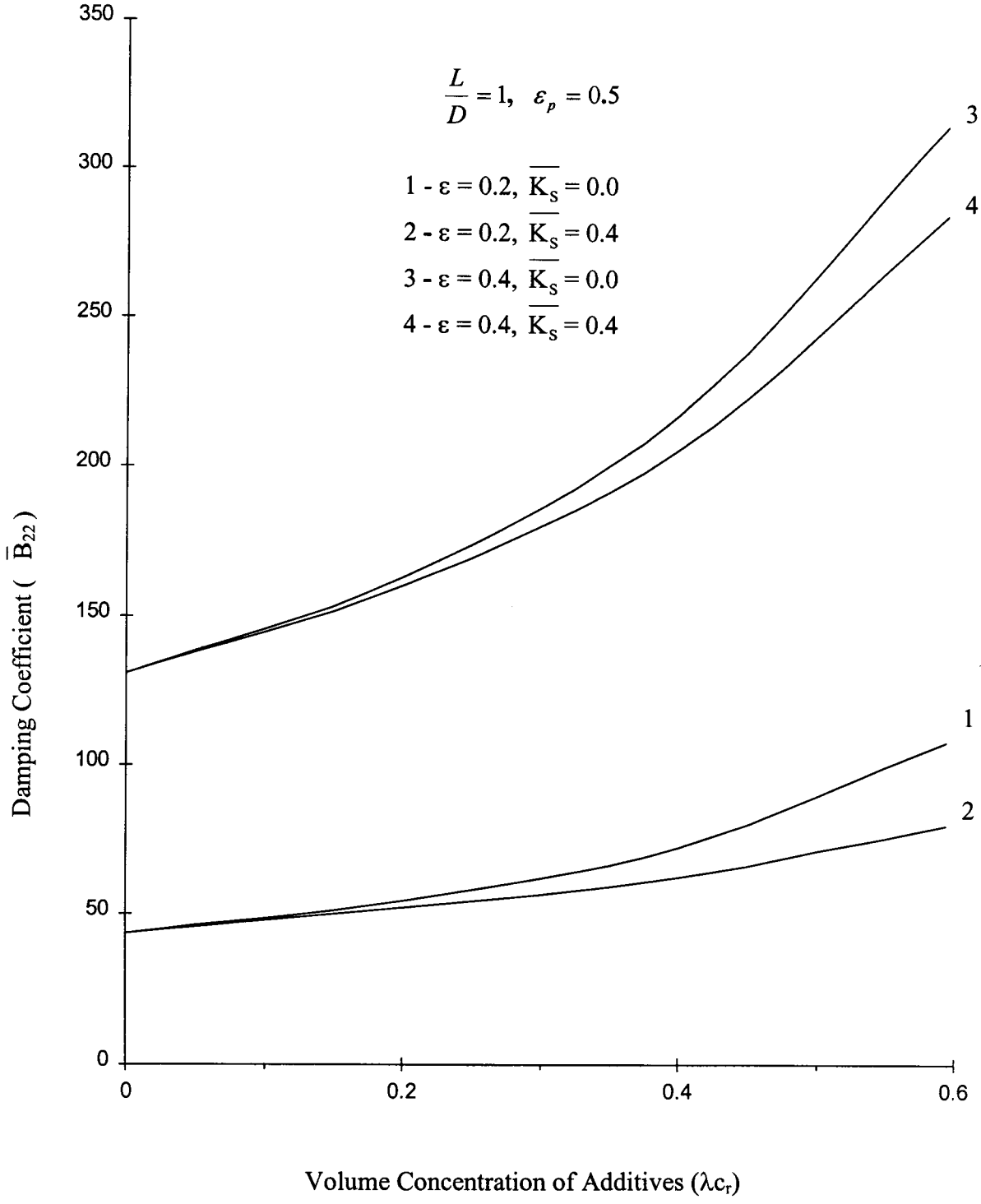

Fig. 5.68 Damping Coefficient($\bar{B}_{22}$) vs Volume Concentration of Additives (λc_r) in Three Lobe Bearing

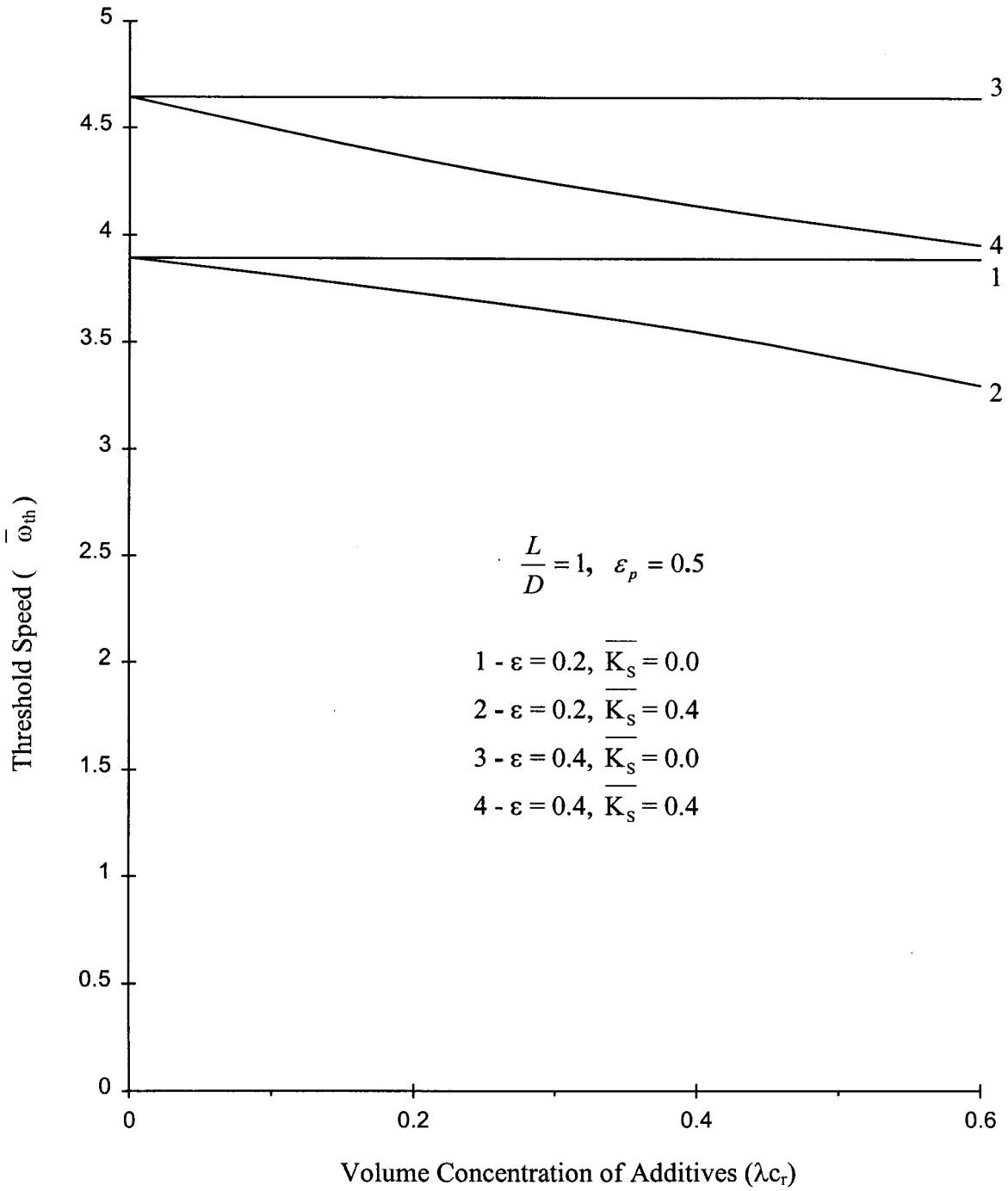

Fig. 5.69 Threshold Speed (ω_{th})vs Volume Concentration of Additives (λc_r) in Three Lobe Bearing

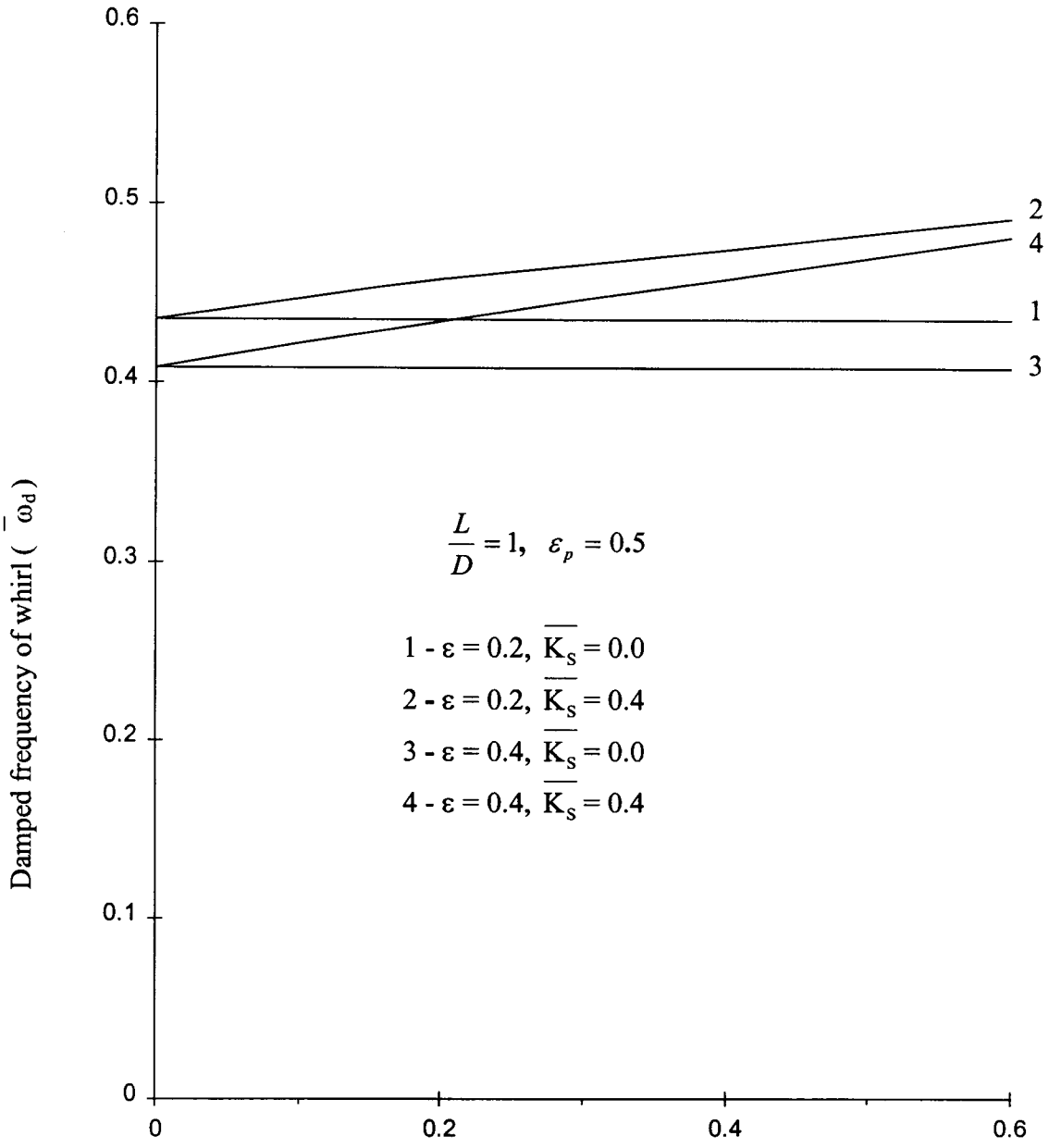

Fig. 5.70 Damped frequency of whirl ($\bar{\omega}_d$) vs Volume Concentration of Additives (λCr) in Three Lobe Bearing

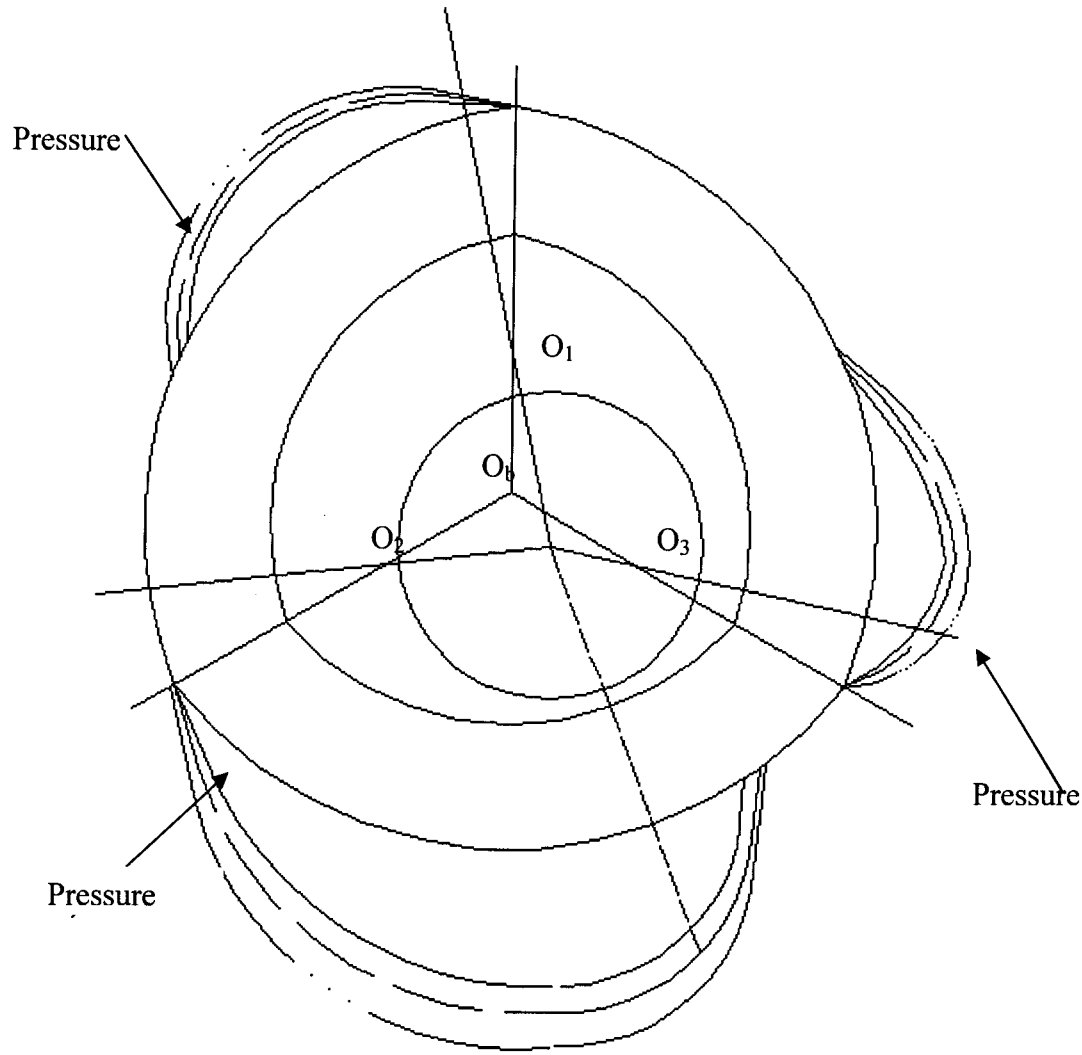

—————— $\varepsilon = 0.2; \lambda c_r = 0.0; K_x = 0.0; \psi = 0.0$

— — $\varepsilon = 0.2; \lambda c_r = 0.2; K_x = 0.4; \psi = 0.0$

—...— $\varepsilon = 0.2; \lambda c_r = 0.4; K_x = 0.4; \psi = 0.0$

Fig. 5.71 Computed Pressure Field For Three Lobe Rigid Bearing

$\bar{S}_{11}, \bar{S}_{12}, \bar{S}_{21}, \bar{S}_{22}$ and $\bar{B}_{11}, B_{12} \approx \bar{B}_{21}, \bar{B}_{22}$, $\bar{\omega}_d$ and $\bar{\omega}_{th}$ with increase in volume concentration of additives are presented in Figs. 5.58 - 5.70. The variations in these performance characteristics are found to show a similar tend as in the case of two lobe bearings. The computed pressure field for three lobe rigid bearing is given in Fig. 5.71.

The dimensional values of various performance characteristics of three lobe bearings operating at $\varepsilon = 0.2$ and $\varepsilon = 0.4$ assuming them to the rigid are given in Table 5.13. From the table it is observed that at $\varepsilon = 0.2$ load carrying capacity changes from 8.11 kN to 14.18 kN when the micropolar effect of the lubricant ($\lambda c_r = 0.4$ and $K_s = 0.4$) is considered.

5.3.2 Elastic Three Lobe Bearings

To authenticate the solution algorithm and computer program developed the load carrying capacity of three lobe bearing obtained from EHD analysis for Newtonian lubricants is compared with published results [70] in Fig. 5.72. The comparison is quite satisfactory. The results obtained from the EHD analysis of three lobe bearings are presented in Figs. 5.72 to 5.86.

The variations of static performance characteristics of three lobe bearings with increase in deformation coefficient are similar to the variations obtained in the case of two lobe bearings.

The variations of dynamic performance characteristics $\bar{S}_{11}, \bar{S}_{12}, \bar{S}_{21}, \bar{S}_{22}$ and $\bar{B}_{11}, B_{12} \approx \bar{B}_{21}, \bar{B}_{22}$, $\bar{\omega}_d$ and $\bar{\omega}_{th}$ obtained with increase in deformation coefficient are shown in Figs. 5.77 - 5.85 for both Newtonian and micropolar lubricants. As observed in the case of two lobe bearings values of all stiffness coefficients except $\bar{S}_{12}$ decrease with increase in deformation coefficient for any value of eccentricity ratio. At any value of deformation coefficient, values of these coefficients except for $\bar{S}_{12}$ increase with increase in volume concentration of additives. It is observed that the damping coefficients are significantly affected due to the variations in the deformation coefficients at any value of eccentricity

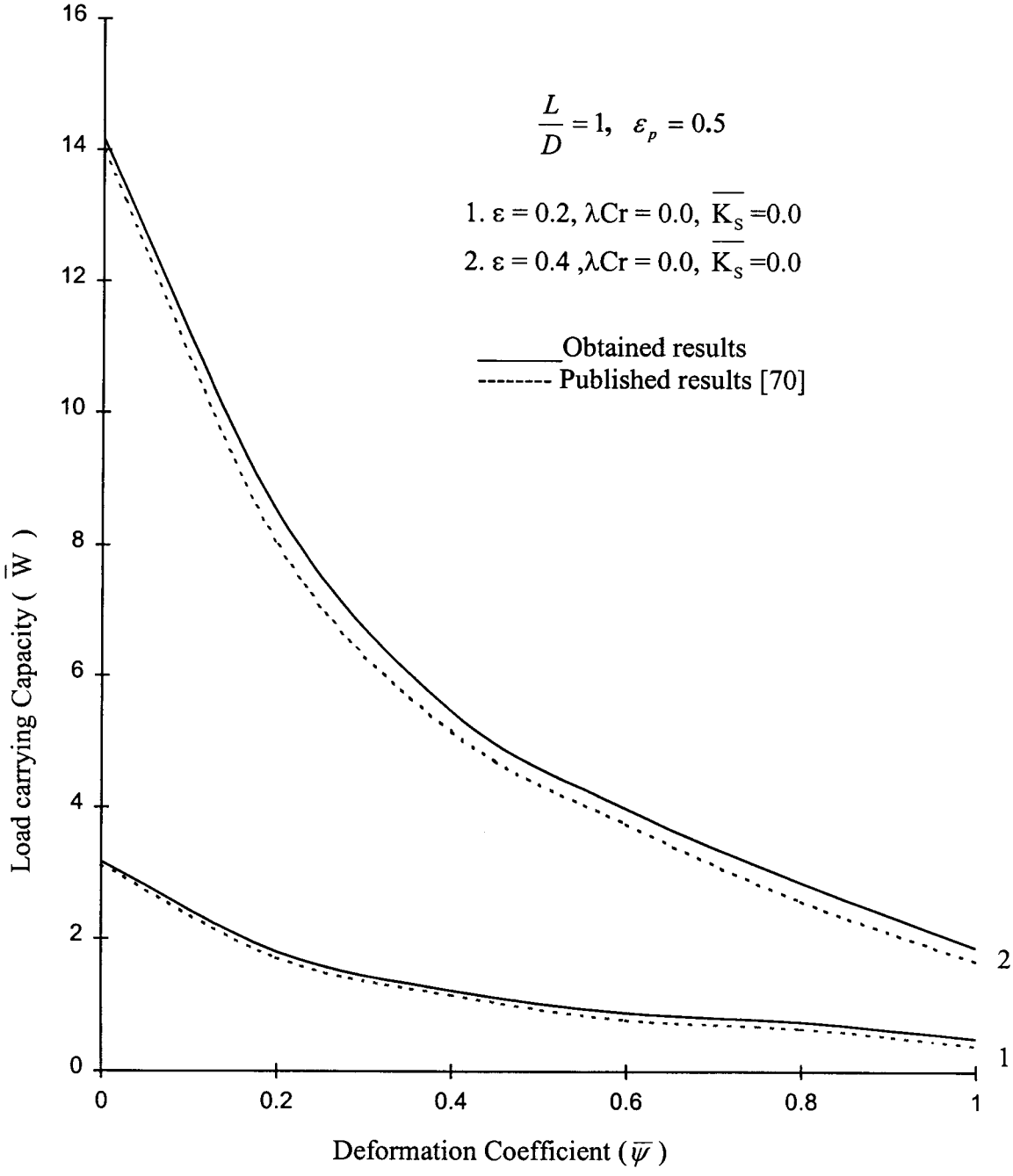

Fig. 5. 72 Load carrying Capacity ($\overline{W}$) vs Deformation Coefficient ($\overline{\psi}$) in Three Lobe Bearing with Newtonian Lubricants

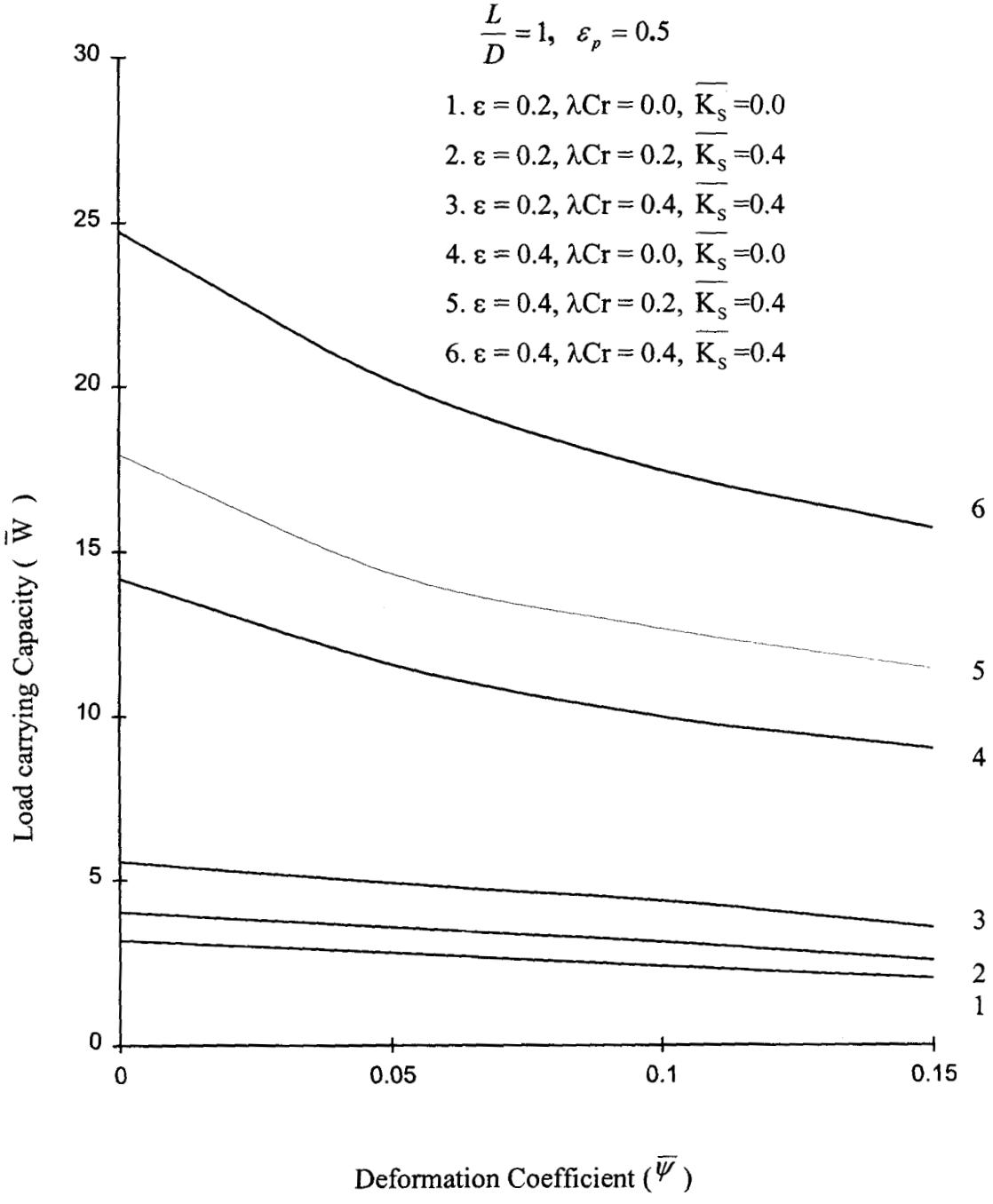

Fig. 5.73 – Load carrying Capacity ($\bar{W}$) vs Deformation Coefficient ($\overline{\psi}$) in Three Lobe Bearing

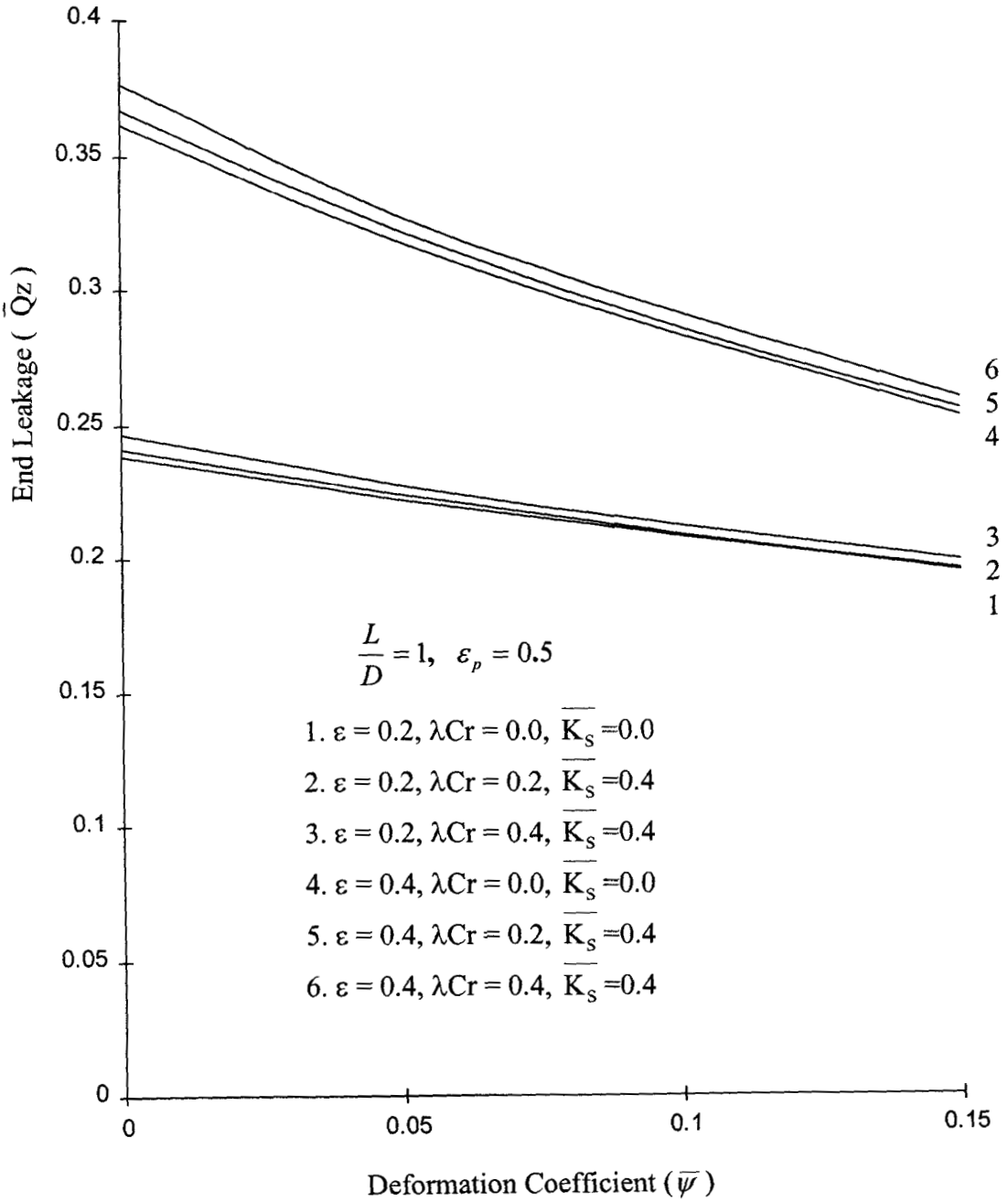

Fig. 5.74 – End Leakage ($\bar{Q}z$) vs Deformation Coefficient ($\bar{\psi}$) in Three Lobe Bearing

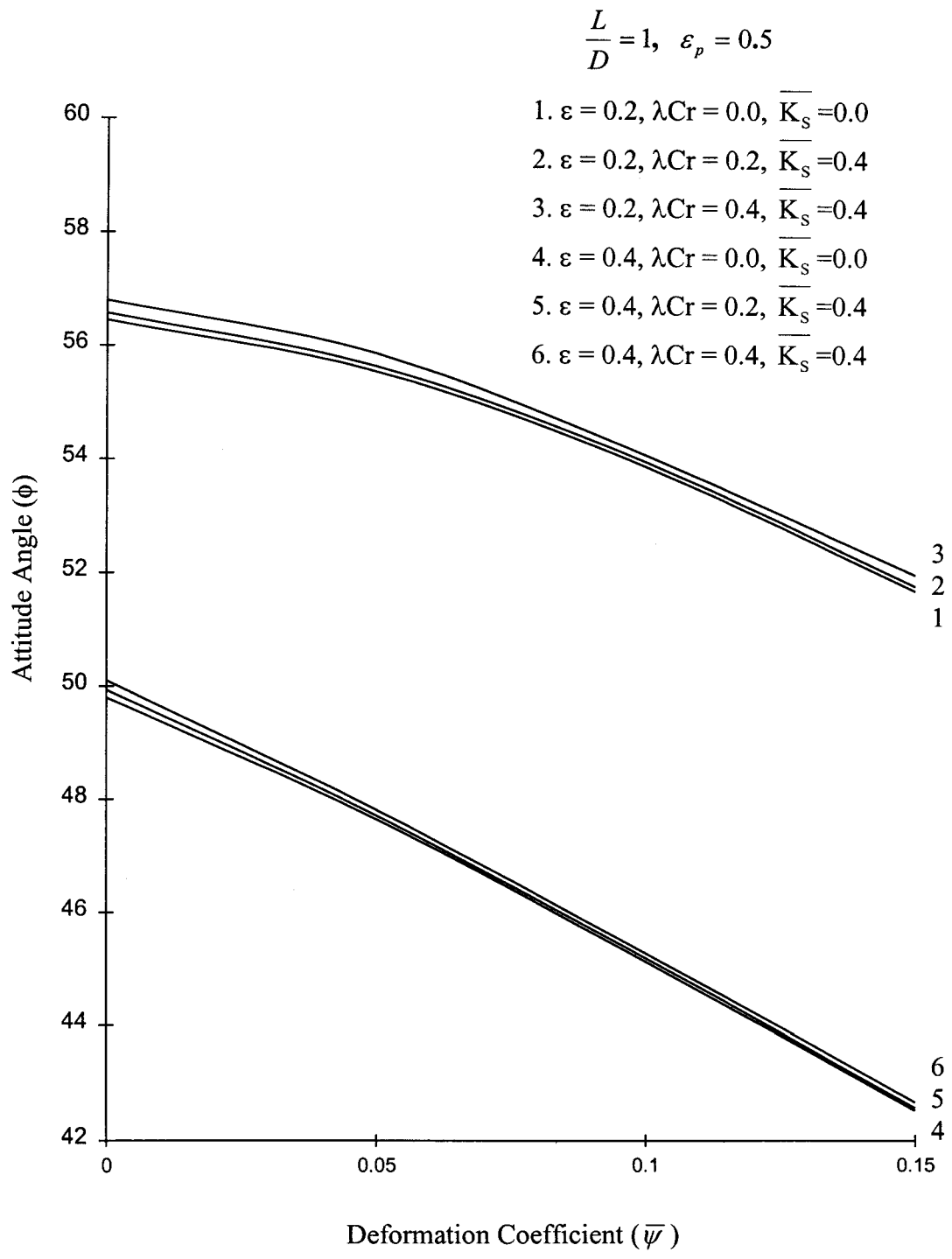

Fig. 5. 75 – Attitude Angle (ϕ) vs Deformation Coefficient ($\overline{\psi}$) in Three Lobe Bearing

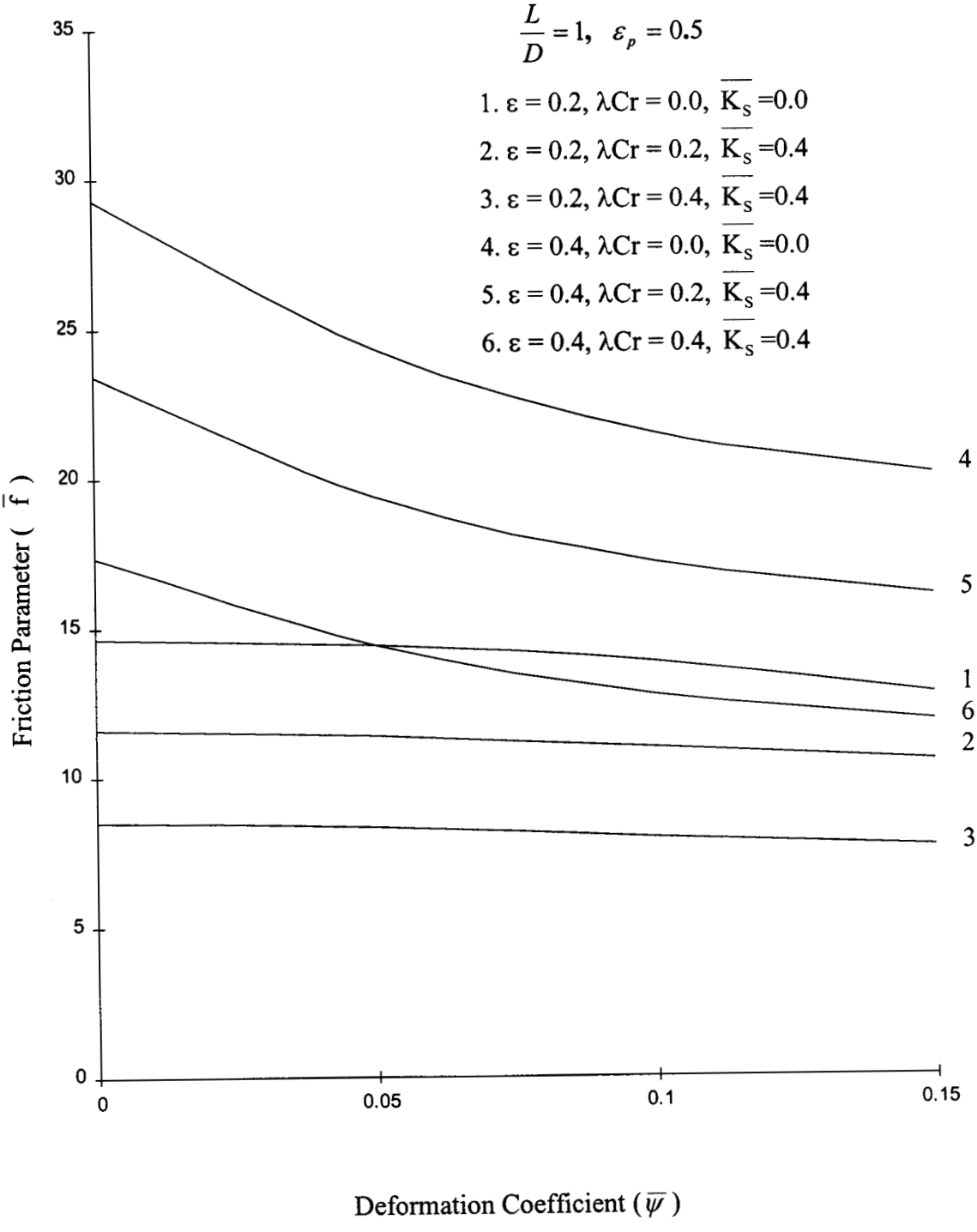

Fig. 5.76 –Friction Parameter ($\bar{f}$) vs Deformation Coefficient ($\overline{\psi}$)in Three Lobe Bearing

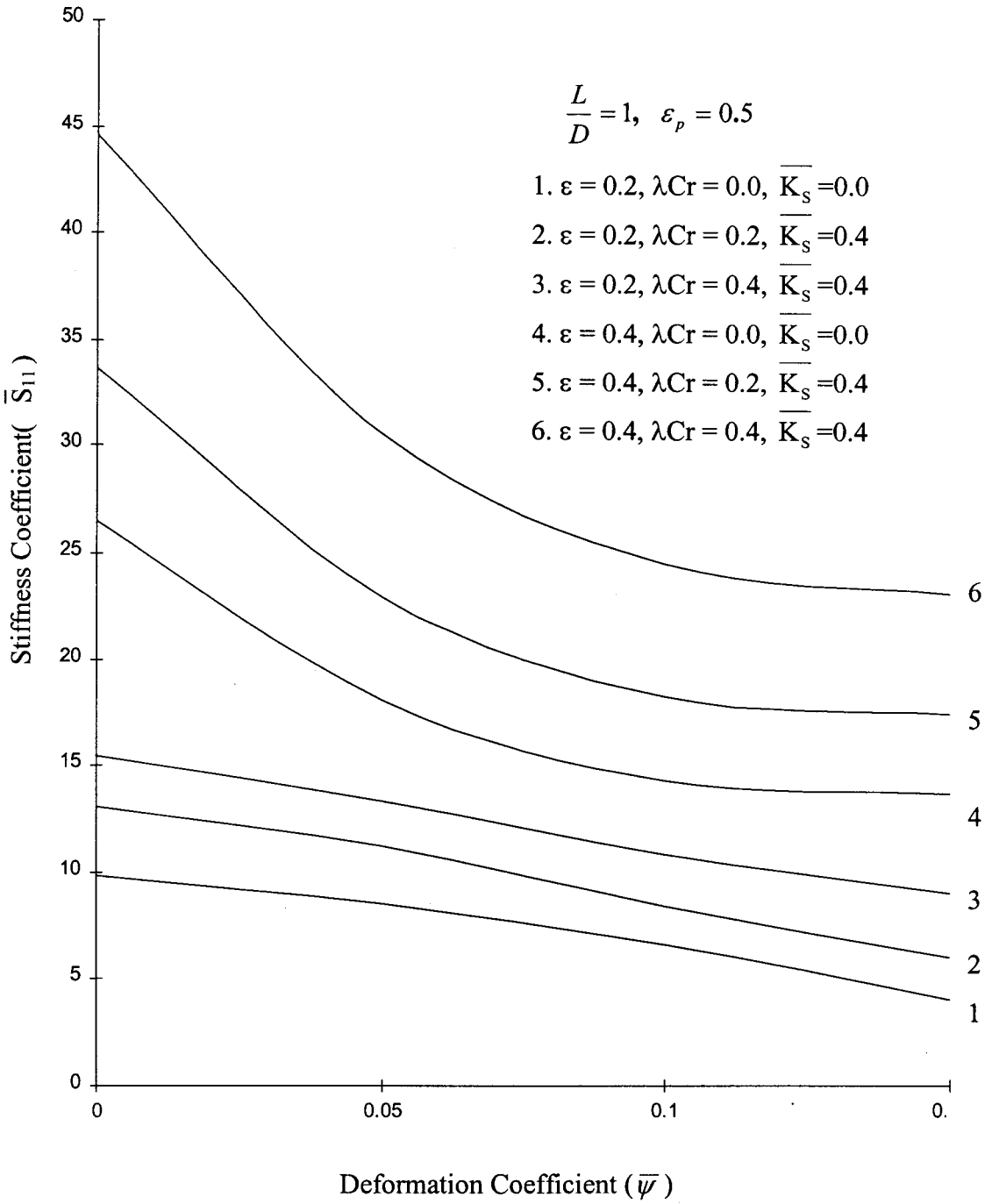

Fig. 5.77 – Stiffness Coefficient($\overline{S}_{11}$) vs Deformation Coefficient ($\overline{\psi}$) in Three Lobe Bearing

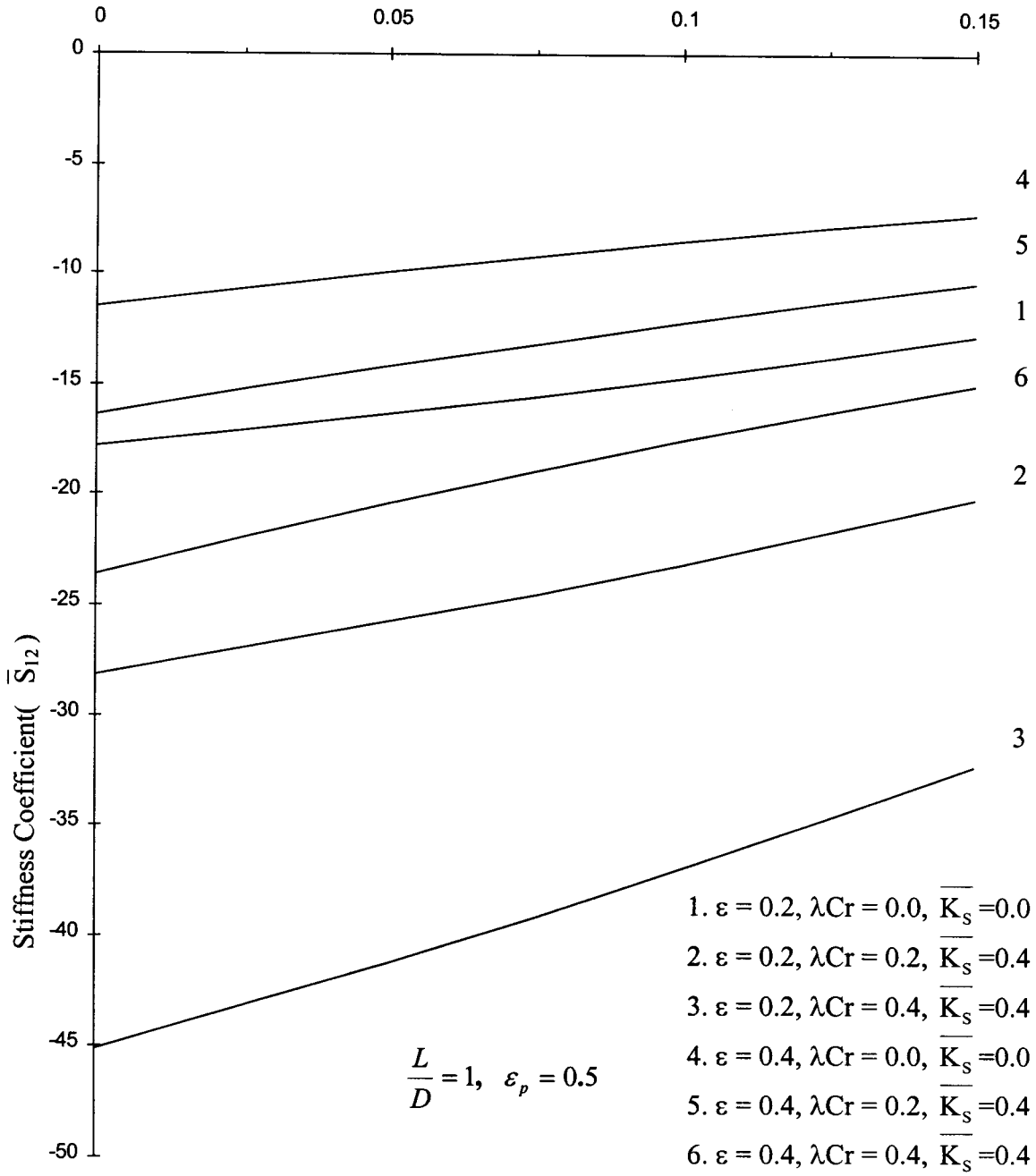

Fig. 5.78 – Stiffness Coefficient($\bar{S}_{12}$) vs Deformation Coefficient ($\bar{\psi}$) in Three Lobe Bearing

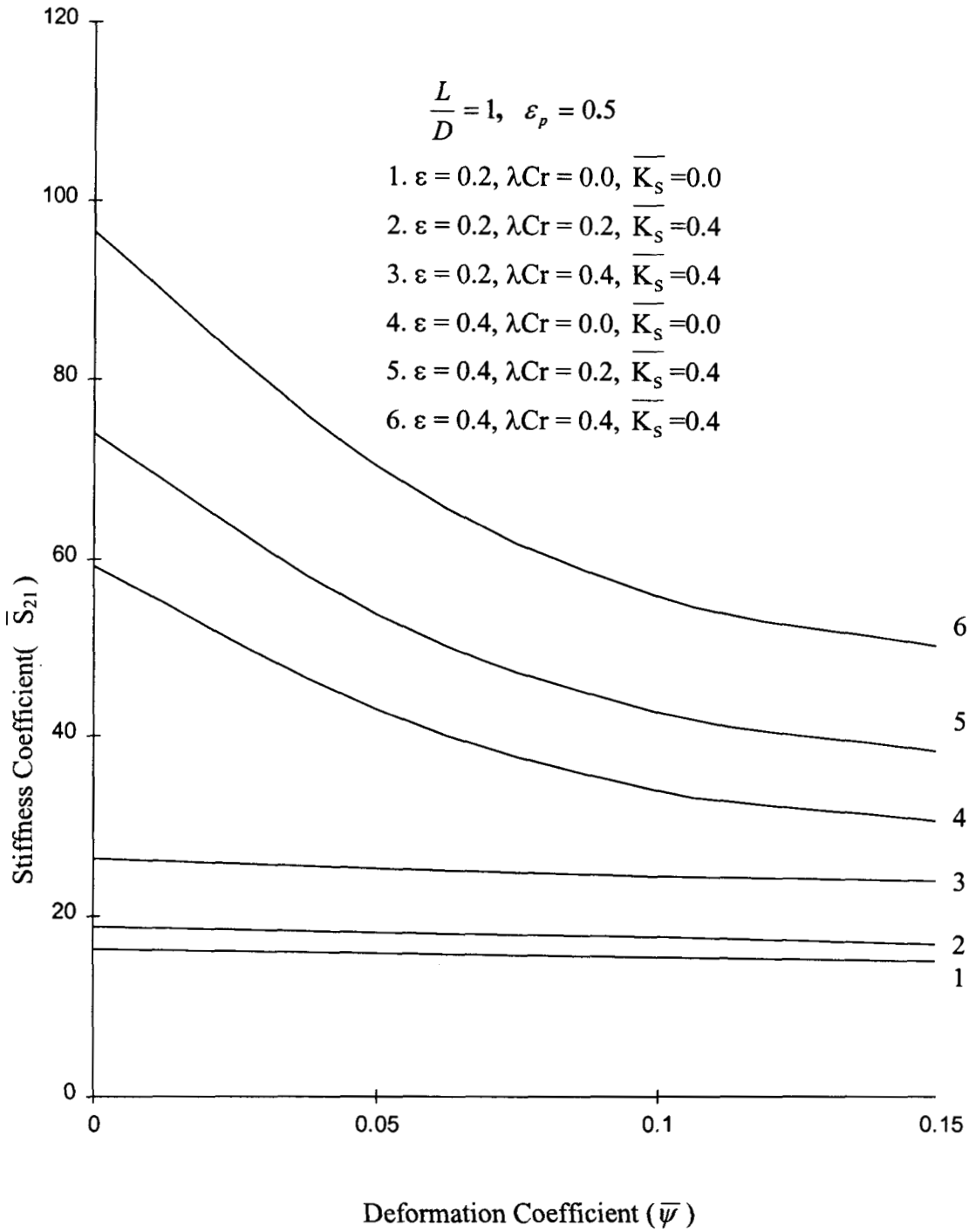

Fig. 5.79 – Stiffness Coefficient($\bar{S}_{21}$) vs Deformation Coefficient ($\overline{\psi}$) in Three Lobe Bearing

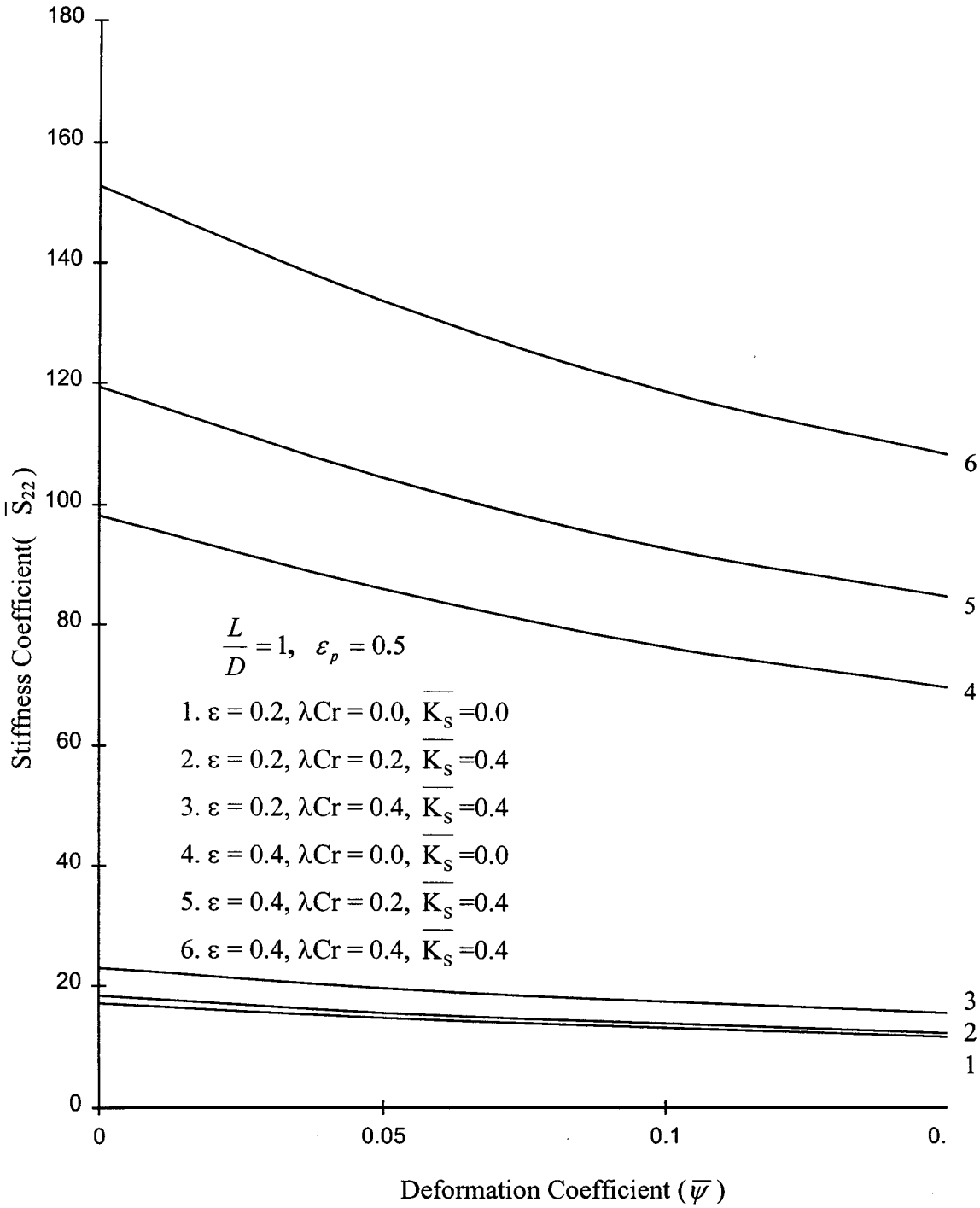

Fig. 5.80 – Stiffness Coefficient($\bar{S}_{22}$) vs Deformation Coefficient ($\bar{\psi}$) in Three Lobe Bearing

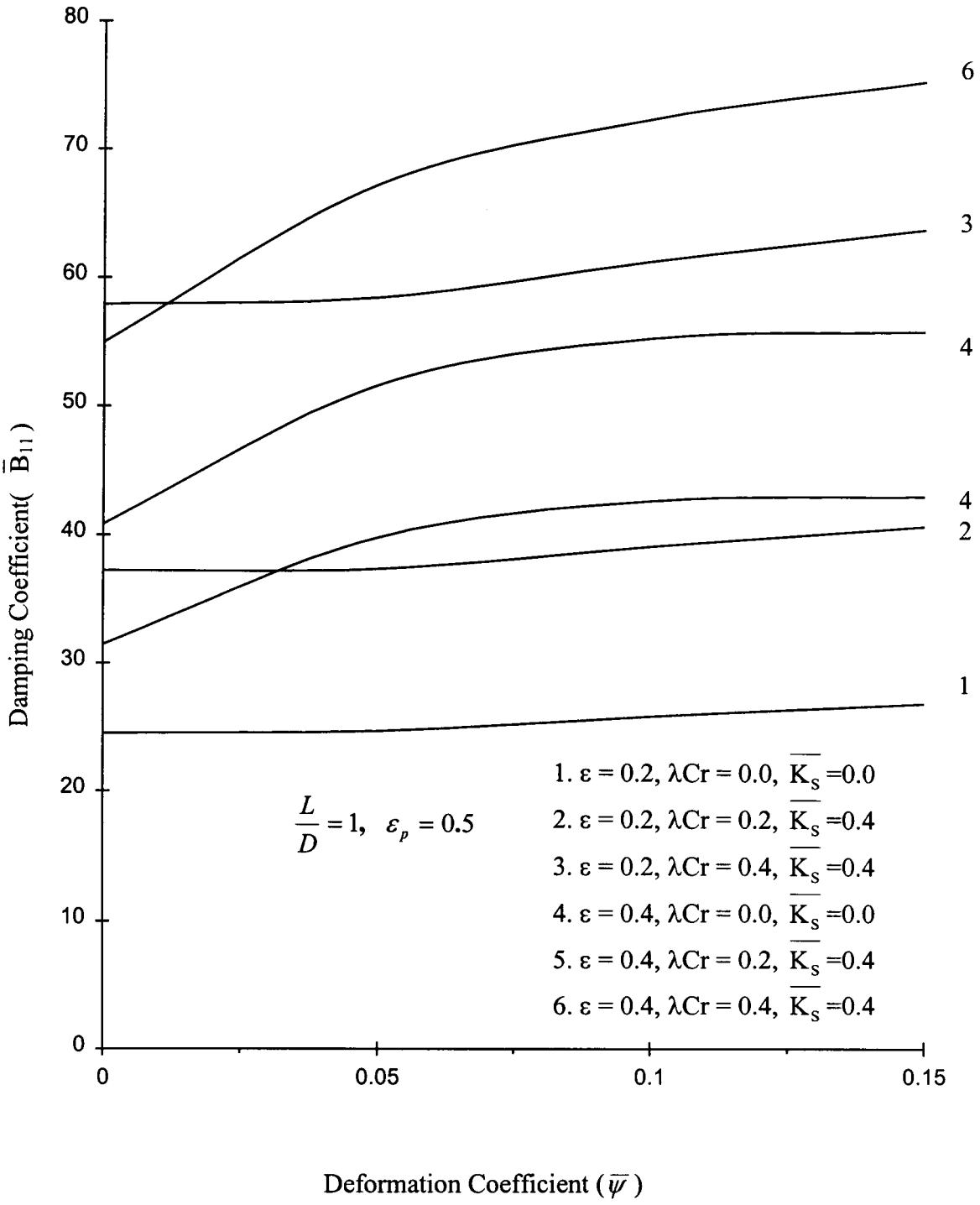

Fig. 5.81– Damping Coefficient($\bar{B}_{11}$) vs Deformation Coefficient ($\bar{\psi}$) in Three Lobe Bearing

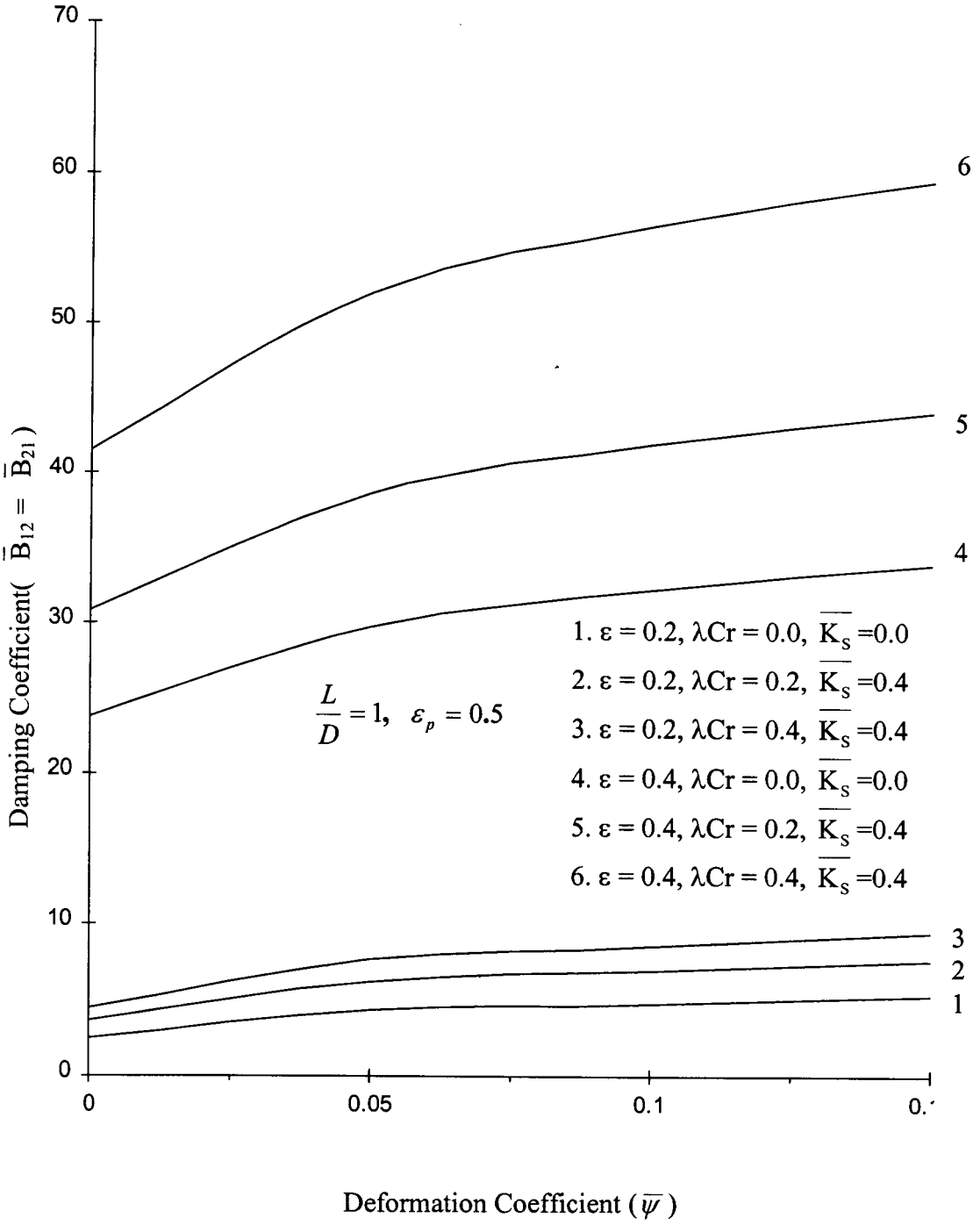

Fig. 5.82– Damping Coefficient($\bar{B}_{12} = \bar{B}_{21}$) vs Deformation Coefficient ($\bar{\psi}$) in Three Lobe Bearing

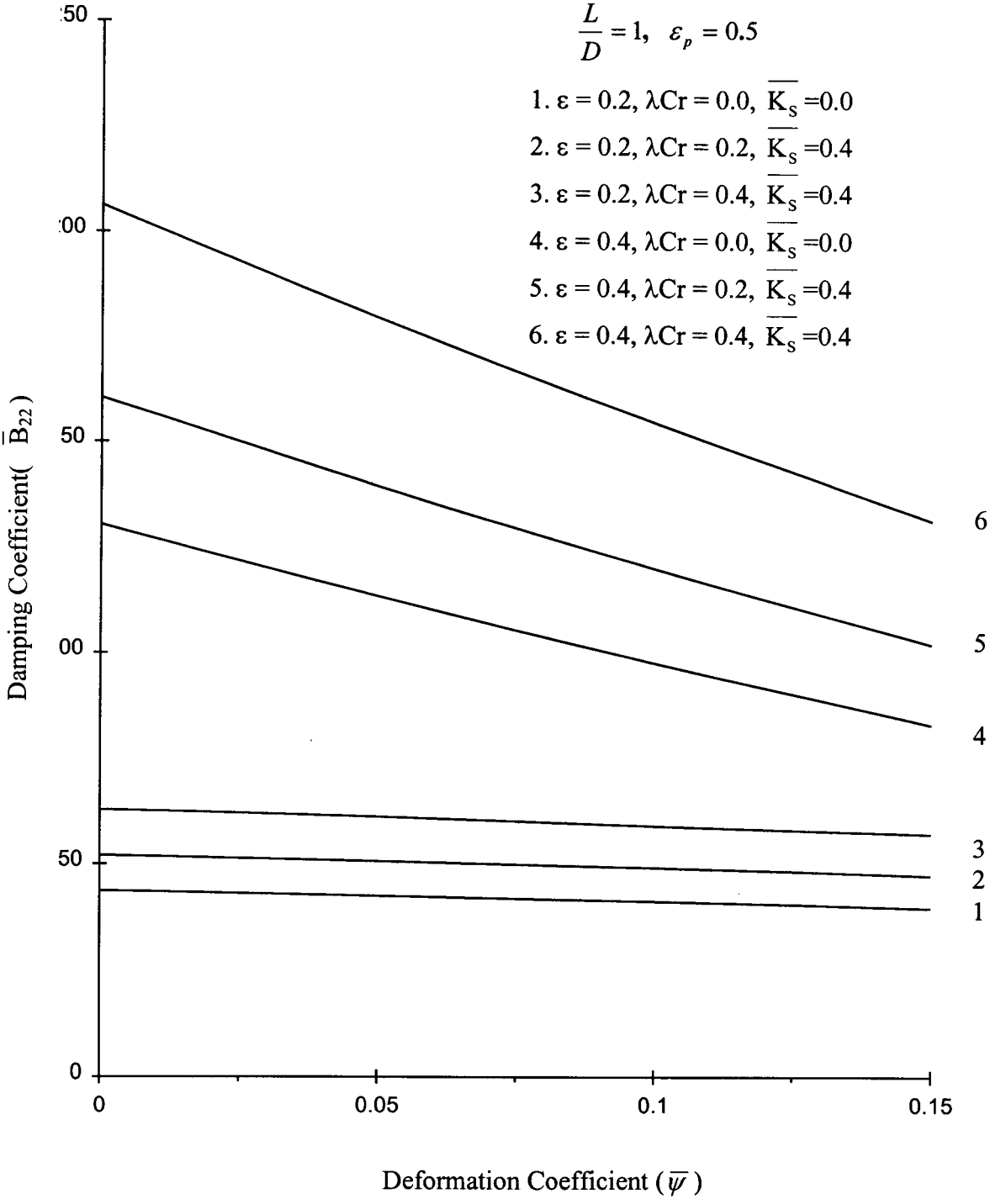

Fig. 5.83– Damping Coefficient($\bar{B}_{22}$) vs Deformation Coefficient ($\bar{\psi}$) in Three Lobe Bearing

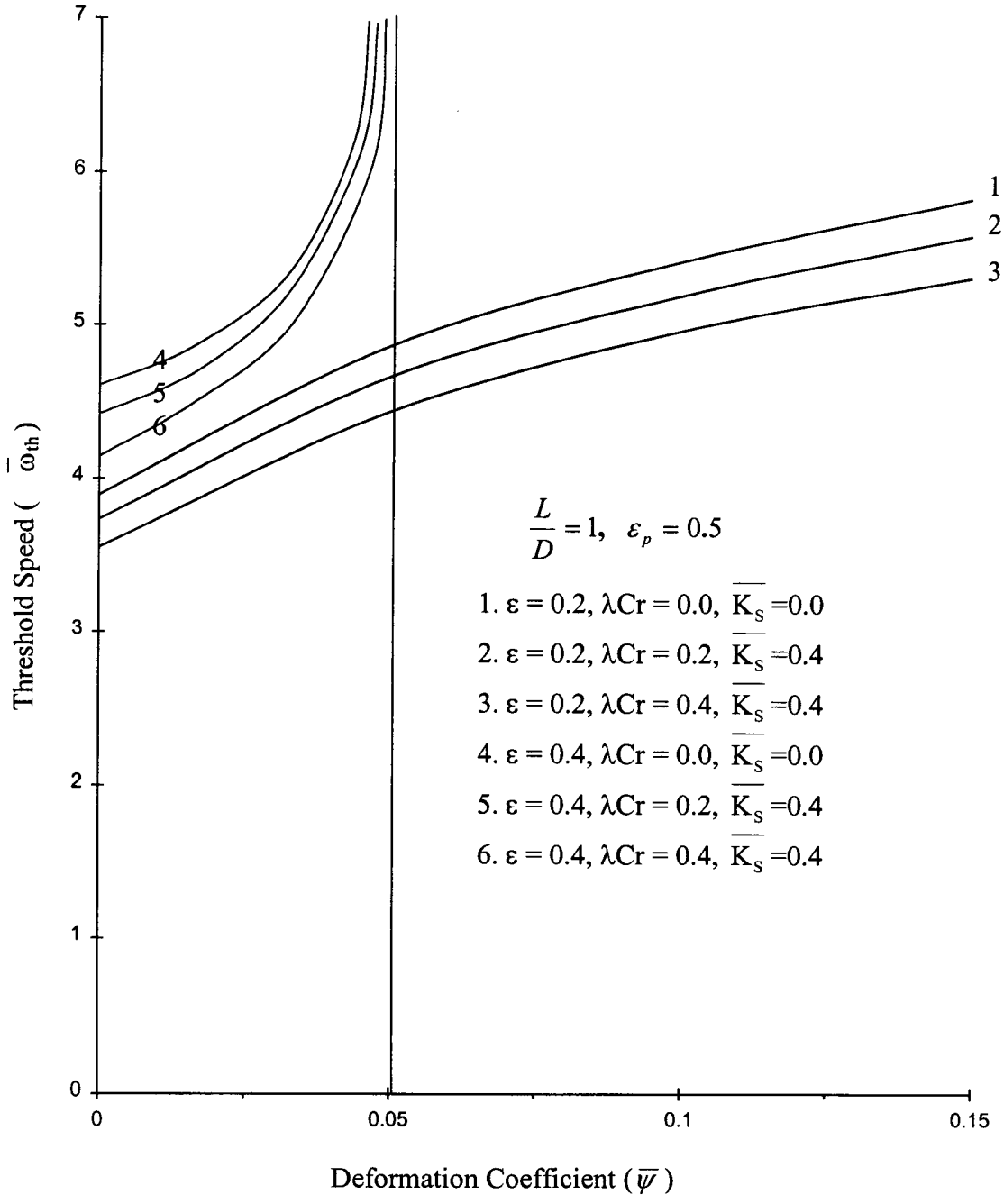

Fig. 5.84 – Threshold Speed ($\bar{\omega}_{th}$) vs Deformation Coefficient ($\bar{\psi}$) in Three Lobe Bearing

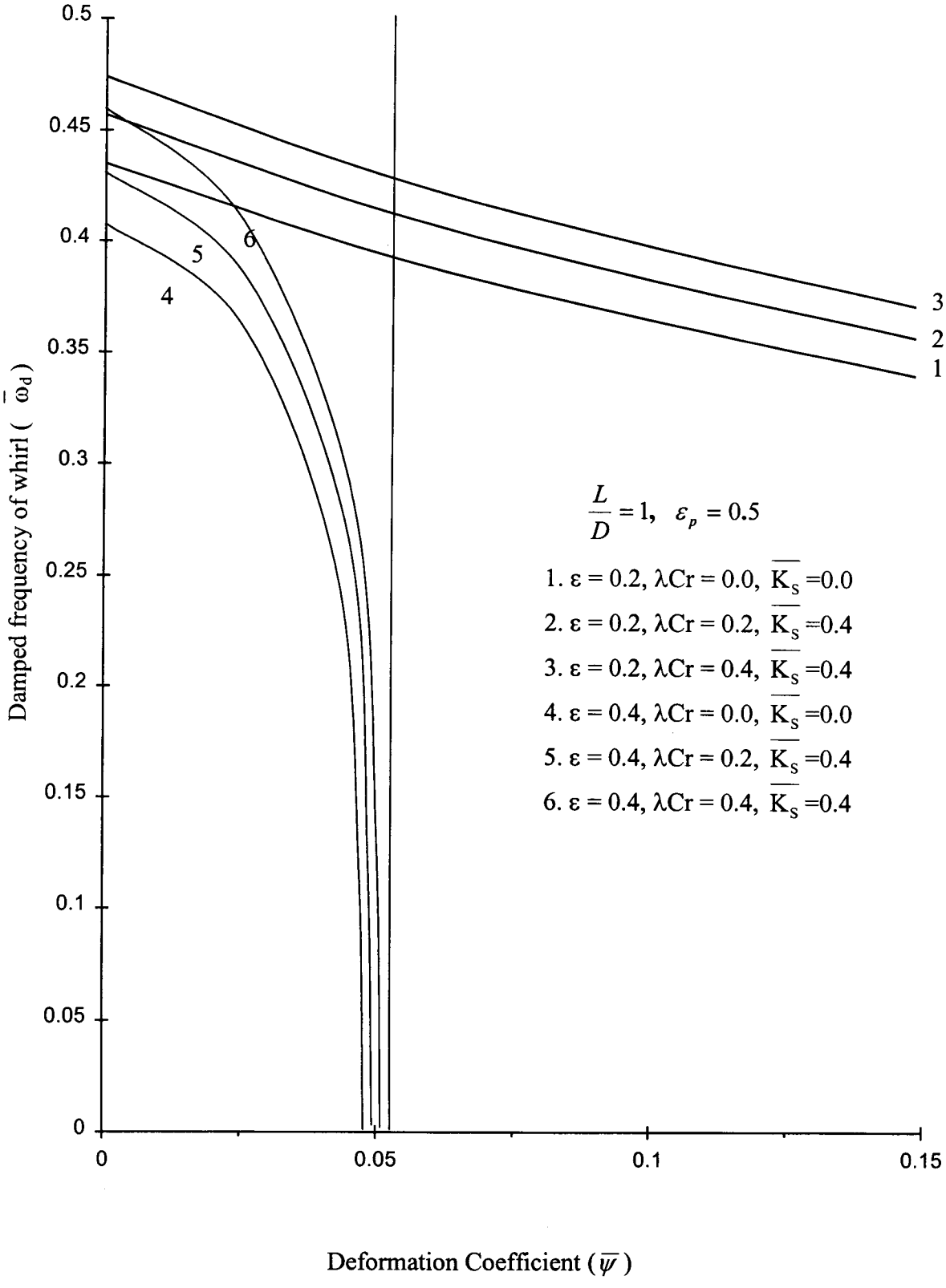

Fig. 5.85 – Damped frequency of whirl ($\bar{\omega}_d$) vs Deformation Coefficient ($\bar{\psi}$) in Three Lobe Bearing

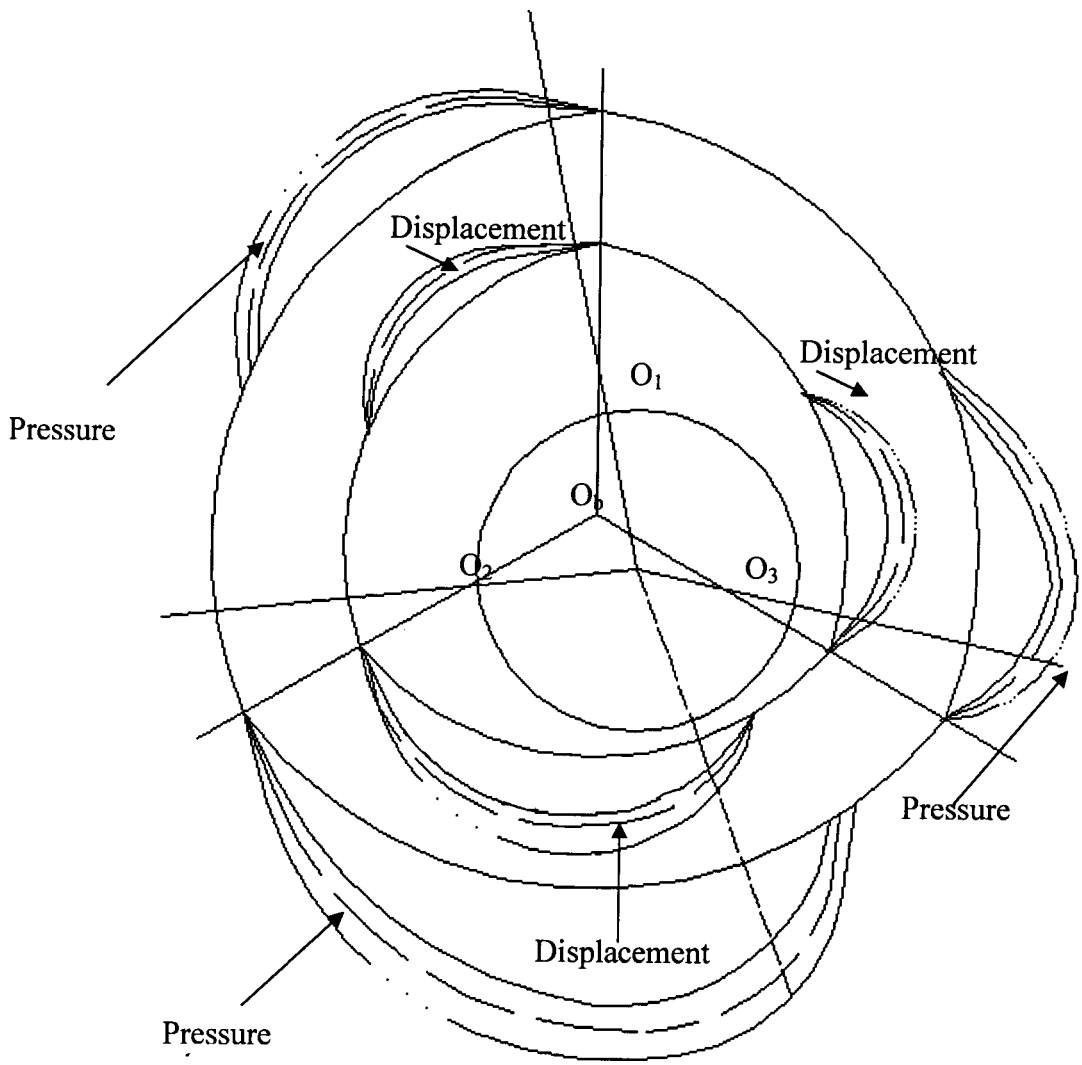

$\varepsilon = 0.2; \lambda c_r = 0.0; K_x = 0.0; \psi = 0.1$

$\varepsilon = 0.2; \lambda c_r = 0.2; K_x = 0.4; \psi = 0.1$

$\varepsilon = 0.2; \lambda c_r = 0.4; K_x = 0.4; \psi = 0.1$

Fig. 5.86 Computed Pressure and Deformation Field in Three Lobe Bearing

ratio. These variations are appreciable especially when bearing operates at high values of deformation coefficients. The mass transfer of additives also changes the values of dynamic characteristics.

The changes in the values of threshold speed and damped frequency of whirl with increase in $\overline{\psi}$ for both micropolar and Newtonian fluids are shown in Fig. 5.84 and Fig. 5.85 respectively. These Figures show the effect of bearing deformation on the threshold speed and damped frequency of whirl. At high values of ε, the nature of variations of threshold speed and damped frequency of whirl with increase in $\overline{\psi}$ for three lobe bearings are different from those for circular and two lobe bearings. The threshold speed increases with increase in $\overline{\psi}$ at very low values of $\overline{\psi}$. When deformation coefficient is more than 0.048, the bearing system is stable at any speed of the journal. The damped frequency of whirl decreases with increase in $\overline{\psi}$ when the deformation coefficient is in the range 0 – 0.048. When deformation coefficient exceeds 0.048, if journal centre is disturbed from its equilibrium position, the journal does not oscillate. The above trend is obtained in the case of micropolar fluids also. But at low values of eccentricity ratios the trend of variation of threshold speed and damped frequency of whirl is entirely different from those obtained at high eccentricity ratios. At low values of eccentricity ratios for both micropolar and Newtonian lubricants, threshold speed increases with increase in deformation coefficient. When volume concentration of additives increases threshold speed decreases, but damped frequency of whirl increases. The pressure and deformation fields in the case of three lobe bearings are shown in Fig. 5.86.

Table 5.14 and 5.15 gives dimensional values of performance characteristics of three lobe bearings operating at various eccentricity ratios ($\varepsilon = 0.2$ and $\varepsilon = 0.4$) for deformation coefficients $\overline{\psi} = 0.05$ and $\overline{\psi} = 0.1$. For an eccentricity ratio $\varepsilon = 0.2$ and deformation coefficient $\overline{\psi} = 0.05$ the load carrying capacity is found to increase form 7.19 kN to 12.57 kN when micropolar lubricant with $\lambda c_r = 0.4$ and $K_s = 0.4$ is considered instead of Newtonian lubricant. The

percentage deviations in the performance characteristics of three lobe bearings compared to rigid bearings operating with Newtonian lubricants are given in Tables 5.16 and 5.17.

5.4 CONCLUSIONS

Based on the results presented in the preceding sections, the following conclusions are drawn for rigid and flexible circular and non circular journal bearing with Newtonian and micropolar lubricants.

i) For any ε, the peak pressure developed in the fluid film of rigid and circular bearing and in each lobe of non circular bearing, load carrying capacity and frictional force increase with increase in volume concentration of additives (λc_r).

ii) For both rigid circular and non circular bearings the end leakage and attitude angle are independent of volume concentration of additives for any value of ε when mass transfer rate of additives (K_s) equal to zero.

iii) When the mass transfer rate of additives (K_s) is present, the peak pressure, load carrying capacity end leakage, and frictional force increase with increase in volume concentration of additives at any value of ε.

iv) For all the three types of bearing studied the dynamic coefficients (stiffness and damping) change appreciably with increase in λc_r especially when ε is large.

v) The threshold speed and damped frequency of whirl are independent of volume concentration of additives when the mass transfer rate is zero, for all the three types of bearings studied.

vi) For micropolar lubricants, the value of threshold speed obtained are less than that obtained for Newtonian lubricant at any value of ε.

vii) For all the three rigid bearing configuration, the damped frequency of whirl increases with increase in λc_r for any value of ε when mass transfer of additives is present.

viii) The stability of rigid circular and non circular (two lobe and three lobe) bearings obtained for micropolar lubricants is less than that obtained for Newtonian lubricant at any value of ε.

ix) At any value of λc_r and ε, the threshold speed decreases but damped frequency of whirl increases when mass transfer rate of additives increases.

x) For any ε, the peak pressure developed in the fluid film of circular bearing and each lobe of non-circular bearings, the load capacity, attitude angle, end leakage and frictional force decrease with increase in $\overline{\psi}$ and significant reduction occurs when $\overline{\psi}$ is large. Reduction in the end leakage with increase in $\overline{\psi}$ is a favourable design condition.

xi) For micropolar lubricant, at any $\overline{\psi}$, the values of load carrying capacity, end leakage, attitude angle and frictional force are more than those obtained with Newtonian lubricants for all the three bearing configurations studied.

xii) For all the bearings studied, appreciable changes in all the dynamic coefficients are obtained with increase in $\overline{\psi}$ especially when $\overline{\psi}$ is high for both Newtonian and micropolar lubricants.

xiii) For both Newtonian and micropolar lubricants at small ε, the threshold speed increase with increase in $\overline{\psi}$ for all the three bearing configurations. For large ε and if $\overline{\psi}$ is small the circular bearing system is always stable whereas the three lobe bearing system remains stable when the value of $\overline{\psi}$ exceeds 0.048 in the case of Newtonian lubricant and 0.049 in the case of micropolar lubricant ($\lambda c_r = 0.4$, $K_s = 0.4$).

xiv) For micropolar lubricant the value of threshold speed obtained is less than that obtained for Newtonian lubricant at any ε and $\overline{\psi}$ for all the bearings.

xv) For all the bearing configurations and lubricants studied, the damped frequency of whirl decreases with increase in $\overline{\psi}$ at small ε. For large ε, at small values of $\overline{\psi}$ in the case of circular bearing and at any value of $\overline{\psi}$ greater than 0.049 in the case of three lobe bearing, the journal when it is disturbed, returns to its equilibrium position without whirl.

xvi) At any ε and $\overline{\psi}$, the values of damped frequency of whirl obtained for micropolar lubricant are more than those obtained for Newtonian lubricant in all the case of bearings studied.

xvii) At any ε and $\overline{\psi}$, threshold speed decreases when mass transfer rate increases but damped frequency of whirl increases for all the bearing configurations.

5.5 SCOPE FOR FUTURE WORK

The work carried out can be extended to obtain performance characteristics of rigid and deformable circular and non circular journal bearings including the effect of variation of viscosity with increase in temperature on the performance. For this purpose thermohydrodynamic analysis should be carried out along with EHD analysis. These performance characteristics (static and dynamic) can be obtained for elastohydrodynamic circular and non circular bearings with micropolar lubricants. In high speed applications the bearing may operate in the turbulent regime. The viscosity will be varied due to turbulence. The effect of turbulence on the performance characteristics of elastothermohydrodynamic bearing operating under micropolar lubricants can also be studied by extending the work.

Table 5.1 Cases studied

Types of Bearings	Cases Studied	Eccentricity Ratio	Volume Concentration of additives (λc_r)	Mass transfer rate (K_s)	Deformation Coefficient $\overline{\psi}$
Circular	Rigid	0.2, .0.6	0.1, 0.2, 0.3, 0.4, 0.5, 0.6.	0.2, 0.4	0.0
	Flexible	0.4, 0.8	0.1, 0.2, 0.3, 0.4, 0.5, 0.6.	0.2, 0.4	0.1, 0.2, 0.3, 0.4, 0.5.
Two lobe	Rigid	0.25, 0.45	0.1, 0.2, 0.3, 0.4, 0.5, 0.6.	0.2, 0.4	0.0
	Flexible	0.25, 0.45	0.1, 0.2, 0.3, 0.4, 0.5, 0.6.	0.2, 0.4	0.05, 0.1, 0.15
Three lobe	Rigid	0.2, 0.4	0.1, 0.2, 0.3, 0.4, 0.5, 0.6.	0.2, 0.4	0.0
	Flexible	0.2, 0.4	0.1, 0.2, 0.3, 0.4, 0.5, 0.6.	0.2, 0.4	0.05, 0.1, 0.15

Table 5.2 Deformation coefficient for different bearing liner materials

Liner Material	Modulus of Elasticity MPa	Poisson's Ratio	Deformation Coefficient ($\overline{\psi}$)
Steel	2.0×10^5	0.3	0.0012
Brass	0.98×10^5	0.33	0.0025
Cast Iron	0.9×10^5	0.27	0.0028
Bronze	0.76×10^5	0.35	0.0033
Babbit (Tin Base)	0.52×10^5	-	0.0048
Babbit (Lead Base)	0.29×10^5	-	0.0088
Texolite	4.8×10^3	0.4	0.053
Nylon	2×10^3	-	0.127
Teflon	0.4×10^3	0.5	0.635

Table 5.3. Dimensional values of performance characteristics of rigid circular bearing for $\varepsilon = 0.4$ and $\varepsilon = 0.8$

Characteristics	$\varepsilon = 0.4$				$\varepsilon = 0.8$			
	$\lambda c_r = 0.0$ $K_s = 0.0$	$\lambda c_r = 0.2$ $K_s = 0.0$	$\lambda c_r = 0.2$ $K_s = 0.4$	$\lambda c_r = 0.4$ $K_s = 0.4$	$\lambda c_r = 0.0$ $K_s = 0.0$	$\lambda c_r = 0.2$ $K_s = 0.0$	$\lambda c_r = 0.2$ $K_s = 0.4$	$\lambda c_r = 0.4$ $K_s = 0.4$
$\overline{W}\times10^{-3}$ N	6.01	7.65	7.98	9.71	34.33	42.82	42.92	55.58
$\bar{Q}_z\times10^{6}$ m^3/s	3.94	3.94	4.18	4.58	7.84	7.84	8.25	8.63
ϕ	62.59	62.59	63.27	66.5	36.37	36.37	37.18	37.26
$\bar{S}_{11}\times10^{-8}$ N/m	2.81	3.79	3.81	4.39	15.75	19.68	20.01	26.49
$\bar{S}_{12}\times10^{-8}$ N/m	-2.25	-2.65	-3.49	-4.91	8.84	6.02	4.49	2.55
$\bar{S}_{21}\times10^{-8}$ N/m	5.12	6.41	6.43	8.24	32.53	40.65	40.66	53.06
$\bar{S}_{22}\times10^{-8}$ N/m	2.55	3.18	2.85	3.40	43.68	54.5	53.25	67.75
$\bar{B}_{11}\times10^{-6}$ N/ms	2.13	2.66	3.21	5.02	5.12	6.05	6.20	8.22
$\bar{B}_{12}\times10^{-6}$ N/m	1.10	1.38	1.59	1.97	6.57	8.22	8.53	11.49
$\bar{B}_{22}\times10^{-6}$ N/m	3.84	4.79	4.81	5.53	22.88	28.60	29.10	36.13
$\overline{\omega}_d\times10^{-2}$ rad/s	1.26	1.26	1.32	1.40	-	-	-	-
$\overline{\omega}_{th}\times10^{-2}$ rad/s	63.09	63.09	61.52	56.54	-	-	-	-

Table 5.4. Dimensional values of performance characteristics of flexible ($\overline{\psi}$ = 0.1) circular bearing for ε = 0.4 and ε = 0.8

Characteristics	ε = 0.4				ε = 0.8			
	λc_r= 0.0 K_s= 0.0	λc_r = 0.2 K_s = 0.0	λc_r = 0.2 K_s = 0.4	λc_r = 0.4 K_s = 0.4	λc_r = 0.0 K_s = 0.0	λc_r = 0.2 K_s = 0.0	λc_r = 0.2 K_s = 0.4	λc_r = 0.4 K_s = 0.4
$\overline{W}\times10^{-3}$ N	5.62	7.03	7.25	9.12	16.08	20.04	20.09	26.02
$\overline{Q}_z\times10^{6}$ m^3/s	3.67	3.67	3.92	3.98	7.06	7.06	7.46	7.85
ϕ	59	59	59.64	62.16	34.22	34.22	34.98	35.06
$\bar{S}_{11}\times10^{-8}$ N/m	2.31	3.13	3.27	3.68	10.37	12.97	13.18	16.68
$\bar{S}_{12}\times10^{-8}$ N/m	-2.57	-3.06	-3.86	-5.78	3.502	1.278	0.319	-1.15
$\bar{S}_{21}\times10^{-8}$ N/m	4.42	5.54	5.19	7.12	12.23	15.28	15.30	19.95
$\bar{S}_{22}\times10^{-8}$ N/m	1.98	2.48	2.26	2.65	10.17	12.65	12.37	16.36
$\bar{B}_{11}\times10^{-6}$ N/ms	2.33	2.91	3.53	5.46	5.57	6.97	7.14	9.46
$\bar{B}_{12}\times10^{-6}$ N/m	0.986	1.23	1.42	1.77	4.26	5.32	5.52	7.25
$\bar{B}_{22}\times10^{-6}$ N/m	3.33	4.17	4.23	4.81	12.54	15.50	15.95	19.82
$\overline{\omega}_d\times10^{-2}$ rad/s	1.22	1.22	1.29	1.33	0.956	0.956	1.03	1.09
$\overline{\omega}_{th}\times10^{-2}$ rad/s	66.39	66.39	64.66	60.34	89.03	86.42	84.29	80.11

Table 5.5 Dimensional values of performance characteristics of flexible ($\overline{\psi}$ =0.2) circular bearing for ε = 0.4 and ε = 0.8

Characteristics	ε = 0.4				ε = 0.8			
	λc_r= 0.0 K_s= 0.0	λc_r = 0.2 K_s = 0.0	λc_r = 0.2 K_s = 0.4	λc_r = 0.4 K_s = 0.4	λc_r = 0.0 K_s = 0.0	λc_r = 0.2 K_s = 0.0	λc_r = 0.2 K_s = 0.4	λc_r = 0.4 K_s = 0.4
$\overline{W}\times10^{-3}$ N	5.19	6.52	6.71	8.18	10.66	13.09	13.29	17.25
$\bar{Q}_z\times10^{6}$ m^3/s	3.53	3.53	3.73	3.86	6.54	6.54	6.87	7.07
ϕ	57.3	57.3	57.92	60.5	33.32	33.32	34.07	34.15
$\bar{S}_{11}\times10^{-8}$ N/m	1.99	2.68	2.71	2.87	7.06	8.82	8.97	11.24
$\bar{S}_{12}\times10^{-8}$ N/m	-2.74	-3.31	-4.14	-6.18	0.338	-1.33	-2.09	-3.17
$\bar{S}_{21}\times10^{-8}$ N/m	3.71	4.63	4.36	6.01	7.66	9.58	9.59	12.51
$\bar{S}_{22}\times10^{-8}$ N/m	1.67	2.09	1.94	2.23	4.35	5.43	5.28	7.03
$\bar{B}_{11}\times10^{-6}$ N/ms	2.39	2.99	3.61	5.61	6.10	7.63	7.81	10.34
$\bar{B}_{12}\times10^{-6}$ N/m	0.923	1.16	1.34	1.65	3.27	4.09	4.25	5.37
$\bar{B}_{22}\times10^{-6}$ N/m	3.00	3.76	3.85	4.33	8.44	10.59	10.73	13.33
$\overline{\omega}_d\times10^{-2}$ rad/s	1.20	1.20	1.26	1.31	0.791	0.791	0.837	0.942
$\overline{\omega}_{th}\times10^{-2}$ rad/s	68.06	68.06	66.31	61.78	95.55	93.20	90.84	86.13

Table 5.6 Percentage deviation in the performance characteristics of circular bearing compared to corresponding values of rigid bearing without additives for $\varepsilon = 0.4$

Characteristics	$\overline{\psi} = 0.1$				$\overline{\psi} = 0.2$			
	$\lambda c_r = 0.0$ $K_s = 0.0$	$\lambda c_r = 0.2$ $K_s = 0$	$\lambda c_r = 0.2$ $K_s = 0.4$	$\lambda c_r = 0.4$ $K_s = 0.4$	$\lambda c_r = 0$ $K_s = 0$	$\lambda c_r = 0.2$ $K_s = 0$	$\lambda c_r = 0.2$ $K_s = 0.4$	$\lambda c_r = 0.4$ $K_s = 0.4$
$\overline{W}$	-6.28	17.20	17.83	51.1	-13.55	8.32	8.93	38.06
$\overline{Q}_z$	-6.64	-6.64	-0.13	-0.33	-10.20	-10.20	-4.05	-1.92
ϕ	-5.73	-5.73	-4.71	-0.687	-8.45	-8.45	-7.46	-3.33
$\overline{F}$	-5.49	-4.82	-4.78	-4.05	-10.27	-10.12	-9.55	-8.82
$\overline{S}_{11}$	-17.42	11.46	9.19	31.25	-29.25	-4.45	-6.50	13.73
$\overline{S}_{12}$	-14.65	-36.3	-72.1	-108.01	-60.81	-85.52	-96.32	-113.06
$\overline{S}_{21}$	-13.59	7.96	-0.561	39.02	-27.68	-9.60	-16.67	17.20
$\overline{S}_{22}$	-21.87	-2.51	-19.64	4.01	-34.23	-18.04	-31.82	-12.28
$\overline{B}_{11}$	9.88	37.29	65.88	157.12	12.50	40.62	69.90	164.02
$\overline{B}_{12}$	-10.46	11.72	29.21	60.23	-15.78	5.27	21.67	49.60
$\overline{B}_{22}$	-13.03	8.64	3.75	25.23	-21.67	-2.09	-6.54	12.84
$\overline{\omega}_d$	-3.11	-3.11	1.67	5.59	-4.76	-4.76	-0.207	3.72
$\overline{\omega}_{th}$	2.21	2.21	-0.443	-7.09	4.79	4.79	2.09	-4.87

$$\text{Percentage deviation} = \frac{(\text{parameter}|_{\text{elastic}} - \text{parameter}|_{\text{rigid}}) \times 100}{\text{parameter}|_{\text{rigid}}}$$

Table 5.7 Percentage deviation in the performance characteristics of circular bearing compared to corresponding values of rigid bearing without additives for $\varepsilon = 0.8$

Characteristics	$\overline{\psi} = 0.1$				$\overline{\psi} = 0.2$			
	$\lambda c_r = 0.0$ $K_s = 0.0$	$\lambda c_r = 0.2$ $K_s = 0$	$\lambda c_r = 0.2$ $K_s = 0.4$	$\lambda c_r = 0.4$ $K_s = 0.4$	$\lambda c_r = 0$ $K_s = 0$	$\lambda c_r = 0.2$ $K_s = 0$	$\lambda c_r = 0.2$ $K_s = 0.4$	$\lambda c_r = 0.4$ $K_s = 0.4$
$\overline{W}$	-53.19	-41.49	-41.23	-24.24	-68.96	-61.31	-61.21	-49.76
$\overline{Q}_z$	-9.18	-9.18	-4.34	0.584	-16.52	-16.52	-11.85	-9.68
ϕ	-5.91	-5.91	-3.82	-3.57	-8.38	-8.38	-6.32	-6.13
$\overline{F}$	-27.13	-26.61	-26.43	-25.7	-38.59	-37.00	-36.91	-36.82
$\overline{S}_{11}$	-34.11	-17.65	-16.31	5.87	-55.21	-44.01	-43.08	-28.6
$\overline{S}_{12}$	-14.65	-36.21	-72.1	-128.72	-96.12	-115.12	-123.61	-135.81
$\overline{S}_{21}$	-62.23	-52.99	-52.91	-38.65	-76.4	-70.52	-70.50	-61.52
$\overline{S}_{22}$	-76.71	-70.88	-71.93	-62.54	-90.04	-87.56	-87.91	-89.75
$\overline{B}_{11}$	15.11	43.91	47.58	95.13	25.92	57.41	61.13	111.13
$\overline{B}_{12}$	-35.28	-19.11	-16.04	42.07	-50.24	-37.81	-35.47	-18.36
$\overline{B}_{22}$	-45.17	-32.25	-30.28	-13.37	-63.14	-53.71	-53.12	-41.75
$\overline{\omega}_d$	-	-	-	-	-	-	-	-
$\overline{\omega}_{th}$	-	-	-	-	-	-	-	-

$$\text{Percentage deviation} = \frac{(\text{parameter}|_{\text{elastic}} - \text{parameter}|_{\text{rigid}}) \times 100}{\text{parameter}|_{\text{rigid}}}$$

Table 5.8 Dimensional values of performance characteristics of rigid two lobe bearing for $\varepsilon = 0.25$ and $\varepsilon = 0.45$

Characteristics	$\varepsilon = 0.25$				$\varepsilon = 0.45$			
	$\lambda c_r = 0.0$ $K_s = 0.0$	$\lambda c_r = 0.2$ $K_s = 0.0$	$\lambda c_r = 0.2$ $K_s = 0.4$	$\lambda c_r = 0.4$ $K_s = 0.4$	$\lambda c_r = 0.0$ $K_s = 0.0$	$\lambda c_r = 0.2$ $K_s = 0.0$	$\lambda c_r = 0.2$ $K_s = 0.4$	$\lambda c_r = 0.4$ $K_s = 0.4$
$\overline{W} \times 10^{-3}$ N	9.23	11.55	11.68	16.06	36.99	46.27	46.78	64.23
$\overline{Q}_z \times 10^{6}$ m^3/s	3.16	3.16	3.22	3.26	3.87	3.87	3.93	3.98
ϕ	84.85	85.01	85.35	86.31	65.31	65.43	65.86	66.42
$\overline{S}_{11} \times 10^{-8}$ N/m	2.25	3.03	3.04	3.83	13.71	17.14	17.43	23.06
$\overline{S}_{12} \times 10^{-8}$ N/m	-7.39	-9.24	-11.68	-18.72	-0.15	-0.19	-0.22	-0.32
$\overline{S}_{21} \times 10^{-8}$ N/m	9.60	11.99	11.04	15.72	36.63	45.97	45.88	59.78
$\overline{S}_{22} \times 10^{-8}$ N/m	14.08	17.60	14.82	19.12	56.81	71.01	69.07	88.42
$\overline{B}_{11} \times 10^{-6}$ N/ms	3.60	4.49	5.44	8.51	5.84	7.30	7.58	10.21
$\overline{B}_{12} \times 10^{-6}$ N/m	-4.60	-5.74	-6.64	-8.24	3.20	4.01	4.16	5.61
$\overline{B}_{22} \times 10^{-6}$ N/m	11.47	14.38	14.04	17.08	30.13	37.66	37.03	47.61
$\overline{\omega}_d \times 10^{-2}$ rad/s	1.21	1.21	1.28	1.34	0.98	0.98	1.05	1.10
$\overline{\omega}_{th} \times 10^{-2}$ rad/s	8.19	8.19	7.78	7.50	10.40	10.40	9.76	9.27

Table 5.9 Dimensional values of performance characteristics of flexible ($\overline{\psi}$ = 0.05) two lobe bearing for ε = 0.25 and ε = 0.45

Characteristics	ε = 0.25				ε = 0.45			
	λc_r= 0.0 K_s= 0.0	λc_r = 0.2 K_s = 0.0	λc_r = 0.2 K_s = 0.4	λc_r = 0.4 K_s = 0.4	λc_r = 0.0 K_s = 0.0	λc_r = 0.2 K_s = 0.0	λc_r = 0.2 K_s = 0.4	λc_r = 0.4 K_s = 0.4
$\overline{W}\times10^{-3}$ N	9.101	11.377	11.516	15.821	26.623	33.28	33.67	46.22
$\bar{Q}_z\times10^{6}$ m^3/s	3.121	3.124	3.162	3.203	3.848	3.848	3.900	3.946
ϕ	84.032	84.031	84.375	85.045	62.015	62.015	62.449	62.780
$\bar{S}_{11}\times10^{-8}$ N/m	2.314	3.124	3.074	3.613	10.827	13.535	13.761	18.209
$\bar{S}_{12}\times10^{-8}$ N/m	-7.152	-8.943	-11.293	-18.102	-0.136	-0.171	-0.195	-0.281
$\bar{S}_{21}\times10^{-8}$ N/m	9.431	11.802	10.856	15.178	26.064	32.575	32.609	42.536
$\bar{S}_{22}\times10^{-8}$ N/m	11.374	17.161	14.277	18.326	35.729	44.658	43.44	55.606
$\bar{B}_{11}\times10^{-6}$ N/ms	3.662	4.583	5.535	8.655	6.614	7.707	7.998	10.773
$\bar{B}_{12}\times10^{-6}$ N/m	-4.461	-5.574	-6.434	-7.975	3.437	4.294	4.458	6.005
$\bar{B}_{22}\times10^{-6}$ N/m	11.382	14.223	13.583	16.394	22.268	27.834	27.370	35.19
$\overline{\omega}_d\times10^{-2}$ rad/s	1.213	1.216	1.276	1.312	0.971	0.971	1.031	1.089
$\overline{\omega}_{th}\times10^{-2}$ rad/s	8.324	8.325	7.983	7.983	10.731	10.731	10.272	9.785

Table 5.10 Dimensional values of performance characteristics of flexible ($\overline{\psi}$ = 0.1) two lobe bearing for ε = 0.25 and ε = 0.45

Characteristics	ε = 0.25				ε = 0.45			
	λc_r= 0.0 K_s= 0.0	λc_r = 0.2 K_s = 0.0	λc_r = 0.2 K_s = 0.4	λc_r = 0.4 K_s = 0.4	λc_r = 0.0 K_s = 0.0	λc_r = 0.2 K_s = 0.0	λc_r = 0.2 K_s = 0.4	λc_r = 0.4 K_s = 0.4
$\overline{W}\times10^{-3}$ N	9.001	11.255	11.383	15.591	202.22	253.10	255.91	357.92
$\bar{Q}_z\times10^{6}$ m^3/s	3.023	3.025	3.062	3.113	3.782	3.782	3.835	3.881
ϕ	82.102	82.106	82.436	83.156	59	59	59.3	59.7
$\bar{S}_{11}\times10^{-8}$ N/m	2.234	3.002	2.957	3.454	8.929	10.801	11.351	15.021
$\bar{S}_{12}\times10^{-8}$ N/m	-7.015	-8.763	-10.073	-17.263	-0.102	-0.128	-0.146	-0.211
$\bar{S}_{21}\times10^{-8}$ N/m	9.106	11.385	10.472	1.445	19.583	24.607	24.298	31.957
$\bar{S}_{22}\times10^{-8}$ N/m	12.783	15.984	13.281	18.322	26.697	32.597	32.456	41.545
$\bar{B}_{11}\times10^{-6}$ N/ms	3.714	4.642	5.604	8.911	6.357	7.934	8.244	11.108
$\bar{B}_{12}\times10^{-6}$ N/m	-4.066	-5.083	-5.875	-7.383	3.618	4.541	4.693	6.323
$\bar{B}_{22}\times10^{-6}$ N/m	11.158	13.944	13.316	16.138	18.940	27.832	23.281	29.93
$\overline{\omega}_d\times10^{-2}$ rad/s	1.197	1.19	1.255	1.307	0.955	0.955	1.015	1.075
$\overline{\omega}_{th}\times10^{-2}$ rad/s	8.483	8.482	8.135	7.726	11.047	11.047	10.366	9.895

Table 5.11 Percentage deviation in the performance characteristics of two lobe bearing compared to corresponding values of rigid bearing without additives for $\varepsilon = 0.25$

Characteristics	$\overline{\psi} = 0.05$				$\overline{\psi} = 0.1$			
	$\lambda c_r = 0.0$ $K_s = 0.0$	$\lambda c_r = 0.2$ $K_s = 0$	$\lambda c_r = 0.2$ $K_s = 0.4$	$\lambda c_r = 0.4$ $K_s = 0.4$	$\lambda c_r = 0$ $K_s = 0$	$\lambda c_r = 0.2$ $K_s = 0$	$\lambda c_r = 0.2$ $K_s = 0.4$	$\lambda c_r = 0.4$ $K_s = 0.4$
$\overline{W}$	-1.49	23.13	25.06	71.25	-2.62	21.74	23.18	68.71
$\overline{Q}_z$	-1.24	-1.24	0.01	1.24	-4.31	-4.31	-3.10	-1.86
ϕ	-1.16	-1.16	-0.765	-0.021	-3.24	-3.24	-2.85	-2.00
$\overline{f}$	-3.26	-22.2	-23.1	-43.52	-6.91	-25.14	-26.00	-45.15
$\overline{S}_{11}$	2.584	38.31	39.32	59.02	-1.12	33.48	30.92	53.36
$\overline{S}_{12}$	-3.21	-20.81	-52.72	-144.71	-5.23	-18.32	-49.51	-138.52
$\overline{S}_{21}$	-1.01	23.69	13.89	59.2	-4.42	19.46	9.93	51.01
$\overline{S}_{22}$	-1.42	23.16	23.8	31.46	-8.25	14.68	4.68	22.38
$\overline{B}_{11}$	1.75	27.18	53.64	140.33	3.11	28.88	55.67	147.59
$\overline{B}_{12}$	3.18	-20.9	-39.06	-73.3	11.62	-10.40	-27.60	-60.5
$\overline{B}_{22}$	-0.808	23.9	18.38	42.85	-2.81	21.48	16.00	40.63
$\overline{\omega}_d$	-0.646	-0.646	4.31	8.18	-1.51	-1.51	3.23	7.32
$\overline{\omega}_{th}$	1.34	1.34	-2.58	-7.28	3.58	3.58	0.671	-5.69

$$\text{Percentage deviation} = \frac{(\text{parameter}|_{\text{elastic}} - \text{parameter}|_{\text{rigid}}) \times 100}{\text{parameter}|_{\text{rigid}}}$$

Table 5.12 Percentage deviation in the performance characteristics of two lobe bearing compared to corresponding values of rigid bearing without additives for $\varepsilon = 0.45$

	$\overline{\psi} = 0.05$				$\overline{\psi} = 0.1$			
	$\lambda c_r = 0.0$ $K_s = 0.0$	$\lambda c_r = 0.2$ $K_s = 0$	$\lambda c_r = 0.2$ $K_s = 0.4$	$\lambda c_r = 0.4$ $K_s = 0.4$	$\lambda c_r = 0$ $K_s = 0$	$\lambda c_r = 0.2$ $K_s = 0$	$\lambda c_r = 0.2$ $K_s = 0.4$	$\lambda c_r = 0.4$ $K_s = 0.4$
$\overline{W}$	-28.03	-9.96	-8.95	24.92	-45.31	-31.57	-30.80	-3.24
$\overline{Q}_z$	-0.759	-0.759	0.591	1.772	-2.44	-2.44	-1.09	0.084
ϕ	-5.19	-5.19	-4.52	-4.00	-9.82	-9.82	-9.36	-8.75
$\overline{f}$	-16.67	-32.71	-33.42	-50.61	-26.41	-40.56	-41.2	-55.66
$\overline{S}_{11}$	-21.06	-1.35	0.326	32.3	-34.91	-21.25	-17.24	9.49
$\overline{S}_{12}$	14.92	-8.18	-23.91	-78.6	35.12	-18.96	-7.2	-34.11
$\overline{S}_{21}$	28.8	-11.09	-10.99	16.01	-46.54	-32.82	-10.98	-12.76
$\overline{S}_{22}$	-37.1	-21.39	-23.53	-21.2	-53.00	-42.62	-42.8	-26.8
$\overline{B}_{11}$	5.46	36.83	31.81	84.32	8.76	35.74	41.49	90.12
$\overline{B}_{12}$	7.15	33.86	38.96	87.2	12.68	41.53	46.24	97.02
$\overline{B}_{22}$	-26.09	-7.61	-9.15	16.79	-37.13	-22.12	-22.72	-0.656
$\overline{\omega}_d$	-1.32	-1.32	4.78	10.63	-2.92	-2.92	4.73	9.31
$\overline{\omega}_{th}$	3.17	3.17	-1.35	-6.13	6.19	6.19	-0.352	-4.88

$$\text{Percentage deviation} = \frac{(\text{parameter}|_{\text{elastic}} - \text{parameter}|_{\text{rigid}}) \times 100}{\text{parameter}|_{\text{rigid}}}$$

Table 5.13 Dimensional values of performance characteristics of rigid three lobe bearing for $\varepsilon = 0.2$ and $\varepsilon = 0.4$

Characteristics	$\varepsilon = 0.2$				$\varepsilon = 0.4$			
	$\lambda c_r = 0.0$ $K_s = 0.0$	$\lambda c_r = 0.2$ $K_s = 0.0$	$\lambda c_r = 0.2$ $K_s = 0.4$	$\lambda c_r = 0.4$ $K_s = 0.4$	$\lambda c_r = 0.0$ $K_s = 0.0$	$\lambda c_r = 0.2$ $K_s = 0.0$	$\lambda c_r = 0.2$ $K_s = 0.4$	$\lambda c_r = 0.4$ $K_s = 0.4$
$\overline{W} \times 10^{-3}$ N	8.11	10.12	10.27	14.18	36.22	45.25	45.86	63.20
$\overline{Q}_z \times 10^{6}$ m^3/s	1.56	1.56	1.57	1.59	2.38	2.38	2.41	2.44
ϕ	56.45	56.45	56.54	56.72	49.86	49.86	49.93	50.03
$\bar{S}_{11} \times 10^{-8}$ N/m	6.31	8.51	8.62	9.86	16.93	21.17	21.53	28.49
$\bar{S}_{12} \times 10^{-8}$ N/m	-11.39	-14.24	-18.00	-28.85	-7.32	-9.15	-10.46	-15.07
$\bar{S}_{21} \times 10^{-8}$ N/m	10.48	13.11	14.03	16.88	37.79	47.24	47.29	61.68
$\bar{S}_{22} \times 10^{-8}$ N/m	10.96	13.71	11.39	14.63	62.71	78.41	76.28	97.64
$\bar{B}_{11} \times 10^{-6}$ N/ms	5.98	7.48	9.03	14.14	7.68	9.60	9.96	13.42
$\bar{B}_{12} \times 10^{-6}$ N/m	0.602	0.752	0.869	1.076	5.79	7.24	7.52	10.13
$\bar{B}_{22} \times 10^{-6}$ N/m	10.65	13.31	12.69	15.34	31.85	39.83	39.96	50.29
$\overline{\omega}_d \times 10^{-2}$ rad/s	1.13	1.13	1.19	1.24	1.06	1.06	1.14	1.19
$\overline{\omega}_{th} \times 10^{-2}$ rad/s	10.18	10.18	9.76	9.29	12.14	12.14	11.38	10.81

Table 5.14 Dimensional values of performance characteristics of flexible ($\overline{\psi}$ = 0.05) three lobe bearing for ε = 0.2 and ε = 0.4

Characteristics	ε = 0.2				ε = 0.4			
	λc_r= 0.0 K_s= 0.0	λc_r = 0.2 K_s = 0.0	λc_r = 0.2 K_s = 0.4	λc_r = 0.4 K_s = 0.4	λc_r = 0.0 K_s = 0.0	λc_r = 0.2 K_s = 0.0	λc_r = 0.2 K_s = 0.4	λc_r = 0.4 K_s = 0.4
$\overline{W}\times10^{-3}$ N	7.19	8.97	9.10	12.57	29.55	36.53	36.63	51.59
$\overline{Q}_z\times10^{6}$ m^3/s	1.45	1.45	1.46	1.48	2.08	20.08	2.11	2.14
ϕ	55.56	55.56	55.65	55.83	47.66	47.66	47.73	47.82
$\bar{S}_{11}\times10^{-8}$ N/m	5.46	7.37	7.43	8.55	11.55	14.43	14.67	19.57
$\bar{S}_{12}\times10^{-8}$ N/m	-10.41	-13.00	-16.43	-26.33	-6.32	-7.91	-9.04	-13.02
$\bar{S}_{21}\times10^{-8}$ N/m	10.14	12.67	11.67	16.32	27.56	34.43	34.47	44.97
$\bar{S}_{22}\times10^{-8}$ N/m	9.43	11.77	9.97	12.57	54.94	68.67	66.79	85.51
$\bar{B}_{11}\times10^{-6}$ N/ms	6.05	7.56	9.14	14.29	9.73	12.16	16.62	16.43
$\bar{B}_{12}\times10^{-6}$ N/ms	1.05	1.31	1.52	1.88	7.27	9.09	9.44	12.71
$\bar{B}_{22}\times10^{-6}$ N/ms	10.41	13.01	12.42	15.00	27.75	34.69	34.11	43.85
$\overline{\omega}_d\times10^{-2}$ rad/s	1.03	1.03	1.08	1.12	-	-	-	-
$\overline{\omega}_{th}\times10^{-2}$ rad/s	12.72	12.72	12.22	11.62	-	-	-	-

Table 5.15 Dimensional values of performance characteristics of flexible ($\overline{\psi}$ = 0.1) three lobe bearing for ε = 0.2 and ε = 0.4

Characteristics	ε = 0.2				ε = 0.4			
	λc_r= 0.0 K_s= 0.0	λc_r = 0.2 K_s = 0.0	λc_r = 0.2 K_s = 0.4	λc_r = 0.4 K_s = 0.4	λc_r = 0.0 K_s = 0.0	λc_r = 0.2 K_s = 0.0	λc_r = 0.2 K_s = 0.4	λc_r = 0.4 K_s = 0.4
$\overline{W}\times10^{-3}$ N	6.34	7.92	8.02	11.19	25.56	31.95	32.36	44.74
$\overline{Q}_z\times10^{6}$ m^3/s	1.36	1.36	1.37	1.39	1.85	1.85	1.87	1.90
ϕ	53.9	53.9	53.98	54.1	45.15	45.15	45.21	45.3
$\overline{S}_{11}\times10^{-8}$ N/m	4.73	6.39	5.43	7.28	9.21	11.51	11.69	15.72
$\overline{S}_{12}\times10^{-8}$ N/m	-9.36	-11.69	-14.78	-23.58	-5.42	-6.78	-7.75	-11.16
$\overline{S}_{21}\times10^{-8}$ N/m	9.97	12.46	11.47	15.78	21.92	28.12	27.43	35.79
$\overline{S}_{22}\times10^{-8}$ N/m	8.43	10.54	8.89	11.25	48.87	68.67	59.42	76.06
$\overline{B}_{11}\times10^{-6}$ N/ms	6.34	7.93	9.58	14.99	10.44	13.06	13.54	17.72
$\overline{B}_{12}\times10^{-6}$ N/ms	1.17	1.45	1.69	2.11	7.91	9.95	10.26	13.81
$\overline{B}_{22}\times10^{-6}$ N/ms	10.16	12.69	12.12	14.52	23.92	30.03	29.43	37.84
$\overline{\omega}_d\times10^{-2}$ rad/s	0.958	0.958	1.00	1.04	-	-	-	-
$\overline{\omega}_{th}\times10^{-2}$ rad/s	14.18	14.18	13.61	13.01	-	-	-	-

Table 5.16 Percentage deviation in the performance characteristics of three lobe bearing compared to corresponding values of rigid bearing without additives for $\varepsilon = 0.2$

Characteristics	$\bar{\psi} = 0.05$				$\bar{\psi} = 0.1$			
	λc_r=0.0 K_s=0.0	λc_r =0.2 K_s =0	λc_r =0.2 K_s =0.4	λc_r =0.4 K_s =0.4	λc_r =0 K_s =0	λc_r =0.2 K_s =0	λc_r =0.2 K_s =0.4	λc_r =0.4 K_s =0.4
$\bar{W}$	-11.3	10.87	12.45	55.22	-21.81	-2.26	-0.88	38.08
$\bar{Q}_z$	-6.72	-6.72	-5.88	-7.56	-12.60	-12.60	-12.18	-10.92
ϕ	-1.57	-1.57	-1.41	-1.11	-4.51	-4.51	-4.36	-4.16
$\bar{f}$	-1.51	-20.77	-21.87	-42.78	-5.26	-23.78	-24.81	-45.18
$\bar{S}_{11}$	-13.33	16.99	14.59	35.68	-24.8	1.41	13.8	15.61
$\bar{S}_{12}$	-8.72	-14.06	-44.15	-131.01	-17.92	-2.60	-29.68	-106.89
$\bar{S}_{21}$	3.32	-2.08	-11.23	-55.52	4.95	-18.78	-9.34	-50.46
$\bar{S}_{22}$	-14.08	-7.34	-9.13	-14.63	-23.1	-3.89	-19.04	-2.51
$\bar{B}_{11}$	1.036	26.32	52.63	138.71	6.05	32.56	60.14	150.57
$\bar{B}_{12}$	74.91	118.31	152.43	188.64	94.48	126.91	171.46	199.68
$\bar{B}_{22}$	-2.26	22.13	16.63	40.78	-4.67	19.15	13.84	36.34
$\bar{\omega}_d$	-9.19	-9.19	-4.59	-0.919	-15.86	-15.86	-11.72	-8.27
$\bar{\omega}_{th}$	24.80	24.80	19.91	14.02	39.18	39.18	33.61	27.76

$$\text{Percentage deviation} = \frac{(\text{parameter}|_{\text{elastic}} - \text{parameter}|_{\text{rigid}}) \times 100}{\text{parameter}|_{\text{rigid}}}$$

Table 5.17 Percentage deviation in the performance characteristics of three lobe bearing compared to corresponding values of rigid bearing without additives for $\varepsilon = 0.4$

Characteristics	$\overline{\psi}$ =0.05				$\overline{\psi}$ =0.1			
	λc_r=0.0 K_s=0.0	λc_r =0.2 K_s =0	λc_r =0.2 K_s =0.4	λc_r =0.4 K_s =0.4	λc_r =0 K_s =0	λc_r =0.2 K_s =0	λc_r =0.2 K_s =0.4	λc_r =0.4 K_s =0.4
$\overline{W}$	-18.41	-0.854	1.17	42.42	-29.42	-11.7	-10.60	23.5
$\overline{Q}_z$	-12.39	-12.39	-11.29	-9.91	-22.03	-22.03	-21.21	-19.83
ϕ	-4.41	-4.41	-4.27	-4.09	-9.44	-9.44	-9.32	-9.14
$\overline{f}$	-17.02	-32.85	-33.7	-50.87	-26.54	-41.65	-41.31	-56.49
$\overline{S}_{11}$	-31.8	-14.82	-13.39	15.5	-45.68	-32.12	-30.96	-7.21
$\overline{S}_{12}$	-13.63	-7.92	-23.35	-77.76	-26.02	-7.52	-5.73	-52.4
$\overline{S}_{21}$	-27.8	-8.89	-8.79	18.97	-41.91	-25.61	-22.76	-5.309
$\overline{S}_{22}$	-12.41	9.45	6.45	36.28	-22.1	-0.162	-5.28	21.23
$\overline{B}_{11}$	26.71	58.39	64.33	113.91	36.04	70.05	76.35	130.41
$\overline{B}_{12}$	25.55	56.88	62.82	119.31	36.46	71.57	76.96	138.41
$\overline{B}_{22}$	-12.87	8.91	7.08	36.67	-24.81	-5.73	-7.61	18.79
$\overline{\omega}_d$	-	-	-	-	-	-	-	-
$\overline{\omega}_{th}$	-	-	-	-	-	-	-	-

$$\text{Percentage deviation} = \frac{(\text{parameter}|_{\text{elastic}} - \text{parameter}|_{\text{rigid}}) \times 100}{\text{parameter}|_{\text{rigid}}}$$

REFERENCES

1. Pinkus O, 'Solution of Reynold's Equation for Arbitrarily Loaded Journal Bearings', J. Basic Engg., Trans. ASME, Series D, Vol.3, 1961, p. 145.
2. Orcutt. F.K and Arwas. E.B., 'The Steady State and Dynamic Characteristics of a Full Circular Bearing and Partial Arc Bearing in Laminar and Turbulent Regimes'. J. Lub. Tech., Trans. ASME, Vol. 89, 1967, p. 143.
3. Smith. D. M., 'Dynamic Characteristics of Turbine Journal Bearings', Conventions of Lubrication and Wear, Inst. Of Mech. Engrs., London, 1963.
4. Singh D. V., R. Sinhasan, R.C. Ghai, 'Analysis of Hydrostatic Journal Bearings by FEM', First National Conference on Industrial Tribology at Madras, 1974, pp. B 12 – 85.
5. Singh. D.V., Sinhasan. R., and Kumar. A., 'A Variaional Solution of Two Lobe Bearings, Mechanical and Machine Theory', J. IFTOMM, Vol.12, 1977, p. 323.
6. Lund. J. W. and Thomsen. K. K., 'A Calculation Method and Data for the Dynamic Coefficients of Oil Lubricant Journal Bearings', Topics in Fluid Film Bearings and Rotor Bearing System Design and Optimization, The ASME Design Engineering Conference, 1978, p. 1.
7. M.M.Reddi, 'Finite Element Solution of Incompressive Lubrication Problem', Trans ASME, July 1969, pp524-533.
8. M.M.Reddi, T.Y.Chu, 'Finite Element Solution of The Steady State Compressible Lubrication Problem', Trans. ASME, J.of Lub.Tech., July 1970, pp.495-503.
9. Singh D.V., Sinhasan. R., and Soni. S. C, 'Static and Dynamic Analysis of Hydrodynamic Bearings in Laminar and Superlaminar Flow Regimes by Finite Element Method', ASLE Trans., Vol. 26 (2), 1983, p. 225
10. S.Heller, 'Static and Dynamic Performance of Externally Pressurised Fluid Film Journal Bearings in the Turbulant Regime', Trans. ASME, J.of Lub.Tech., July 1974, pp.381-390.

11. C.M.Ettler and H.G.Anderson, 'The use of Higher order Finite Element Method for the use of Reynold's Equation', Tribology Trans., Vol.33, 1990, pp. 163-170.
12. H.N.Chandrawat and R.S.Sinhasan, 'A Comparison between two numerical techniques for Hydrodynamic Journal Bearing Problems', Wear, Vol.119, 1987, pp.77-87.
13. P.K.Goenka, 'Dynamically Loaded Bearings: Finite Element Method Analysis', J. of Tribology, Vol.106, 1984, pp.429-439.
14. Y.Chang, 'Starting Pressure Boundary Conditions for Perturbed Reynold's Equation',J.of Tribology,Vol.112,1990,pp.551-555.
15. A.Akers,S.Michaelson and Cameron, 'Stability Contours for a Whirling Finite Journal Bearing', Trans.ASME, J.of Lub.Tech., Jan.1971,pp.177-190.
16. J.L.Nikolajsen, 'The Effect of Variable Viscosity on the Stability of Plain Journal Bearings and Floating Ring Journal Bearings',Trans.ASME, J.of Lub.Tech., Oct.1973, pp.447-456.
17. P.shelly and C.Etliest, 'The application of a Finite Element Method to the Evaluation of Oil Whirl Characteristics', J. of Mech. Engg. Sciences, Vol.16, 1974, pp.101-108.
18. S.M. Rohde and H.A. Ezzat, 'On the Dynamic Behavior of Hybrid Journal Bearing', Trans ASMT, J.of Lub. Tech., Vol.98. 1976, p:90.
19. T. Etsion, O. Pinkus, 'Analysis of short Journal Bearings with New Upstream Boundary Conditions' Trans ASME, J. of Lub Tech, Vol.96, 1974, pp: 489 - 496.
20. R. Taylor, 'A Numerical Solution of the Dynamic Characteristics of an Aerostatic, Porous Thrust Bearing having a Uniform Film Subjected to Linear Axial Load Variations', J. of Mech. Engg Science, Vol. 19, 1977, pp.120 – 130.
21. Wilcock D.F., 'Turbulent Lubrication-Its Genisis and Role in Modern Design',Trans.ASME, J.of Lub.Tech.,Vol.96,1974, pp.1-6.

22. K.Venkiteswarlu, N.J.Rao, E.V.Venugopal and S.Akella, 'Three Dimensional Laminar and Turbulent Lubrication in Journal Bearings', Wear, Vol.126, 1990, pp.263-279.
23. W.W.Gardner and J.G.Ulschmid, 'Turbulence Effects in two Journal Bearing Applications', Trans.ASME, J.of Lub.Tech., Jan.1974, pp.15-21.
24. Y.C.Hsu, 'Non Newtonian flow in Infinite-length Full Journal Bearing', Trans. ASME, J.of Lub. Tech., Vol.89, 1967, pp.329-333.
25. H.Hyashi, S.Wada and N. Nakarai, 'Hydrodynamic Lubrication of Journal Bearing by Non Newtonian Lubricants', Bull. Of JSME., Vol.20, 1977, pp.224-231.
26. S.T.N.Swamy B.S.Prabhu and B.V.A.Rao, 'Steady State and Stability Characteristics of a Hydrodynamic Journal Bearing with a Non Newtonian Lubricant', Wear, Vol.42, 1977, pp.229-244.
27. J.K. Dien and H.G. Elrod, 'A Generalized steady state Raymold's Equation for Non-Newtonian Fluids with Application to Journal Bearing', Tran ASME, J. Lub. Tech. Vol.105, 1983, p. 385.
28. M. Malik, Bhagwan Dass and R. Sinhasan, 'The Analysis of Hydrodynamic Journal Bearings using Non-Newtonian Lubricants by Viscosity Averaging Across the Film', ASLE Trans., Vol. 26, 1983, pp.125 – 131.
29. P. K. Goenka and J. F. Booker, 'Effects of Surface Eliptivity on Dynamically Loaded Cylindrical Bearing', Trans ASME, J. of Lub Tech., Vol. 105, 1983, p:1
30. Ashok Kumar,R.Sinhasan and D.V.Singh, 'Performance Characteristics of Two Lobe Hydrodynamic Journal Bearings',ASME Trans., J.of Lub.Tech., Vol102,1980, pp.425-429.
31. Kumar Vaidyanathan and Theo G.Keith Jr., 'Performance Characteristics of Cavitated Non Circular Journal Bearings in the Turbulent Flow Regime',Tribology Transactions,Vol.34,1991, pp.35-44.
32. Malik. M., Sinhasan. R. and Chandra M., 'Design Data for Three –Lobe Bearings', ASLE Trans., Vol. 24 (3), 1981, p. 345

33. M. Malik, M. Chandra and R. Sinhasan, 'Performance Characteristics of Tilted Three-Lobe Journal Bearing Configurations', Trib. Int., Vol. 5, 1981, p:345.

34. Li. D. F., Choy. K. C and Allaire. P. E., 'Stability and Transient Characteristics of Four Multilobe Journal Bearing Configurations', Trans. ASME, J. of Lub. Tech., Vol. 102, 1980, p. 241.

35. Osterle, F., and Saibel. E., 'Surface Deformation in the Hydrodynamic Slider Bearing Problems and their Effects on the Pressure Development', Proceedings of the Conference on Lubrication and Wear', Inst. Mech. Engrs., 1957, p. 53

36. Osterle. F. and Saibel. E, 'The Effect of Bearing deformation in Slider Bearing Lubrication', ASLE Trans., Vol.18, 1958, p. 213

37. Higginson G. R.,'The Theoretical Effects of Elastic Deformation of Bearing Liner on Journal Bearing Performance', Proceedings of Symposium of Elastohydrodynamic Lubrication, Inst. of Mech Engrs London, Vol. 180,1965, p.31.

38. Carl. T.E., 'The Experimental Investigation of a Cylindrical Journal Bearing Under Constant and Sinusoidal Loading', Proceedings of 2nd Convention on Lubrication and Wear, Inst. of Mech Engrs. London, 1964, p. 100.

39. O' Donoghue. J. D., Brighton. D. K. and Hook. C. T., 'The Effect of Elastic Distortions on Journal Bearings Performance', Trans. ASME, J. Lub. Tech., Vol. 89, 1967, p. 409.

40. O' Donoghue. J. D, Koch. P. R. and Hook C. T, 'Approximate Short Bearing Analysis and Experimental Results using Plastic Bearing Liner', Proceedings of Inst. of Mech. Engrs., Vol. 184, 1969, p.216

41. Bozaci A., Dudley. B. R., Middleton V. and Allen D. G, ' Steady Load Performance of a Journal Bearing with an Elastic Housing', Proc. Fifth Leeds – Lyon Symposium Tribology, Leeds, Paper IX (II), 1978 , p. 320.

42. Jain S. C., Sinhasan R. and Signh D. V, 'Elastohydrodynamic Analysis of a Cylindrical Journal Bearing with a Flexible Bearing Shell', Wear, Vol. 78, 1982, p.325

43. Prabhakaran Nair. K, Sinhasan R. and Singh D. V., 'A Study of Elastohydrodynamic Lubrication: Finite Element Treatment for Rigid and Elastic Surfaces', National Conference on Industrial Tribology held at Bombay, India, 1986, p. II – 1-13.

44. Benjamin M. K. and Castelli. V., 'A theoretical investigation of compliant Surface Journal Bearings', Trans ASME, J. of Lub. Tech., Vol. 93, 1971, p. 191.

45. Oh K.P. and Huebner K. H., 'Solution of Elastohydrodynamic Finite Bearing Problems', Trans. ASME, J. of Lub. Tech, Vol. 95, 1973, pp. 342-352.

46. Jain. S. C., Sinhasan. R and Singh. D. V., 'On Plane Slider Bearing with the Flexible Bearing Pad'., Proc. IVth ISME Conference, Roorkee, India, 1981, p. 59..

47. Stafford A. C., Henshell R. D. and Dudley B. R., 'Finite Element Analysis in Elastohydrodynamic Lubrication', Proceedings of Fifth Leeds – Leyon Symposium on Tribology, Leeds, Paper ix (iii), 1978, p. 329

48. Frene. J., Deasailly R. and Fantino B., 'Hydrodynamics of an Elastic Connecting Rod Bearing: Comparison of Theoretical and Experimental Results', Proc. V Leeds-Lyon, Sym. on Tribology; Leeds, Paper ix (iv), 1978, pp:335.

49. Fantino B., Godet, M. and Frene, J., 'Dynamic Behaviour of an Elastic Connecting-Rod; Theoretical Study', Proceedings of Inst. Mech. Engrs., Paper No.830307/02/82., p.23.

50. Labouff, G.A. and Booker J.F., 'Dynamically Loaded Journal Bearings: A Finite Element Treatment for Rigid and Elastic Surface', Trans. ASME., J. Trib., Vol.107, 1985, pp. 505-515.

51. Conway H.D and Engel P.A., 'The Elastohydrodynamic Lubrication Problems', ASLE Trans., Vol. 21 (3), 1978, p. 261.

52. Conway H.D., Lee H.C., 'The Analysis of Lubrication of a Flexible Journal Bearing', Trans. ASME, J. of Lub. Tech., Vol. 97, 1975, p. 599

53. Conway, H.D. and Lee H.C., 'The Lubrication of Short Flexible Journal Bearings', Trans. ASME, J. Lub. Tech., Vol. 99, 1977, p.3 76.

54. Taylor, C. and O'Callaghan, J.F., 'A Numerical Solution of Elastohydrodynamic Lubrication Problem using Finite Elements', J. Mech. Engg. Sci., Vol 14, 1972, pp.229-237.

55. Jain S.C. and Sinhasan R., 'Performance of Flexible Shell Journal Bearing with Variable Viscosity Lubricants', Trib. International, 1986, p p. 331-339.

56. Jain S.C. Sinhasan R.and Singh D.V., 'A Study of Elastohydrodynamic Lubrication with Piezoviscous Lubricants', ASLE Trans., Vol.27, 1984, pp.168-176.

57. R. Sinhasan and H. N. Chandrawat, 'An Elastohydrodynamic Study on Two- Axial-Groove Journal Bearings', Trib. International, Vol. 88, 1988, p. 341.

58. Mak. W.C. and Conway. H. D., 'The Lubrication of Long Porous Flexible Journal Bearing', Trans ASME, J. Lub. Tech., Vol. 99, 1977, pp. 449-454.

59. Mak W. C. and Conway H.D., 'Analysis of a Short Porous Flexible Journal Bearing', Int. J Mech. Sci., Vol. 19, p 78.

60. Jain S. C., Sinhasan R. and Singh D. V., 'The Performance Characteristics of Thin Compliant Shell Bearing', Wear, Vol.81 1982, p. 251.

61. Sinhasan R., Jain S.C. and Sharma S.C., 'Orifice Compensated Flexible Pad Thrust Bearings of Different Configuration', Trib. International, Vol. 19,1986, p. 244.

62. Fantino B., Frene J. and Du Parquet J., 'Elastic Connecting Rod Bearing with Piezoviscous Lubricant, Analysis of the Steady Characteristics', Trans. ASME. J. Lub. Tech., Vol 101, 1979, p: 190.

63. Jain S.C., Sinhasan R. and Singh D.V., 'A Study of EHD Lubrication of Centrally Loaded 120 Arc Partial Bearing in Different Flow Regimes', J. of Mech. Engg. Sci., Part C, Vol.197, 1983, p.97.

64. K. KohnoS. Takahashi and K. Saki, 'Elasto-hydrodynamic lubrication analysis of journal bearings with combined use of boundary elements and

finite elements', Engineering Analysis with Boundary Elements, Vol. 13, 1994, pp.273-281.

65. B. J. Hamrock and D. Dowson, 'Elastohydrodynamic Lubrication of Elliptical Contacts for Materials of Low Elastic Modulus', Trans. ASME, J. of Lub. Tech., Vol. 101, 1979, p. 92.
66. Tae- Jo Park and Kyung- Woong Kim, 'A numerical Analysis of the Elastohydrodynamic Lubrication of Elliptical Contacts', Elsevier Sequoias, Netherlands, Vol 164, 1990, pp. 299-312.
67. Prabhakaran Nair K, Singh D. V. and Sinhasan R., 'Elastohydrodynamic Effects in Elliptical Bearing', Wear, Vol. 118, 1987, pp. 129 – 145.
68. Goyal K.C. and Sihanasan R., 'Elastohydrodynamic Studies of Two-Lobe Journal Bearings with Non-Newtonian Lubricants', J. Wear, Vol.145, 1991,pp. 329-345.
69. H. N. Chandrawat and R. Sinhasan, 'A study of a two-lobe journal bearing considering elastohydrodynamic effects', Wear, Vol.127, 1988, pp 161-177.
70. Prabhakaran Nair K, Singh D.V. and Sinhasan R., 'A Study of Elastohydrodynamic Effects in a Three – Lobe Journal Bearing', Tribology International, Vol. 20,1987, No. 3, pp. 125 – 132.
71. Chandravat H.N.and Sinhasan R, 'A study of Elastohydrodynamic Lubrication in Three Lobe Journal Bearing', Wear,Vol. 137, 1990, pp. 1 – 13.
72. Prabhakaran Nair K., and Regi Joseph., 'Study of Skewed Bearing with Piezoviscous Lubricants using Finite Element Method', ASME International Periodicals, Modeling, Measurement and Control, Vol. 45, No. 3, 1992, pp. 11-35.
73. Lakshminarayana V.,Kanth N.L.,Nair K.P. and Nair R.R., 'Static and Dynamic Analysis to Journal Bearings Using FEM ,Considering Skewed Axes and Piezo Viscous Nature of the Lubricant', Proc.15th AIMTDR Conference, Coimbatore (India),Dec.1992, pp.262-267.

74. Nair K.P.,Joy M.L.,Reddy K.V. and Nair R.R.., 'Thermohydrodynamic Analysis of Journal Bearing Using Finite Element Method',Proc.15th AIMTDR Conference, Coimbatore (India), Dec.1992, pp.224-238.

75. Nair K.P.and Joy M.L., 'Static Analysis of Thermohydrodynamic Journal Bearings',Proc. 6th International Congress of Tribology (EUROTRIB-93), Budapest, August 1993.

76. Nair K.P.,Joy M.L. and Indulekha T.P., 'Thermofluid Analysis of Circular Bearing using FEM', J. Thermofluid Dynamics, Vol.39,1994, pp.367-371.

77. Nair K.P. and Joy M.L., 'Thermohydrodynamic Analysis of Circular Bearing using Finite Element Modeling', AMSE International Periodical, Modeling,Measurement and Control-B,Vol.48 No:3,1993, pp.45-64.

78. Nair K.P., Joy M.L.and Harshan P.B., 'A Study of Thermohydrodynamic Lubrication in Circular Bearings', Proc. of International Conference on Tribology, Budapest, August 1993.

79. Nair K.P. and Joy M.L., 'Elastothermohydrodynamic Analysis of a Circular Bearing', Proc. National Conference on Design of Mechanical Systems, IIT, Kharagpur, India, Dec.23-24,1993.

80. Lakshminarayana V.and Nair K.P., 'THD Analysis of a Finite Two-Lobe Journal Bearing', National Conference Design of Mech. Systems (NACOMM), IIT, Kharagpur (India), December 23-24,1993.

81. Lakshminarayana V.and Nair K.P., 'THD Analysis of a Two-Lobe Journal Bearing using Finite Element Model', J.AMSE, Vol.54, No: 2, 1994, pp1-14.

82. Eringen A.C., 'Simple Microfluids', Int. J. of Engg. Sciences, Vol.2,1964, pp.205-217.

83. Eringen A.C., 'Theory of Micropolar Fluids', J, Math. & Mech., Vol.16, No.1, 1966, pp.1-18.

84. Allen S.J and Kline K.A, 'Lubrication theory for Micropolar Fluids', ASME Journal of Applied Mechanics, Sept. 1971, pp.646-649.

85. J.B. Shukla, 'Effects of Aditives and impurities in Lubrication', Proceedings of First World Conference in Industrial Tribology, New Delhi, 1972, pp. B5.1-B5.10.

86. M.S. Khader and R.L. Vachon, 'Theoretical effects of solid particles in hydrostatic bearing lubricant', Trans. ASME, J. Lub. Tech.,Vol. 95 (1973), pp. 104–106.

87. J. B. Shukla and M. Isa, 'Generalized Reynolds equation for Micropolar lubricants and its applications to optimum one dimensional slider bearings, effects of solid particle additives in solution', J. Mech. Engineering Science VI 7, (1975), pp. 280-284.

88. Zaheeruddin K. H and Isa M, 'Micropolar fluid lubrication of one dimensional Journal Bearing', Wear, 1978, Vol.50, pp. 211-220.

89. J. Prakash and P. Sinha, 'Squeze Film theory for micropolar fluids, Tran ASME,. J. of Lub. Tech. Vol. 98, 1976 pp. 139-144.

90. Prakash J and Sinha P, 'A study of Squeezing flow in Micropolar Fluid Lubricated Journal Bearing', Wear, Vol. 38, 1976, pp. 17-28.

91. Balaram M, 'Micropolar Sqeeze Film', Trans. ASME, J. Lub. Tech., Oct. 1975, pp. 635-637.

92. Albert E. Yousif and Thamer M. Ibrahim, 'Lubrication of a slider bearing with oils containing additives and contaminats' Wear V 81 1982, pp.33-45.

93. Prakash J, and Prawal Sinha, , 'Lubrication Theory for Micropolar Fluids and Its Application to a Journal Bearing', In, J. Engg Sci, Vol.13, 1975, pp.217-232.

94. Albert E. Yousif and Somer M. Nacy, 'Hydrodynamic behaviour of Two-phase (Liquid-solid) Lubricants', Wear Vol. 66, 1981, pp. 223-240.

95. Nicolae Tipei, 'Lubrication with Micropolar Liquids and its Application to short bearings', Trans. ASME, J. Lub. Tech, Vol. 101, 1979, pp. 356-363.

96. Tsai-Wang HuangCheng-I Weng and Chao-Kuang Chen, 'Analysis of finite width journal bearings with micropolar fluids', Wear, Volume 123, Issue 1, 1988, pp. 1-12.

97. M.M. Khonsari and D.E. Brewe, 'On the performance of finite journal bearing lubricated with micropolar fluid', Tribol. Trans. 32 (1989), pp. 155–160.

98. C.C. Narayanan, R. Narayanan and K. Prabhakaran Nair, 'Effects of Mass Transfer of Additives in Finite Journal Bearing Using Micropolar Lubricant', Proceedings of XI NCIT, 1995, pp. 136-141.

99. R. Narayanan, C.C. Narayanan and K. Prabhakaran Nair, 'Analysis of Mass transfer effects on the performance of journal bearings using Micropolar Lubricant', Heat and Mass Transfer, Vol. 30, 1995, p.429.

100. Albert E. Yousif and Thamir M. Ibrahim, 'Lubrication of infinitely long thrust bearings with micropolar fluids', Wear, Volume 89, Issue 2, 1983, pp. 137-150

101. Jaw-Ren Lin, 'Static and dynamic characteristics of externally pressurized circular step thrust bearings lubricated with couple stress fluids', Tribology International, Vol. 32, 1999, pp. 207-216.

102. G. Lukaszevicz, 'Long time behaviour of 2 D Micropolar Fluid Flows', Mathematical and Computer Modelling, Vol. 34, 2001, pp.487-509.

103. K.Raghunandana and B.C.Majumdar, 'Stability of Journal Bearing Systems using non-Newtonian Lubricants : A Nonlinear Transient Analysis', Tribology International,Vol.32,1999,pp.179-184.

104. S.Das. S.K. Ghua and A.K. Chattopadhyay, 'On the steady-state performance of misaligned hydrodynamic journal bearings lubricated with Micropolar Fluids', Tribology International, Vol. 135, 2002, pp. 201-210.

105. O'Connar.J.J and John B, 'Standard hand book of lubrication Engineering', McGraw Hill Book Co. Inc., New York, 1968.

106. O.C. Zienkiewicz, 'The Finite Element Method', McGraw Hill book Co., New York, 1977.

107. Hewbner K.H., 'The Finite Element Method for Engineers', John Wiley and Sons', New York, 1975.

LIST OF TECHNICAL PAPERS PUBLISHED

1. V.P. Sukumaran Nair and K Prabhakaran Nair, 'Finite Element Analysis of Elastohydrodynamic Circular Journal Bearing with Micropolar Lubricants', Int. J. Finite Element Analysis and Design (Accepted).
2. V.P. Sukumaran Nair and K Prabhakaran Nair, 'Static analysis of a three lobe bearing operating with micropolar lubricants', All India seminar on manufacturing strategies for 21st century, Thrissur, November 26-28, 2003.
3. V.P. Sukumaran Nair and K Prabhakaran Nair, 'Static Analysis of an Elliptical Bearing with Micropolar Lubricants using Finite Element Method', Second National Conference on Power Conversion and Industrial Control (PCIC), NSSCE, Palakkad, July 9-10,2004 (Accepted).
4. V.P. Sukumaran Nair and K Prabhakaran Nair, 'Finite Element Analysis of Elastohydrodynamic Three Lobe Journal Bearing with Micropolar Lubricants', Second National Conference on Power Conversion and Industrial Control (PCIC), NSSCE, Palakkad, July 9-10, 2004 (Accepted).
5. V.P. Sukumaran Nair and K Prabhakaran Nair, 'Finite Element Modeling of Elastohydrodynamic Circular Bearing operating under Micropolar Lubricants, AMSE System Modeling & Simulation – (Under Review).
6. V.P. Sukumaran Nair and K Prabhakaran Nair, 'Elastohydrodynamic Analysis of Noncircular Bearings operating under Micropolar Lubricants', International Journal of Computer Aided Design – (Under Review).

Appendix - A1

NON CIRCULAR BEARING GEOMETRY

The non circular (two-lobe, three lobe) bearing geometries are as follows.

A 1.1 Two-Lobe Bearing

The two lobe bearing consists of two circular halves with centers O_1 and O_2 (Fig. A 1.1) with offset ε_p on either side of the geometric centre O_b of the bearing. The eccentricities ε_1 and ε_2 and attitude angles ϕ_1 and ϕ_2 for any journal centre O_3 can be calculated by using the following equations.

For lower lobe:

$$\varepsilon_1 = \left\{\varepsilon^2 + \varepsilon_p^2 + 2\varepsilon\varepsilon_p \cos\phi\right\}^{1/2} \tag{A 1.1}$$

$$\phi_1 = \tan^{-1}\left\{\frac{\varepsilon \sin\phi}{\varepsilon_p + \varepsilon\cos\phi}\right\} \tag{A 1.2}$$

For upper lobe:

$$\varepsilon_1 = \left\{\varepsilon^2 + \varepsilon_p^2 - 2\varepsilon\varepsilon_p \cos\phi\right\}^{1/2} \tag{A 1.3}$$

$$\phi_2 = \pi - \tan^{-1}\left\{\frac{\varepsilon \sin\phi}{\varepsilon_p + \varepsilon\cos\phi}\right\} \tag{A 1.4}$$

A 1.2 Three-Lobe Bearing

The three lobe bearing consists of three non concentric arcs Fig. A 1.2 and the various geometric parameters of a three lobe bearing are related as follows.

Lobe 1:

$$\varepsilon_1 = \left\{\varepsilon^2 + \varepsilon_p^2 + 2\varepsilon\varepsilon_p \cos\phi\right\}^{1/2} \tag{A 1.5}$$

$$\phi_1 = \tan^{-1}\left\{\frac{\varepsilon \sin\phi}{\varepsilon_p + \varepsilon\cos\phi}\right\} \tag{A 1.6}$$

Lobe 2:

$$\varepsilon_1 = \left\{ \varepsilon^2 + \varepsilon_p^2 - 2\varepsilon\varepsilon_p \cos\left(\frac{\pi}{3} + \phi\right) \right\}^{1/2} \tag{A 1.7}$$

$$\phi_2 = \frac{2\pi}{3} - \tan^{-1}\left\{ \frac{\varepsilon \sin\left(\frac{\pi}{3} + \phi\right)}{\varepsilon_p - \varepsilon \cos\left(\frac{\pi}{3} + \phi\right)} \right\} \tag{A 1.8}$$

Lobe 3:

$$\varepsilon_1 = \left\{ \varepsilon^2 + \varepsilon_p^2 - 2\varepsilon\varepsilon_p \cos\left(\frac{\pi}{3} - \phi\right) \right\}^{1/2} \tag{A 1.9}$$

$$\phi_2 = \frac{2\pi}{3} - \tan^{-1}\left\{ \frac{\varepsilon \sin\left(\frac{\pi}{3} - \phi\right)}{\varepsilon_p - \varepsilon \cos\left(\frac{\pi}{3} - \phi\right)} \right\} \tag{A 1.10}$$

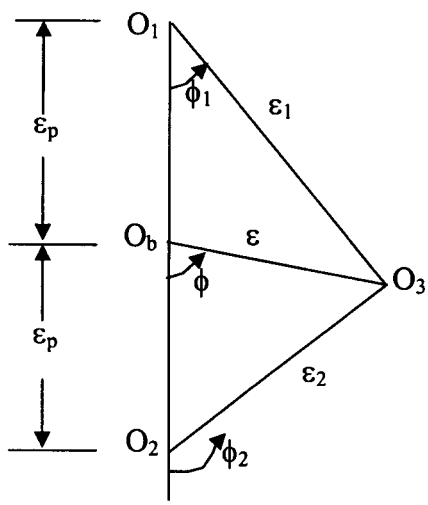

Fig. A 1.1 Geometry of two lobe bearing

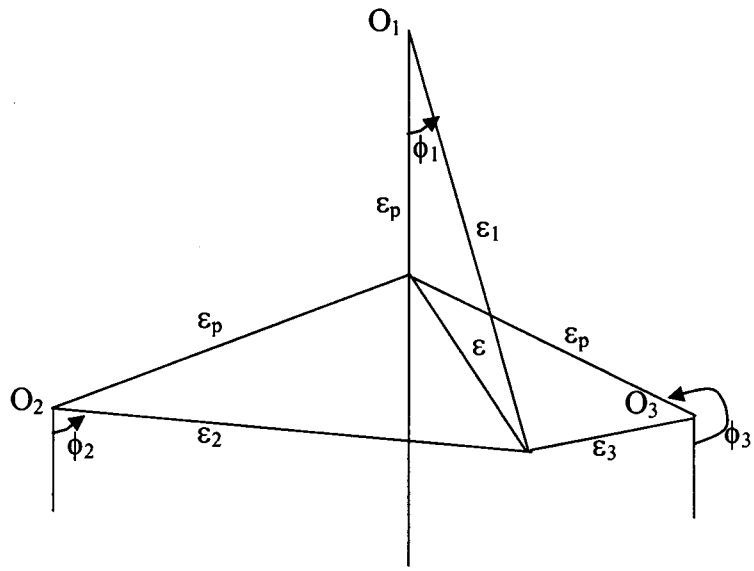

Fig. A 1.2 Geometry of three lobe bearing

Appendix-A2

THE TRANSFORMATION OF STIFFNESS AND DAMPING COEFFICIENTS

The fluid film damping forces which depend on velocities $\dot{\xi}$ and $\dot{\eta}$ are given by its horizontal and vertical components and these components can be written as shown below.

$$W_1 = -(b_{1\xi}\,\dot{\xi} + b_{1\eta}\,\dot{\eta}) \tag{A 2.1}$$

$$W_2 = -(b_{2\xi}\,\dot{\xi} + b_{2\eta}\,\dot{\eta}) \tag{A 2.2}$$

Equations A 2.1 and A 2.2 can be written in matrix form as

$$\begin{bmatrix} W_1 \\ \\ W_2 \end{bmatrix} = \begin{bmatrix} b_{1\xi} / \varepsilon & b_{1\eta} \\ \\ b_{2\xi} / \varepsilon & b_{2\eta} \end{bmatrix} \begin{bmatrix} \varepsilon\dot{\xi} \\ \\ \dot{\eta} \end{bmatrix} \tag{A 2.3}$$

ε, $\dot{\xi}$ and $\dot{\eta}$ can be written in terms of $\dot{x}_1$ and $\dot{x}_2$ as given below.

$$\begin{bmatrix} \varepsilon\dot{\xi} \\ \\ \dot{\eta} \end{bmatrix} = \begin{bmatrix} \cos\theta & -\sin\theta \\ \\ \sin\theta & \cos\theta \end{bmatrix} \begin{bmatrix} \dot{x}_1 \\ \\ \dot{x}_2 \end{bmatrix} \tag{A 2.4}$$

Thus equation A 2.3 can be written as

$$\begin{bmatrix} W_1 \\ \\ W_2 \end{bmatrix} = \begin{bmatrix} b_{1\xi} / \varepsilon & b_{1\eta} \\ \\ b_{2\xi} / \varepsilon & b_{2\eta} \end{bmatrix} \begin{bmatrix} \cos\theta & -\sin\theta \\ \\ \sin\theta & \cos\theta \end{bmatrix} \begin{bmatrix} \dot{x}_1 \\ \\ \dot{x}_2 \end{bmatrix} \tag{A 2.5}$$

NB4550

The fluid film damping force components can be written in terms of damping coefficients and velocities as given below.

$$\begin{bmatrix} W_1 \\ \\ W_2 \end{bmatrix} = \begin{bmatrix} B_{11} & B_{12} \\ \\ B_{21} & B_{22} \end{bmatrix} \begin{bmatrix} \dot{x}_1 \\ \\ \dot{x}_2 \end{bmatrix} \qquad \text{(A 2.6)}$$

Comparing equations A 2.5 and 2.6

$$\begin{bmatrix} B_{11} & B_{12} \\ \\ B_{21} & B_{22} \end{bmatrix} = \begin{bmatrix} b_{1\xi} & b_{1\eta} \\ \\ b_{2\xi} & b_{2\eta} \end{bmatrix} \begin{bmatrix} \frac{\cos\theta}{\varepsilon} & \frac{-\sin\theta}{\varepsilon} \\ \\ \sin\theta & \cos\theta \end{bmatrix} \qquad \text{(A 2.7)}$$

As the displacements and velocities are in the same direction similar transformation can be used for stiffness coefficients also.

$$\begin{bmatrix} S_{11} & S_{12} \\ \\ S_{21} & S_{22} \end{bmatrix} = \begin{bmatrix} s_{1\xi} & s_{1\eta} \\ \\ s_{2\xi} & s_{2\eta} \end{bmatrix} \begin{bmatrix} \frac{\cos\theta}{\varepsilon} & \frac{-\sin\theta}{\varepsilon} \\ \\ \sin\theta & \cos\theta \end{bmatrix} \qquad \text{(A 2.8)}$$